SZKOŁA DOKTORSKA
BioMedChem
Uniwersytetu Łódzkiego
i Instytutów Polskiej
Akademii Nauk w Łodzi

INSTYTUT
ERCE BiolMed

Mateusz Grabowski

Praca doktorska:

Modyfikacja polilaktydu poprzez wprowadzenie do struktury polimeru ugrupowania zawierającego podatne na termiczną dysocjację wiązanie kowalencyjne

Doctoral thesis:

Modification of polylactide by introducing into the polymer structure a moiety containing a covalent bond susceptible to thermal dissociation

- Promotor/Supervisor
  dr hab. Melania Bednarek
  Centrum Badań Molekularnych i Makromolekularnych
  Polskiej Akademii Nauk
- Promotor pomocniczy/Assistant Supervisor
  dr Bartłomiej Kost
  Centrum Badań Molekularnych i Makromolekularnych
  Polskiej Akademii Nauk

Podziękowania:

Serdecznie dziękuję Promotorowi Pani dr hab. Melanii Bednarek za inspirację do podjęcia pracy badawczej, za pomoc merytoryczną, cierpliwość, wsparcie i okazaną życzliwość.

Dziękuję również promotorowi pomocniczemu dr Bartłomiejowi Kost za pomoc naukową, przekazaną wiedzę oraz wsparcie w prowadzeniu badań.

Z całego serca pragnę podziękować moim rodzicom za ich niezłomne wsparcie i wiarę we mnie, które towarzyszyły mi na każdym etapie mojej drogi akademickiej.

Praca finansowana w ramach projektu badawczego OPUS NCN:
2018/31/B/ST8/01969: „Wykorzystanie kowalencyjnych wiązań o charakterze odwracalnym do otrzymywania odwracalnych sieci polilaktydowych i kopolimerów laktydu”
(Narodowe Centrum Nauki)

Praca doktorska wykonana w Centrum Badań Molekularnych i Makromolekularnych
Polskiej Akademii Nauk

Spis treści

Przedmowa

Przedstawiona rozprawa doktorska zatytułowana „Modyfikacja polilaktydu poprzez wprowadzenie do struktury polimeru ugrupowania zawierającego podatne na termiczną dysocjację wiązanie kowalencyjne” składa się z pięciu oryginalnych monotematycznych publikacji i jednej publikacji przeglądowej opublikowanych w czasopismach o zasięgu międzynarodowym (z tzw. Listy Filadelfijskiej). Autoreferat, który jest komentarzem do załączonych publikacji, rozpoczynają streszczenia w języku polskim i angielskim. W kolejnej pierwszej opisowej części zamieszczono wstęp, z którego wynika znaczenie podjętych badań i omówiono podstawowe zagadnienia związane z badanymi w pracy układami polimerowymi. Część druga zawiera opis właściwych badań, będący przewodnikiem opisującym główne osiągnięcia badawcze szczegółowo przedstawione w publikacjach. Trzecia część zawiera kopie sześciu publikacji (wraz z opisami badań dodatkowych zawartymi w „Suplementarny Information”) oraz oświadczenia współautorów o ich wkładzie w wykonane badania.

Cykl publikacji szczegółowo opisuje badania dotyczące różnych możliwości modyfikacji polilaktydu wynikających z wprowadzenia do jego struktury szczególnego typu wiązania kowalencyjnego o charakterze odwracalnym, mianowicie wiązania węgiel-węgiel w grupie tetrafenyloetanu podatnego na termiczną dysocjację.

W zakres pracy doktorskiej wchodzą następujące publikacje:

1. Mateusz Grabowski, Bartłomiej Kost, Bartłomiej Gostyński, Melania Bednarek. Can tetraphenylethane (TPE) “iniferter” group be introduced into the polymer chain by coupling TPE diol with diisocyanate? *Polymer*. 2022;246:124738. doi:10.1016/j.polymer.2022.124738
2. Mateusz Grabowski, Bartłomiej Kost, Przemysław Kubisa, Melania Bednarek. A New Approach to The Synthesis of Polylactide/Polyacrylonitrile Block Copolymers. *Polymers*. 2022;14(8):1529. doi:10.3390/ polym14081529
3. Mateusz Grabowski, Bartłomiej Kost, Agnieszka Bodzioch, Melania Bednarek. Functionalization of Polylactide with Multiple Tetraphenylethane Inifer Groups to Form PLA Block Copolymers with Vinyl Monomers. *Int. J. Mol. Sci*. 2023;24(1):19. doi:10.3390/ijms24010019
4. Mateusz Grabowski, Bartłomiej Kost, Mateusz Bartniak, Dorota Bociąga, Witold Szymański, Melania Bednarek. Copolymerization of lactide with functional epoxide as a way to the polymer network with dually active tetraphenylethane groups. *Polymer*. 2024;312:127673 doi:10.1016/j.polymer.2024.127673

5. Melania Bednarek, Mateusz Grabowski, Magdalena Lipińska, Andrzej Pawlak. Reversible polymer networks based on polylactide with tetraphenylethane thermally dissociating groups in crosslinks. *Polym. Adv. Technol*. 2024;35(4):e6390. doi:10.1002/pat.6390
6. Melania Bednarek, Mateusz Grabowski. Polylactide/poly(vinyl monomer) block copolymers for specific applications. *Polymer Reviews*. 2024;64(3):898-938. doi:10.1080/15583724.2024.2310105

Streszczenie

Celem pracy była modyfikacja polilaktydu (PLA) poprzez wprowadzenie do jego struktury ugrupowania zawierającego podatne na termiczną dysocjację wiązanie kowalencyjne. Jako ugrupowanie wytypowano grupę tetrafenyloetanu (TPE), która na skutek dostarczenia ciepła dysocjuje z wytworzeniem rodników. Wprowadzenie grup TPE do struktury PLA otworzyło drogę do jego modyfikacji na różne sposoby.

Pierwszym zadaniem badawczym było wprowadzenie ugrupowania TPE do łańcucha PLA. W tym celu przeprowadzono badania wstępne mające na celu przeanalizowanie reaktywności komercyjnego tetrafenyloetano-1,2-diolu (TPED) jako związku pozwalającego na wprowadzenie grup TPE do struktury PLA. Badania wykazały niewystarczającą reaktywność trzeciorzędowych grup -OH w TPED zarówno w reakcji inicjowania polimeryzacji laktydu jak też w reakcji z diizocyjanianami w celu sprzęgnięcia z diolem PLA. Opracowano alternatywne metody wprowadzenia ugrupowania TPE, w tym celu zsyntezowano pochodne benzofenonu (BP) z reaktywnymi grupami -OH będące prekursorami grup TPE. Wykorzystując otrzymane pochodne opracowano dwie metody wprowadzenia grup TPE do makrocząsteczki PLA: pierwsza - poprzez inicjowanie otrzymaną pochodną BP_ET kationowej polimeryzacji laktydu, w wyniku której, w następstwie sprzęgania, otrzymano łańcuchy PLA z wbudowaną jedną grupą TPE, druga - poprzez reakcję sprzęgania pochodnej TPE-diET z oligodiolem PLA z użyciem diizocyjanianu, w wyniku której otrzymano poliestro-uretan zawierający wiele grup TPE w łańcuchu. Wprowadzenie grup TPE do łańcucha polimerowego opartego na polilaktydzie otworzyło drogę do kopolimerów blokowych PLA z monomerami winylowymi, co stanowiło pierwszy kierunek pracy. Otrzymane polilaktydy z grupami TPE w środku wykorzystano jako makroinifertery w celu inicjowania polimeryzacji monomerów winylowych. W ten sposób po raz pierwszy z zastosowaniem metody inifertera otrzymano kopolimery blokowe PLA/poli(monomer winylowy).

Drugim wątkiem rozwijanym w pracy było wykorzystanie ugrupowania TPE do syntezy odwracalnych/dynamicznych kowalencyjnych sieci polilaktydowych. Opracowano dwie metody syntezy sieci z ugrupowaniami TPE w węzłach sieci. W pierwszej metodzie wykorzystano zsyntezowany monomer epoksydowy BP_EP jako komonomer w reakcji kopolimeryzacji z laktydem. Otrzymany kopolimer (LA-co-BP_EP) następnie usieciowano w wyniku reakcji sprzęgania bocznych grup BP na skutek promieniowania UV. Wykazano odwracalny charakter otrzymanej sieci poprzez przeprowadzenie badań reologicznych. Obecność grup TPE w węzłach sieci mających zdolność inicjowania polimeryzacji

monomerów winylowych, wykorzystano również do wprowadzenia jednostek AN do struktury sieci. Wykazano, że wprowadzenie bloków PAN do struktury sieci skutkuje poprawą odporności termicznej oraz poprawą właściwości mechanicznych. Druga metoda otrzymywania sieci zawierających w swojej strukturze grupy TPE oparta została na sprzęganiu gwiaździstych PLA zawierających grupy TPE w rdzeniu, za pomocą diizocyjanianu. Badania reologiczne, pozwoliły na wykazanie dynamicznego charakteru sieci. Zademonstrowano również zdolność otrzymanych sieci do naprawy po uszkodzeniu.

Abstract

The aim of the study was to modify polylactide (PLA) by introducing a group containing a covalent bond susceptible to thermal dissociation into the PLA structure. The group selected was tetraphenylethane (TPE), which, upon heating, dissociates to form radicals. Introducing TPE groups into the PLA structure opened up pathways for modifying PLA in various ways.

The first research objective was the introduction of the TPE group into the PLA chain. For this purpose, preliminary research was conducted to analyze the reactivity of tetraphenylethane-1,2-diol (TPED) as a compound allowing the introduction of TPE groups into the PLA structure. The studies showed insufficient reactivity of TPED's tertiary -OH groups in both lactide polymerization initiation and reactions with diisocyanates to couple with PLA diol. Alternative methods for introducing the TPE group were developed, including the synthesis of benzophenone (BP) derivatives with reactive -OH groups, which serve as precursors to TPE groups. Using the obtained derivatives, two methods were developed to introduce TPE groups into the PLA macromolecule. The first method was cationic polymerization of lactide (LA) initiated by the obtained BP_ET derivative, followed by chains coupling which resulted in PLA with single embedded TPE group in the middle of the chain. The second method involved coupling the TPE-diET derivative with PLA oligodiol using diisocyanate, yielding a polyester-urethane containing multiple TPE groups in the chain. The introduction of TPE groups into the polylactide-based polymer chain paved the way for PLA block copolymers with vinyl monomers, which formed the first direction of the research. The obtained polylactides with TPE groups in the center were used as macroinitiators to initiate the polymerization of vinyl monomers. In this way, for the first time using the iniferter method, PLA/poly(vinyl monomer) block copolymers were obtained.

The second focus of the research was the use of TPE groups for the synthesis of reversible/dynamic covalent polylactide networks. Two methods for synthesizing networks with TPE groups at the network nodes were developed. In the first method, the epoxy ring containing derivative (BP_EP) was used as a comonomer in the copolymerization reaction with LA. The resulting (LA-co-BP_EP) copolymer was then cross-linked through UV-induced coupling of the BP side groups. The reversible nature of the resulting network was demonstrated through rheological studies. The presence of TPE groups at the network nodes, capable of initiating vinyl monomer polymerization, was also used to introduce AN units into the network structure. It was shown that the introduction of PAN blocks into the network structure improved

thermal resistance and mechanical properties. The second method for producing networks containing TPE groups in their structure involved coupling star-shaped PLA containing TPE groups in the core, using diisocyanate. Rheological studies demonstrated the dynamic nature of the networks. The networks' ability to self-repair after damage was also demonstrated.

1. Wstęp

1.1. Wprowadzenie

Odkąd Staudinger zaproponował istnienie ‘makromoleküle’[1,2] ich wkład w transformację otaczającego nas świata przeszedł najśmielsze oczekiwania. Polimery zrewolucjonizowały świat materiałów poprzez swoją nieporównywalną w stosunku do klasycznych materiałów (ceramiki, metali, drewna) możliwość przystosowania oraz różnorodność[3]. Dziś po ponad stu latach od rewolucyjnej koncepcji kowalencyjnie związanych makromolekuł Staudingera, wyprodukowano dotychczas ponad 9 miliardów ton polimerów[4], w samym roku 2022 globalna produkcja tworzyw sztucznych wyniosła ok 400 mln ton, z czego tylko 1% wyprodukowane z polimerów otrzymanych z surowców odnawialnych[5]. Oprócz oczywistych zalet materiałów polimerowych, niosą one ze sobą również wady, większość obecnie produkowanych polimerów są to polimery pochodzące z surowców nieodnawialnych, do produkcji których wykorzystano monomery ropopochodne. Choć przejście na model gospodarki o zamkniętym obiegu nabiera tempa, niestety ogromna większość materiałów otrzymanych z polimerów ropopochodnych nie wchodzi w jej skład, co oznacza, że znaczna ich część trafia na wysypiska śmieci, gdzie może być składowana bez końca[3]. Szacuje się, że w samej Unii Europejskiej rocznie generowane jest ok 32 mln ton odpadów pochodzących z tworzyw sztucznych, mniej niż 30% jest poddawane recyklingowi, reszta trafia na wysypiska śmieci, z czego 50% ulega spalaniu z odzyskiem energii[6]. Nadal część odpadów powstałych np. z materiałów opakowaniowych nie jest właściwie utylizowana i trafia w sposób niekontrolowany do środowiska[3]. Należy w tym miejscu zaznaczyć również rosnący problem mikroplastiku[7].

Dlatego też od wielu lat trwają badania nad otrzymywaniem zrównoważonych polimerów (z ang. „sustainable polymers”), mogących zastąpić polimery ropopochodne. Aby polimer był uważany za zrównoważony musi być otrzymywany z surowców odnawialnych, które nie szkodzą zdrowiu człowieka oraz środowisku, jednocześnie spełniając wymogi konsumenta (będąc konkurencyjnym w cenie i mającym porównywalne właściwości mechaniczne i termiczne, w porównaniu z obecnie wykorzystywanymi polimerami)[3]. Obecnie zaawansowanym technologicznie polimerem o ugruntowanej pozycji na rynku wśród polimerów otrzymywanych z surowców odnawialnych jest polilaktyd/poli(kwas mlekowy). Produkcja polilaktydu systematycznie rośnie i odpowiada obecnie za 31% globalnej produkcji polimerów otrzymywanych z surowców odnawialnych[8]. Choć jego cena jest nadal zdecydowanie wyższa niż konkurencyjnych konwencjonalnych polimerów otrzymywanych z paliw kopalnych, staje się coraz bardziej dostępny, poprzez wprowadzanie innowacyjnych wielkotonażowych procesów produkcyjnych takich jak firmy NatureWorks Co. (USA)[9].

1.2. Polilaktyd - otrzymywanie i właściwości

Polilaktyd jest alifatycznym poliestrem otrzymywanym z surowców odnawialnych np.: kukurydzy, trzciny cukrowej czy ryżu. Swoje różnorodne zastosowanie zawdzięcza w szczególności degradowalności (kompostowalności), biokompatybilności oraz właściwościom mechanicznym zbliżonymi do takich polimerów jak polistyren bądź poli(teraftalan etelenu). Polilaktyd jest termoplastem, zatem może być łatwo przetworzony poprzez termoforowanie, wtryskiwanie, wytłaczanie, wytłaczanie rozdmuchowe, przędzenie[10]. Dzięki swoim właściwościom jest uważany za potencjalny substytut polimerów ropopochodnych. W biomedycynie dzięki biozgodności i degradowalności znalazł jedne z najbardziej zaawansowanych technologicznie zastosowań, gdzie wykorzystywany jest do produkcji nici chirurgicznych, rusztowań w inżynierii tkankowej, stentów kardiologicznych, bypassów, platform diagnostycznych, a także systemów dostarczania leków[10–12]. Jego zastosowanie rozwijane jest również w innych gałęziach przemysłu od opakowaniowego, rolniczego, elektronicznego, aż po motoryzacyjny[10]. W przemyśle włókna polilaktydowe cenione są ze względu na niską retencję zapachu oraz posiadają doskonałe właściwości odprowadzania wilgoci. Polilaktydowe butelki, folie i termoformowane pojemniki są coraz popularniejsze ze względu na odporność na tłuszcze, oleje i zdolność do „blokowania” smaków i zapachów[13].

Możliwe są dwie główne drogi syntezy PLA: polikondensacja kwasu mlekowego i polimeryzacja z otwarciem pierścienia (ROP) laktydu, cyklicznego dimeru kwasu mlekowego. Polikondensacja nie prowadzi do otrzymania polilaktydów o dużych masach molowych i wymaga usuwania produktu ubocznego w postaci wody. Powszechnie wykorzystywaną metodą pozwalającą na otrzymanie dużych mas molowych PLA o małej dyspersji jest ROP. Laktyd ze względu na obecność dwóch centrów chiralnych, występuje w postaci 3 stereoizomerów: S,S-laktydu (L-laktydu), R,R-laktydu (D-laktydu) oraz R,S- laktydu (mezo-laktydu) (Rys. 1). Ta asymetria sprawia, że możliwe jest otrzymanie trzech rodzajów PLA odpowiednio PLLA, PDLA oraz różniącego się właściwościami fizykochemicznymi PDLLA.

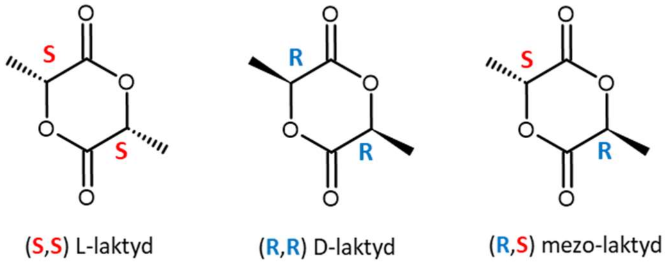

Rys. 1 Struktury stereoizomerów laktydu[14]

W wyniku polimeryzacji optycznie czystych L- i D-laktydów otrzymuje się izotaktyczne homopolimery, odpowiednio PLLA i PDLA. Wielkocząsteczkowe PLLA i PDLA są semikrystaliczne i wykazują T_m ok. 180 °C oraz $T_g \sim$ 55-65 °C[12]. Polimery o krystalicznej strukturze mogą być otrzymane, gdy zachowana jest kontrola stereo-regularności jednostek D i L. W praktyce ich krystaliczność i T_m zwykle zmniejszają się wraz ze spadkiem czystości optycznej jednostek laktydu. Z mieszaniny L- i D-laktydu czyli racemicznego laktydu otrzymuje się ataktyczne i heterotaktyczne PDLLA, które są amorficznymi polimerami o $T_g \sim$ 30 °C[15]. Możliwe jest również otrzymanie syndiotaktycznego PDLLA z mezo-laktydu, który jest semikrystalicznym polimerem, jednakże jego synteza wymaga zastosowania specjalistycznych katalizatorów, które muszą ograniczać transestryfikacje. Izotaktyczny PLA charakteryzuje się największą sztywnością (moduł Younga 4 GPa, wytrzymałość na rozciąganie 50-70 MPa, moduł zginania ~ 5 GPa, wytrzymałość na zginanie ~ 100 MPa oraz wydłużenie przy zerwaniu ~ 4%), jednocześnie ataktyczny PLA jest najbardziej elastyczny (moduł Younga 1,2 GPa, wytrzymałość na rozciąganie 59 MPa, wytrzymałość na zginanie 88 MPa)[12,16].

Obecnie znane są dwa mechanizmy polimeryzacji z otwarciem pierścienia LA: jonowy i koordynacyjno-insercyjny[17,18]. Najczęściej wykorzystywaną metodą w przemyśle jest polimeryzacja z otwarciem pierścienia laktydu według mechanizmu koordynacyjno-insercyjnego, który wymaga obecności metaloorganicznego katalizatora[19–22]. Ze względu na dużą aktywność katalityczną i dobrą rozpuszczalność w układzie polimeryzacyjnym najczęściej stosowane są związki cyny (oktanian cyny (II), $Sn(Oct)_2$). W polimeryzacji laktydu katalizowanej $Sn(Oct)_2$, najczęściej stosowanymi inicjatorami są związki zawierające grupy hydroksylowe, zwykle są to alkohole, bądź też makrocząsteczki z hydroksylowymi grupami końcowymi. Możliwe jest również wykorzystanie amin oraz tioli jako inicjatorów[23–25]. W pierwszym etapie alkohol reaguje z $Sn(Oct)_2$ tworząc alkoholan cyny. Następnie jeden z karbonylowych atomów tlenu z pierścienia LA czasowo koordynuje z atomem cyny katalizatora w formie alkoholanowej, a grupa alkoksylowa katalizatora koordynuje z karbonylowym atomem węgla LA. Otwarcie pierścienia następuje poprzez pęknięcie wiązania pomiędzy węglem grupy acylowej, a atomem tlenu, umożliwiając insercję cząsteczki otwartego monomeru do wiązania cyna-tlen katalizatora. Propagacja przebiega w następstwie analogicznej koordynacji poprzez ten sam mechanizm i kolejne cząsteczki laktydu ulegają insercji do wiązania cyna-tlen (Rys. 2)[20,26]. Oktanian cyny umożliwia otrzymywanie polilaktydów o dużym ciężarze cząsteczkowym i małym rozrzucie mas molowych. Jest skutecznym katalizatorem zarówno w polimeryzacji w masie jak i w roztworze.

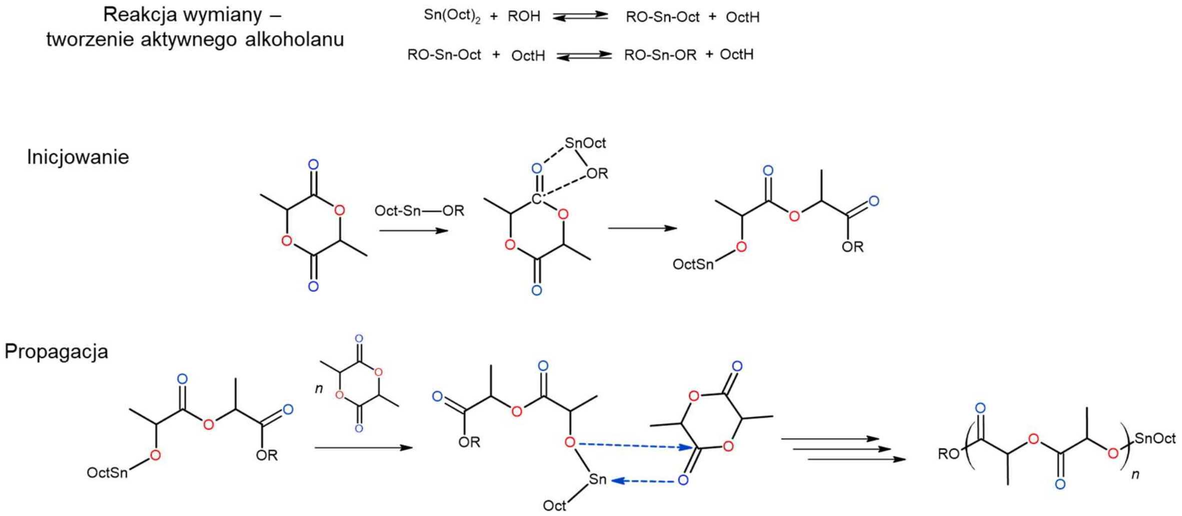

Rys. 2 Schemat mechanizmu polimeryzacji koordynacyjno-insercyjnej LA z zastosowaniem oktanianu cyny jako katalizatora i prowadzonej w obecności alkoholu jako inicjatora

Alternatywą dla polimeryzacji koordynacyjnej laktydu jest polimeryzacja kationowa. W tego rodzaju polimeryzacji monomerów heterocyklicznych jako katalizatory wykorzystywane są mocne kwasy protonowe lub kwasy Lewisa. Kationowa polimeryzacja z otwarciem pierścienia cyklicznych monomerów zawierających atom(y) tlenu zazwyczaj przebiega według mechanizmu Aktywnego Końca Łańcucha (Active Chain End, ACE), w którym centra aktywne odpowiedzialne za propagację stanowią trzeciorzędowe jony oksoniowe znajdujące się na końcu rosnącego łańcucha polimerowego[27]. Jeśli kationowa polimeryzacja cyklicznych eterów, estrów i acetali (w tym laktydu) prowadzona jest w obecności związków zawierających grupy hydroksylowe i silnych kwasów protonowych, wówczas dominującym mechanizmem jest mechanizm Aktywowanego Monomeru (AM)[28,29] (Rys. 3).

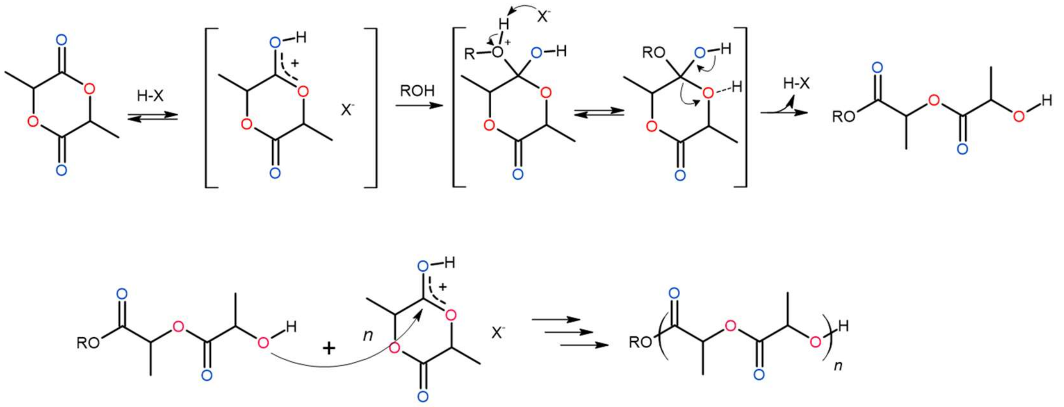

Rys. 3 Schemat wzrostu łańcucha polilaktydowego według mechanizmu Aktywowanego Monomeru[30]

W polimeryzacji według AM, na etapie inicjowania, pierścień aktywowanego poprzez protonowanie monomeru, ulega otwarciu w wyniku ataku nukleofilowego tlenu grupy hydroksylowej inicjatora. Proces wzrostu łańcucha przebiega podobnie, tzn. protonowany monomer, stanowiący naładowane centrum aktywne polimeryzacji reaguje z nienaładowaną grupą hydroksylową rosnącej makrocząsteczki (w wyniku ataku nukleofilowego atomu tlenu grupy hydroksylowej na atom węgla w protonowanym monomerze)[28,31,32]. W omawianym układzie kwas pełni rolę katalizatora, nie jest związany z rosnącym łańcuchem polimeru i może być użyty w niedomiarze w stosunku do jednostek inicjatora. Proces polimeryzacji kationowej według mechanizmu AM przy zachowaniu odpowiednich warunków zachodzi w sposób kontrolowany, nie prowadzi do otrzymania polimerów o bardzo dużych masach molowych, ale umożliwia otrzymanie oligodioli, polioli i makromonomerów do dalszego wykorzystania w syntezie polimerów[30]. Zarówno mechanizmowi koordynacyjno-insercyjnymu jak i kationowemu może towarzyszyć transestryfikacja między- i wewnątrzcząsteczkowa skutkująca szerszym rozkładem masy molowej oraz w przypadku transestryfikacji wewnątrzcząsteczkowej dodatkowo niższym M_n [33].

PLA pomimo swoich zalet, posiada również wady, ponieważ jego T_g mieści się w zakresie 55-65 °C[12], w temperaturze pokojowej jest on materiałem sztywnym i kruchym, posiada słabą stabilność termiczną, charakteryzuje się również słabą krystalicznością, a także niską hydrofilowością. Ogranicza to jego wykorzystanie w biomedycynie oraz w zastosowaniach gdzie wytrzymałość mechaniczna i parametry takie jak: udarność oraz wysokie wydłużenie przy zerwaniu są wymagane (śruby i płytki chirurgiczne)[13]. W celu poprawy owych właściwości, aby rozszerzyć zakres zastosowań PLA, opracowano szereg metod modyfikacji chemicznych oraz fizycznych PLA. Do metod fizycznych możemy zaliczyć plastyfikacje, dodatek wypełniaczy oraz tworzenie kompozytów. Wśród metod chemicznych możemy wyróżnić sieciowanie, wprowadzenie innych ugrupowań chemicznych oraz kopolimeryzację[34].

1.3. Kopolimeryzacja laktydu z monomerami winylowymi

Kopolimeryzacja LA jest uniwersalnym narzędziem, ponieważ pozwala na modyfikację makrocząsteczki już na etapie polimeryzacji, oraz pozwala na otrzymanie wielu interesujących kopolimerów o różnej mikrostrukturze (i taktyczności) oraz topologii (Rys. 4).

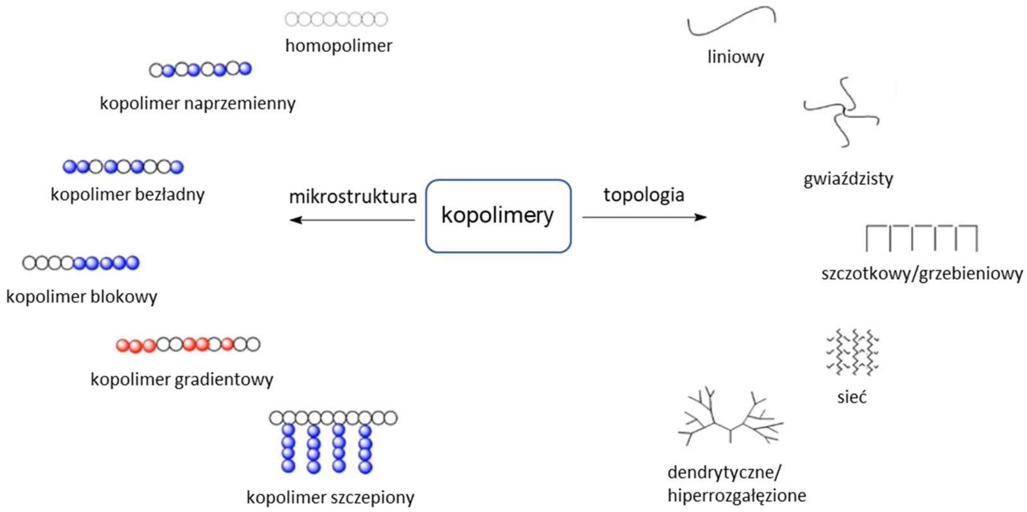

Rys. 4 Podział kopolimerów ze względu na mikrostrukturę i topologię

Spośród różnych typów kopolimerów laktydu możemy wyróżnić grupę kopolimerów blokowych. Według IUPAC kopolimer blokowy składa się z makrocząsteczek, w których sąsiednie bloki różnią się jednostką konstytucyjną, pochodzącą z różnych rodzajów merów, lub z tego samego meru, ale o innym składzie lub rozkładzie sekwencji jednostek konstytucyjnych[35]. Możemy wyróżnić kopolimery diblokowe, triblokowe oraz multiblokowe.

Kopolimeryzacja LA z innymi cyklicznymi estrami, węglanami i eterami (jak: Ɛ-kaprolakton (CL), tlenek etylenu (EO), glikolid (GA), valerolakton (VL), węglan trimetylenu (TMC))[36], w celu poprawy właściwości PLA takich jak hydrofilowość, krystaliczność czy plastyczność jest szeroko opisana w literaturze[36]. Jednakże o ile synteza kopolimerów laktydu z innymi monomerami cyklicznymi jest łatwiejsza do przeprowadzenia (często wobec tego samego katalizatora) o tyle synteza kopolimerów LA z monomerami polimeryzującymi według innego mechanizmu niż ROP jest bardziej wymagająca i skomplikowana.

Istnieją różne metody syntezy kopolimerów blokowych LA z monomerami polimeryzującymi według innego mechanizmu np. z monomerami winylowymi (vinyl monomer, VM). Metody te obejmują wykorzystanie podwójnie działających inicjatorów, modyfikacje grup końcowych PLA grupami inicjującymi polimeryzację drugiego bloku oraz sprzęganie uprzednio otrzymanych łańcuchów polimerowych poprzez wprowadzenie do łańcuchów grup reagujących ze sobą. Jednakże metody te posiadają swoje ograniczenia np. modyfikacja grup końcowych jest procesem często skomplikowanym i wieloetapowym. Polimeryzacja nowego monomeru wymaga wcześniejszego oczyszczenia otrzymanego makroinicjatora i doboru nowego katalizatora. Dlatego prowadzone są badania rozwijające nowe uproszczone metody syntezy kopolimerów blokowych PLA/poli(monomer winylowy).

Kopolimeryzacja laktydu z monomerami winylowymi jest jednym ze sposobów modyfikacji PLA i jego właściwości[37,38,39]. Obecność bloków PVM pozwala na poprawę właściwości PLA takich jak: hydrofilowość[40], stabilność termiczna[39] czy wytrzymałość mechaniczna[39]. Lepsza odporność termiczna oraz właściwości mechaniczne są szczególnie ważne w przypadku zastosowań opakowaniowych[39], produkcji włókien i filamentów PLA do druku 3D oraz produkcji materiałów codziennego użytku[10,39]. Hydrofilowość z kolei jest bardzo ważna z punktu widzenia zastosowań biomedycznych np.: implantów (sztywnych jak i miękkich) i systemów dostarczania leków (w postaci organożeli, membran, ale głównie w postaci nano(mikro)cząstek)[41]. Blokowe kopolimery amfifilowe PLA/PVM wykazują tendencję do samoorganizacji w odpowiednich rozpuszczalnikach i temperaturach pozwalając na otrzymanie zróżnicowanych struktur nano- i mikrocząstek. Jednakże nie tylko amfifilowe kopolimery blokowe ulegają samoorganizacji. Kopolimery składające się z dwóch lub więcej bloków, o różnej naturze chemicznej, ulegają separacji faz w ciele stałym, a ich makrocząsteczki często samoorganizują się tworząc ciekawe morfologie, wykorzystywane m.in.. do otrzymywania materiałów porowatych[37].

1.4. Kontrolowana polimeryzacja rodnikowa z wykorzystaniem inifertera

W celu uzyskania lepszej kontroli nad przebiegiem polimeryzacji rodnikowej opracowano wiele metod kontrolowanej polimeryzacji rodnikowej*, wśród których najczęściej stosowanymi są: ATRP (Atom Transfer Radical Polymerization), RAFT (Reversible Addition-Fragmentation chain-Transfer) czy NMP (Nitroxide-Mediated Polymerization)[42]. Metody te pozwalają na kontrolę nad składem, architekturą i funkcyjnością polimerów. Obecnie

---

*) Obecnie zalecaną przez IUPAC nazwą jest: „polimeryzacja rodnikowa z odwracalną dezaktywacją”.

wykorzystując metody kontrolowanej polimeryzacji rodnikowej możliwe wydaje się przygotowanie różnorodnych skomplikowanych architektur z wykorzystaniem wielu monomerów winylowych, w typowych reakcjach polimeryzacji w roztworze, masie, zawiesinie czy emulsji.

Koncepcją, która wyprzedzała wyżej wymienione rozwinięte metody kontrolowanej polimeryzacji rodnikowej była koncepcja inifertera, którą zaproponował już w 1982r Takayuki Otsu. Według Otsu iniferter to związek chemiczny, który jednocześnie pełni rolę inicjatora (INItiate), przenośnika (transFER) oraz terminatora (TERminate) w kontrolowanej polimeryzacji rodnikowej. W swoich pracach Otsu jako inifertery wykorzystał związki ditiokarbaminianów[43] oraz disulfidów[44] w celu polimeryzacji styrenu i metakrylanu metylu. W badaniach wykazał pewnego rodzaju „żyjący” charakter polimeryzacji rodnikowych, w których masy molowe, choć ich dyspersja była szeroka, rosły liniowo wraz z konwersją, co było ówcześnie nie obserwowane w polimeryzacjach rodnikowych. Polimeryzacja z użyciem inifertera jest procesem kilkuetapowym[45,46]. W pierwszym etapie następuje dysocjacja inifertera, (termiczna, fotochemiczna, a także radiacyjna) z wytworzeniem karborodników. Powstałe karborodniki są bardzo reaktywne i inicjują polimeryzację poprzez reakcję z podwójnym wiązaniem monomeru tworząc makrorodnik. Następnie zachodzi wzrost łańcucha i po addycji określonej liczby jednostek monomerycznych, makrorodnik rekombinuje z drugim makrorodnikiem rosnącego łańcucha, bądź też kolejnym karborodnikiem pochodzącym od inifertera powodując czasową dezaktywację. Kolejne etapy polimeryzacji prowadzonej w obecności inifertera przedstawia Rys. 5.

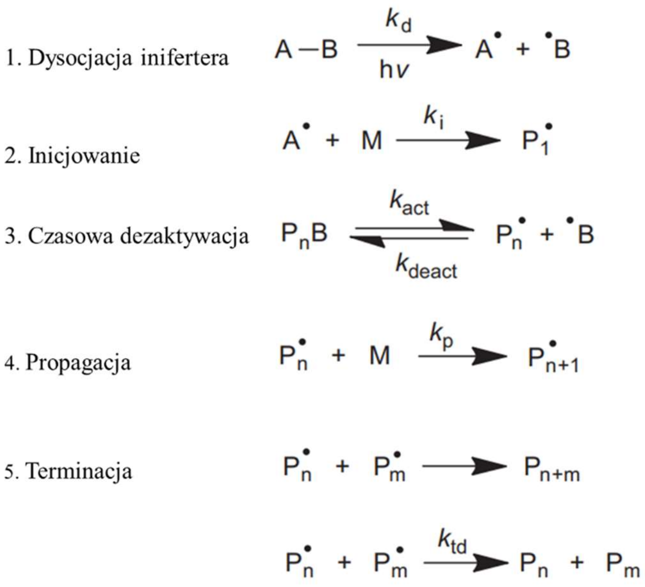

Rys. 5 Schemat polimeryzacji z użyciem inifertera

Polimeryzacja z użyciem inifertera zachodzi w sposób kontrolowany, gdzie aktywny i uśpiony koniec propagującego łańcucha są w stanie odwracalnej równowagi w czasie trwania polimeryzacji. Ponadto musi spełniać inne charakterystyczne cechy wspólne dla metod polimeryzacji kontrolowanych. W trakcie polimeryzacji, konwersja i masa molowa rosną liniowo w czasie. Stała szybkości dysocjacji infertera powinna być znacznie wyższa niż stała szybkości propagacji. Wówczas wszystkie łańcuchy powinny być inicjowane na początku procesu, powinny rosnąć z podobną szybkością i pozostać aktywne do końca polimeryzacji. Na przestrzeni lat zidentyfikowano wiele związków pełniących rolę iniferterów. Otsu podzielił związki stosowane początkowo jako inifertery pod względem budowy na asymetryczne A-B (związki zawierające sulfidy, aminy, alkoksyaminy, tiole) i symetryczne B-B (nadtlenki, disulfidy, tetrafenyloetany). W zależności od czynnika aktywującego polimeryzację wyróżnił fotoinifertery i inifertery termiczne[47].

Równolegle z pracami Otsu pojawiły się także prace Brauna i Bledzkiego, dotyczące procesów polimeryzacji monomerów winylowych inicjowanych nowym typem inicjatora zawierającym ugrupowanie tetrafenyloetanu (TPE)[48,49]. Ugrupowanie TPE na skutek dostarczenia ciepła dysocjuje z wytworzeniem rodników (Rys. 6) zdolnych do inicjowania polimeryzacji monomerów winylowych polimeryzujących według mechanizmu rodnikowego. Zdolność do termicznej dysocjacji wynika z obecności słabego wiązania C-C w przypadku podstawienia atomów węgla czterema pierścieniami fenylowymi którego energia wynosi ~200 kJ·mol^{-1} i jest, dla porównania, znacznie niższa niż energia wiązania C-C w etanie (377 kJ·mol^{-1})[50].

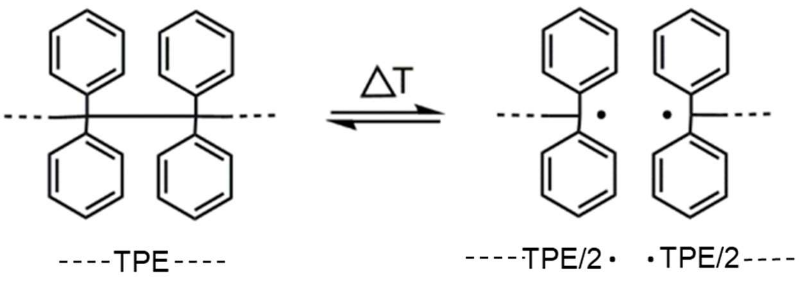

Rys. 6 Odwracalna dysocjacja termiczna ugrupowania TPE

Małocząsteczkowe związki zawierające grupę TPE traktowane były również jako iniferter przez wspomnianego wcześniej Otsu[43,44,51]. Ugrupowanie TPE może zostać wykorzystane jako iniferter nie tylko w postaci małocząsteczkowego związku, ale również poprzez wprowadzenie do łańcucha polimeru, a otrzymane makrocząsteczki polimeru z grupami TPE mogą zostać użyte jako makroiniferter. Istnieje literatura, w której postulowano syntezę poliuretanu zawierającego ugrupowanie TPE[52–55]. Ugrupowanie TPE wprowadzono również do poliuretanów na bazie oligodioli: politetrahydrofuranu, politlenku etylenu, politlenku propylenu, oraz poli(Ɛ-kaprolaktonu). Poliuretany te wykorzystano jako makroinifertery w polimeryzacji styrenu i metakrylanów [56–60].

1.5. Otrzymywanie sieci polilaktydowych

PLA w pobliżu temperatury topnienia (165°C) traci swoją wytrzymałość mechaniczną. Jednym ze sposobów zapobiegania pogorszeniu właściwości fizycznych PLA w podwyższonych temperaturach, jest proces sieciowania. Proces ten nie tylko ogranicza ruchy rotacyjne, ale i swobodę przemieszczania się łańcuchów polimeru względem siebie sprawiając, że polimer staje się nietopliwy. Opracowano wiele metod sieciowania polilaktydu[13,61,62].

Chemiczne sieciowanie może dotyczyć wielkocząsteczkowego polilaktydu, gdzie dodaje się nadtlenki (niekiedy wraz z wielofunkcyjnymi związkami sieciującymi), ale również sieciowanie dotyczy reakcji pomiędzy grupami funkcyjnymi oligomerycznego polilaktydu i związku sprzęgającego. W drugim przypadku reakcjami prowadzącymi do usieciowania w zależności od wprowadzonych grup funkcyjnych mogą być reakcje kondensacji/addycji lub polimeryzacji rodnikowej. Oprócz powyższych metod istnieją przykłady syntezy sieci poprzez kopolimeryzację laktydu z multifunkcyjnym komonomerem. Chemiczne sieciowanie polilaktydu jest najczęściej procesem dwuetapowym. W pierwszej kolejności przygotowany jest reaktywny prepolimer, a następnie reaktywne grupy biorą udział w procesie sieciowania. Tego rodzaju chemiczne sieciowanie wiąże się z wprowadzeniem nowych ugrupowań chemicznych, powodując modyfikację struktury polimeru, co w efekcie daje materiały o zmienionych właściwościach. Modyfikowanie składu chemicznego sieci pozwala również na nadawanie funkcyjności sieciom polimerowym.

Właściwości usieciowanych polimerów zależą od struktury chemicznej i topologii[63]. Na poziomie molekularnym cechy sieci są głównie determinowane przez skład chemiczny. Jednakże takie cechy jak elastyczność, porowatość czy pęcznienie zależą od topologii sieci polimerowej. Za topologię odpowiada gęstość usieciowania, wiszące nieprzereagowane łańcuchy bądź połączenia, splątania i pętle różnych rzędów[63]. Sieci polimerowe tworzą amorficzną lub semikrystaliczną trójwymiarową strukturę z kowalencyjnymi węzłami sieci[64]. Kowalencyjne wiązania nie ulegają łatwo rozerwaniu nawet w wysokich temperaturach i polimer zwykle ulega degradacji przed stopieniem. Polimery usieciowane nie mogą być poddane recyklingowi i powtórnie przetworzone. Aby połączyć wytrzymałość i trwałość polimerów usieciowanych z możliwością powtórnego przetwarzania termoplastów, opracowano dynamiczne polimerowe sieci kowalencyjne. Dynamiczne polimerowe sieci kowalencyjne są to materiały zawierające w swojej strukturze odwracalne wiązania kowalencyjne[65]. Ich odwracalność mogą indukować takie czynniki jak temperatura, katalizator, światło oraz pH. Przy braku wymienionych czynników materiały te zachowują charakter polimerów usieciowanych, natomiast ich struktura może ulec wielokrotnemu przegrupowaniu po aktywacji dynamicznych wiązań. Oprócz możliwości poddania odwracalnych sieci recyklingowi posiadają one również dodatkowe właściwości takie jak: ciągliwość, pamięć kształtu oraz możliwość samonaprawy. W ostatnich dwóch dekadach w dziedzinie dynamicznych sieci kowalencyjnych nastąpił ogromny postęp i opracowano wiele ciekawych usieciowanych struktur wykorzystując bardzo różne ugrupowania o charakterze odwracalnym do ich konstrukcji[66].

2. Cel pracy

Głównym celem przedstawionej pracy było opracowanie nowej metody modyfikacji polilaktydu (PLA) poprzez wprowadzenie do jego łańcucha/struktury ugrupowania tetrafenyloetanu (TPE). W pierwszej części pracy, ugrupowanie TPE posiadające zdolność do termicznej dysocjacji z wytworzeniem rodników, wykorzystano jako iniferter w celu inicjowania polimeryzacji rodnikowej monomerów nienasyconych. Opracowano zatem stosunkowo łatwą i efektywną metodę syntezy kopolimerów PLA z monomerami polimeryzującymi według mechanizmu rodnikowego. W drugiej części pracy, ugrupowanie TPE wykorzystano do syntezy odwracalnych/dynamicznych kowalencyjnych sieci polilaktydowych.

W pracy postawione zostały szczegółowe cele badawcze:

- Opracowanie syntezy pochodnej hydroksybenzofenonu (BP_ET), a następnie pochodnej tetrafenyloetanodiolu (TPE_diET) zawierającej pierwszorzędowe grupy hydroksylowe, oraz badania potwierdzające reaktywność otrzymanego diolu w reakcji z diizocyjanianami.
- Synteza polilaktydu zawierającego jedną grupę TPE w makrocząsteczce poprzez inicjowanie polimeryzacji LA pochodną BP_ET, a następnie sprzęganie otrzymanych łańcuchów PLA w warunkach naświetlania promieniowaniem UV; Otrzymanie kopolimerów triblokowych PLA/poli(monomer winylowy) poprzez wykorzystanie otrzymanego makroinifertera do inicjowania polimeryzacji monomeru winylowego.
- Otrzymanie poliestro-uretanu (PLA_PU) na bazie PLA z wieloma grupami TPE, w wyniku reakcji diolu PLA z pochodną TPE (TPE_diET) z użyciem diizocyjanianu; Wykorzystanie otrzymanego poliestro-uretanu jako makroinifertera do syntezy kopolimerów multiblokowych PLA/poli(monomer winylowy).
- Opracowanie syntezy pochodnej hydroksybenzofenonu zawierającej pierścień epoksydowy (BP_EP); Wykorzystanie BP_EP jako komonomeru w reakcji kopolimeryzacji z LA; Usieciowanie otrzymanego kopolimeru (LA-co-BP_EP) z podwieszonymi grupami benzofenonu, w wyniku naświetlania promieniowaniem UV; Wykazanie odwracalności otrzymanej sieci oraz wykorzystanie jej jako makroinifertera w celu inicjowania polimeryzacji monomerów winylowych, w efekcie wprowadzenie nowych jednostek monomerycznych do struktury sieci.

- Opracowanie syntezy difunkcyjnej pochodnej dihydroksybenzofenonu, zawierającej dwie pierwszorzędowe grupy -OH (BP_diET); Polimeryzacja LA z wykorzystaniem pochodnej BP_diET jako inicjatora; Sprzęganie otrzymanych łańcuchów PLA do gwiazd zawierających ugrupowanie TPE w rdzeniu; Synteza sieci polimerowych poprzez sprzęganie gwiaździstych PLA z użyciem diizocyjanianu; Charakterystyka i badanie dynamicznego charakteru sieci.

Ponadto przygotowano i opublikowano pracę przeglądową tematycznie ściśle związaną z badaniami prowadzonymi w ramach pracy doktorskiej, w której omówiono szerokie wykorzystanie kopolimerów blokowych PLA/PVM głównie do zastosowań w biomedycynie, ale też w typowych zastosowaniach technologicznych.

3. Badania własne

3.1. Badania reaktywności tetrafenyloetano-1,2-diolu (TPED)

Zrealizowanie celu zawartego w temacie pracy doktorskiej wymagało wprowadzenia do łańcucha polilaktydu grup TPE zdolnych do termicznej dysocjacji. Ich zdolność do termicznej dysocjacji z wytworzeniem rodników mogłaby następnie posłużyć do różnych modyfikacji PLA. Spośród możliwych sposobów wprowadzenia wytypowane zostały dwa najprostsze mianowicie, zastosowanie tetrafenyloetano-1,2-diolu (handlowego produktu znanego również jako benzopinakol, TPED) jako małocząsteczkowego diolu do sprzęgania z diolem PLA z użyciem diizocyjanianu oraz zastosowanie TPED jako inicjatora polimeryzacji laktydu. Pierwszy ze sposobów zdawał się być racjonalny ponieważ istniała spora literatura, w której opisywano syntezę poliuretanów z zastosowaniem TPED oraz dioli poli(tetrahydrofuranu), poli(tlenku etylenu), poli(tlenku propylenu) oraz poli(Ɛ-kaprolaktonu)[52–55,57]. Wstępne syntezy mające na celu sprzęgnięcie diolu TPED z diolem PLA z użyciem diizocyjanianu pokazały, że w wyniku polimeryzacji w rozpuszczalniku nie można tą drogą wprowadzić grup TPE do łańcucha polimeru. Prawdopodobną przyczyną była zbyt mała reaktywność trzeciorzędowych grup -OH cząsteczki TPED, które według doniesień literaturowych, są o dwa rzędy wielkości mniej reaktywne w porównaniu z grupami pierwszorzędowymi, a reaktywność ta może być jeszcze mniejsza w przypadku dużej zawady sterycznej w postaci pierścieni fenylowych[67].

Celem potwierdzenia braku reaktywności diolu TPED przeprowadzono badania kinetyczne reakcji sprzęgania tego diolu z oligodiolami dwóch różnych polimerów tzn. PLA oraz PTHF (politetrahydrofuran) za pomocą dwóch różnych diizocyjanianów, tzn. alifatycznego heksametyleno diizocyjanianu (HDI) oraz aromatycznego diizocyjanianu difenylometanu (MDI). Badania wykonano za pomocą metody spektroskopii FTIR (Fourier Transform Infrared Spectroscopy), która na podstawie analizy intensywności pasma charakterystycznego dla grupy izocyjanianowej pozwoliła na wyznaczenie konwersji tych grup. Reakcję prowadzono dwuetapowo: w pierwszym etapie dodawano dwukrotny nadmiar diizocyjanianu do diolu PLA lub THF, a gdy połowa grup -NCO przereagowała dodawano TPED. Po wprowadzeniu do mieszaniny reakcyjnej TPED nie obserwowano dalszej konwersji grup -NCO. Na brak konwersji grup -NCO wskazywały również badania kinetyczne reakcji samego TPED z diizocyjanianami. Wykonana analiza produktów reakcji oligodioli PLA oraz PTHF z diizocyjanianami, z wykorzystaniem spektroskopii FTIR oraz ^{1}H NMR wskazała na obecność wiązań uretanowych, nie obserwowano ich natomiast w przypadku użycia samego TPED.

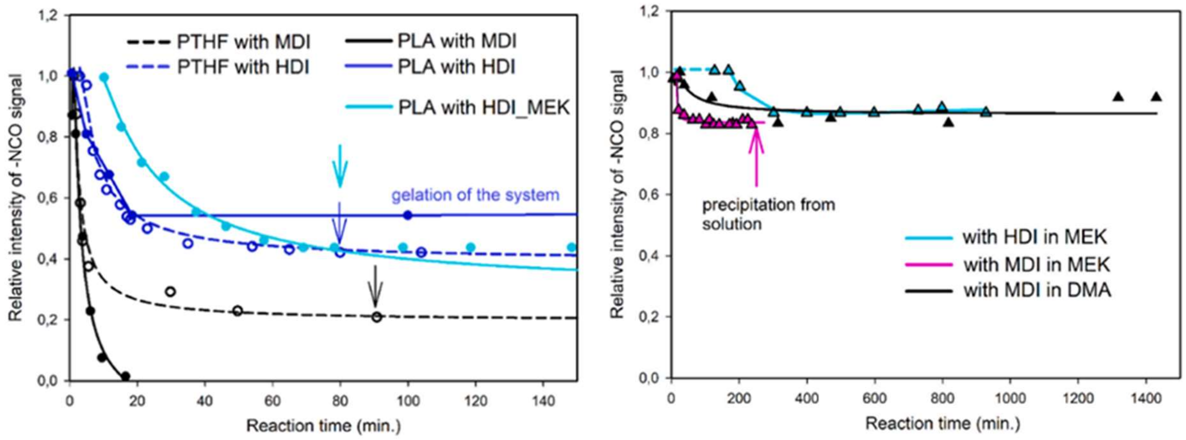

Rys. 7 Konwersja grup izocyjanianowych w czasie dla reakcji dioli PTHF oraz PLA z diizocyjanianami i TPED (a), reakcji samego TPED z diizocyjanianami (b). Strzałki oznaczają moment dodania TPED do układu

Brak reaktywności grup -OH związanych z TPED w reakcji z izocyjanianami w zastosowanych warunkach potwierdzono w wyniku badań z wykorzystaniem modelowania molekularnego. Badania te wykazały, że czynniki konformacyjne i steryczne uniemożliwiają utworzenie aktywnego kompleksu z katalizatorem, zaś czynniki elektronowe ograniczają znacznie nukleofilowość grup -OH.

Zarówno wyniki badań kinetycznych jak i obliczeniowych potwierdziły brak reaktywności diolu TPED, a zatem brak możliwości wprowadzenia go do łańcucha PLA poprzez sprzęganie TPED z oligomerycznym diolem z użyciem diizocyjanianów prowadzone w rozpuszczalniku. (Wyniki badań reaktywności wraz z ich szeroką dyskusją przedstawiono w *publikacji 1*).

Niezależnie zbadano możliwość wykorzystania TPED jako inicjatora polimeryzacji LA. Ten sposób wprowadzenia grupy TPE do łańcucha polimerowego okazał się również nieskuteczny ze względu na niską reaktywność grup -OH oraz reakcje uboczne zachodzące w obecności katalizatora (przegrupowanie pinakolowe w środowisku kwaśnym[59] lub rozpad w środowisku zasadowym[68,69]).

W związku z powyższymi wynikami podjęto dalsze prace mające na celu opracowanie alternatywnych metod wprowadzenia grup TPE, poprzez syntezę pochodnych TPE z reaktywnymi grupami -OH, co dokładniej zostanie przedstawione w kolejnym rozdziale.

3.2. Synteza związków niezbędnych do wprowadzenia grup tetrafenyloetanu (TPE) do łańcucha PLA

W celu otrzymania pochodnych będących prekursorami grup TPE charakteryzujących się wysoką reaktywnością jako substrat wyjściowy postanowiono wykorzystać 4-hydroksybenzofenon (HBP), zawierający aromatyczną grupę -OH. HBP przeprowadzono w pochodną zawierającą pierwszorzędową grupę -OH (BP_ET) w wyniku reakcji syntezy eterów Williamsona (Rys. 8) (szczegółowy opis syntezy oraz analiz został przedstawiony w *Publikacji 1 i 2*).

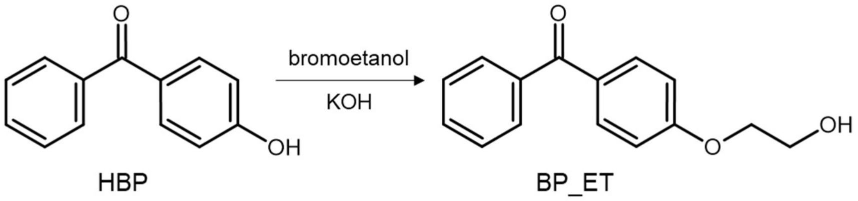

Rys. 8 Schemat syntezy pochodnej BP_ET

Analogicznie, 4,4-dihydroksybenzofenon (diHBP) zawierający w swojej strukturze dwie aromatyczne grupy -OH przeprowadzono w pochodną z dwiema pierwszorzędowymi grupami -OH (BP_diET) (Rys. 9) (szczegółowy opis syntezy oraz wykonanych analiz przedstawiony jest w *Publikacji 5*).

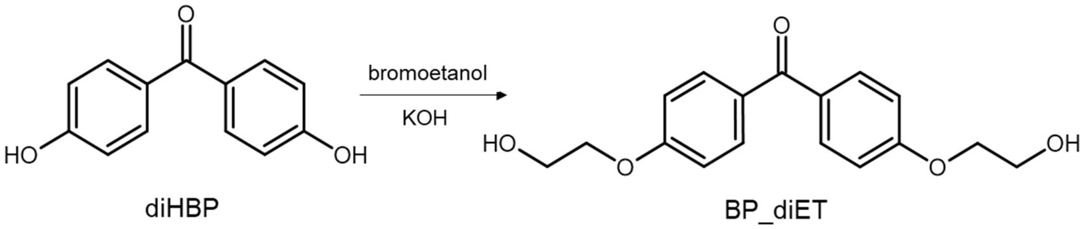

Rys. 9 Schemat syntezy pochodnej BP_diET

Następnie z wykorzystaniem tego samego mechanizmu reakcji zsyntezowano również pochodną HBP zawierającą pierścień epoksydowy (BP_EP), wychodząc z HBP i epichlorohydryny (ECH) (Rys. 10) (szczegółowy opis syntezy oraz wykonanych analiz przedstawiono w *Publikacji 4*).

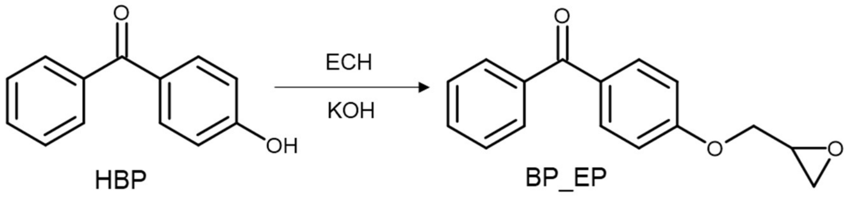

Rys. 10 Schemat syntezy pochodnej BP_EP

Struktura każdego z produktów została potwierdzona z wykorzystaniem spektroskopii NMR i GC-MS. Wykorzystując reakcję sprzęgania pinakolowego[70] (przebiegającego w obecności donora atomów wodoru) otrzymane związki użyto następnie do wprowadzenia w różny sposób grup TPE do łańcucha PLA, o czym będzie mowa w kolejnych rozdziałach. Grupy BP poddane sprzęganiu były umiejscowione bądź to w małocząsteczkowej pochodnej BP_ET, prowadząc do otrzymania pochodnej TPE_diET (Rys. 12), bądź też związane z łańcuchem polimerowym (Rys. 11) (Szczegółowy opis reakcji sprzęgania oraz zbiór analiz znajdują się w *publikacjach 1, 2, 3, 4 i 5*).

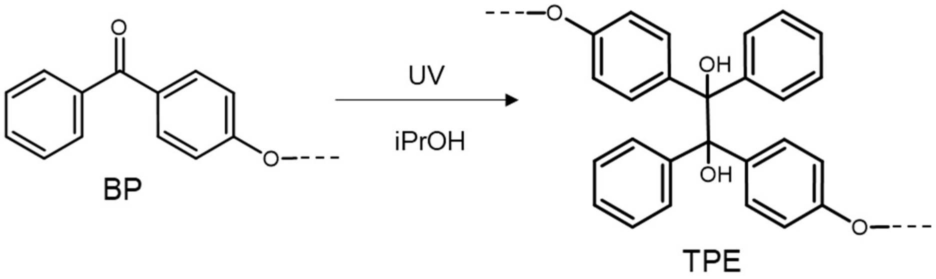

Rys. 11 Schemat sprzęgania pinakolowego pochodnej BP do TPE

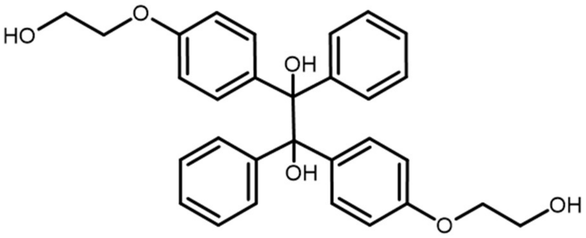

Rys. 12 Pochodna TPE_diET

3.3. Wykorzystanie grup TPE wprowadzonych do łańcucha PLA do syntezy kopolimerów blokowych

3.3.1. Synteza kopolimerów triblokowych PLA/PAN

Do otrzymania kopolimerów triblokowych użyto polilaktydów o różnych masach molowych, zawierających jedno ugrupowanie TPE.

Początkowo w celu otrzymania wspomnianych polilaktydów, rozważano użycie zsyntezowanego według schematu na Rys. 12 TPE-diET z dwiema pierwszorzędowymi grupami -OH, do inicjowania polimeryzacji laktydu. Jednakże zawiera on w swojej strukturze cały fragment TPED, zatem może również ulegać reakcjom ubocznym[68,69] i rozpadowi w środowisku kwaśnym bądź zasadowym[60]. Dlatego też opracowano metodę, w której punktem wyjścia było inicjowanie kationowej polimeryzacji laktydu przez pochodną benzofenonu BP_ET zawierającą pierwszorzędową grupę hydroksylową, opisaną w rozdziale 3.2. Pozwoliło to na otrzymanie szeregu polilaktydów z dobrą kontrolą masy molowej. Otrzymane łańcuchy PLA zakończone jedną grupą BP, w następnej kolejności sprzęgnięto, z wykorzystaniem reakcji sprzęgania pinakolowego grup BP pod wpływem promieniowania UV. W wyniku reakcji sprzęgania otrzymano łańcuchy PLA z jedną grupą TPE w środku (TPE_diET_PLA) (Rys 13). Struktura otrzymanych polimerów została potwierdzona za pomocą spektroskopii ^{1}H NMR (szczegółowy opis reakcji i zbiór analiz przedstawiono w *publikacji 2*).

Rys. 13 Schemat syntezy PLA z jednym ugrupowaniem TPE w środku

Analiza otrzymanych widm ^{1}H NMR, gdzie obserwowano charakterystyczne sygnały pochodzące od utworzonego ugrupowania TPE, w korelacji z dwukrotnym wzrostem masy molowej wyznaczonej metodą SEC pozwoliła na potwierdzenie sprzęgnięcia ugrupowań BP do TPE.

W dalszej części pracy otrzymane polilaktydy z wbudowanym ugrupowaniem TPE, o różnych masach molowych wykorzystano jako makroinifertery, w celu wprowadzenia jednostek monomeru winylowego do struktury polimeru. Do reakcji kopolimeryzacji wybrany został akrylonitryl jako modelowy monomer winylowy, ponieważ nie polimeryzuje on termicznie w zastosowanej temp. 85°C oraz terminacja polimeryzacji zachodzi poprzez rekombinację w określonych warunkach[71], co było kluczowym warunkiem do otrzymania kopolimerów triblokowych. W wyniku reakcji otrzymano kopolimery triblokowe PLA-PAN-PLA (Rys. 14), których struktury zostały potwierdzone z zastosowaniem spektroskopii NMR (^{1}H NMR, ^{13}C NMR) oraz SEC (opisy reakcji kopolimeryzacji wraz z widmami znajdują się w *publikacji 2*).

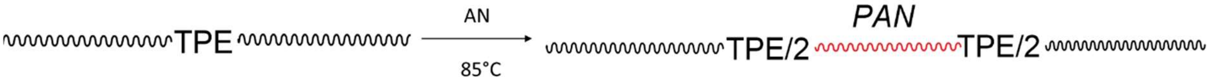

Rys. 14 Schemat reakcji otrzymywania kopolimerów triblokowych PLA-PAN-PLA

Zastosowana metoda pozwoliła na osiągnięcie konwersji AN na poziomie 62-73% w ciągu 24h (Tabela 1). Wykazano również, że skład kopolimerów może być regulowany poprzez zmianę stosunku AN w stosunku do PLA (co wpływa na ilość wbudowanych jednostek AN), a także poprzez zmianę masy cząsteczkowej PLA zawierającego ugrupowanie TPE.

Tabela 1. Polimeryzacja akrylonitrylu z wykorzystaniem makroinifertera w temp. 85°C w czasie 24h

TPE_diET_ PLA	Stosunek molowy AN/LA w m.r. (wag.)	Konwersja AN [%] (24h)	Kopolimery PLA-PAN-PLA	
M_n			AN/LA (stos. mol)	M_n ^{1}H NMR (SEC)
1400	4.2 (1)	73	11.1	5130 (4250)
2200	1.7 (0.5)	65	2.5	5760 (4580)
	3.2 (1)	69	3.45	5670 (4780)
	7.0 (2)	71	9.9	9370 (8500)
3300	3.5 (1)	62	2.3	6070 (5850)

m.r. – mieszanina reakcyjna

W wyniku analizy ^{13}C NMR potwierdzono mechanizm polimeryzacji z zastosowaniem ugrupowania TPE jako inifertera, polegający na inicjowaniu polimeryzacji rodnikiem powstałym w wyniku rozpadu grupy TPE poprzez addycję do podwójnego wiązania monomeru winylowego, a nie poprzez przeniesienie rodnika od inicjatora do monomeru jak postulował w swoich pracach Braun[48]. Powyższe wyniki wraz z porównaniem oznaczonych mas molowych kopolimerów z teoretycznymi potwierdziły otrzymanie kopolimeru triblokowego PLA-PAN-PLA. Opracowana metoda może zostać wykorzystana nie tylko do syntezy kopolimerów z AN, ale również z innymi monomerami winylowymi.

3.3.2. Synteza kopolimerów multiblokowych PLA/PVM

Do syntezy kopolimerów multiblokowych laktydu i monomerów winylowych wyjściowym polimerem był polilaktyd zawierający wiele grup TPE.

W celu otrzymania tak zaprojektowanego polilaktydu niezbędne było opracowanie metody wprowadzenia wielu ugrupowań TPE do łańcucha PLA. Opracowano dwuetapową reakcję syntezy poliestro-uretanu (Rys. 15). Do syntezy wykorzystano pochodną TPE zawierającą pierwszorzędowe grupy -OH (TPE_diET) przedstawioną w rozdziale 3.2. W pierwszym etapie przeprowadzono reakcję oligodiolu PLA z diizocyjanianem, następnie do układu wprowadzono pochodną TPE_diET. Stopień przereagowania grup funkcyjnych kontrolowano za pomocą spektroskopii ^{1}H NMR. Otrzymany poliestro-uretan PLA-PU oczyszczono i scharakteryzowano za pomocą spektroskopii ^{1}H NMR oraz FTIR. Analiza widm ^{1}H NMR wskazała na obecność charakterystycznych sygnałów pochodzących od utworzonych wiązań uretanowych oraz przesunięcia sygnałów odpowiadającym grupom końcowymi PLA oraz etylenowym TPE_diET. Jednocześnie dokładne przypisanie sygnałów w widmach FTIR również umożliwiło potwierdzenie pojawienia się charakterystycznych drgań odpowiadających powstaniu wiązań uretanowych. Wyniki analiz pozwoliły potwierdzić chemiczne związanie grupy TPE z łańcuchem polimeru. Otrzymany polimer o M_n ~37000 (SEC) charakteryzował się monomodalnym rozkładem mas molowych (opis syntezy oraz szczegółowe analizy widm znajdują się w *publikacji 3)*. W przypadku otrzymanego poliestro-uretanu, przed przystąpieniem do wykorzystania go jako makroinifertera do inicjowania polimeryzacji monomerów winylowych, postanowiono sprawdzić zdolność wbudowanego TPE do rozpadu na rodniki.

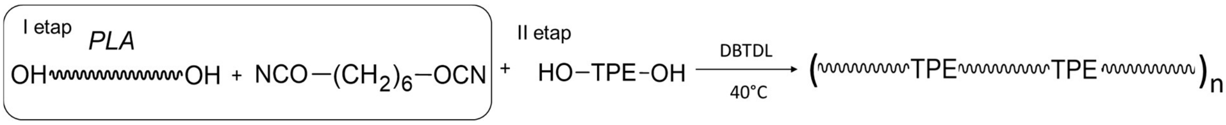

Rys. 15 Schemat syntezy PLA_PU

Ugrupowanie TPE znane jest ze zdolności do termicznej dysocjacji z wytworzeniem rodników, które są w stanie inicjować polimeryzację monomerów nienasyconych, co wykazano w szeregu prac[52–55,57] w tym w *publikacji 2*. W celu potwierdzenia zdolności ugrupowania TPE znajdującego się w poliestro-uretanie PLA-PU do rozpadu z wytworzeniem rodników, wykonano analizę metodą spektroskopii elektronowego rezonansu paramagnetycznego (EPR). Spektroskopia EPR pozwala na badanie próbek posiadających niesparowane elektrony. Spektrometry EPR rejestrują widmo substancji paramagnetycznej w postaci krzywej absorpcji, dokładna analiza kształtu krzywych pozwala na identyfikację rodników[72]. Pomiar wykonany dla próbki PLA-PU w obecności sondy spinowej TEMPO (2,2,6,6-tetrametylo-1-oksopiperydyny), wykazał malejące stężenie rodników TEMPO na skutek ich reakcji z coraz większą ilością powstających rodników …-TPE/2• (Rys. 16a). W ten sposób potwierdzono rosnący rozpad TPE z wytworzeniem rodników w funkcji rosnącej temperatury (Rys. 16b). Jednocześnie wyznaczono optymalną temperaturę prowadzenia polimeryzacji monomeru winylowego (tzn. temp. nasycenia powstawania rodników) na 85 °C. (opisy przeprowadzonych pomiarów wraz ze szczegółową dyskusją wyników znajdują się w *publikacji 3*).

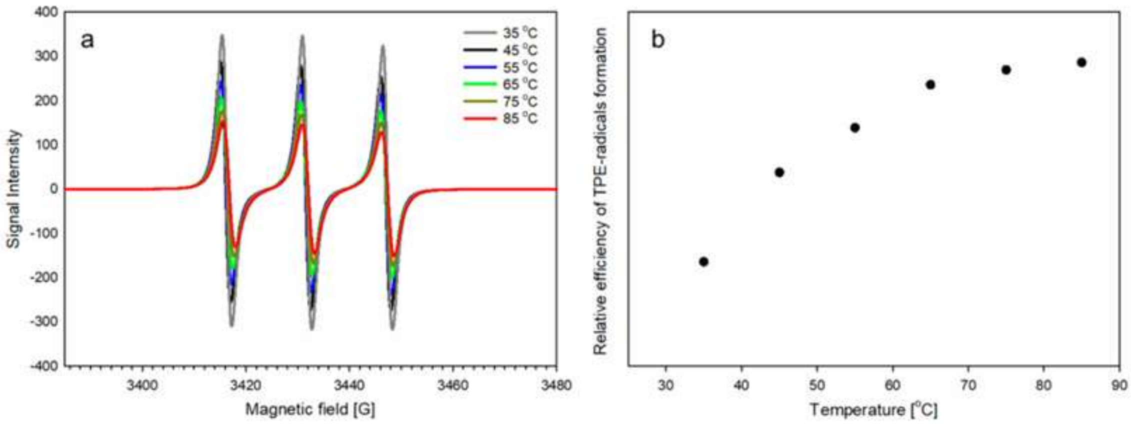

Rys. 16 (a) Widmo EPR PLA-PU/TEMPO zarejestrowane w różnych temperaturach w obecności TEMPO; (b) Postęp rozpadu grup TPE wbudowanych do struktury polimeru PLA-PU wraz z rosnącą temperaturą

W kolejnym etapie badań otrzymany poliestro-uretan zawierający wiele grup TPE w łańcuchu polimerowym, wykorzystano jako makroiniferter w celu inicjowania polimeryzacji styrenu (ST) i akrylonitrylu (AN). Ponownie, monomery te zostały wybrane ze względu na dominujący mechanizm terminacji poprzez rekombinację [71,73] (Rys. 17).

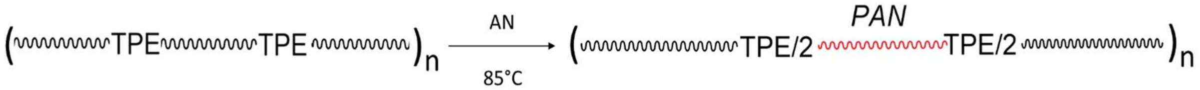

Rys. 17 Schemat syntezy kopolimerów multiblokowych PLA/PAN

Wyniki kopolimeryzacji podsumowuje Tabela 2. Kopolimeryzację przeprowadzono z zastosowaniem takiego samego stosunku masowego monomeru winylowego do PLA-PU, z zastosowaniem rozpuszczalników o różnej polarności.

Tabela 2. Polimeryzacja VM z wykorzystaniem makroinifertera PLA-PU (M_n PLA-PU ~37000, SEC) w temp. 85 °C w czasie 24h

Substraty			Konwersja VM [%]	Kopolimery PLA/PVM	
Monomer winylowy VM	Stosunek mol. VM/LA w m.r.	Rozpuszczalnik		VM/LA, ^{1}H NMR	$M_{n,}$ SEC
AN	4.8	DMF	85	7.0	b.d.
	4.8	Anizol	70	3.8	16600
ST	2.5	DMF	37	0.4	b.d.
	2.5	DMF	45 (95 °C)	1.2	13000
	2.5	Anizol	33	0.5	11600

m.r. – mieszanina reakcyjna b.d. – brak danych

Analiza otrzymanych kopolimerów PLA/PAN oraz PLA/PST z wykorzystaniem spektroskopii ^{1}H NMR, pozwoliła na określenie konwersji monomerów winylowych oraz stosunku monomeru winylowego do laktydu w strukturze kopolimeru. Zastosowana metoda makroinifertera skutkowała uzyskaniem stosunkowo wysokiej konwersji AN w obu rozpuszczalnikach, wynoszącej 70-85%, ale względnie niskiej konwersji ST na poziomie 33-45%. Wyniki analizy SEC wskazały na monomodalny, ale szeroki rozkład mas molowych otrzymanych produktów, co w połączeniu z analizą widm ^{1}H NMR potwierdziło powstanie kopolimerów. Dodatkowe potwierdzenie uzyskano w wyniku zastosowania spektroskopii DOSY NMR. Widma dyfuzyjne DOSY (Diffusion Ordered Spectroscopy) pozwalają na rozseparowanie wszystkich widm ^{1}H NMR poszczególnych składników mieszanin na podstawie wartości współczynników dyfuzji. Jako że współczynniki dyfuzji są związane z objętością hydrodynamiczną cząsteczki, metoda ta jest bardzo przydatna w pomiarze mas molowych polimerów, kinetyce polimeryzacji oraz analizie kopolimerów[74]. Na podstawie wyznaczonych współczynników dyfuzji możliwe było potwierdzenie otrzymania kopolimerów blokowych oraz kowalencyjne związanie wszystkich elementów budulcowych kopolimerów. Zbadany został również wpływ wprowadzonych bloków PVM na właściwości termiczne otrzymanych kopolimerów. Do wyznaczenia temperatury zeszklenia otrzymanych kopolimerów zastosowano metodę DSC (różnicowej kalorymetrii skaningowej). Pomiar wskazał na jedną temperaturę zeszklenia kopolimerów i brak separacji faz. Jednocześnie warto zaobserwować, że wprowadzenie bloków PVM skutkowało wzrostem T_g kopolimeru w porównaniu z wyjściowym poliestro-uretanem. Wyniki badań przedstawione w pracy wskazały na łatwość i efektywność zastosowanej metody syntezy kopolimerów multiblokowych PLA/PVM z wykorzystaniem inifertera. (szczegółowy opis reakcji kopolimeryzacji, widma ^{1}H NMR, SEC, DOSY i termogramy wraz z ich szczegółową analizą znajdują się w *publikacji 3*).

3.4. Synteza sieci PLA zawierających termicznie odwracalne wiązania TPE i ich dynamiczny charakter

Jedną z metod modyfikacji polilaktydu jest otrzymanie polimeru usieciowanego. Proces ten prowadzi do poprawy właściwości termicznych i mechanicznych polilaktydu. Jednakże wytworzenie usieciowanych materiałów polimerowych uniemożliwia ich dalsze przetwarzanie. W celu połączenia zalet kowalencyjnych sieci polimerowych z zaletami termoplastów, w niniejszej pracy zsyntezowano sieci polilaktydowe zawierające odwracalne wiązania kowalencyjne w swojej strukturze.

3.4.1. Sieci polimerowe otrzymane na bazie kopolimeru laktydu z epoksydem BP_EP

Jednym ze sposobów otrzymania sieci polimerowych jest sprzęganie liniowych łańcuchów polimerowych na skutek reakcji pomiędzy reaktywnymi grupami bocznymi. W niniejszej pracy postanowiono wprowadzić boczne grupy benzofenonu (BP) do łańcuchów polimeru opartego na polilaktydzie, aby w wyniku ich sprzęgania otrzymać polimer usieciowany i jednocześnie wygenerować grupy TPE w jego strukturze.

Grupy BP wprowadzono poprzez kopolimeryzację LA ze sfunkcjonalizowanym monomerem epoksydowym BP_EP (opisanym w rozdziale 3.2). W wyniku reakcji otrzymano kopolimer LA-co-BP_EP (Rys. 18) z bocznymi grupami BP, którego strukturę scharakteryzowano za pomocą metod SEC, MALDI TOF oraz spektroskopii ^{1}H i ^{13}C NMR.

Rys. 18 Schemat syntezy kopolimeru LA-co-BP_EP

Szczegółowa analiza wyników (opisana w *publikacji 4*, wraz z zamieszczonymi widmami) wskazała na średnią ilość grup BP w jednej makrocząsteczce wynoszącą 3 jednostki. W celu zwiększenia liczby grup BP, łańcuch kopolimeru przedłużono poprzez sprzęganie z użyciem diizocyjanianu. W efekcie wraz z trzykrotnym wzrostem masy cząsteczkowej, liczba grup BP w jednej makrocząsteczce wzrosła do 9. Tak otrzymany kopolimer LA-co-BP_EP/HDI usieciowano w wyniku reakcji sprzęgania pinakolowego podwieszonych grup BP, w warunkach naświetlania promieniowaniem UV (przebiegającego w obecności donora atomów wodoru). W efekcie otrzymano sieć PLA-TPE_EP, zawierającą odwracalne grupy TPE w węzłach sieci. Analiza sygnałów widm FITR otrzymanej sieci pozwoliła na potwierdzenie sprzęgnięcia grup BP do grup TPE. Otrzymana sieć polimerowa charakteryzowała się wysoką zawartością żelu >95%. Wyniki badań przeprowadzonych w statycznych próbach jednoosiowego rozciągania próbek sieci wykazały wytrzymałość na rozciąganie równą 16 MPa oraz wydłużenie przy zerwaniu porównywalne do komercyjnego PLA (widma ^{1}H NMR, SEC kopolimeru LA-co-BP_EP/HDI, a także widma FTIR, termogramy oraz wyniki badań wytrzymałościowych otrzymanych sieci wraz z dyskusją wyników znajdują się w *publikacji 4*).

3.4.1.1. Badania reologiczne - wykazanie odwracalnego charakteru sieci PLA-TPE_EP

Wprowadzenie do struktury sieci ugrupowań TPE zawierających wiązania zdolne do odwracalnej termicznej dysocjacji powinno skutkować otrzymaniem odwracalnej/dynamicznej sieci polimerowej opartej na PLA. W celu wykazania odwracalnego charakteru sieci polimerowej wykonano badania reologiczne. Pomiar z wykorzystaniem reometrii oscylacyjnej pozwolił na określenie zachowania materiału pod wpływem przyłożonej siły oscylacyjnej w temperaturze zapewniającej zaawansowaną dysocjację grup TPE (120 °C). Jak wykazały badania, próbka poddana w pierwszym etapie dużemu odkształceniu, po zredukowaniu odkształcenia do bardzo małej wartości, całkowicie relaksowała w krótkim czasie.

Ponadto w celu potwierdzenia zdolności sieci do odzyskania właściwości mechanicznych wykonano eksperyment, polegający na poddaniu próbki filmu sieci naprzemiennym dużym i małym odkształceniom w stałej temp. 120 °C, podczas których rejestrowano reakcję materiału na naprężenie oscylacyjne. Wyniki pomiarów (Rys. 19) pokazały jak moduły: zachowawczy (G') i stratności (G") wracają do swoich pierwotnych wartości przy kilku kolejnych odkształceniach. Widać, że przy każdym dużym odkształceniu wartości modułów spadają, jednocześnie moduł stratności przewyższa moduł zachowawczy. Oznacza to, że w wyższej temperaturze, w której odwracalna dysocjacja termiczna grup TPE jest zaawansowana, przy dużych odkształceniach przeważają właściwości plastyczne, a przy małych właściwości sprężyste badanej próbki sieci PLA-TPE_EP (warunki przeprowadzonych pomiarów i szczegółowe wyniki wraz z dyskusją znajdują się w *publikacji 4*).

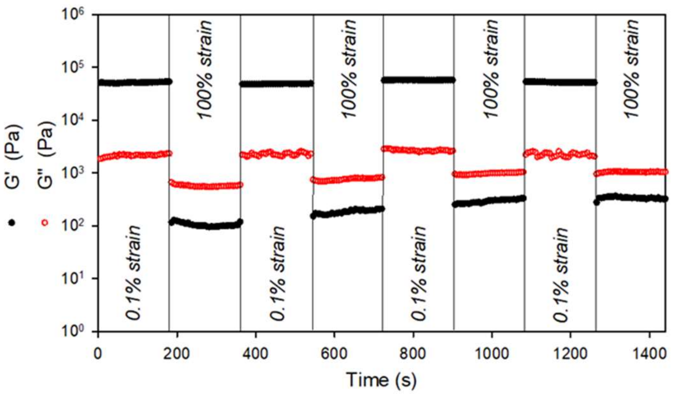

Rys. 19 Zależność modułu stratności i modułu zachowawczego sieci PLA-TPE_EP poddanej naprzemiennie małym i dużym odkształceniom. Pomiar prowadzony w 120 °C

Otrzymane wyniki są potwierdzeniem tezy, że sieć PLA-TPE_EP jest w stanie w pełni odzyskać swoje właściwości mechaniczne dzięki wymianie między grupami TPE na skutek ich termicznej dysocjacji.

3.4.1.2. Wprowadzenie nowych jednostek monomerycznych do struktury sieci PLA-TPE_EP

Gdy grupy inicjujące polimeryzację są wbudowane do struktury sieci polimerowej, pozwala to na łatwą modyfikację sieci po etapie syntezy, zmieniając niekiedy diametralnie jej właściwości. W literaturze istnieje niewiele przykładów zastosowania inifertera w celu modyfikacji sieci polimerowych, jednym z nich może być wykorzystanie tritiowęglanu jako fotoinifertera w celu wprowadzenia bloków poli(N-izopropyloakryloamidu) do struktury żeli opartych na poli(tlenku etylenu)[75].

W prezentowanej pracy już wcześniej udowodniono efektywność ugrupowania TPE w inicjowaniu polimeryzacji VM (rozdział 3.3), dlatego też postanowiono wykorzystać zdolność do odwracalnej termicznej dysocjacji grup TPE z wytworzeniem rodników w celu wprowadzenia jednostek monomeru winylowego do struktury otrzymanej sieci PLA-TPE_EP. Polimeryzację przeprowadzono poprzez ogrzewanie próbki sieci w temp. 85 °C w roztworze akrylonitrylu. W wyniku reakcji otrzymano sieć PLA-TPE_EP/PAN z wbudowanymi jednostkami AN, o stosunku jednostek AN/LA wynoszącym ~20. Zastosowanie metod spektroskopowych ^{13}C NMR w ciele stałym oraz FTIR pozwoliło na potwierdzenie obecności bloków PAN w strukturze sieci. W celu zbadania wpływu wprowadzenia jednostek AN do struktury sieci na jej odporność termiczną wykonano pomiar metodą TGA (termograwimetryczną). Analiza otrzymanych termogramów wskazała na rozkład sieci z wbudowanymi blokami PAN w znacznie wyższych temperaturach w porównaniu do wyjściowej sieci PLA-TPE_EP. Za zwiększenie odporności termicznej niewątpliwie odpowiadają wprowadzone bloki PAN. W celu zbadania właściwości mechanicznych otrzymanych sieci zawierających bloki PAN, wykonano badanie twardości i modułu elastyczności metodą nanoindentacji. Jak pokazały wyniki, twardość próbki i moduł rosną wraz z ilością wprowadzonych jednostek AN. Powyższe wyniki wykazały prostotę i skuteczność zastosowanej metody modyfikacji nierozpuszczalnej sieci polimerowej poprzez wykorzystanie koncepcji inifertera (szczegółowy opis reakcji kopolimeryzacji wraz z wynikami analiz i ich szczegółową dyskusją znajdują się w *publikacji 4*).

3.4.2. Sieci polimerowe otrzymane na bazie gwiaździstych PLA zawierających grupy TPE w rdzeniu

W ramach prowadzonych badań otrzymano również sieci polilaktydowe zawierające w swojej strukturze odwracalne wiązania kowalencyjne (grupy TPE), poprzez sprzęganie gwiaździstych PLA zawierających grupy TPE w rdzeniu, za pomocą diizocyjanianu.

W pierwszym etapie pracy w wyniku reakcji polimeryzacji LA inicjowanej pochodną BP_diET (opisaną w rozdziale 3.2) otrzymano telecheliczne polilaktydy o różnych masach molowych, tzn. ok. 3000 (TPE-PLA3), oraz ok. 6000 (TPE-PLA6). W kolejnym kroku tak otrzymane liniowe makrocząsteczki z grupą BP w środku sprzęgnięto, pod wpływem naświetlania UV (w obecności donora atomów wodoru), do gwiaździstych polilaktydów zawierających ugrupowanie TPE w rdzeniu (Rys. 20). Dodatkowo zsyntezowano referencyjną sieć na bazie gwiaździstego PLA zawierającą rdzeń bez grup TPE (PLAref2.5), w celu wykorzystania jej do badań porównawczych. Masy molowe otrzymanych liniowych i gwiaździstych PLA (po sprzęgnięciu) zostały oznaczone metodami ^{1}H NMR oraz SEC i zestawione w Tabeli 3 (Szczegółowy opis syntez oraz wykonanych analiz został przedstawiony w *publikacji 5*).

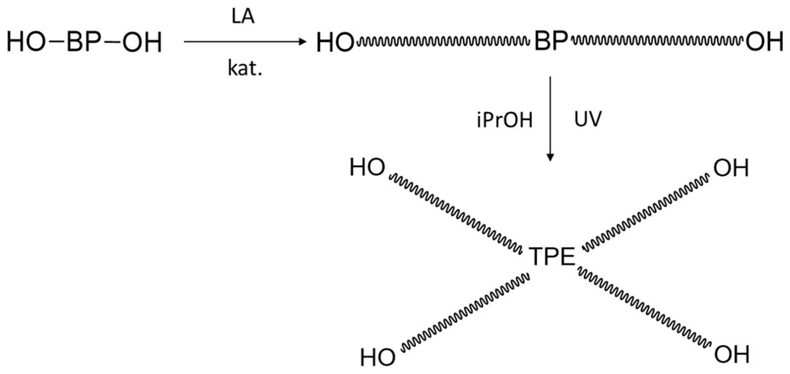

Rys. 20 Schemat syntezy liniowych i gwiaździstych PLA

Tabela 3. Otrzymane liniowe PLA i gwiaździste PLA (po sprzęgnięciu)

Polimer	Wyjściowy liniowy polimer	Gwiazdy TPE-PLA	Sieć	
	M_n, ^{1}H NMR	M_n, ^{1}H NMR	Zawartość żelu [%]	T_g, DSC [°C]
TPE-PLA3	1600	3200	99	49.9
TPE-PLA6	3400	6400	99	48.2
PLAref2.5	-	2500	99	50.3

Tak otrzymane gwiaździste polilaktydy z ugrupowaniem TPE w rdzeniu następnie sprzęgnięto z użyciem diizocyjanianu i w wyniku reakcji otrzymano sieci polimerowe z ugrupowaniami TPE w węzłach sieci. Wykorzystanie wyjściowych polimerów o różnych masach molowych pozwoliło na otrzymanie rzadziej i gęściej usieciowanych polilaktydów. Utworzenie sieci potwierdzono metodą spektroskopii FTIR, obserwując w widmach IR sygnały odpowiadające utworzonym wiązaniom uretanowym. Wysoka zawartość żelu, na poziomie 99%, wskazywała na efektywne usieciowanie polimeru. Celem zbadania właściwości mechanicznych, próbki filmów sieci zostały poddane próbie rozciągania. Zgodnie z oczekiwaniami gęściej usieciowany polimer wykazał większą wytrzymałość na rozciąganie, natomiast rzadziej usieciowany wykazał większe wydłużenie przy zerwaniu (widma FTIR, termogramy oraz wyniki badań mechanicznych wraz z dyskusją znajdują się w *publikacji 5*).

3.4.2.1. Badanie dynamicznego charakteru sieci

W celu potwierdzenia dynamicznego charakteru sieci przeprowadzono badania relaksacji w różnych temperaturach. Na podstawie modelu Maxwella dla lepkosprężystych cieczy wyznaczono czasy relaksacji τ*, będące czasami potrzebnymi do relaksacji 63% początkowego naprężenia[76]. Wykazano, że sieci relaksują w bardzo krótkim czasie, poniżej 1 s (Rys 21), co można przypisać szybkiej wymianie rodnikowej pomiędzy grupami TPE. Dla porównania, sieć referencyjna nie relaksowała w tym samym czasie pomiaru. Warto zauważyć, że nie tylko temperatura, ale też gęstość usieciowania miała wpływ na proces relaksacji, gdzie w przypadku gęściej usieciowanego polimeru, całkowita relaksacja nastąpiła dopiero po dłuższym czasie. (szczegółowy opis pomiarów reologicznych, wraz z wynikami i ich dyskusją znajdują się w *publikacji 5*).

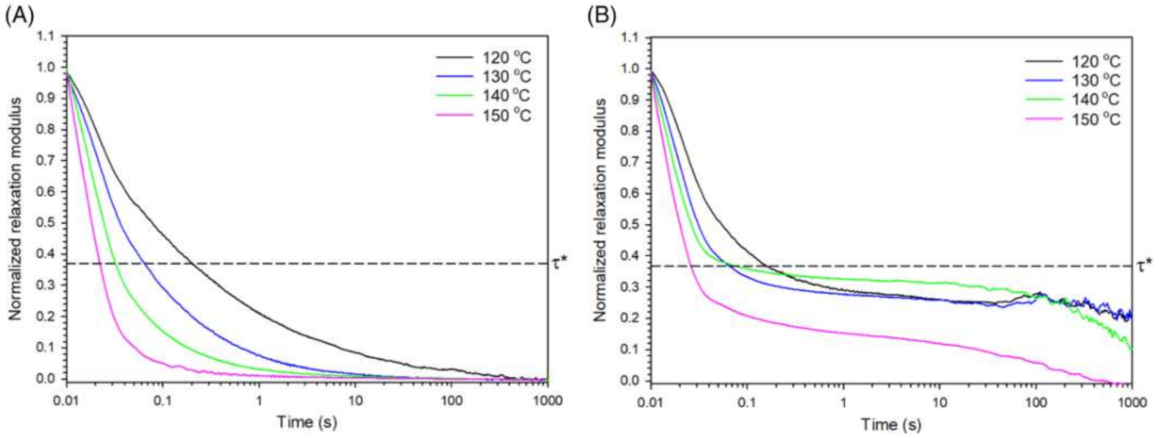

Rys 21 Normalizowany moduł relaksacji dla TPE-PLA6 (A) i TPE-PLA3 (B) w różnych temperaturach

Otrzymane usieciowane polimery poddano również eksperymentowi mającemu na celu wykazanie zdolności do naprawy po uszkodzeniu. Jak pokazały rezultaty eksperymentu, sieci z wbudowanymi grupami TPE zdolne są do naprawy co wynika z możliwości rozpadu istniejących i tworzenia się nowych wiązań kowalencyjnych grup TPE, przy czym zostają zachowane ich właściwości wytrzymałościowe (opis przeprowadzania eksperymentu wraz z dyskusją wyników znajduje się w *publikacji 5*).

4. Podsumowanie

W ramach niniejszej pracy doktorskiej opracowano nową metodę modyfikacji PLA poprzez wprowadzenie do jego struktury ugrupowania tetrafenyloetanu (TPE). Ugrupowanie to ulega termicznej dysocjacji z wytworzeniem rodników, dzięki czemu wykorzystano je zarówno jako iniferter w celu syntezy kopolimerów blokowych PLA/PVM jak też jako odwracalne wiązanie kowalencyjne w syntezie odwracalnych/dynamicznych sieci PLA. Osiągnięte w wyniku prowadzonych badań rezultaty można podsumować następująco:

1. Opracowano syntezę pochodnej hydroksybenzofenonu (BP_ET), a następnie pochodnej tetrafenyloetanodiolu (TPE_diET) zawierającej pierwszorzędowe grupy hydroksylowe. Struktury związków potwierdzono z wykorzystaniem metod spektroskopowych. Wykonano badania potwierdzające reaktywność otrzymanej pochodnej.

2. Wykorzystując pochodną BP_ET jako inicjator polimeryzacji LA, otrzymano PLA z grupą BP na końcu łańcuchu. W wyniku sprzęgnięcia grup BP na skutek promieniowania UV otrzymano polilaktyd z jednym ugrupowaniem TPE w środku. Stosując metody spektroskopowe i SEC potwierdzono strukturę otrzymanych polimerów.

Otrzymany polilaktyd z jednym ugrupowaniem TPE w środku łańcucha wykorzystano jako makroiniferter do inicjowania polimeryzacji AN w prosty sposób, mianowicie ogrzewając PLA w obecności AN. W wyniku opracowanej metody możliwe było otrzymanie kopolimerów triblokowych PLA/PAN o długości bloków regulowanej poprzez zastosowanie różnych warunków polimeryzacji. Strukturę kopolimeru potwierdzono z wykorzystaniem metod spektroskopowych i SEC.

3. Stosując metodę dwuetapowej syntezy poliestro-uretanu w wyniku reakcji diolu PLA z pochodną TPE (TPE_diET) z użyciem diizocyjanianu, otrzymano poliestro-uretan PLA-PU zawierający w swojej strukturze wiele ugrupowań TPE. Strukturę otrzymanych polimerów potwierdzono stosując metody spektroskopowe i SEC.

Otrzymany poliestro-uretan z wbudowanymi wieloma grupami TPE wykorzystano do inicjowania polimeryzacji monomerów winylowych (styrenu i akrylonitrylu). Wykazano, że można w ten stosunkowo prosty sposób otrzymać kopolimery multiblokowe PLA/PAN oraz PLA/PST. Strukturę otrzymanych kopolimerów potwierdzono stosując metody spektroskopowe i SEC.

4. Opracowano syntezę pochodnej hydroksybenzofenonu zawierającą pierścień epoksydowy (BP_EP). W wyniku kopolimeryzacji BP_EP i LA otrzymano kopolimer PLA/poliepoksyd (LA-co-BP_EP), który w następnym etapie usieciowano sprzęgając grupy boczne BP. Otrzymaną sieć PLA-TPE_EP z wbudowanymi ugrupowaniami TPE scharakteryzowano z zastosowaniem metod spektroskopowych.

Przeprowadzając badania reologiczne, wykazano odwracalny charakter sieci i zmianę właściwości reologicznych w podwyższonej temperaturze korzystną dla potencjalnego przetwórstwa. Sieci z wbudowanymi ugrupowaniami TPE wykorzystano jako makroinifertery w celu wprowadzenia jednostek monomeru winylowego (akrylonitrylu) do struktury sieci. W ten sposób wskazano łatwą drogę modyfikacji nierozpuszczalnych sieci, również tych opartych na innych polimerach.

5. Zsyntezowano difunkcyjną pochodną hydroksybenzofenonu (BP_diET), zawierającą dwie pierwszorzędowe grupy -OH, którą wykorzystano jako inicjator polimeryzacji LA. Makrocząsteczki PLA z grupą BP w środku sprzęgnięto w warunkach naświetlania UV, otrzymując gwiaździste PLA z grupą TPE w rdzeniu. Otrzymano sieci polimerowe na bazie zsyntezowanych gwiaździstych PLA, w wyniku ich reakcji z diizocyjanianem. Sieci scharakteryzowano z wykorzystaniem odpowiednich metod analitycznych. Wykazano ich odwracalny/dynamiczny charakter przeprowadzając badania reologiczne. Zademonstrowano również zdolność do naprawy sieci po uszkodzeniu.

Dodatkowo przygotowano i opublikowano pracę przeglądową, w której omówiono szerokie wykorzystanie kopolimerów blokowych PLA/PVM w szczególności do zastosowań w biomedycynie, będącą rozszerzeniem wstępu teoretycznego prezentowanej pracy doktorskiej i jednocześnie uwypuklającą motywację przeprowadzonych badań.

5. Literatura

1. Staudinger H. Über Polymerisation. *Ber dtsch Chem Ges A/B*. 1920;53(6):1073-1085. doi:10.1002/cber.19200530627

2. Percec V, Xiao Q. The Legacy of Hermann Staudinger: Covalently Linked Macromolecules. *Chem*. 2020;6(11):2855-2861. doi:10.1016/j.chempr.2020.10.007

3. Schneiderman DK, Hillmyer MA. 50th Anniversary Perspective: There Is a Great Future in Sustainable Polymers. *Macromolecules*. 2017;50(10):3733-3749. doi:10.1021/acs.macromol.7b00293

4. Geyer R, Jambeck JR, Law KL. Production, use, and fate of all plastics ever made. *Sci Adv*. 2017;3(7):e1700782. doi:10.1126/sciadv.1700782

5. Chinthapalli R, Skoczinski P, Carus M, et al. Biobased Building Blocks and Polymers—Global Capacities, Production and Trends, 2018–2023. *Industrial Biotechnology*. 2019;15(4):237-241. doi:10.1089/ind.2019.29179.rch

6. The Circular Economy for Plastics – A European Analysis 2024 • Plastics Europe. Plastics Europe. Accessed September 25, 2024. https://plasticseurope.org/knowledge-hub/the-circular-economy-for-plastics-a-european-analysis-2024/

7. Hale RC, Seeley ME, La Guardia MJ, Mai L, Zeng EY. A Global Perspective on Microplastics. *Journal of Geophysical Research: Oceans*. 2020;125(1):e2018JC014719. doi:10.1029/2018JC014719

8. European Bioplastics e.V. Accessed March 25, 2024. https://www.european-bioplastics.org/bioplastics/materials/

9. Wellenreuther C, Wolf A, Zander N. *Cost Structure of Bio-Based Plastics: A Monte-Carlo-Analysis for PLA*. Hamburgisches WeltWirtschaftsInstitut (HWWI); 2021. https://hdl.handle.net/10419/235600

10. Balla E, Daniilidis V, Karlioti G, et al. Poly(lactic Acid): A Versatile Biobased Polymer for the Future with Multifunctional Properties—From Monomer Synthesis, Polymerization Techniques and Molecular Weight Increase to PLA Applications. *Polymers*. 2021;13(11):1822. doi:10.3390/polym13111822

11. Bednarek M, Grabowski M. Polylactide/poly(vinyl monomer) block copolymers for specific applications. *Polymer Reviews*. 2024;64(3):898-938. doi:10.1080/15583724.2024.2310105

12. Farah S, Anderson DG, Langer R. Physical and mechanical properties of PLA, and their functions in widespread applications — A comprehensive review. *Advanced Drug Delivery Reviews*. 2016;107:367-392. doi:10.1016/j.addr.2016.06.012

13. Anderson K, Schreck K, Hillmyer M. Toughening Polylactide. *Polymer Revs*. 2008;48(1):85-108. doi:10.1080/15583720701834216

14. Michell RM, Ladelta V, Silva ED, Müller AJ, Hadjichristidis N. Poly(lactic acid) stereocomplexes based molecular architectures: Synthesis and crystallization. *Progress in Polymer Science*. 2023;146:101742. doi:https://doi.org/10.1016/j.progpolymsci.2023.101742

15. Chile LE, Mehrkhodavandi P, Hatzikiriakos SG. A Comparison of the Rheological and Mechanical Properties of Isotactic, Syndiotactic, and Heterotactic Poly(lactide). *Macromolecules*. 2016;49(3):909-919. doi:10.1021/acs.macromol.5b02568

16. Garlotta D. A Literature Review of Poly(Lactic Acid). *Journal of Polymers and the Environment*. 2001;9(2):63-84. doi:10.1023/A:1020200822435

17. Gupta AP, Kumar V. New emerging trends in synthetic biodegradable polymers – Polylactide: A critique. *European Polymer Journal*. 2007;43(10):4053-4074. doi:10.1016/j.eurpolymj.2007.06.045

18. Dechy-Cabaret O, Martin-Vaca B, Bourissou D. Controlled Ring-Opening Polymerization of Lactide and Glycolide. *Chem Rev*. 2004;104(12):6147-6176. doi:10.1021/cr040002s

19. Kricheldorf HR, Kreiser-Saunders I, Stricker A. Polylactones 48. SnOct2-Initiated Polymerizations of Lactide: A Mechanistic Study. *Macromolecules*. 2000;33(3):702-709. doi:10.1021/ma991181w

20. Kowalski A, Duda A, Penczek S. Kinetics and Mechanism of Cyclic Esters Polymerization Initiated with Tin(II) Octoate. 3. Polymerization of l,l-Dilactide. *Macromolecules*. 2000;33(20):7359-7370. doi:10.1021/ma000125o

21. Majerska K, Duda A, Penczek S. Kinetics and mechanism of cyclic esters polymerisation initiated with tin(II) octoate, 4. Influence of proton trapping agents on the kinetics of ε-caprolactone and L,L-dilactide polymerisation. *Macromolecular Rapid Communications*. 2000;21(18):1327-1332. doi:10.1002/1521-3927(20001201)21:18<1327::AID-MARC1327>3.0.CO;2-9

22. R. Kricheldorf H, M. Weidner S. Syntheses of polylactides by means of tin catalysts. *Polymer Chemistry*. 2022;13(12):1618-1647. doi:10.1039/D2PY00092J

23. Kamber NE, Jeong W, Waymouth RM, Pratt RC, Lohmeijer BGG, Hedrick JL. Organocatalytic Ring-Opening Polymerization. *Chem Rev*. 2007;107(12):5813-5840. doi:10.1021/cr068415b

24. Duda A, Biela T, Kowalski A, Libiszowski J. Amines as (co)initiators of cyclic esters' polymerization. *Polimery*. 2005;50(7-8):501-508.

25. Suzuki M, Watanabe A, Kawai R, Sato R, Matsuoka S ichi, Kawauchi S. Ring-opening polymerization of thiolactide by using thiol-amine combination. *Polymer*. 2021;215:123386. doi:10.1016/j.polymer.2021.123386

26. Ryner M, Stridsberg K, Albertsson AC, von Schenck H, Svensson M. Mechanism of Ring-Opening Polymerization of 1,5-Dioxepan-2-one and l-Lactide with Stannous 2-Ethylhexanoate. A Theoretical Study. *Macromolecules*. 2001;34(12):3877-3881. doi:10.1021/ma002096n

27. Matyjaszewski K. *Cationic Polymerizations : Mechanisms, Synthesis, and Applications*. Marcel Dekker; 1996.

28. Bednarek M, Biedron T, Kaluzynski K, Kubisa P, Pretula J, Penczek S. Ring-opening polymerization processes involving activated monomer mechanism. Cationic polymerization of cyclic ethers containing hydroxyl groups. *MACROMOLECULAR SYMPOSIA*. 2000;157:1-11. doi:10.1002/1521-3900(200007)157:1<1::AID-MASY1>3.0.CO;2-X

29. Kubisa P, Penczek S. Cationic activated monomer polymerization of heterocyclic monomers. *Progress in Polymer Science*. 1999;24(10):1409-1437. doi:10.1016/S0079-6700(99)00028-3

30. Baśko M, Kubisa P. Cationic polymerization of L,L-lactide. *Journal of Polymer Science Part A: Polymer Chemistry*. 2010;48(12):2650-2658. doi:10.1002/pola.24048

31. Basko M. Activated monomer mechanism in the cationic polymerization of L,L-lactide. *Pure and Applied Chemistry*. 2012;84(10):2081-2088. doi:10.1351/PAC-CON-11-10-19

32. Baśko M, Kubisa P. Mechanism of propagation in the cationic polymerization of L,L -lactide. *J Polym Sci A Polym Chem*. 2008;46(23):7919-7923. doi:10.1002/pola.23074

33. Slomkowski S, Penczek S, Duda A. Polylactides—an overview. *Polymers for Advanced Technologies*. 2014;25(5):436-447. doi:10.1002/pat.3281

34. Puthumana M, Santhana Gopala Krishnan P, Nayak SK. Chemical modifications of PLA through copolymerization. *International Journal of Polymer Analysis and Characterization*. 2020;25(8):634-648. doi:10.1080/1023666X.2020.1830650

35. Jenkins AD, Kratochvíl P, Stepto RFT, Suter UW. Glossary of basic terms in polymer science (IUPAC Recommendations 1996). *Pure and Applied Chemistry*. 1996;68(12):2287-2311. doi:doi:10.1351/pac199668122287

36. Södergård A, Stolt M. Properties of lactic acid based polymers and their correlation with composition. *Progress in Polymer Science*. 2002;27(6):1123-1163. doi:10.1016/S0079-6700(02)00012-6

37. Bednarek M, Grabowski M. Polylactide/poly(vinyl monomer) block copolymers for specific applications. *Polymer Reviews*. Published online February 5, 2024:1-41. doi:10.1080/15583724.2024.2310105

38. Gigmes D, Trimaille T. Advances in amphiphilic polylactide/vinyl polymer based nano-assemblies for drug delivery. *Advances in Colloid and Interface Science*. 2021;294:102483. doi:10.1016/j.cis.2021.102483

39. Nagarajan V, Mohanty AK, Misra M. Perspective on Polylactic Acid (PLA) based Sustainable Materials for Durable Applications: Focus on Toughness and Heat Resistance. *ACS Sustainable Chem Eng*. 2016;4(6):2899-2916. doi:10.1021/acssuschemeng.6b00321

40. Rasal RM, Janorkar AV, Hirt DE. Poly(lactic acid) modifications. *Progress in Polymer Science (Oxford)*. 2010;35(3):338-356. doi:10.1016/j.progpolymsci.2009.12.003

41. Oh JK. Polylactide (PLA)-based amphiphilic block copolymers: synthesis, self-assembly, and biomedical applications. *Soft Matter*. 2011;7:5096-5108. doi:10.1039/c0sm01539c

42. Matyjaszewski K. General Concepts and History of Living Radical Polymerization. In: *Handbook of Radical Polymerization*. John Wiley & Sons, Ltd; 2002:361-406. doi:https://doi.org/10.1002/0471220450.ch8

43. Otsu T, Yoshida M, Tazaki T. A model for living radical polymerization. *Makromol Chem, Rapid Commun*. 1982;3(2):133-140. doi:10.1002/marc.1982.030030209

44. Otsu T, Yoshida M. Role of initiator-transfer agent-terminator (iniferter) in radical polymerizations: Polymer design by organic disulfides as iniferters. *Makromol Chem, Rapid Commun*. 1982;3(2):127-132. doi:10.1002/marc.1982.030030208

45. Otsu T. Iniferter concept and living radical polymerization. *Journal of Polymer Science Part A: Polymer Chemistry*. 2000;38(12):2121-2136. doi:10.1002/(SICI)1099-0518(20000615)38:12<2121::AID-POLA10>3.0.CO;2-X

46. Atilla Tasdelen M, Yagci Y. Controlled/Living Radical Polymerization in the Presence of Iniferters. In: Tsarevsky NV, Sumerlin BS, eds. *Fundamentals of Controlled/Living Radical Polymerization*. The Royal Society of Chemistry; 2013:78-111. doi:10.1039/9781849737425-00078

47. Otsu T, Matsumoto A. Controlled Synthesis of Polymers Using the Iniferter Technique: Developments in Living Radical Polymerization. In: DiMari S, Funke W, Haralson MA, et al., eds. *Microencapsulation Microgels Iniferters*. Springer; 1998:75-137. doi:10.1007/3-540-69682-2_3

48. Błedzki A, Braun D. Polymerisationsauslösung mit substituierten Ethanen, 1. Polymerisation von Methylmethacrylat mit 1,1,2,2-Tetraphenyl-1,2-diphenoxyethan. *Makromol Chem*. 1981;182(4):1047-1056. doi:10.1002/macp.1981.021820405

49. Braun VD, Becker KH. Aromatische Pinakole als Polymerisationsinitiatoren. *Angew Makromol Chem*. 1969;6(1):186-189. doi:10.1002/apmc.1969.050060119

50. Yao XQ, Hou XJ, Wu GS, et al. Estimation of C−C Bond Dissociation Enthalpies of Large Aromatic Hydrocarbon Compounds Using DFT Methods. *J Phys Chem A*. 2002;106(31):7184-7189. doi:10.1021/jp020607x

51. Otsu T, Matsumoto A, Tazaki T. Radical polymerization of methyl methacrylate with some 1,2-disubstituted tetraphenylethanes as thermal iniferters. *Polymer Bulletin*. 1987;17(4):323-330. doi:10.1007/BF00955715

52. Tharanikkarasu K, Radhakrishnan G. A novel polyurethane macroinitiator for free radical polymerization. *European Polymer Journal*. 1994;30(12):1351-1355. doi:10.1016/0014-3057(94)90262-3

53. Tharanikkarasu K, Radhakrishnan G. Tetraphenylethane Iniferters. 3. “Living” Radical Polymerization of Methyl Methacrylate Using Toluene-Diisocyanate-Based Polyurethane Iniferter. *Journal of Macromolecular Science, Part A*. 1996;33(4):417-437. doi:10.1080/10601329608010868

54. Tharanikkarasu K, Radhakrishnan G. Tetraphenylethane iniferters. II. Toluene diisocyanate-based polyurethane iniferter for “living” radical polymerization of acrylonitrile. *J Polym Sci A Polym Chem*. 1996;34(9):1723-1731. doi:10.1002/(SICI)1099-0518(19960715)34:9<1723::AID-POLA9>3.0.CO;2-S

55. Tharanikkarasu K, Radhakrishnan G. ‘Living’ Radical Polymerization of Styrene Using Tetraphenylethane-based Polyurethane Iniferter. *Polym Int*. 1997;43(1):13-21. doi:10.1002/(SICI)1097-0126(199705)43:1<13::AID-PI731>3.0.CO;2-J

56. Tharanikkarasu K, Radhakrishnan G. Tetraphenylethane iniferters: Polyurethane-polystyrene multiblock copolymers through “living” radical polymerization. *Journal of Applied Polymer Science*. 1997;66(8):1551-1560. doi:10.1002/(SICI)1097-4628(19971121)66:8<1551::AID-APP16>3.0.CO;2-6

57. Tharanikkarasu K, Kim BK. Modification of aqueous polyurethane dispersions via tetraphenylethane iniferters. *Journal of Applied Polymer Science*. 1999;73(14):2993-3000. doi:10.1002/(SICI)1097-4628(19990929)73:14<2993::AID-APP24>3.0.CO;2-B

58. Sundar S, Tharanikkarasu K, Dhathathreyan A, Radhakrishnan G. Aqueous dispersions of poly(urethane- co -vinylpyridine) synthesised from polyurethane macroiniferter. *Colloid & Polymer Science*. 2002;280(10):915-921. doi:10.1007/s00396-002-0707-y

59. Kim BK, Tharanikkarasu K, Lee JS. Polyurethane-polymethacrylic acid multiblock copolymer dispersions through polyurethane macroiniferters. *Colloid Polym Sci*. 1999;277(2):285-290. doi:10.1007/PL00013758

60. Zhou G, Ma C, Zhang G. Synthesis of polyurethane-g-poly(ethylene glycol) copolymers by macroiniferter and their protein resistance. *Polym Chem*. 2011;2(6):1409-1414. doi:10.1039/C1PY00016K

61. Södergård A, Näsman JH. Stabilization of poly(l-lactide) in the melt. *Polymer Degradation and Stability*. 1994;46(1):25-30. doi:10.1016/0141-3910(94)90104-X

62. Bednarek M, Borska K, Kubisa P. New Polylactide-Based Materials by Chemical Crosslinking of PLA. *Polymer Reviews*. 2021;61(3):493-519. doi:10.1080/15583724.2020.1855194

63. Gu Y, Zhao J, Johnson JA. Polymer Networks: From Plastics and Gels to Porous Frameworks. *Angewandte Chemie International Edition*. 2020;59(13):5022-5049. doi:10.1002/anie.201902900

64. Vidil T, Tournilhac F, Musso S, Robisson A, Leibler L. Control of reactions and network structures of epoxy thermosets. *Progress in Polymer Science*. 2016;62:126-179. doi:10.1016/j.progpolymsci.2016.06.003

65. Bowman C, Prez FD, Kalow J. Introduction to chemistry for covalent adaptable networks. *Polym Chem*. 2020;11(33):5295-5296. doi:10.1039/D0PY90102D

66. Zheng N, Xu Y, Zhao Q, Xie T. Dynamic Covalent Polymer Networks: A Molecular Platform for Designing Functions beyond Chemical Recycling and Self-Healing. *Chem Rev*. 2021;121(3):1716-1745. doi:10.1021/acs.chemrev.0c00938

67. Ionescu M. *Chemistry and Technology of Polyols for Polyurethanes*. Second edition. Smithers Rapra; 2016.

68. Muñiz MK. The Pinacol Rearrangement. *Comprehensive Organic Synthesis: Second Edition*. 2014;3:741-756. doi:10.1016/B978-0-08-097742-3.00319-0

69. Zalibera M, Nesvadba P, Gescheidt G. Reaction of Benzopinacol with Non-ionic Bases: Reversing the Pinacol Coupling. *Org Lett*. 2013;15(18):4627-4629. doi:10.1021/ol402253s

70. Chatterjee A, Joshi NN. Evolution of the stereoselective pinacol coupling reaction. *Tetrahedron*. 2006;62(52):12137-12158. doi:10.1016/j.tet.2006.09.002

71. Li X, Ogihara T, Kato T, Nakamura Y, Yamago S. Evidence for Polarity- and Viscosity-Controlled Pathways in the Termination Reaction in the Radical Polymerization of Acrylonitrile. *Macromolecules*. 2021;54(10):4497-4506. doi:10.1021/acs.macromol.1c00158

72. Schweiger A, Jeschke G. *Principles of Pulse Electron Paramagnetic Resonance*. Oxford University Press; 2001.

73. Nakamura Y, Yamago S. Termination Mechanism in the Radical Polymerization of Methyl Methacrylate and Styrene Determined by the Reaction of Structurally Well-Defined Polymer End Radicals. *Macromolecules*. 2015;48(18):6450-6456. doi:10.1021/acs.macromol.5b01532

74. Groves P. Diffusion ordered spectroscopy (DOSY) as applied to polymers. *Polym Chem*. 2017;8(44):6700-6708. doi:10.1039/C7PY01577A

75. Chen M, Gu Y, Singh A, et al. Living Additive Manufacturing: Transformation of Parent Gels into Diversely Functionalized Daughter Gels Made Possible by Visible Light Photoredox Catalysis. *ACS Cent Sci*. 2017;3(2):124-134. doi:10.1021/acscentsci.6b00335

76. Capelot M, Unterlass MM, Tournilhac F, Leibler L. Catalytic Control of the Vitrimer Glass Transition. *ACS Macro Lett*. 2012;1(7):789-792. doi:10.1021/mz300239f

6. Spis publikacji i wystąpień konferencyjnych

Publikacje

1. Mateusz Grabowski, Bartłomiej Kost, Bartłomiej Gostyński, Melania Bednarek. Can tetraphenylethane (TPE) “iniferter” group be introduced into the polymer chain by coupling TPE diol with diisocyanate? *Polymer*. 2022;246:124738. doi:10.1016/j.polymer.2022.124738
2. Mateusz Grabowski, Bartłomiej Kost, Przemysław Kubisa, Melania Bednarek. A New Approach to The Synthesis of Polylactide/Polyacrylonitrile Block Copolymers. *Polymers*. 2022;14(8):1529. doi:10.3390/ polym14081529
3. Mateusz Grabowski, Bartłomiej Kost, Agnieszka Bodzioch, Melania Bednarek. Functionalization of Polylactide with Multiple Tetraphenylethane Inifer Groups to Form PLA Block Copolymers with Vinyl Monomers. *Int. J. Mol. Sci*. 2023;24(1):19. doi:10.3390/ijms24010019
4. Mateusz Grabowski, Bartłomiej Kost, Mateusz Bartniak, Dorota Bociąga, Witold Szymański, Melania Bednarek. Copolymerization of lactide with functional epoxide as a way to the polymer network with dually active tetraphenylethane groups. *Polymer.* 2024;312:127673 doi:10.1016/j.polymer.2024.127673
5. Melania Bednarek, Mateusz Grabowski, Magdalena Lipińska, Andrzej Pawlak. Reversible polymer networks based on polylactide with tetraphenylethane thermally dissociating groups in crosslinks. *Polym. Adv. Technol*. 2024;35(4):e6390. doi:10.1002/pat.6390
6. Melania Bednarek, Mateusz Grabowski. Polylactide/poly(vinyl monomer) block copolymers for specific applications. *Polymer Reviews*. 2024;64(3):898-938. doi:10.1080/15583724.2024.2310105

Komunikaty ustne

1. Mateusz Grabowski, Melania Bednarek, Bartłomiej Kost, Polylactide modification by introducing groups with a thermally diisociating covalent bond into the polymer structure. XIII Scientific Conference – Controlled Polymerization, Łódź 03.06.2024
2. Mateusz Grabowski, Melania Bednarek, Bartłomiej Kost, Methods of polylactide copolymer synthesis by generating tetraphenylethane inifer groups in the PLA structure. 14th Advanced Polymers via Macromolecular Engineering, Paris 23-27.04.2023
3. Mateusz Grabowski, Melania Bednarek, Bartłomiej Kost, Methods of polylactide copolymer synthesis by generating tetraphenylethane inifer groups in the PLA structure, The 12th International Congress of Societas Humboldtiana Polonorum, Łódź, 30.06-02.07.2023
4. Mateusz Grabowski, Melania Bednarek, Bartłomiej Kost, Metody syntezy kopolimerów polilaktydu poprzez wprowadzenie ugrupowania inifera do struktury PLA, XIV Sesja Magistrantów i Doktorantów Łódzkiego Środowiska Chemików, Łódź, 13.06.2023
5. Mateusz Grabowski, Melania Bednarek, Bartłomiej Kost, Modyfikacja polilaktydu poprzez wprowadzenie do struktury polimeru ugrupowania zawierającego podatne na termiczną dysocjację wiązanie kowalencyjne, Krajowa konferencja naukowa studencko-doktorancka: IX Łódzkie Sympozjum Doktorantów Chemii, Łódź, 19-20.05.2022

Plakaty

1. Mateusz Grabowski, Melania Bednarek, Bartłomiej Kost, Methods of polylactide copolymer synthesis by generating tetraphenylethane inifer groups in the PLA structure. Chemical Science symposium 2023: Chemistry of polymers, London, 26-27.10.2023
2. Mateusz Grabowski, Melania Bednarek, Bartłomiej Kost, Metody syntezy kopolimerów polilaktydu poprzez wprowadzenie ugrupowania inifera do struktury PLA, 65. Zjazd Naukowy Polskiego Towarzystwa Chemicznego, Toruń, 18-22.09.2023
3. Mateusz Grabowski, Melania Bednarek, Bartłomiej Kost, Methods of polylactide copolymer synthesis by generating tetraphenylethane inifer groups in the PLA structure, The 12th International Congress of Societas Humboldtiana Polonorum, Łódź, 30.06-02.07.2023

4. Mateusz Grabowski, Melania Bednarek, Bartłomiej Kost, Synteza kopolimerów blokowych polilaktydu z zastosowaniem makroinifertera opartego na PLA 64. Zjazd Naukowy Polskiego Towarzystwa Chemicznego, Lublin, 11-16.09.2022
5. Mateusz Grabowski, Melania Bednarek, Bartłomiej Kost, Polylactide containing tetraphenylethane groups as a new approach to PLA copolymers, Bordeaux Polymer Conference 2022, 13-16.06.2022
6. Mateusz Grabowski, Melania Bednarek, Bartłomiej Kost, Silesian Meetings on Polymer Materials POLYMAT 2022, Polylactide containing tetraphenylethane groups as a new approach to PLA copolymers, Zabrze, 17.03.22
7. Mateusz Grabowski, Melania Bednarek, Bartłomiej Kost, Introduction of tetraphenylethane units to polylactide structure, resulting in obtaining new materials based on PLA, 7th Young Polymer Scientists Conference and Short Course- Lodz, 27-28.09.2021
8. Mateusz Grabowski, Melania Bednarek, Bartłomiej Kost, Wprowadzenie grup tetrafenyloetanu do struktury polilaktydu i wynikające stąd możliwości uzyskania nowych materiałów opartych na PLA, 63. Zjazd Naukowy Polskiego Towarzystwa Chemicznego, Łódź, 13-17.09 2021

7. Oświadczenia współautorów i załączone publikacje

Publikacja 1:

Mateusz Grabowski, Bartłomiej Kost, Bartłomiej Gostyński, Melania Bednarek. Can tetraphenylethane (TPE) “iniferter” group be introduced into the polymer chain by coupling TPE diol with diisocyanate? *Polymer*. 2022;246:124738. doi:10.1016/j.polymer.2022.124738

Publikacja 2:

Mateusz Grabowski, Bartłomiej Kost, Przemysław Kubisa, Melania Bednarek. A New Approach to The Synthesis of Polylactide/Polyacrylonitrile Block Copolymers. *Polymers*. 2022;14(8):1529. doi:10.3390/ polym14081529

Publikacja 3:

Mateusz Grabowski, Bartłomiej Kost, Agnieszka Bodzioch, Melania Bednarek. Functionalization of Polylactide with Multiple Tetraphenylethane Inifer Groups to Form PLA Block Copolymers with Vinyl Monomers. Int. J. Mol. Sci. 2023;24(1):19. doi:10.3390/ijms24010019

Publikacja 4:

Mateusz Grabowski, Bartłomiej Kost, Mateusz Bartniak, Dorota Bociąga, Witold Szymański, Melania Bednarek. Copolymerization of lactide with functional epoxide as a way to the polymer network with dually active tetraphenylethane groups. *Polymer.* 2024;312:127673

Publikacja 5:

Melania Bednarek, Mateusz Grabowski, Magdalena Lipińska, Andrzej Pawlak. Reversible polymer networks based on polylactide with tetraphenylethane thermally dissociating groups in crosslinks. *Polym. Adv. Technol*. 2024;35(4):e6390. doi:10.1002/pat.6390

Publikacja 6:

Melania Bednarek, Mateusz Grabowski. Polylactide/poly(vinyl monomer) block copolymers for specific applications. *Polymer Reviews*. 2024;64(3):898-938. doi:10.1080/15583724.2024.2310105

mgr inż. Mateusz Grabowski
Centrum Badań Molekularnych
i Makromolekularnych
Polskiej Akademii Nauk

Łódź dn. 10.10.2024

Oświadczenie współautora publikacji

Oświadczam, że w ramach przygotowania następujących artykułów naukowych:

1. Grabowski M, Kost B, Gostyński B, Bednarek M. Can tetraphenylethane (TPE) "iniferter" group be introduced into the polymer chain by coupling TPE diol with diisocyanate? *Polymer*. 2022;246:124738. doi:10.1016/j.polymer.2022.124738

2. Grabowski M, Kost B, Kubisa P, Bednarek M. A New Approach to The Synthesis of Polylactide/Polyacrylonitrile Block Copolymers. *Polymers*. 2022;14(8):1529. doi:10.3390/ polym14081529

3. Grabowski M, Kost B, Bodzioch, A, Bednarek M. Functionalization of Polylactide with Multiple Tetraphenylethane Inifer Groups to Form PLA Block Copolymers with Vinyl Monomers. *Int. J. Mol. Sci*. 2023;24(1):19. doi:10.3390/ijms24010019

4. Grabowski M, Kost B, Bartniak M, Bociąga D, Szymański W, Bednarek M. Copolymerization of lactide with functional epoxide as a way to the polymer network with dually active tetraphenylethane groups. *Polymer.* 2024;312:127673 doi:10.1016/j.polymer.2024.127673

5. Bednarek M, Grabowski M, Lipińska M, Pawlak A. Reversible polymer networks based on polylactide with tetraphenylethane thermally dissociating groups in crosslinks. *Polym Adv Technol*. 2024;35(4):e6390. doi:10.1002/pat.6390

6. Bednarek M, Grabowski M. Polylactide/poly(vinyl monomer) block copolymers for specific applications. *Polymer Reviews*. 2024;64(3):898-938. doi:10.1080/15583724.2024.2310105

W wyżej przedstawionych publikacjach wykonałem następujące zadania:

Ad. 1. Przeprowadziłem syntezę pochodnej benzofenonu (BP_ET), a następnie pochodnej tetrafenyloetanodiolu (TPE_diET). Brałem udział w badaniach potwierdzających reaktywność otrzymanej pochodnej. Tworzyłem tekst manuskryptu.

Ad. 2 Przeprowadziłem syntezę polilaktydów z jedną grupą TPE w środku łańcucha. Otrzymane polilaktydy wykorzystałem jako makroinifertery w celu otrzymania kopolimerów triblokowych PLA/PAN. Scharakteryzowałem otrzymane polimery. Tworzyłem tekst manuskryptu.

Ad. 3 Opracowałem i przeprowadziłem syntezę poliestro-uretanu zawierającego wiele ugrupowań TPE w łańcuchu. Wykorzystując otrzymane polimery jako makroinifertery przeprowadziłem syntezę kopolimerów multiblokowych PLA/PVM. Scharakteryzowałem otrzymane polimery. Przygotowałem materiał do badań oraz brałem udział w analizie rezultatów badania EPR, mającego na celu wykazanie zdolności ugrupowania TPE znajdującego się w poliestro-uretanie PLA-PU do rozpadu z wytworzeniem rodników. Tworzyłem tekst manuskryptu.

Ad. 4 Przeprowadziłem syntezę sfunkcjonalizowago monomeru epoksydowego BP_EP. Przeprowadziłem kopolimeryzację laktydu z monomerem BP_EP. Na bazie otrzymanego kopolimeru LA-co-BP_EP zsyntezowałem sieci polimerowe zawierającą odwracalne grupy TPE w węzłach sieci. Wyjściowe kopolimery i otrzymane sieci scharakteryzowałem. Brałem udział w doborze parametrów badań reologicznych mających na celu wykazanie odwracalnego charakteru sieci polimerowych i analizowałem ich rezultaty. Wprowadziłem jednostki monomeru winylowego do struktury sieci i analizowałem rezultaty badań wykazujących wpływ wprowadzenia jednostek monomeru winylowego na właściwości termiczne i mechaniczne sieci. Tworzyłem tekst manuskryptu.

Ad. 5 Przeprowadzałem syntezę gwiaździstych polilaktydów z grupą TPE w rdzeniu. Na bazie otrzymanych gwiaździstych polilaktydów zsyntezowałem sieci polimerowe z ugrupowaniem TPE w węzłach sieci. Otrzymane polimery i sieci polimerowe scharakteryzowałem. Brałem udział w doborze parametrów i analizowałem wyniki badań reologicznych mających na celu wykazanie dynamicznego charakteru sieci. Przeprowadziłem eksperyment wykazujący zdolność sieci z wbudowanymi grupami TPE do naprawy po uszkodzeniu. Tworzyłem tekst manuskryptu.

Ad. 6 Współuczestniczyłem w przeszukiwaniu dostępnej literatury. Brałem udział w tworzeniu manuskryptu.

mgr inż. Mateusz Grabowski

Łódź dn. 27.09.2024

Dr hab. Melania Bednarek
Centrum Badań Molekularnych
i Makromolekularnych
Polskiej Akademii Nauk

Oświadczenie współautora publikacji

Oświadczam, że w ramach przygotowania następujących artykułów naukowych:

1. Grabowski M, Kost B, Gostyński B, Bednarek M. Can tetraphenylethane (TPE) "iniferter" group be introduced into the polymer chain by coupling TPE diol with diisocyanate? *Polymer*. 2022;246:124738. doi:10.1016/j.polymer.2022.124738

2. Grabowski M, Kost B, Kubisa P, Bednarek M. A New Approach to The Synthesis of Polylactide/Polyacrylonitrile Block Copolymers. *Polymers*. 2022;14(8):1529. doi:10.3390/ polym14081529

3. Grabowski M, Kost B, Bodzioch, A, Bednarek M. Functionalization of Polylactide with Multiple Tetraphenyethane Inifer Groups to Form PLA Block Copolymers with Vinyl Monomers. *Int. J. Mol. Sci*. 2023;24(1):19. doi:10.3390/ijms24010019

4. Bednarek M, Grabowski M, Lipińska M, Pawlak A. Reversible polymer networks based on polylactide with tetraphenylethane thermally dissociating groups in crosslinks. *Polym Adv Technol*. 2024;35(4):e6390. doi:10.1002/pat.6390

5. Grabowski M, Kost B, Bartniak M, Bociąga D, Szymański W, Bednarek M. Copolymerization of lactide with functional epoxide as a way to the polymer network with dually active tetraphenylethane groups. *Polymer*. 2024;312:127673 doi:10.1016/j.polymer.2024.127673

6. Bednarek M, Grabowski M. Polylactide/poly(vinyl monomer) block copolymers for specific applications. *Polymer Reviews*. 2024;64(3):898-938. doi:10.1080/15583724.2024.2310105

W wyżej przedstawionych publikacjach wykonałam następujące zadania:

Ad. 1-5. Prowadziłam merytoryczny nadzór nad badaniami, byłam pomysłodawcą zakresów prac, uczestniczyłam w eksperymentach kinetycznych opisanych w artykule z pozycji 1, uczestniczyłam w interpretacji wyników analiz oraz tworzeniu i korekcie manuskryptu.

Ad. 6. Zaplanowałam zakres przeglądu i jego strukturę, współuczestniczyłam w przeszukiwaniu dostępnej literatury, byłam głównym autorem tekstu.

M. Bednarek

dr hab. Melania Bednarek

Oświadczenie wydane na prośbę mgr. inż. Mateusza Grabowskiego w związku z przygotowaniem pracy doktorskiej.

dr Bartłomiej Kost
Centrum Badań Molekularnych
i Makromolekularnych
Polskiej Akademii Nauk

Łódź dn. 10.10.2024

Oświadczenie współautora publikacji

Oświadczam, że w ramach przygotowania następujących artykułów naukowych:

1. Grabowski M, Kost B, Gostyński B, Bednarek M. Can tetraphenylethane (TPE) "iniferter" group be introduced into the polymer chain by coupling TPE diol with diisocyanate? *Polymer*. 2022;246:124738. doi:10.1016/j.polymer.2022.124738

2. Grabowski M, Kost B, Kubisa P, Bednarek M. A New Approach to The Synthesis of Polylactide/Polyacrylonitrile Block Copolymers. *Polymers*. 2022;14(8):1529. doi:10.3390/ polym14081529

3. Grabowski M, Kost B, Bodzioch, A, Bednarek M. Functionalization of Polylactide with Multiple Tetraphenyethane Inifer Groups to Form PLA Block Copolymers with Vinyl Monomers. *Int. J. Mol. Sci*. 2023;24(1):19. doi:10.3390/ijms24010019

4. Bednarek M, Grabowski M, Lipińska M, Pawlak A. Reversible polymer networks based on polylactide with tetraphenylethane thermally dissociating groups in crosslinks. *Polym Adv Technol*. 2024;35(4):e6390. doi:10.1002/pat.6390

5. Grabowski M, Kost B, Bartniak M, Bociąga D, Szymański W, Bednarek M. Copolymerization of lactide with functional epoxide as a way to the polymer network with dually active tetraphenylethane groups. *Polymer*. 2024;312:127673

W wyżej przedstawionych publikacjach wykonałem następujące zadania:

Ad. 1-5. Prowadziłem merytoryczny nadzór nad badaniami, brałem udział w projektowaniu pochodnych benzofenonu w publikacjach 1-3 i 5. Uczestniczyłem w eksperymentach kinetycznych opisanych w artykule z pozycji 1, uczestniczyłem w interpretacji wyników analiz oraz korekcie manuskryptów.

Kost Bartłomiej
dr Bartłomiej Kost

Oświadczenie wydane na prośbę mgr. inż. Mateusza Grabowskiego w związku z przygotowaniem pracy doktorskiej.

prof. dr hab. Przemysław Kubisa
Centrum Badań Molekularnych
i Makromolekularnych
Polskiej Akademii Nauk

Łódź dn. 15.10.2024

Oświadczenie współautora publikacji

Oświadczam, że w ramach przygotowania następujących artykułów naukowych:

1. Grabowski M, Kost B, Kubisa P, Bednarek M. A New Approach to The Synthesis of Polylactide/Polyacrylonitrile Block Copolymers. *Polymers*. 2022;14(8):1529. doi:10.3390/ polym14081529

W wyżej przedstawionej publikacji wykonałem następujące zadania:

Ad. 1. Prowadziłem merytoryczny nadzór nad badaniami, uczestniczyłem w interpretacji wyników analiz oraz korekcie manuskryptu.

prof. dr hab. Przemysław Kubisa

Oświadczenie wydane na prośbę mgr. inż. Mateusza Grabowskiego w związku z przygotowaniem pracy doktorskiej.

dr Bartłomiej Gostyński
Centrum Badań Molekularnych
i Makromolekularnych
Polskiej Akademii Nauk

Łódź dn. 26.07.2024

Oświadczenie współautora publikacji

Oświadczam, że w ramach przygotowania następującego artykułu naukowego:

1. Grabowski, M.; Kost, B.; Gostyński, B.; Bednarek, M. Can tetraphenylethane (TPE) “iniferter” groups be introduced into polymer chains by coupling TPE diol with diisocyanates? Polymer 2022, 246, 124738. https://doi.org/10.1016/j.polymer.2022.124738.

W wyżej przedstawionej publikacji wykonałem następujące zadania:

Opracowałem warunki oraz wykonałem badania obliczeniowe, mające na celu wykazanie braku reaktywności grup hydroksylowych zawartych w strukturze tetrafenyloetanodiolu. Brałem udział w tworzeniu manuskryptu.

B.Gostyński
dr Bartłomiej Gostyński

Oświadczenie wydane na prośbę mgr. inż. Mateusza Grabowskiego w związku z przygotowaniem pracy doktorskiej.

dr Agnieszka Bodzioch

Łódź dn. 01.07.2024

Oświadczenie współautora publikacji

Oświadczam, że w ramach przygotowania następującego artykułu naukowego:

1. Grabowski, M.; Kost, B.; Bodzioch, A.; Bednarek, M. Functionalization of Polylactide with Multiple Tetraphenyethane Inifer Groups to Form PLA Block Copolymers with Vinyl Monomers. Int. J. Mol. Sci. 2023, 24, 19. https://doi.org/10.3390/ijms24010019

W wyżej przedstawionej publikacji wykonałam następujące zadania:

Opracowałam warunki oraz wykonałam badania, potwierdzające rozpad grup TPE wbudowanych do struktury polimeru z wytworzeniem rodników, z wykorzystaniem metody spektroskopowej EPR.

dr Agnieszka Bodzioch

A. Bodzioch

Oświadczenie wydane na prośbę mgr. inż. Mateusza Grabowskiego w związku z przygotowaniem pracy doktorskiej.

dr hab. Andrzej Pawlak, profesor instytutu
Centrum Badań Molekularnych
i Makromolekularnych
Polskiej Akademii Nauk

Łódź dn. 26.07.2024

Oświadczenie współautora publikacji

Oświadczam, że w ramach przygotowania następującego artykułu naukowego:

1. Bednarek M, Grabowski, M, Lipińska M, Pawlak A. Reversible polymer networks based on polylactide with tetraphenylethane thermally dissociating groups in crosslinks. Polym Adv Technol. 2024;35(4):e6390. doi:10.1002/pat.6390

W wyżej przedstawionej publikacji wykonałem następujące zadania:

Opracowałem warunki oraz wykonałem badania wytrzymałości na rozciąganie próbek sieci polimerowych.

APawlak

Dr hab. inż. Andrzej Pawlak

Oświadczenie wydane na prośbę mgr. inż. Mateusza Grabowskiego w związku z przygotowaniem pracy doktorskiej.

dr inż. Witold Szymański
Instytut Inżynierii Materiałowej
Wydział Mechaniczny
Politechnika Łódzka
ul. Stefanowskiego 1/15
90-537 Łódź

08.10.2024

Oświadczenie współautora publikacji

Oświadczam, że w ramach przygotowania następującego artykułu naukowego:

1. Grabowski, M.; Kost, B.; Bartniak, M.; Bociąga, D.; Szymański, W; Bednarek, M. Copolymerization of lactide with functional epoxide as a way to the polymer network with dually active tetraphenylethane groups. Polymer. 2024;312:127673. doi:10.1016/j.polymer.2024.127673

W wyżej przedstawionej publikacji wykonałem następujące zadania:

Opracowałem warunki oraz wykonałem badania twardości i modułu sprężystości wzdłużnej próbek sieci polimerowych metodą nanoindentacji.

.

dr inż. Witold Szymański

Oświadczenie wydane na prośbę mgr. inż. Mateusza Grabowskiego w związku z przygotowaniem pracy doktorskiej.

dr hab. inż. Magdalena Lipińska
Instytut Technologii Polimerów i Barwników
Wydział Chemiczny
Politechnika Łódzka
ul. Stefanowskiego 16
90-537 Łódź

Łódź dn. 11.07.2024

Oświadczenie współautora publikacji

Oświadczam, że w ramach przygotowania następującego artykułu naukowego:

1. Bednarek M, Grabowski M, Lipińska M, Pawlak A. Reversible polymer networks based on polylactide with tetraphenylethane thermally dissociating groups in crosslinks. Polym Adv Technol. 2024;35(4):e6390. doi:10.1002/pat.6390

W wyżej przedstawionej publikacji wykonałam następujące zadania:

Opracowałam warunki oraz wykonałam badania reologiczne, mające na celu scharakteryzowanie i zbadanie dynamicznego charakteru sieci polimerowych.

dr hab. inż. Magdalena Lipińska

Magdalena Lipińska

Oświadczenie wydane na prośbę mgr. inż. Mateusza Grabowskiego w związku z przygotowaniem pracy doktorskiej.

mgr inż. Mateusz Bartniak
Instytut Inżynierii Materiałowej
Wydział Mechaniczny
Politechnika Łódzka
ul. Stefanowskiego 1/15
90-537 Łódź

08.10.2024

Oświadczenie współautora publikacji

Oświadczam, że w ramach przygotowania następującego artykułu naukowego:

1. Grabowski, M.; Kost, B.; Bartniak, M.; Bociąga, D.; Szymański, W; Bednarek, M. Copolymerization of lactide with functional epoxide as a way to the polymer network with dually active tetraphenylethane groups. Polymer. 2024;312:127673. doi:10.1016/j.polymer.2024.127673

W wyżej przedstawionej publikacji wykonałem następujące zadania:

Opracowałem warunki oraz wykonałem badania reologiczne próbek sieci polimerowych.

.

Mateusz Bartniak

mgr inż. Mateusz Bartniak

Oświadczenie wydane na prośbę mgr. inż. Mateusza Grabowskiego w związku z przygotowaniem pracy doktorskiej.

dr hab. inż. Dorota Bociąga, prof. uczelni
Instytut Inżynierii Materiałowej
Wydział Mechaniczny
Politechnika Łódzka
ul. Stefanowskiego 1/15
90-537 Łódź

08.10.2024

Oświadczenie współautora publikacji

Oświadczam, że w ramach przygotowania następującego artykułu naukowego:

1. Grabowski, M.; Kost, B.; Bartniak, M.; Bociąga, D.; Szymański, W; Bednarek, M. Copolymerization of lactide with functional epoxide as a way to the polymer network with dually active tetraphenylethane groups. Polymer. 2024;312:127673. doi:10.1016/j.polymer.2024.127673

W wyżej przedstawionej publikacji wykonałam następujące zadania:

Prowadziłam merytoryczny nadzór nad badaniami reologicznymi próbek sieci polimerowych.

Dorota Bociąga

dr hab. inż. Dorota Bociąga, prof. uczelni

Oświadczenie wydane na prośbę mgr. inż. Mateusza Grabowskiego w związku z przygotowaniem pracy doktorskiej.

Publikacja 1:

Mateusz Grabowski, Bartłomiej Kost, Bartłomiej Gostyński, Melania Bednarek. Can tetraphenylethane (TPE) “iniferter” group be introduced into the polymer chain by coupling TPE diol with diisocyanate? *Polymer*. 2022;246:124738. doi:10.1016/j.polymer.2022.124738

Polymer 246 (2022) 124738

Contents lists available at ScienceDirect

Polymer

journal homepage: www.elsevier.com/locate/polymer

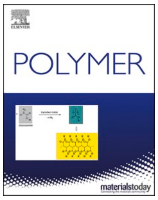

Can tetraphenylethane (TPE) “iniferter” groups be introduced into polymer chains by coupling TPE diol with diisocyanates?

Mateusz Grabowski, Bartłomiej Kost, Bartłomiej Gostyński, Melania Bednarek *

Centre of Molecular and Macromolecular Studies, Polish Academy of Sciences, Sienkiewicza 112, 90-363, Lodz, Poland

ARTICLE INFO

Keywords:
Tetraphenylethane
Benzopinacol
Iniferter
Diisocyanates
Polyurethane

ABSTRACT

Several different articles have appeared in recent years concerning the application of tetraphenylethane (TPE) groups, which are able to dissociate to free radicals under mild heating, for the initiation of radical polymerization of vinyl monomers. It has been claimed that the TPE group is introduced into the polymer chain by the reaction of 1,1,2,2-tetraphenyl-1,2-ethanediol (TPED) with diisocyanate, optionally with the application of the additional oligodiol. This approach is based on the presumed reaction of the isocyanate group with a tertiary hydroxyl group that is supposed to form urethane linkages. In the present study, we checked whether such a reaction can indeed occur under the applied conditions. A kinetic study of the reaction of poly(tetrahydrofuran) diol plus TPED or polylactide diol plus TPED with diisocyanate (aromatic or aliphatic) was performed in two different solvents, and conversion of isocyanate groups was followed by FT IR spectroscopy. Independently, the kinetics of the reaction of TPED alone with diisocyanates were investigated. The products of the reactions were analyzed by the ^{1}H NMR method for the expected consumption of tertiary –OH groups and urethane bond formation. Theoretical calculations for the reactivity of tertiary –OH groups in TPED with isocyanate groups are presented as additional proof that this reaction should not proceed under the conditions applied in earlier papers. A new approach to the introduction of TPE units into polymer structures is suggested.

1. Introduction

The methods for polyurethane synthesis have been described in numerous scientific monographs and are the subject of many scientific articles [1–6]. Polyurethane (PU) preparation is a technological process known for many years that is still being improved and modified according to specific requirements. Thus, it can be concluded that the reactions proceeding during the PU preparation are well known as well as the way of conducting the process. The reaction of diisocyanates with different di- or multihydroxyl compounds – low molecular weight and oligomeric in nature – is also useful as a method for introducing desired functional groups or oligomeric segments into the polymer structure. The conditions of such reactions should be selected individually for each reaction, as the reactivities of the –NCO and –OH groups can vary considerably. Adapting the procedure described in one article may not work with the use of a different reagent.

A coupling reaction with diisocyanates was also applied to introduce the initiating group into the polymer structure for the polymerization of a new monomer. Prepared in such a way, polyurethane serves as a “macroiniferter”. The concept of an iniferter that initiates, transfers, and/or terminates free radical polymerization has been developed to have better control over the polymerization process [7]. As an iniferter, the tetraphenylethane (TPE) has been used among many others. This group undergoes homolytic cleavage at a temperature above 60 °C with the generation of radicals (see Scheme 1), which can react with unsaturated compounds [8–11].

Several articles have appeared wherein PU iniferter synthesized by coupling TPE diol with diisocyanate has been used to initiate the polymerization of styrene (St) and acrylates [12–15]. There are also several works in which TPE groups are placed into PU-containing segments of other polymers, such as poly(tetrahydrofuran) (PTHF), poly(ethylene oxide) (PEO), poly(propylene oxide) (PPO), or poly(ε-caprolactone) (PCL) [16–22]. These polyurethanes act as “macroiniferters” for the polymerization of styrene and methacrylates. Macroiniferters are prepared via two steps. First, oligodiol is reacted with a diisocyanate in the bulk at elevated temperature with a twofold excess of aromatic diisocyanate – toluene diisocyanate (TDI) or 4,4′-diphenylmethane diisocyanate (MDI). When half of the –NCO group is reacted (as claimed by

---

* Corresponding author.
E-mail address: bednarek@cbmm.lodz.pl (M. Bednarek).

https://doi.org/10.1016/j.polymer.2022.124738
Received 21 December 2021; Received in revised form 7 March 2022; Accepted 8 March 2022

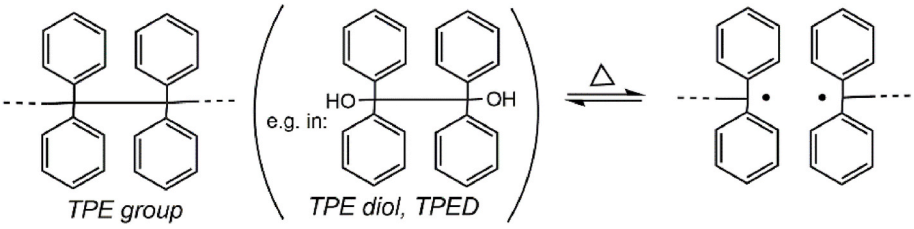

Scheme 1. TPE group dissociation.

the authors), the reacting system is cooled to 25–35 °C, and then TPED (alone or in a solvent) is added and reacted for 24 or 48 h at this temperature [16–22]. In the performed syntheses of polyurethanes, the –NCO group reacts with the primary –OH group of PTHF diol (or secondary –OH in the case of PPO) in the first step, and in the following step, the remaining –NCO groups, according to the authors, react with tertiary –OH hindered by bulky phenyl groups.

We attempted to introduce TPE groups into the polylactide chain by adapting the described procedures, but the coupling of polylactide (PLA) diol with TPED using diisocyanates did not proceed. This observation suggests that perhaps the –OH groups present in TPED diol are not sufficiently reactive and prompted us to take a closer look at papers that have been published earlier.

As proven by extensive research, the reactivity of the –NCO group toward different hydroxyl compounds has been studied and differs markedly. Whereas the reactivity of the –NCO group toward primary –OH in the uncatalyzed reaction is 100 in relative units, the reactivity toward secondary –OH is 30 and toward tertiary –OH is only 0.5 [6] and can still be reduced when the –OH group is surrounded by bulky groups such as phenyl groups in TPED. Thus, the reactivity of tertiary –OH is at least two orders of magnitude lower than that of primary –OH groups. In light of these data, it appears that the reaction of a diisocyanate with TPED to form polyurethane cannot proceed under the available reaction conditions.

Based on the texts of the abovementioned articles, it is not clear if the TPE moiety is introduced into the formed "polyurethane" via chemical (urethane) linkages. Although -NH- groups are shown in the ^{1}H NMR spectra and some of them are assigned to urethane groups formed by the reaction of tertiary –OH from TPED, it was not verified [16]. The number of TPE units in the PU chain was calculated from the molecular weight of the polymer with the assumption that all reacted TPED should be incorporated into the polymer chain. Obtained in this way, PU was washed with methanol to remove unreacted TPED; however, there is no evidence that the remaining TPED is chemically bound to the polymer. It was shown that the next step, i.e., initiation of styrene polymerization is successful. It appears that for the case of PEO diol, the formed PU contains chemically bound TPE because the M_n of PU increases with the conversion of St, and essentially one peak is present in the GPC curve (although a small fraction of lower M_n remains, as indicated by a shoulder for this main peak). For the case of PU prepared from poly(propylene oxide) diol, where terminal secondary –OH groups of the diol are supposed to be much less efficient in PU formation, the authors obtained PU with a smaller M_n and bimodal distribution. The lower M_n was explained by inefficient initiation of St polymerization. It appears that inefficient initiation may explain the smaller M_n but not the bimolecular GPC curve. The polymerization of styrene resulting in the St homopolymer can be explained by the initiation with TPED not incorporated in the PU chain, as well as by styrene thermal polymerization. Other authors have presented ^{1}H NMR spectra for polyurethanes prepared by a similar procedure using PTHF and TPED in which only signals corresponding to all components of PU synthesis are visible. [21,22]. Signals corresponding to -NH- protons from the formed urethane were omitted. Additionally, in the IR spectra, urethane groups are not highlighted at all.

As mentioned above, during our preliminary study concerning the introduction of TPE groups into the polymer chain by coupling polylactide diols with TPED using diisocyanate, we encountered considerable difficulties. After repeated washing of the obtained polyurethane with methanol, it was found to contain only traces of TPE groups. Thus, we decided to perform a kinetic study of the reaction of a diisocyanate with oligodiols, such as poly(tetrahydrofuran) diol (PTHF) or polylactide diol and TPED, performed in two steps. First, oligodiol was reacted with diisocyanate added in twofold excess, and then TPED was added. Aromatic diisocyanate (MDI) was used for the coupling reaction with PTHF diol bearing primary –OH groups, similar to previous works described by some authors in a few of the abovementioned articles [16,21,22], and aliphatic hexamethylene diisocyanate (HDI) was used independently. The same diisocyanates were further applied for coupling reactions with the application of PLA diol (the reaction pathway is presented in Scheme 2). The conversion of –NCO groups was followed by the ATR-FT IR method. The same conditions for both stages, i.e., synthesis of oligodiol prepolymer bearing isocyanate groups and addition of TPED to this prepolymer were applied. This is the difference between our method of PU synthesis compared with that presented in previous articles where the first step is performed in the bulk at higher temperature (60–70 °C) [16,21,22] and the addition of TPED is performed in solution at 30–35 °C. Thus, we took into account that our first step for the synthesis will proceed more slowly than that described in the

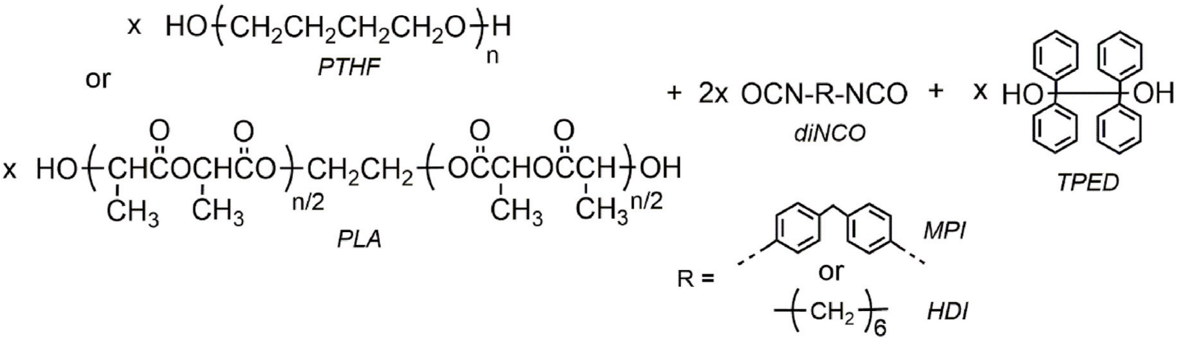

Scheme 2. Components of the kinetic investigation.

reported articles, but the crucial second step should proceed similarly. The obtained products were analyzed with respect to their composition and structure by ^{1}H NMR and IR methods. However, the aim of this work was not to obtain specific polyurethanes and their precise analysis but only to show that TPED is not reactive with isocyanate under the conditions described in previous articles.

2. Experimental

2.1. Materials

L,L-Lactide from Purac was recrystallized from 2-propanol, sublimated and stored under vacuum. PTHF, M_n 650 (600 as determined by ^{1}H NMR) was received from Sigma-Aldrich and dried in vacuum at 50 °C. Tetraphenylethane diol (TPED, 99%), hexamethylene diisocyanate (HDI, 99%), 4,4′-methylenebis(phenyl isocyanate) (MDI, 98%), 2-bromoethanol (95%), and 4-hydroxybenzophenone (HBP, 98%), all from Sigma–Aldrich, were used as received.

Ethylene glycol (EG, 99.8%) was purchased from Sigma–Aldrich and distilled before use. Trifluoromethanesulfonic acid from Aldrich (trifilic acid, 99%) was distilled under vacuum, and dibutyltin dilaurate (DBTDL, 98%) from ABCR was used as received. Dichloromethane (DCM, 99,8%), dichloroethane (DCE, pure p.a.), and dimethylacetamide (DMA, pure p.a.) from POCH Poland, 2-butanone (MEK, 99%) from Sigma–Aldrich were dried with $CaH_{2,}$ distilled before use and then stored over molecular sieves (4 Å). Chloroform (pure p.a.), 2-propanol (pure p.a.), methanol (pure p.a.) and hexane (99%), all from POCH, were used as received. Potassium hydroxide (pure p.a.) from POCH and magnesium sulfate ($MgSO_4$, 99%) from CHEMPUR Poland were used as received.

2.2. Synthesis of polylactide diol

Three grams (20 mmol) of L-lactide together with a stirring bar was placed into a Schlenk flask, which was evacuated for 0.5 h and then backfilled with N_2. Then, 9 mL of DCE was introduced through the rubber septum with a syringe, followed by the addition of ethylene glycol as an initiator (95 μL, 1.69 mmol) and triflic acid as a catalyst (60 μL, 0.68 mmol). Polymerization was performed at room temperature for 24 h. The polymer was precipitated to methanol and hexane.

2.3. Kinetic experiments

In all kinetic experiments for the reaction of polymer diol with diisocyanaate followed by the addition of TPED (where possible), the initial molar ratio of diisocyanate to polymer was equal to 2, while in experiments where only the kinetics of TPED with diisocyanate were studied, the ratio of diNCO to TPED was equal to 1. Reactants and solvents were dried before being placed into the reaction flask. When HDI was applied as diNCO, it was injected into the total amount of reacting solution. When MDI was applied, the starting reagent was dissolved in half of the solvent, and MPI was dissolved in the second half of the total volume. For the exemplary kinetics of PTHF-diol with HDI in DMA, 0.55 g of PTHF (M_n = ~600, 0.92 mmol) was dissolved in 4 mL of DMA in a flask containing 3 inlets from which the vertical inlet had a diameter appropriate for the connection with the measuring arm connected to the IR spectrometer. The flask containing the polymer solution and stirring bar was connected to the IR arm and purged with argon through side inlets. The inlets were closed rapidly with a stopcock and rubber septum and additionally protected from moisture by parafilm. The flask was immersed in an oil bath preheated to 40 °C. Then, HDI (1.84 mmol, 309 mg, 294 μL) was added to the vessel through the septum with a syringe, followed by the addition of the catalyst (15 mL, 1,4 mol.% with respect to –NCO groups). The IR spectra were recorded from the moment of adding diNCO. The observed changes in the intensity of the –NCO signal at ~2270 cm^{-1} allowed for the determination of the time for 50% conversion at which TPED should be added. Thus, ~2 mL of reacting solution was withdrawn and introduced with a syringe to a small flask containing TPED (337 mg, 0.92 mmol) closed with a rubber septum under an inert atmosphere. After dissolving TPED, the solution was reintroduced with the syringe to the reaction mixture. The progress of the reaction was followed up to the stabilization of the concentration of –NCO groups (or up to their consumption in one experiment).

2.4. Synthesis of TPED derivative containing primary hydroxyl groups (TPED_diET)

A total of 1.68 g (43 mmol) of potassium hydroxide was dissolved in 2.5 ml of distilled water in a beaker. Then, the solution was added to 5 g (25 mmol) of 4-hydroxybenzophenone in a round bottom flask. The resulting yellow reaction mixture was stirred at 70 °C until HBP was dissolved. Next, 4 ml (54 mmol) of 2-bromoethanol was added via a syringe, and the stirring was continued for 24 h. The aqueous phase was subjected to extraction with chloroform 3 times, and the organic phase was extracted with distilled water 3 times. The combined organic extracts were dried with $MgSO_4$. The solvent was evaporated under vacuum, and the resulting product was recrystallized by dissolving in 4 mL of ethanol while heating. Then, excess diethyl ether was added and cooled down, which resulted in crystal growth. The white crystals of HBP_ET were dried under vacuum and obtained with a yield of 50%. In the next step, HBP_ET was placed into a quartz flask to which isopropanol (8 mL for every 1 g) was added. The flask was closed with a rubber septum and purged with nitrogen (with a needle) for 15 min. Then, the flask content was slightly heated until the mixture was dissolved. The homogenous solution was exposed to ultraviolet light (365 nm) for 24 h. The resulting white precipitate TPED_diET was then centrifuged from the rest of the reaction mixture and dried under vacuum (>99% pure, ^{1}H NMR, Fig. S2 in Supporting Information).

2.5. Computational methods

All calculations were performed with the B3LYP-GD3/LANL2DZ level of theory; the solvent (N,N-dimethylacetamide) was modeled as a polarizable continuum model (CPCM), and the temperature was set to 315.15 K. Geometry minimization and relaxed potential energy surface (PES) scans with a subsequent further optimization of their stationary points were performed. Vibrational analysis (no frequency scaling factor used) confirmed that PES stationary points found in the course of the computations are indeed proper minima and first-order transition states. ESP mapping was performed with an isovalue for the total electron density equal to 0.0004.

2.6. Instrumental methods

^{1}H NMR spectra for the synthetized PLA polymers were recorded in $CDCl_3$ using a Bruker Avance 400 Neo instrument operating at 400 MHz.

Size exclusion chromatography (SEC) was performed using an Agilent Pump 1100 Series with an Agilent G1379A Degasser, a set of two PL-Gel 5 μm mixed-C columns, and a Wyatt Optilab Rex interferometric refractometer for the analysis of oligodiols. Dichloromethane was used as an eluent at a flow rate of 0.8 mL·min^{-1} at room temperature. The system was calibrated with polystyrene standards. The product of the kinetic reaction of PLA oligodiol with TPED_diET and HDI was analyzed with a Wyatt (Dernbach, Germany) instrument equipped with two Perfect Separation Solutions (PSS) columns and one guard column (GRAM Linear, (10 μm, *Mn* between 800 and 1,000,000 Da) and differential refractometer (RI) and light scattering (LS) detectors. The measurement was performed in DMF as an eluent, containing 50 mmol LiBr, at a flow rate of 1 mL/min (calibration with polystyrene standards).

Matrix-assisted laser desorption ionization – time of flight (MALDI TOF MS) experiments were performed using an Axima-Performance TOF

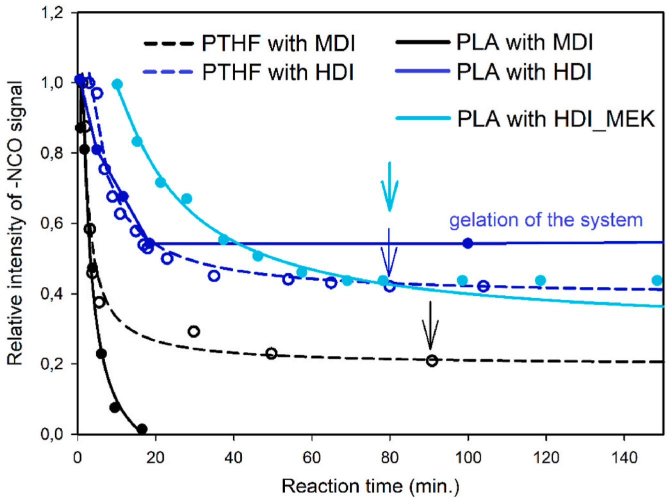

Fig. 1. Conversion of –NCO groups versus time for reactions of PTHF-diol (dashed line) and PLA-diol (solid line) with diisocyanates performed in DMA, plus additional reaction of PLA in MEK. Reactions performed at 40 °C; Arrows indicate the addition of TPED.

spectrometer (Shimadzu Biotech, Manchester, UK) equipped with a nitrogen laser (337 nm). The pulsed extraction ion source accelerated the ions to a kinetic energy of 20 keV. Dithranol was used as a matrix and KBr was used as a cationating agent.

Fourier transform infrared spectroscopy (FTIR) measurements were performed using a Thermo Scientific Nicolet 6700 instrument with an ATR (attenuated total reflectance) GoldenGate accessory and a DTGS (deuterated triglycine sulfate) detector. The spectra were obtained by adding 64 scans at a resolution of 2 cm^{-1}.

UV coupling was performed in a photochemical reactor (RayonetRPR-200, Southern New England, USA) equipped with 12 UV lamps ($\lambda = 365$ nm) and a magnetic stirrer.

3. Results and discussion

3.1. Kinetics for the reaction of oligodiols and TPED with diisocyanates by FT IR measurements

The reaction was performed in solution (in DMA or in MEK) to enable its course to be followed by IR measurements. The oligodiol (PTHF or PLA) was dissolved in a solvent in a reaction vessel, and after purging the vessel with nitrogen and reaching the reaction temperature of 40 °C, the diisocyanate (dissolved in DMA for the case of MDI) with a molar ratio of 2:1 with respect to oligodiol was added through the septum followed by the addition of a catalyst (with the same amount used in all experiments, i.e., 1.8 mol% with respect to –NCO groups). After approximately half of the initial amount of –NCO groups was reacted, TPED equimolar to oligodiol was introduced (where possible) without additional solvent (see Experimental section). The changes in the intensity of the signal corresponding to –NCO groups in the IR spectra represent the conversion of these groups with time. Fig. 1 presents kinetic curves for the reactions performed for diisocyanates with diols.

It is visible in Fig. 1 that oligodiols react with –NCO groups at different rates depending on the type of hydroxyl group at the end of the oligodiol and on the type of diisocyanate (reactivity of –NCO group). In all experiments, after the introduction of diisocyanate to the reaction vessel, a signal corresponding to –NCO groups is observed, whose intensity is decreased after the addition of the catalyst, and this decrease is noticeably faster (at least at the first stage of the reaction) for aromatic diisocyanate. For the case of the reaction with PTHF diol with MDI performed in DMA solution, after relatively fast consumption of half of the initial amount of –NCO groups, they still react slowly, and after addition of TPED, when the amount of –NCO groups are stabilized at the level of 0.2 of the initial amount, further conversion is stopped. The reason that the consumption of –NCO groups in the first step of the reaction does not stop at the level of 0.5 is explained further in the text. During 20 h of the kinetic study, no further consumption of –NCO was observed at relatively low temperatures, i.e., 40 °C (kinetic plot for the whole time range of the reaction is presented in Fig. S5). For the case of aliphatic diNCO, the reaction with PTHF is stopped after half of the –NCO groups are reacted. For the case of PLA diol, the reaction proceeds differently depending on the diisocyanate used. When aromatic MDI is added, the concentration of –NCO groups drops to zero in a short time. When aliphatic HDI is used, the concentration of –NCO drops to a certain value and then remains at this level to decrease slowly with time. However, gelation of the reaction mixture was observed after approximately 1.5 h; thus, no addition of TPED was performed. To explain the different rates for the studied reactions, the reactivities of different diisocyanates with different diols (with hydroxyl groups of different reactivity) should be compared (Table 1).

Table 1
Experimental effective rate constants for reactions of 1,3-butandiol (1,3-BD) and 1,4-butandiol (1,4-BD) with aliphatic and aromatic diisocyanates [23].

C_{cat} x 10^4 mol/L	Effective rate constant k_{eff} x 10^5, L/(g-equiv. s)							
	HDI [a]		TDI [a]				MDI [a]	
	1,3-BD	1,4-BD	1,3-BD		1,4-BD		1,3-BD	1,4-BD
			k_1 [b]	k_2	k_1 [b]	k_2		
0	0.3	0.5	12	0.3	45	1.0	1.8	5.2
4	64	130	292	42	750	92	480	520

[a] HDI = hexamethylene diisocyanate, TDI = toluene diisocyanate, MDI = 4,4′-diphenylmethane diisocyanate.

[b] Calculated values.

Based on the results of other researchers, it is obvious that aromatic diisocyanate is noticeably more reactive than aliphatic diisocyanate. The rate constant of the uncatalyzed reaction of MDI with a diol possessing primary –OH groups is approximately 10 times higher than that of the reaction of HDI. The catalyst increases the rate constant values many times (up to 260 times!) and reduces the difference between those for aromatic and aliphatic diisocyanates (in the presence of a catalyst, the rate constant for the reaction of the primary diol with aromatic diisocyanate is 4 times higher than that for the reaction with aliphatic diisocyanate). From the data given in Table 1, it is also evident that diol containing one secondary –OH group reacts slower than the diol with two primary groups (for the uncatalyzed reaction, the rate constant is approximately 3 times lower for aromatic MDI and 2 times lower for aliphatic HDI). The presented data may be helpful in explaining the kinetics observed for the system studied here.

As shown by the kinetic plots, aromatic diisocyanate reacts relatively quickly with the terminal primary –OH group in PTHF diol. Surprisingly, PLA diol with secondary –OH end-groups reacts even faster with aromatic diisocyanate than PTHF diol. The –NCO groups disappear quickly despite the twofold excess used. Evidently, they are consumed in side reactions, which may be the reaction with DMA solvent (the reaction with amide group) or the uncatalyzed thermal formation of carbodiimides from aryl isocyanate or isocyanurate (cyclic trimer of isocyanate) formation [24–26]. All these side reactions are usually prompted by using aromatic diisocyanate, but for the case when this isocyanate reacts with primary –OH groups, the formation of urethane bonds occurs predominantly. For the case of the reaction of aromatic isocyanate with less reactive tertiary hydroxyl groups, side reactions dominate.

The less reactive aliphatic diisocyanate reacts more slowly with PLA diol (both in DMA and MEK solvents), evidently with limited side reactions. After a certain time, the conversion of the –NCO groups stops. For the case of the reaction in DMA, the reaction mixture forms a gel (this may confirm the side reaction between –NCO groups and DMA),

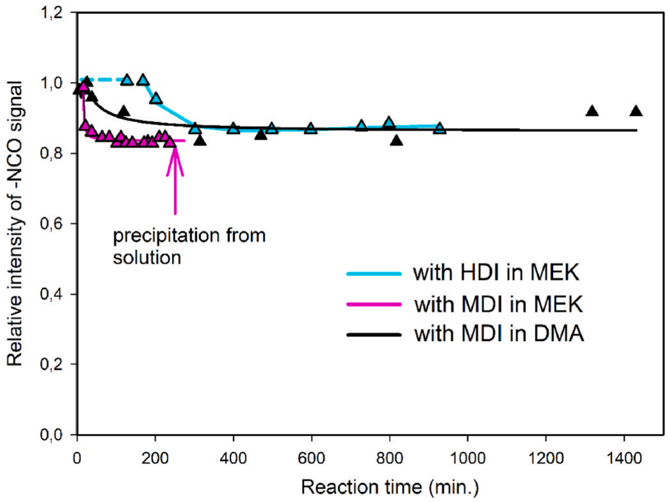

Fig. 2. Conversion of –NCO groups versus time for reactions of TPED with diisocyanates in MEK or DMA solvents; Reactions performed at 40 °C.

which makes it impossible to add TPED. For this reason, the reaction was repeated in MEK. In this case, when the concentration of –NCO groups attained a stable level (approximately half of the initial amount), TPED was introduced, which did not lead to further conversion of the –NCO groups.

To confirm that diisocyanates cannot react with tertiary –OH groups in TPED diol, additional experiments were performed to check the kinetics of the reaction of TPED with an equimolar amount of diisocyanate in the presence of ~1.8 mol% dibutyltin dilaurate catalyst. The results are shown in Fig. 2.

It is evident from the plots presented in Fig. 2 that no more than 10% of the initial amount of –NCO groups is consumed within 24 h of the experimental duration.

3.2. Structure of the products of kinetic investigations

Further confirmation of the inactivity of the –OH groups present in the TPED molecule in the formation of the urethane bond with isocyanates can be found in the ^{1}H NMR spectra obtained for the products of the reactions of TPED with diisocyanates (Fig. 3). The analyzed product of the reaction with HDI is separated from the reaction medium by self-precipitation, and the product of the reaction with MDI is separated by evaporation of solvents (thus, it also contains unreacted diisocyanate).

In both ^{1}H NMR spectra, apart from signals corresponding to the phenyl groups from TPED and phenyl groups from a diisocyanate, when MDI is used, the signals corresponding to –OH groups from TPED are visible. By comparison of the intensities of signals corresponding to -OH groups to those corresponding to phenyl groups (taking into account the number of protons in the groups under consideration - the calculation method is explained in Supporting Information), it can be calculated that after the reaction of TPED with aliphatic diisocyanate and aromatic diisocyanate, 88% and 64% of the -OH groups remain, respectively. The presence of small signals at 7.5–7.8 ppm (close to signals characteristic of TPED aromatic protons) and at 5.75 ppm (close to the signal corresponding to the –OH group from TPED) is indicative of TPED decomposition. These results (although with some error due to inaccuracies resulting from measurements of the signal intensity in the NMR spectra) show that most –OH groups remain unreacted (with a slightly larger conversion obtained when MDI is applied); this is in agreement with kinetic experiments where a small conversion of isocyanate groups is observed, which may also be due to any side reactions mentioned earlier in the text.

Similarly, for the product of the kinetic study of the reaction of polylactide with aliphatic diisocyanate, followed by the addition of TPED, no conversion of –OH groups present in TPED was detected (Fig. 4).

By comparison of the intensities of appropriate signals, it can be calculated that all of the tertiary hydroxyl groups present in TPED (and in the reaction mixture) remain unreacted. In the precipitated product, less than 20% of the used TPED remains, and the remaining TPED also contains unreacted –OH groups.

FT IR analyses for the products of the reaction of diisocyanates with diols in both systems, that is, with or without the PTHF/PLA oligodiol, show that in the IR spectra, the signal corresponding to the formed -NH- group (in the urethane group) at 3230–3470 cm^{-1} is easily detected when oligodiol is used. When only TPED is reacted, this -NH- band is not observed. (see Fig. 5).

Referring to previously cited articles about allegedly obtained polyurethanes with incorporated TPED (with and without additional oligodiol) [12,16], we tried to again analyze the results shown by the authors. From the ^{1}H NMR spectra of the obtained polyurethanes, the signals in the range of 8.5–10.0 ppm, which are assigned to -NH- protons from urethane groups formed by the reaction of toluene diisocyanate (TDI) with TPED, can also correspond to urethane groups formed by the reaction of water or methanol, which was checked within this work by spectral simulation using Mestrec software. In the ^{1}H NMR spectra presented by some other authors [21,22], the signals corresponding to protons from urethane groups are not indicated.

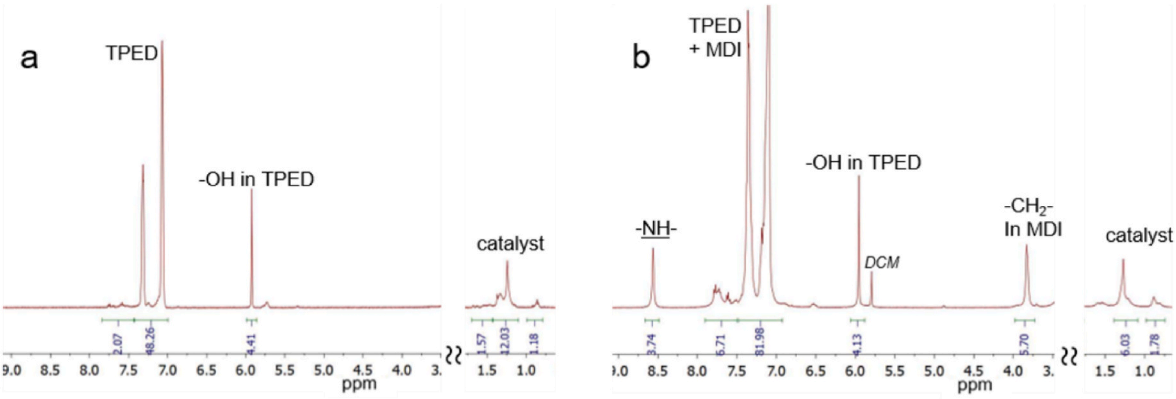

Fig. 3. ^{1}H NMR spectra (DMSO-d_6) for the products of the reaction of TPED with diisocyanates: a) with HDI in MEK as a solvent, b) with MDI in DMA as a solvent.

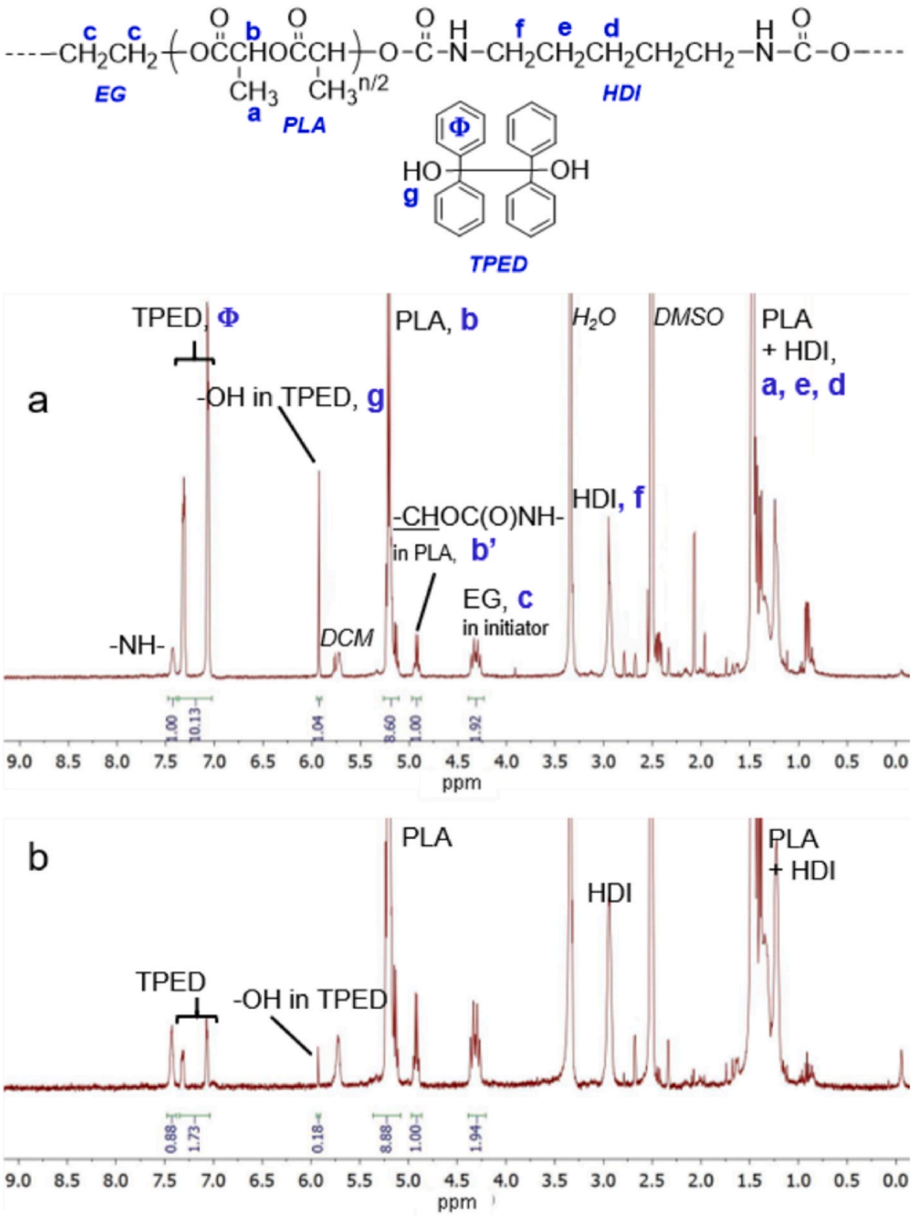

Fig. 4. ^{1}H NMR spectra for the product of the kinetic reaction of PLA with HDI in MEK: a) after evaporation of solvents, b) precipitated to methanol (both evaporation and precipitation after 24 h of the reaction).

3.3. Computational part

The inability of –OH groups present in TPED diol to react was also confirmed by theoretical calculations.

To further clarify the observations about the course of the reaction of TPED with diisocyanates under organotin catalysis discussed above, we decided to perform computational studies concerning the possible obstacles within the mechanistic route proposed in the literature. The latter, according to computational papers [27–30], consists of several stages:

- creation of the DBTDL-alcohol catalytic complex;
- subsequent urethane bond formation;
- release of the newly formed urethane and creation of the catalyst-product complex.

Unfortunately, the cited literature deals mostly (if not only) with the mechanism for monohydroxyl alcohols. However, after detailed scrutiny of the existing literature, we found [31] that the catalytic mechanism postulated for diols differs only to the extent that the diols form a bidental, tetragonal-bipyramid complex with DBTDL (i.e., two instead of one of their –OH groups are engaged in forming the complex) where the two diol-DBTDL bonds form the basis of the pyramid. This very issue appears to us to be the most salient because it could prevent the TPED moiety from successfully forming the catalytic complex as it requires the adaptation of a synclinal/synperiplanar conformation.

Computations were performed for TPED and for much less sterically hindered 1,2-ethandiol (ethylene glycol, EG) for comparison. The results indicate that the most stable TPED conformation is indeed the antiperiplanar conformation (Fig. 6), the antiperiplanar-to-synclinal transition is slightly thermodynamically unfavorable and the energy barrier accompanying the transition state (TS) is considerable; whereas for the case of EG, both thermodynamic factors are much more favorable (Table 2). The control experiment engaging the EG proceeded without any difficulties.

Based on the Eyring equation (Eq. (1):

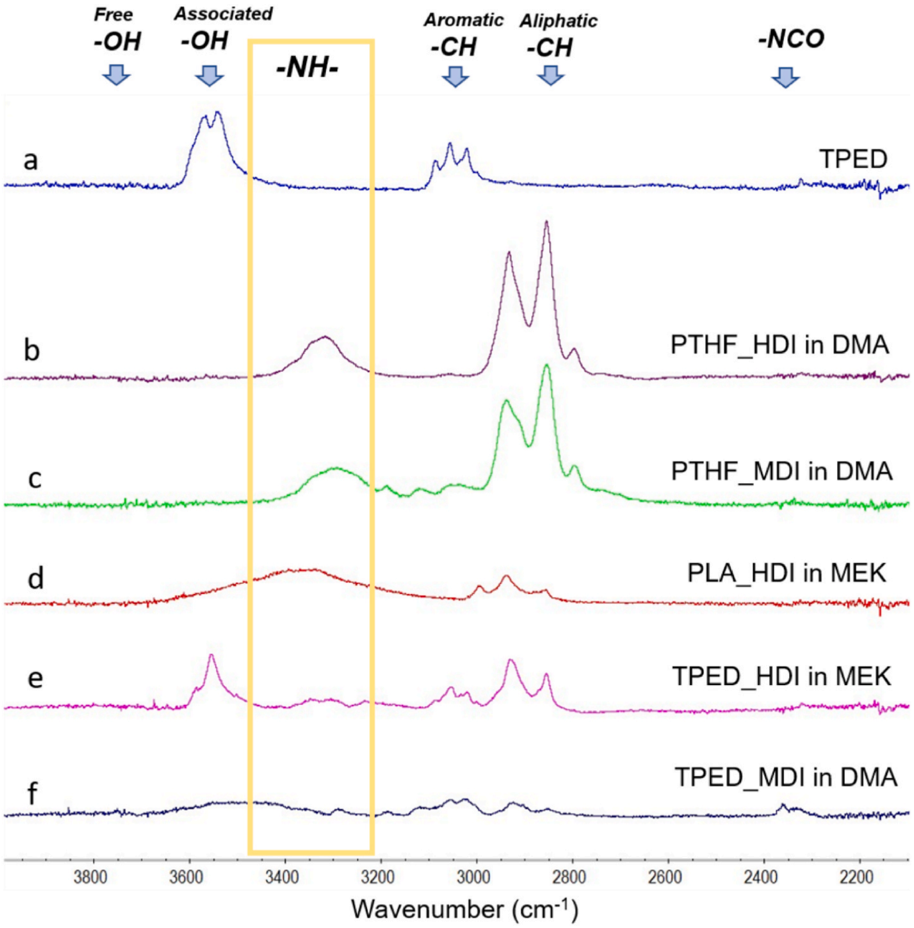

Fig. 5. Fragments of FT IR spectra for the products of kinetic experiments; Products b, c, d (with oligodiols) were separated by precipitation to methanol, Product e was separated by evaporation of the solvent, Product f – by self-precipitation.

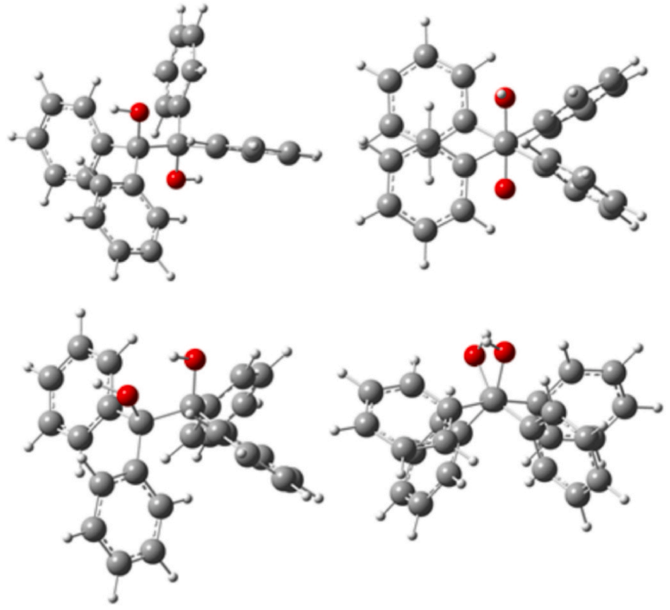

Fig. 6. Antiperiplanar (up) and synclinal (down) conformations of TPED; –OH groups are in red. (For interpretation of the references to color in this figure legend, the reader is referred to the Web version of this article.)

Table 2
ΔG and $\Delta G^{\ddagger}$ (free energy change for the reaction and its Gibbs' activation energy respectively) for antiperiplanar-to-synclinal transition for both examined diols and their rate constants ratio (calculated for T = 315.15 K).

Diol	ΔG [kJ/mol]	$\Delta G^{\ddagger}$ [kJ/mol]	rate constants ratio
TPED	10.5	72.1	$\frac{k_{TPED}}{k_{EG}} = 1.34{\cdot}10^{-10}$
EG	−10.1	12.2	

$$k = \frac{\kappa k_B T}{h} e^{-\frac{\Delta G^{\ddagger}}{RT}} \tag{1}$$

Eq. 1. Eyring equation

we were able to calculate the ratio of the corresponding rate constants. In our denotation, k is the reaction rate, h and k_B are the Planck and Boltzmann constants, respectively, $\Delta G^{\ddagger}$ is the Gibbs' activation energy (whereas ΔG is understood as the overall change of Gibbs' free energy during the course of the reaction), R is the universal gas constant, T is temperature and κ is the transmission coefficient. The latter is frequently considered to be 1 because it reflects what part of the particles that reach TS turns directly into the product without a need to cross TS again. Therefore, $\kappa = 1$ means that the substrate-to-product transition is in fact unstoppable as soon as the molecule reaches TS, which is a sound assumption, especially for the case of conformational transitions that do not require any electron recombination. In light of our above discussion, it is worth noting that reaction barriers $\Delta G^{\ddagger}$ of approximately 67 kJ/mol appear among the unfavorable reactions that are related to a complete rearrangement of the electronic structures of the reagents [32] and not only to simple conformational changes. Such a significantly high

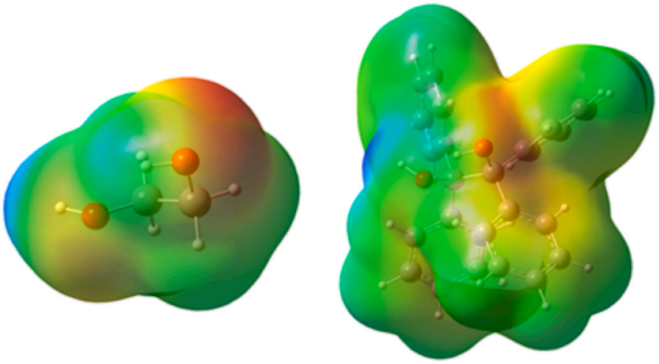

Fig. 7. ESP-mapped surface of the total electronic density for synclinal conformations of EG (left) and TPED (right); The highest electron density is in red. (For interpretation of the references to color in this figure legend, the reader is referred to the Web version of this article.)

barrier for the crucial conformational change as it takes place in our case can easily hamper the TPED ability to undergo the aforementioned polymerization reaction, as indicated by the value of the conformational change rate constant ratio.

The second important factor that needs to be considered is the nucleophilicity of the hydroxyl groups present in both diols. To form the catalyzing complex, hydroxyl groups are required to be sufficiently rich in electrons so as to donate them to the tin center in the later course of the reaction. To obtain some pieces of information about the feasibility of this process, we mapped the electrostatic potential (ESP) on the total density surface for TPED and EG. The results clearly indicate that electrons on at least one of the (H)O- groups of EG are quite easily available (vivid red color), and the EG molecule can, thus, create the catalyzing complex with much more ease than TPED, where the electrons of –OH are buried more deeply and additionally shielded by the steric 'bumps' of the four phenyl rings (Fig. 7).

From the above factors, we conclude that the inability of TPED to undergo reaction even in the presence of the catalyst arises due to steric (high conformational change barrier) and electronic (weak nucleophilicity of –OH groups) factors that prevent the substrate from adapting to both the optimal geometry and reactivity required by the very first steps of the postulated mechanism.

3.4. An alternative method for the introduction of TPE groups into polyurethane structures

All presented results contradict the possibility of creating a urethane linkage in the reaction of TPED diol with diisocyanate. Thus, we decided to obtain a derivative of TPED containing primary hydroxyl groups that could react efficiently with diisocyanate. The first step of this synthesis involved the attachment of the hydroxyethyl group to hydroxybenzophenone (HBP), and the second step involved the coupling of the obtained hydroxyethoxybenzophenone (HBP_ET) to obtain a TPED analog containing two primary –OH groups in the substituents of the phenyl groups (in addition to forming tertiary –OH groups). Coupling step – the reaction known from the synthesis of benzopinacol [33] was performed under UV irradiation in the presence of isopropanol as a proton donor. Scheme 3 presents the reaction pathway.

The obtained TPED derivative was applied by us instead of TPED to introduce a TPE group into a PLA-based polymer by coupling it with PLA diol using HDI as diisocyanate. The kinetics of this reaction were studied in a similar way as for the previous kinetics of PTHF followed by FT IR spectroscopy (see Fig. 8). THF as a solvent was used to replace previous solvents because of the limited solubility of synthesized TPED_diET.

As shown in Fig. 8, isocyanate groups react with PLA diol at a rate that is comparable to reactions in DMA and MEK. When the concentration of –NCO groups reached half of the initial value (and started to stabilize on the kinetic curve), a portion of TPED_diET was added. The concentration of –NCO groups dropped again to reach ~8% of the initial value after approximately 150 min. It is worth remembering that at the same time, HDI diisocyanate practically did not start to react with introduced TPED with tertiary hydroxyl groups in MEK and DMA solutions, as shown above. By showing the huge difference between these data and previous kinetics, the described kinetic experiment with the reactive TPE derivative provides additional support for the inability of isocyanate to react with TPED.

On the other hand, it indicates a way to introduce this group into the polymer chain, although introduced groups contain unreacted tertiary –OH groups, which should be considered when planning further reactions based on this functional polymer approach.

4. Conclusions

Kinetic investigations for the coupling reaction of oligodiols (PTHF or PLA) with tetrafenylethane diol by diisocyanates, performed in two different solvents (DMA and MEK), show that the reaction of the tertiary –OH group present in TPED with isocyanate is not possible at an applied temperature of 40 °C, which is even slightly higher than the temperature used by previous researchers. ^{1}H NMR analyses confirm that the tertiary –OH group remains unreacted in the reaction products. The insufficient

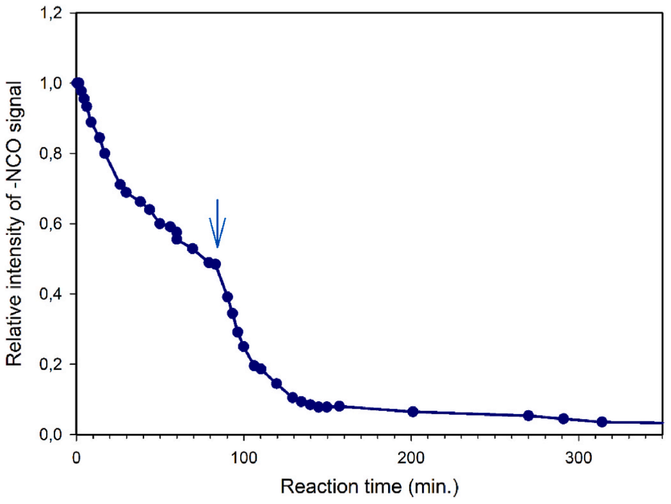

Fig. 8. Conversion of –NCO groups versus time for the reaction of PLA diol with HDI performed in THF at 40 °C; An arrow indicates the addition of TPED_diET.

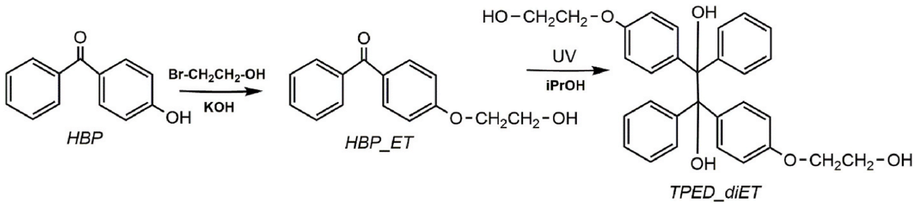

Scheme 3. Synthesis of TPED derivative containing primary hydroxyl groups.

reactivity of tertiary –OH groups (approximately 100 lower than that of primary –OH), as shown by the cited literature data, is unequivocally confirmed by kinetic experiments and thorough analysis of the reaction products. Additional proof for why this reaction does not occur based on steric and electronic factors is obtained from theoretical calculations.

Summarizing the results presented herein, it should be stressed that even if any “polyurethane” material containing TPED inside has been obtained earlier, the TPE group is probably inserted through linkages other than urethane or is physically included inside the prepared polymer (synthesized predominantly from oligodiol and diisocyanate in excess).

Data availability

The raw/processed data required to reproduce these findings cannot be shared at this time due to technical or time limitations.

CRediT authorship contribution statement

Mateusz Grabowski: Investigation, Methodology. **Bartłomiej Kost:** Conceptualization, Methodology, Investigation. **Bartłomiej Gostyński:** Formal analysis, Software. **Melania Bednarek:** Conceptualization, Methodology, Writing – original draft, Writing – review & editing.

Declaration of competing interest

The authors declare that they have no known competing financial interests or personal relationships that could have appeared to influence the work reported in this paper.

Acknowledgements

This work was supported by the National Science Centre in Poland under Grant no 2018/31/B/ST8/01969. This research was supported in part by PL-Grid Infrastructure. Mateusz Grabowski acknowledge Bio-Med-Chem Doctoral School of the University of Lodz and Lodz Institutes of the Polish Academy of Sciences under which this study was conducted.

Appendix A. Supplementary data

Supplementary data to this article can be found online at https://doi.org/10.1016/j.polymer.2022.124738.

References

[1] C. Hepburn, Polyurethane Elastomers, second ed., Elsevier Science Publishers LTD, London and New York, 1992.

[2] J.O. Akindoyo, M.D.H. Beg, S. Ghazali, M.R. Islam, N. Jeyaratnam, A.R. Yuvaraj, Polyurethane types, synthesis and applications-a review, RSC Adv 6 (2016) 114453–114482, https://doi.org/10.1039/c6ra14525f.

[3] J. Datta, P. Kasprzyk, Thermoplastic polyurethanes derived from petrochemical or renewable resources: a comprehensive review, Polym. Eng. Sci. 58 (2018) E14–E35, https://doi.org/10.1002/pen.24633.

[4] F.E. Golling, R. Pires, A. Hecking, J. Weikard, F. Richter, K. Danielmeier, D. Dijkstra, Polyurethanes for coatings and adhesives – chemistry and applications, Polym. Int. 68 (2019) 848–855, https://doi.org/10.1002/pi.5665.

[5] B. Eling, Ž. Tomović, V. Schädler, Current and future trends in polyurethanes: an industrial perspective, Macromol. Chem. Phys. 221 (2020) 1–11, https://doi.org/10.1002/macp.202000114.

[6] M. Ionescu, in: Chemistry and Technology of Polyols for Polyurethanes, 2nd ed., Smithers Rapra Technology Ltd, UK, 2016.

[7] T. Otsu, Iniferter concept and living radical polymerization, J. Polym. Sci. Part A Polym. Chem. 38 (2000) 2121–2136, https://doi.org/10.1002/(SICI)1099-0518(20000615)38:12<2121::AID-POLA10>3.0.CO;2-X.

[8] D. Braun, K.H. Becker, Aromatische pinakole als polymerisationsinitiatoren, Die Angew. Makromol. Chemie. 6 (1969) 186–189.

[9] D. Braun, K.H. Becker, Kinetik der Polymerisationsauslösung mit aromatischen pinakolen, Die Makromol. Chemie. 147 (1971) 91–99, https://doi.org/10.1002/macp.1971.021470108.

[10] D. Braun, K.H. Becker, Aromatic pinacols as polymerization initiators, Ind. Eng. Chem. Prod. Res. Dev. 10 (1971) 386–388, https://doi.org/10.1021/i360040a008.

[11] T. Otsu, A. Matsumoto, T. Tazaki, Radical polymerization of methyl methacrylate with some 1,2-disubstituted tetraphenylethanes as thermal iniferters, Polym. Bull. 17 (1987) 323–330.

[12] K. Tharanikkarasu, G. Radhakrishnan, A novel polyurethane macroinitiator for free radical polymerization, Eur. Polym. J. 30 (1994) 1351–1355.

[13] K. Tharanikkarasu, G. Radhakrishnan, Tetraphenylethane iniferters.3. “living” radical polymerization of methyl methacrylate using toluene-diisocyanate-based polyurethane iniferter, J. Macromol. Sci., Part A Pure Appl. Chem. A33 (1996) 417–437.

[14] K. Tharanikkarasu, G. Radhakrishnan, Tetraphenylethane iniferters. II. Toluene diisocyanate-based polyurethane iniferter for "living radical polymerization of acrylonitrile, J. Polym. Sci. Part A Polym. Chem. 34 (1996) 1723–1731.

[15] K. Tharanikkarasu, G. Radhakrishnan, Living” radical polymerization of styrene using tetraphenylethane-based polyurethane iniferter, Polym. Int. 43 (1997) 13–21.

[16] K. Tharanikkarasu, G. Radhakrishnan, Tetraphenylethane iniferters: polyurethane-polystyrene multiblock copolymers through “living” radical polymerization, J. Appl. Polym. Sci. 66 (1997) 1551–1560.

[17] K. Tharanikkarasu, B.K. Kim, Modification of aqueous polyurethane dispersions via tetraphenylethane iniferters, J. Appl. Polym. Sci. 73 (1999) 2993–3000.

[18] S. Sundar, K. Tharanikkarasu, A. Dhathathreyan, G. Radhakrishnan, Aqueous dispersions of poly(urethane-co-vinyl-pyridine) synthesised from polyurethane macroiniferter, Colloid Polym. Sci. 280 (2002) 915–921, https://doi.org/10.1007/s00396-002-0707-y.

[19] S. Sundar, N. Vijayalakshmi, S. Gupta, R. Rajaram, G. Radhakrishnan, Aqueous dispersions of polyurethane-polyvinyl pyridine cationomers and their application as binder in base coat for leather finishing, Prog. Org. Coating 56 (2006) 178–184, https://doi.org/10.1016/j.porgcoat.2006.04.001.

[20] B.K. Kim, K. Tharanikkarasu, J.S. Lee, Polyurethane-polymethacrylic acid multiblock copolymer dispersions through polyurethane macroiniferters, Colloid Polym. Sci. 277 (1999) 285–290, https://doi.org/10.1007/PL00013758.

[21] G. Zhou, C. Ma, G. Zhang, Synthesis of polyurethane-g-poly(ethylene glycol) copolymers by macroiniferter and their protein resistance, Polym. Chem. 2 (2011) 1409–1414, https://doi.org/10.1039/c1py00016k.

[22] Y. Zhang, L. Wang, Z. Zhang, Y. Zhang, X. Tuo, Synthesis and simultaneous self-assembly of multiblock fluorinated polyurethane in iniferter polymerization, J. Polym. Sci. Part A Polym. Chem. 51 (2013) 2161–2170, https://doi.org/10.1002/pola.26619.

[23] M.A. Zaverkina, V.P. Lodygina, V.V. Komratova, E.V. Stovbun, E.R. Badamshina, Kinetics of diisocyanate reactions with chain-extending agents, Polym. Sci. - Ser. A. 48 (2006) 382–387, https://doi.org/10.1134/S0965545X06040067.

[24] F. Parodi, Isocyanate derived polymers, in: S. R, P.S.G. Eastmond, A. Ledwith (Eds.), Compr. Polym. Sci., Eds, Pergamon Press (Elsevier Sci. Publ.), Oxford, 1989, pp. 387–412.

[25] A. Al Nabulsi, D. Cozzula, T. Hagen, W. Leitner, T.E. Müller, Isocyanurate formation during rigid polyurethane foam assembly: a mechanistic study based on: in situ IR and NMR spectroscopy, Polym. Chem. 9 (2018) 4891–4899, https://doi.org/10.1039/c8py00637g.

[26] P. Athey, N. Wilmot, R. Keaton, D. Babb, C. Boyer, T. Morley, An Isocyanate Trimerisation Catalyst System, a Precursor Formulation, a Process for Trimerising Isocyanates, Rigid Polyisocyanurate/polyurethane Foams Made Therefrom, and a Process for Making Such Foams, 2011, EP2346919A2.

[27] R. Devendra, N.R. Edmonds, T. Söhnel, Computational and experimental investigations of the urethane formation mechanism in the presence of organotin (IV) carboxylate catalysts, J. Mol. Catal. Chem. 366 (2013) 126–139, https://doi.org/10.1016/j.molcata.2012.09.015.

[28] R. Devendra, N.R. Edmonds, T. Söhnel, Organotin carboxylate catalyst in urethane formation in a polar solvent: an experimental and computational study, RSC Adv 5 (2015) 48935–48945, https://doi.org/10.1039/c5ra03367e.

[29] R. Devendra, N.R. Edmonds, T. Söhnel, Insight into the mechanism of the catalysis of urethane formation by organotin(IV) dicarboxylate, React. Kinet. Mech. Catal. 124 (2018) 487–502, https://doi.org/10.1007/s11144-018-1366-4.

[30] R. Devendra, N.R. Edmonds, T. Söhnel, Investigations of catalysis of urethane formation using organotin dicarboxylate, Heliyon 6 (2020), https://doi.org/10.1016/j.heliyon.2020.e04074.

[31] S. Niyogi, S. Sarkar, B. Adhikari, Catalytic activity of DBTDL in polyurethane formation, Indian J. Chem. Technol. 9 (2002) 330–333.

[32] L.R. Domingo, Molecular electron density theory: a modern view of reactivity in organic chemistry, Molecules 21 (2016) 1–15, https://doi.org/10.3390/molecules21101319.

[33] B. Furniss, A. Hannaford, P. Smith, A. Tatchell, Vogel's Textbook of Practical Organic Chemistry, Longman Scientific & Technical, Longman House, London, 1989.

SUPPORTING INFORMATION

Can tetraphenylethane (TPE) “iniferter” groups be introduced into polymer chains by coupling TPE diol with diisocyanate?

*Mateusz Grabowski, Bartłomiej Kost, Bartłomiej Gostyński, Melania Bednarek**

Centre of Molecular and Macromolecular Studies, Polish Academy of Sciences, Sienkiewicza 112, 90-362 Lodz, Poland; e-mail: bednarek@cbmm.lodz.pl

1. Analysis of oligodiols

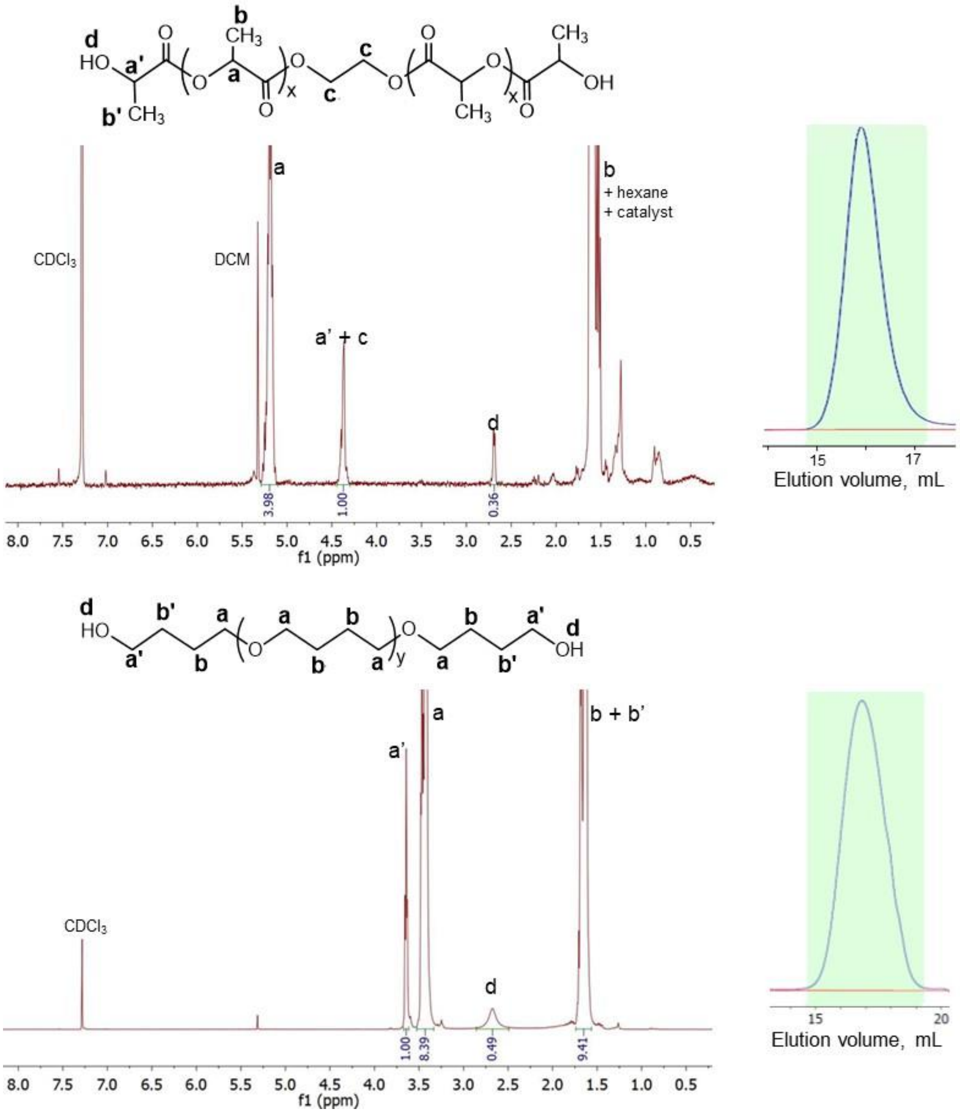

Figure S1. ^{1}H NMR ($CDCl_3$) and SEC (DCM) analyses of synthesized PLA and commercial PTHF diols.

2. Analysis of synthesized derivative of TPED (TPED_diET)

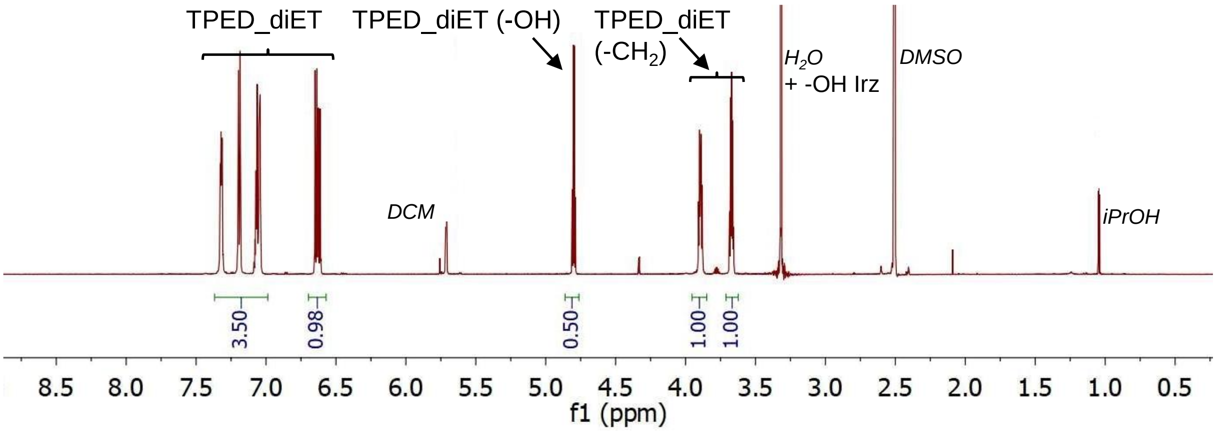

Figure S2. ^{1}H NMR spectrum (DMSO-d_6) of TPED_diET.

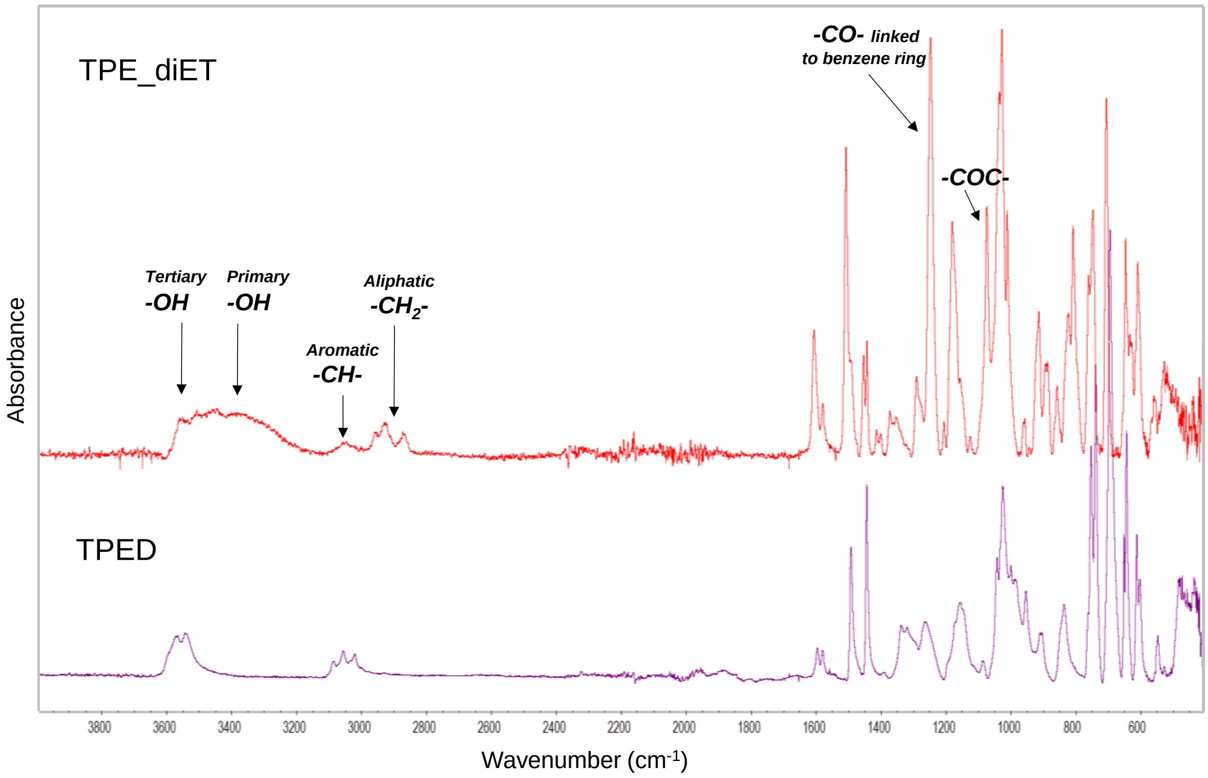

Figure S3. FT IR spectrum of TPED_diET (on the top). The IR spectrum of commercial TPED is also presented for comparison (on the bottom).

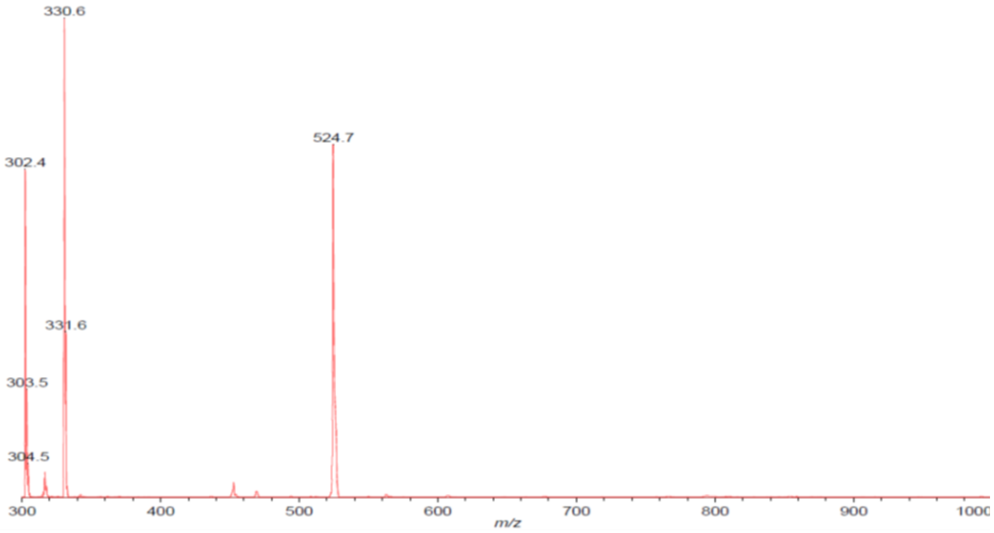

Figure S4. MALDI TOF spectrum of TPED_diET recorded with low laser energy (M of TPED_diET = 486, K^+ as a cation, thus m/z(TPED_diET) should be 486 + 39 = 525); in the region below 350 m/z, signals corresponding to matrix appear.

MALDI TOF was done instead of MS because of dissociation of -$C(Ph)_2$-$C(Ph)_2$ bond at MS analysis conditions.

3. Kinetic experiments

Kinetic plots for all performed experiments are presented in the main text for the region for which kinetic curves started to stabilize. Some experiments were performed during 20 hours, but some were finished earlier because of the observation of gelation or precipitation of the formed product, or full conversion of diisocyanate, or lack of further conversion of -NCO groups. Below exemplary kinetic curves for the reactions proceeding in the same phase to the end are presented.

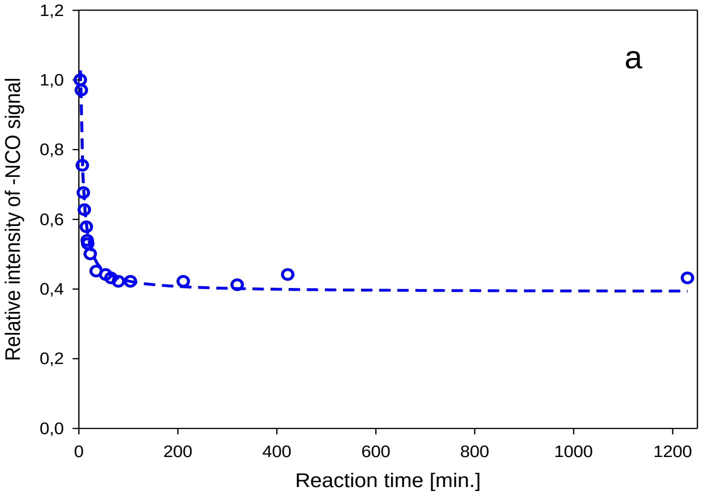

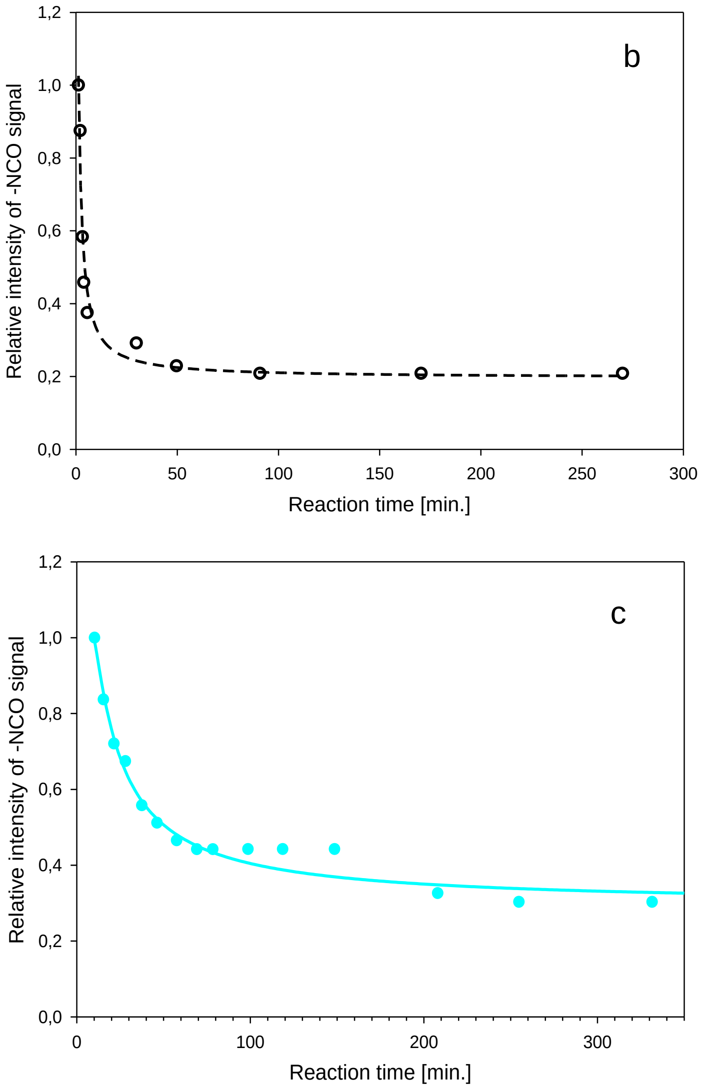

Figure S5. Conversion of -NCO groups versus time during the whole time of the kinetic experiment for the reactions: a) of PTHF diol with HDI, b) PTHF diol with MDI, c) PLA diol with HDI (MEK). In all cases TPED diol was added at time indicated in Figure 1 in the main text.

4. Analysis of products of kinetic experiments

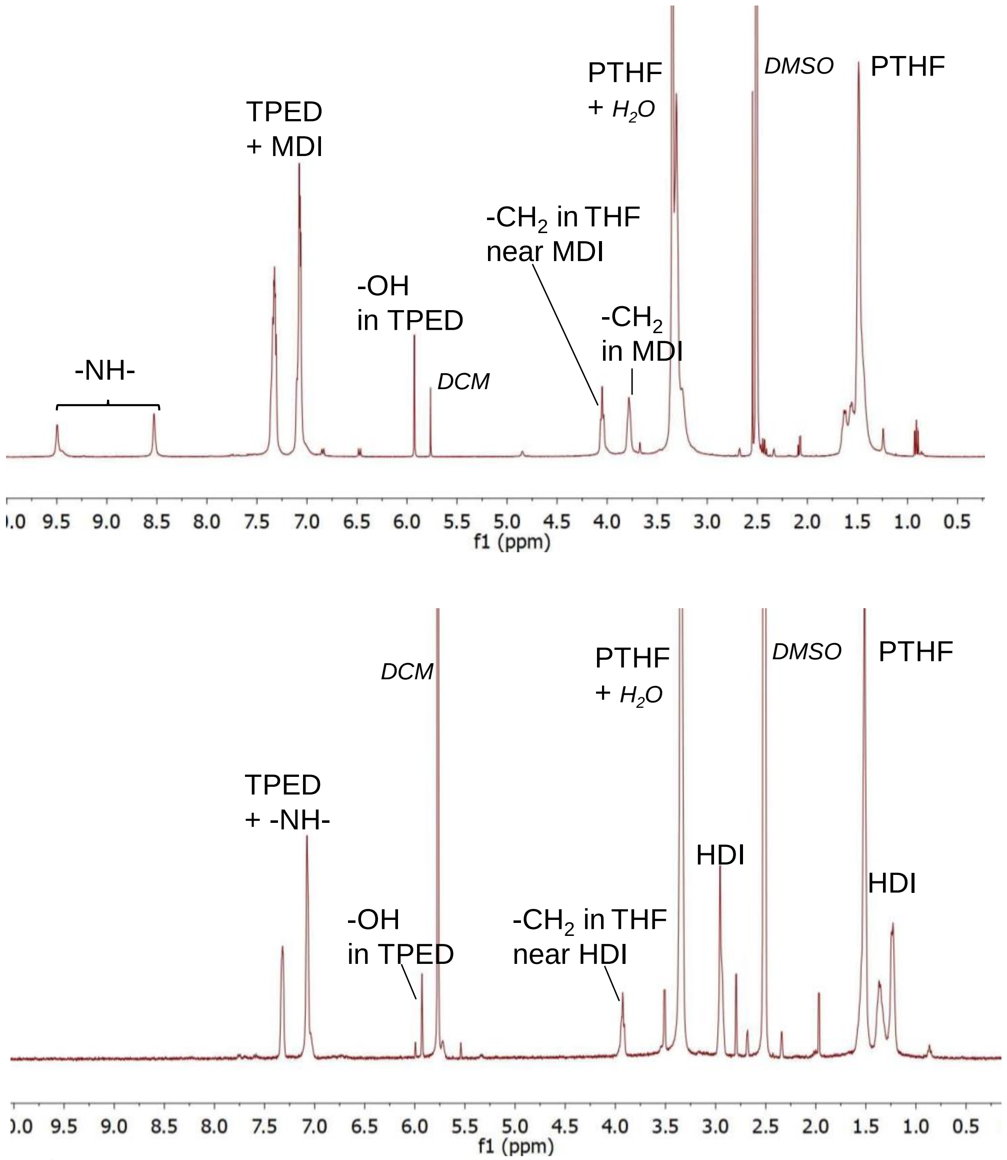

Figure S6. ^{1}H NMR spectra (DMSO-d_6) of the products of reactions PTHF diol with MDI (a) and HDI (b). TPED was added in both reactions. Product (a) was separated by solvents evaporation and washing with methanol, product (b) – by one-time precipitation to methanol. In both spectra the signals corresponding to TPED diol are visible but together with the signal corresponding to unreacted -OH groups.

The way of calculation of the conversion of -OH groups belonging to TPED on the basis of ^{1}H NMR spectra

1. For the reaction with HDI, the intensity of signals at 7.07-7.85 ppm corresponding to aromatic protons from TPED was compared with the intensity of the signal at 5.92-5.95 ppm corresponding to -OH groups in TPED. The ratio of unreacted -OH to aromatic protons from the spectrum was compared with the theoretical ratio for TPED which is equal to 0.1.

2. For the reaction with MDI, the signals between 7.07-7.85 ppm correspond to aromatic protons from both – TPED and MDI, thus to perform calculation as above, firstly the intensity of protons originating from MDI was subtracted. This intensity was calculated as equal to 4 x intensity of the signal at ~3.83 ppm corresponding to methylene group in MDI (2 protons in -CH_2- group, 8 protons in phenyl groups).

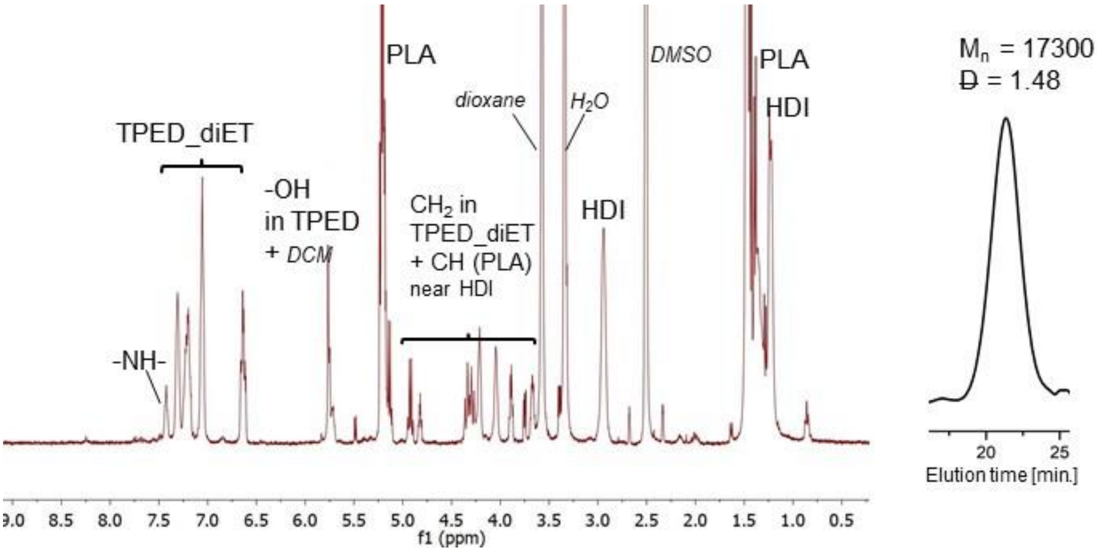

Figure S7. ^{1}H NMR (DMSO-d_6) and SEC (DMF, PSt standards) analyses of the product of the reaction of PLA diol with HDI +TPED_diET.

SEC analyses of the products of other kinetic experiments were not performed because of their poor solubility in accessible solvents.

Publikacja 2:

Mateusz Grabowski, Bartłomiej Kost, Przemysław Kubisa, Melania Bednarek. A New Approach to The Synthesis of Polylactide/Polyacrylonitrile Block Copolymers. *Polymers*. 2022;14(8):1529. doi:10.3390/ polym14081529

polymers

MDPI

Article

A New Approach to The Synthesis of Polylactide/Polyacrylonitrile Block Copolymers

Mateusz Grabowski, Bartłomiej Kost, Przemysław Kubisa and Melania Bednarek *

Centre of Molecular and Macromolecular Studies, Polish Academy of Sciences, Sienkiewicza 112, 90-363 Lodz, Poland; mgrabowski@cbmm.lodz.pl (M.G.); kost@cbmm.lodz.pl (B.K.); pkubisa@cbmm.lodz.pl (P.K.)
* Correspondence: bednarek@cbmm.lodz.pl; Tel.: +48-42-6803219

Abstract: As a result of the search for alternatives to the known methods for the synthesis of PLA/vinyl polymer block copolymers, a new approach based on the "iniferter" concept was demonstrated in this article. In this approach, the introduction of a group that was capable of forming radicals and initiating radical polymerization into the polylactide (PLA) chain was conducted. Then, the obtained functional PLA was heated in the presence of a radically polymerizable monomer. The tetraphenylethane (TPE) group was chosen as a group that could dissociate to radicals. PLA with a TPE group in the middle of the chain was prepared in several steps as follows: (1) the synthesis of 4-(2-hydroxyethoxy)benzophenone (HBP-ET); (2) the polymerization of lactide, which was initiated with HBP-ET; and (3) the coupling of HBP-ET chains under UV radiation to form TPE-diET_PLA. A "macroiniferter", i.e., TPE-diET_PLA, was used to initiate the polymerization of acrylonitrile (AN) by heating substrates at 85 °C. ^{1}H and ^{13}C NMR and SEC analyses of the products indicated that the triblock copolymer PLA-PAN-PLA formed and thus confirmed the assumed mechanism of the initiation of AN polymerization, which relied on the addition of the radical that formed from TPE (linked with the PLA chain) to the monomer molecule. Copolymerizations were performed with the application of prepared TPE-diET_PLA with three different M_n's (1400, 2200, and 3300) and with different AN/PLA ratios, producing copolymers with varied compositions, i.e., with AN/LA ratios in the range of 2.3–11.1 and M_n's in the range of 5100–9400. It was shown that the AN/LA ratio in the copolymer was increasable by the applied excess of AN with respect to the PLA macroiniferter in the feed and that more AN monomer was able to be introduced to PLA with shorter chains.

Keywords: polylactide; copolymer; acrylonitrile; tetraphenylethane; iniferter

check for updates

Citation: Grabowski, M.; Kost, B.; Kubisa, P.; Bednarek, M. A New Approach to The Synthesis of Polylactide/Polyacrylonitrile Block Copolymers. *Polymers* **2022**, *14*, 1529. https://doi.org/10.3390/polym14081529

Academic Editor: Asterios (Stergios) Pispas

Received: 2 March 2022
Accepted: 4 April 2022
Published: 9 April 2022

1. Introduction

Polylactide (PLA), a renewable polyester that originally had a primary use in biomedical applications and as a packaging material, is now being considered as a substitute for petroleum-derived plastics [1,2]. However, in many applications, PLA has several disadvantages including its relatively low thermal stability and brittleness. One of the methods for modifying the properties of PLA is introducing new chemical units into PLA chains. Copolymers of PLA have been synthesized [3–9], and they can be applied in various fields, such as tissue engineering [3], drug delivery systems, diagnostic/imaging platforms [4], orthopedic implants, and packaging applications [5], and are widely described in the scientific literature [3–9].

Among different types of lactide copolymers are block copolymers. Block copolymers with another cyclic monomer are easily synthesized by successive polymerization using the same catalytic system. Problems arise when the other block is built from the polymerization of vinyl monomers according to the radical mechanism. The combination of blocks of PLA and blocks derived from vinyl monomers offers the possibility of modifying the properties of resulting block copolymers within a broad range due to a variety of vinyl monomers and different structures of resulting blocks. There are several approaches to preparing such copolymers, e.g., replacing the end groups of the first block with groups that initiate the polymerization of the monomer forming the second block, using double-acting initiators (initiators containing the ROP initiating group and the group that initiates radical polymerization), or coupling the two previously obtained blocks after introducing groups that react with each other at their ends [9]. Functionalizing PLA to obtain specific functional groups at the ends of macromolecules is often a difficult, multistep process (as polyester, PLA is not very stable under strongly acidic or basic conditions). When polymerizing new monomers, it is necessary to perform purification after the prior synthesis, introduce a new catalyst, and introduce a new solvent. Each of the methods used thus far have certain limitations, so new methods are being sought and developed to replace or simplify the current methods.

In this paper, we describe a method based on the "iniferter" concept [10]. There is a tetraphenylethane (TPE) group among different compounds/groups that acts as an iniferter [10,11]. The TPE group dissociates into free radicals upon heating (see Figure 1). The binding energy between carbon atoms substituted with four phenyl groups is ~200 kJ·mol^{-1} (for $(Ph)_2CH\text{-}CH(Ph)_2$); thus, the binding energy is much lower than that of the C-C bond in ethane (377 kJ·mol^{-1}) [12].

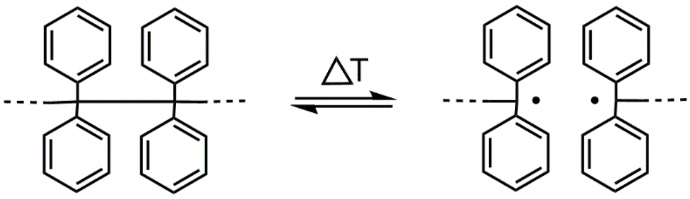

Figure 1. Reversible thermal dissociation of the TPE group.

If a TPE-containing compound (initiator/iniferter) is placed in a medium that contains unsaturated monomers, radicals that are formed upon heating initiate their polymerization [13,14]. According to Braun, when benzopinacol (tetraphenylethanediol, TPED) possessing two tertiary hydroxyl groups is applied as the initiator and the formation of diphenylmethyl radicals has occurred, the initiation proceeds by abstracting the hydrogen radical from the hydroxyl group and adding it to the vinyl monomer [13,14]. However, when -OH groups are blocked, the TPE derivative initiated by an addition to a double bond [15,16].

The TPE group in low-molecular-weight compounds, as well as polymer chains, has been applied as an initiating group in the polymerization of styrene, methyl/butyl/benzyl methacrylate, and acrylonitrile [11,13–20]. Attempts to prepare polyurethanes that contain TPE by reacting tetraphenylethanediol with aromatic diisocyanates have been made and, as claimed by the conductors of such experiments, resulted in "macroiniferters" with several TPE units [11,17–20]. Some polyurethanes (PUs) have been obtained for which an additional oligodiol, such as poly(tetrahydrofuran), poly(propylene oxide), or poly(ε-caprolactone), was used in PU synthesis [21–23]. All polyurethanes served as macroiniferters for the polymerization of vinyl monomers.

We decided to introduce the TPE unit into the PLA chain with the same purpose, i.e., to synthesize the PLA/poly(vinyl monomer) copolymer; however, during our preliminary study, the reaction of isocyanate with tetraphenylethanediol, which contained tertiary -OH groups, was not effective [24]. Other attempts to introduce one TPE unit into the PLA chain by applying TPED as a difunctional initiator of lactide polymerization were also unsuccessful, probably due to the side reactions that occur with benzopinacol in the presence of any catalyst (pinacol rearrangement under acidic conditions [25] or decomposition to benzophenone derivatives under basic conditions) [26]. Thus, we chose another approach, omitting the insufficient reactivity of the sterically hindered tertiary -OH groups in TPED and relying on the preparation of a TPE derivative that contains primary hydroxyl groups that are reactive enough to initiate lactide polymerization.

First, we introduced only one TPE group into the middle of the PLA chain. In our study, the TPE group was introduced into the PLA chain by its formation via the coupling of benzophenone groups that were placed at the polymer chain ends. This type of macroiniferter (PLA-TPE-PLA) should produce triblock copolymer PLA-poly(vinyl monomer)-PLA as a result of heating in the presence of a vinyl monomer. In this study, we examined if PLA copolymers with acrylonitrile (AN) can be obtained by applying a PLA macroiniferter containing TPE units in a specific surrounding. The structures of the obtained copolymers were analyzed, and the mechanism of AN polymerization was suggested. The possibility of regulating the copolymer composition by selecting applied conditions was also examined.

2. Materials and Methods

2.1. Materials

L,L-Lactide from Purac was recrystallized from 2-propanol, sublimated, and stored under vacuum. 2-Bromoethanol (95%) and 4-hydroxybenzophenone (HBP, 98%), which were both from Sigma-Aldrich (St.Luis, MO, USA/Steinheim, Germany), were used as received, and acrylonitrile (AN, 99%) was passed through an inhibitor removal column filled with silica gel and distilled under vacuum.

Trifluoromethanesulfonic acid from Sigma-Aldrich (St.Luis, MO, USA/Steinheim, Germany), (triflic acid, 99%) was distilled under vacuum. Dichloroethane (DCE, pure p.a.), dimethylformamide (DMF, pure p.a.), and dioxane (pure p.a.) from POCH (Gliwice, Poland) were dried over CaH_2, distilled before use, and stored over molecular sieves (4 Å). Chloroform (pure p.a.), 2-propanol (pure p.a.), methanol (pure p.a.), ethanol (pure p.a.), diethyl ether (pure p.a.), and hexane (99%), all from POCH (Gliwice, Poland), were used as received. Potassium hydroxide (pure p.a.) was obtained from POCH (Gliwice, Poland), magnesium sulfate ($MgSO_4$, 99%) was obtained from Chempur (Piekary Śląskie, Poland) and both were used as received.

2.2. Synthesis of the HBP Derivative Containing Primary Hydroxyl Groups (HBP-ET)

The HBP derivative containing primary hydroxyl groups was prepared employing Williamson etherification [27]. A total of 1.68 g (43 mmol) of potassium hydroxide was dissolved in 2.5 mL of distilled water in a beaker. Then, the solution was added to 5 g (25 mmol) of 4-hydroxybenzophenone (HBP) in a round-bottom flask. The resulting yellow reaction mixture was stirred at 70 °C until HBP dissolved. Next, 4 mL (54 mmol) of 2-bromoethanol was added to the syringe, and stirring was continued for 24 h. The aqueous phase was subjected to extraction with chloroform 3 times, and the organic phase was extracted with distilled water 3 times. The combined organic extracts were dried with $MgSO_4$. The solvent was evaporated under a vacuum, and the resulting product was recrystallized by being dissolved in 4 mL of ethanol while heated. Then, an excess amount of diethyl ether was added and cooled down, which resulted in growing crystals. The obtained white crystals of HBP-ET, which were dried under vacuum, were obtained with a yield of 50% (>99% pure, ^1H NMR, GC).

2.3. Synthesis of PLA with HBP-ET Units at One Chain End

PLAs were synthesized by the cationic ring-opening polymerization of L-lactide initiated with HBP-ET [28]. The general procedure was as follows (amounts given for HBP-ET_PLA, M_n = 1100): LA (3.5 g, 24 mmol) and HBP-ET (0.67 g, 2.7 mmol) were placed in a Schlenk flask, vacuumed, backfilled with nitrogen, and dissolved in 9 mL of DCE, which was added with a syringe via a rubber septum. Next, 0.049 mL (0.56 mmol) of triflic acid was added as a catalyst. The reaction flask was put into an oil bath and stirred at 45 °C for 72 h. After that time, the reaction was stopped by adding CaO, and the reaction mixture was filtered from CaO and precipitated to hexane. The resulting polymer was dried under vacuum; the product was obtained with a yield of ~70%.

2.4. Synthesis of PLA with TPE Units in the Middle of the Chain (TPE-diET_PLA)

Polymers were prepared by a radical coupling process that was initiated by UV irradiation [29]. The general procedure was as follows (amounts given for TPE-diET_PLA, M_n = 2200): HBP-ET_PLA (3 g) was placed in a quartz flask to which 6 mL of dioxane and 8 mL of 2-propanol were added (both were purged with nitrogen beforehand). The flask was closed with a rubber septum and purged with nitrogen (with a needle) for 15 min. Then, the flask content was slightly heated until it dissolved. The homogenous solution was exposed to ultraviolet light (365 nm) for 24 h. The resulting solution was evaporated under reduced pressure and dried. Subsequently, the polymer was dissolved in DCE and precipitated to hexane, decanted, and dried under vacuum. The resulting polymer was obtained with a yield of ~90%.

2.5. Polymerization of AN Using TPE-diET_PLA as a Macroiniferter

The synthesis of the TPE-diET_PLA/PAN copolymer was performed using the iniferter concept [10]. TPE-diET_PLA (0.3 g, 0.13 mmol) was placed in a Schlenk flask, vacuumed, and filled with nitrogen. Next, 0.32 mL of AN (4.7 mmol) was added to the reaction flask through a rubber septum. The solution was degassed by freeze–pump–thaw cycles. The flask was filled with nitrogen and placed and heated in an oil bath at 85 °C for 24 h with stirring. The resulting polymer was precipitated to cold methanol, centrifuged, and dried under reduced pressure.

2.6. Instrumental Methods

^{1}H NMR spectra of the synthetized PLA polymers were recorded in $CDCl_3$ and in DMSO-d6 using a Bruker Avance 400 Neo instrument (Bruker, Billerica, MA, USA) operating at 400 MHz.

Size exclusion chromatography (SEC) was performed using an Agilent Pump 1100 Series with an Agilent G1322A Degasser (Santa Carla, CA, USA) for analyses in DCM and a Shimadzu Pump LC-20AD with Shimadzu DGU-20A5 Degasser (Kioto, Prefektura Kioto, Japan) for analyses in DMF. For both systems, a set of two PLgel 5 μm mixed-C columns and a Wyatt Optilab REX interferometric refractometer (Dernbach, Germany) were used. A flow rate of 0.8 $mL \cdot min^{-1}$ was applied for the eluent, and analyses were performed at room temperature in DCM and at 40 °C in DMF. The systems were calibrated with polystyrene standards.

Fourier transform infrared spectroscopy (FTIR) measurements were performed on a Thermo Scientific Nicolet 6700 instrument with an attenuated total reflectance (ATR) GoldenGate accessory (Waltham, MA, USA) and with a deuterated triglycine sulfate (DTGS) detector. The spectra were obtained by adding 64 scans at a 2 cm^{-1} resolution.

UV coupling was performed in a photochemical reactor (RayonetRPR-200, Southern New England, Brandford, CT, USA) equipped with 12 UV lamps (λ = 365 nm) and a magnetic stirrer.

3. Results and Discussion

3.1. Synthesis of a PLA Containing TPE Group in the Middle of the Chain

The synthesis of a PLA-based macroiniferter containing an active group in the middle of the PLA chain was performed using the following steps: (1) functionalization of 4-hydroxybenzophenone with 2-bromoethanol, which led to the introduction of a primary -OH group into the benzophenone derivative 4-(2-hydroxyethoxy)benzophenone (HBP-ET), (2) initiation of lactide polymerization with HBP-ET (HBP-ET_PLA), and (3) coupling of HBP-ET_PLA to the TPE-diET_PLA polymer. The corresponding reaction scheme is presented in Figure 2.

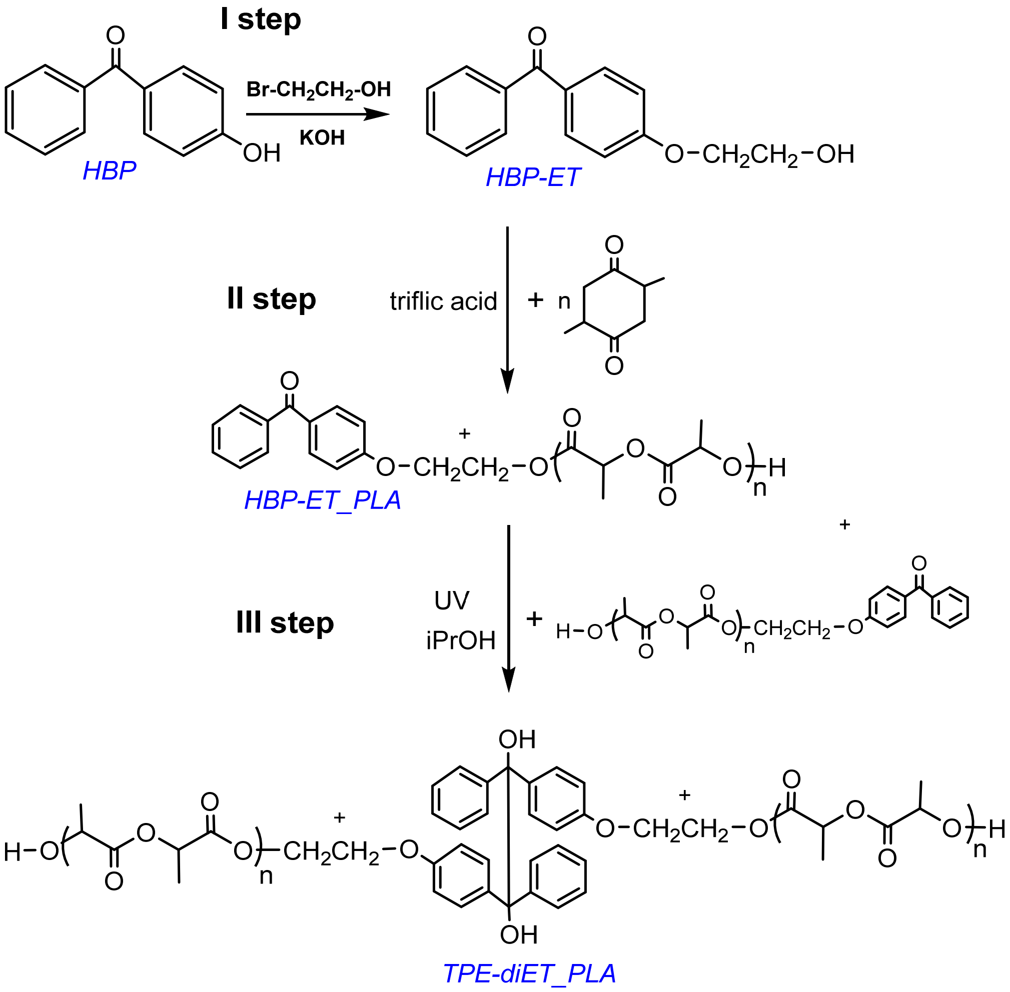

Figure 2. Scheme for the synthesis of PLA with one TPE group in the middle of the chain.

The successful functionalization of 4-hydroxybenzophenone to 4-(2-hydroxyethoxy) benzophenone (HBP-ET) was confirmed by ^{1}H NMR analysis (see Figure S1 in Supporting Information). HBP-ET containing primary hydroxyl groups was used for the initiation of L,L-lactide polymerization, which was catalyzed by triflic acid. PLAs with three different molecular weights were obtained. The molecular weights were M_n = ~700, 1100, and 1600 (M_n determined by ^{1}H NMR, Figure 3, Figures S2 and S3). These polymers possessed a benzophenone moiety at one chain end and were dissolved in a solvent that contained isopropanol as a hydrogen atom donor, and they were subjected to UV radiation, which resulted in the coupling of two PLA chains and the formation of a tetraphenylethane group in the middle of the polymer chain. The expected structure of the coupled PLAs was confirmed by ^{1}H NMR, ^{13}C NMR, ^{1}H^{13}C-HMBC correlation, and FT IR analyses (Figures 3 and S2–S6).

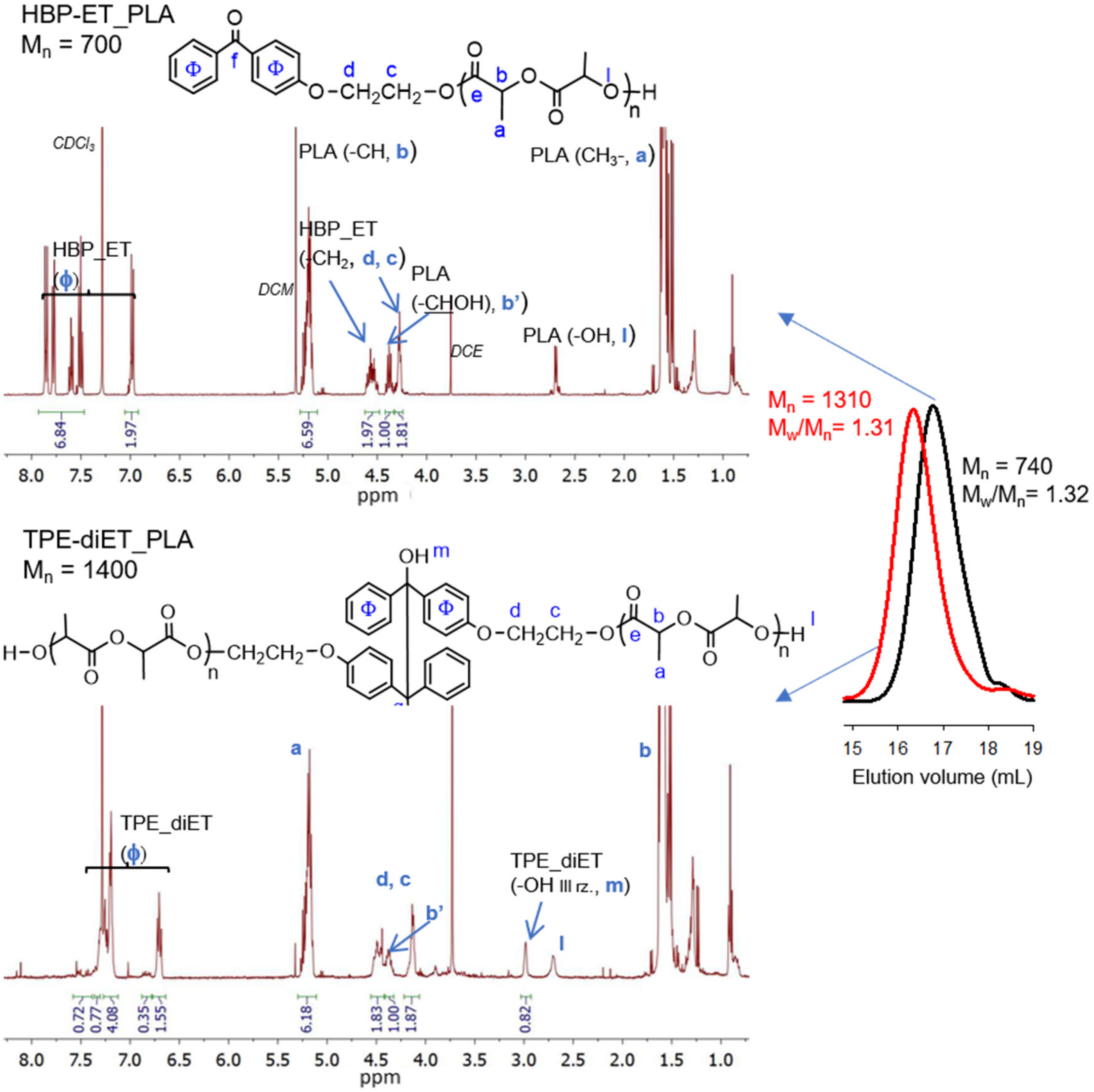

Figure 3. ^{1}H NMR spectra (CDCl$_3$) and SEC curves (DCM) of HBP-ET_PLA, M_n =700 (top, SEC black line) and TPE-diET_PLA, M_n = 1400 (bottom, SEC red line).

3.2. Polymerization of Acrylonitrile Initiated by TPE-diET_PLA

Different vinyl monomers can be polymerized by the radicals that form from the dissociation of the TPE group; however, for our study, we chose a monomer that was not thermally polymerizable. Acrylonitrile was determined to be stable at 85 °C, which is a sufficient temperature for achieving the reasonable decomposition of TPE.

To obtain PLA/PAN copolymers, TPE-diET_PLA was placed in a Schlenk tube, dissolved in a solvent (DMF or DMSO for the kinetic experiment), and mixed with acrylonitrile; after deoxygenation, the flask was immersed in a heated oil bath at 85 °C (a higher temperature can result in faster polymerization but also some side products). After a predetermined time, the solvents were evaporated, and the product was analyzed by ^{1}H NMR (some polymers were also analyzed by ^{13}C NMR) and SEC analyses. SEC curves revealed the additional presence of unreacted PLA homopolymers in a sample; thus, the polymerization product was precipitated with methanol and analyzed again (Polylactide with a small molecular weight is soluble in methanol). Figure 4 presents ^{1}H NMR spectra and SEC curves of the precipitated product from the AN polymerization initiated by TPE -diET_PLA with a relatively low M_n.

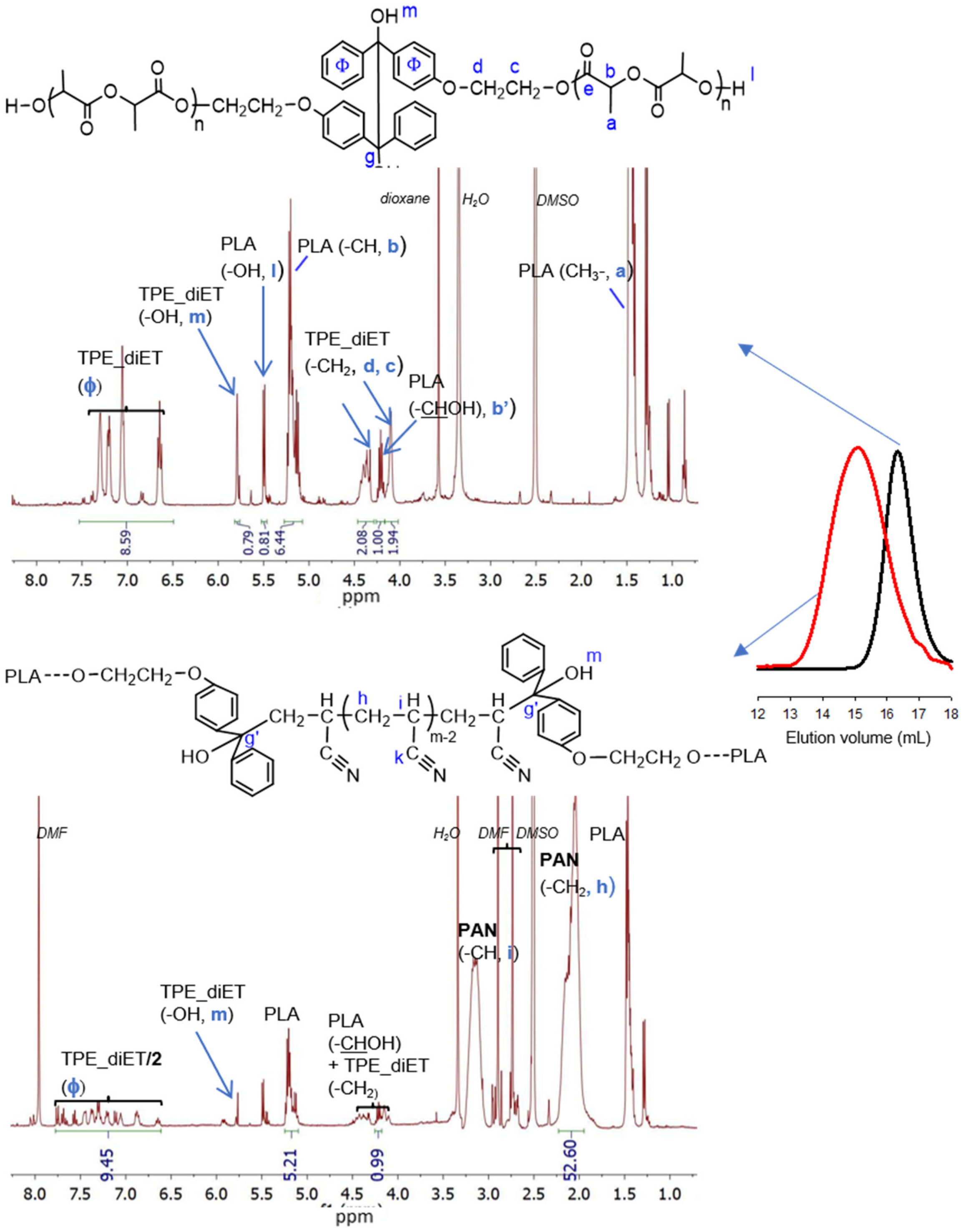

Figure 4. ^{1}H NMR spectra (DMSO-d6) and SEC curves (DMF) of TPE-diET_PLA, M_n = 1400 (on the top, SEC black line), and the precipitated product of the AN polymerization initiated with TPE-diET_PLA; m_{AN}/m_{PLA} in feed =1; 24 h (on the bottom, SEC red line).

In the ^{1}H NMR spectrum, all the signals that were expected for the TPE-diET_PLA/PAN copolymer were present. In comparison with the spectrum for TPE-diET_PLA, new signals corresponding to methylene at 2.0–2.25 ppm and methine protons at 3.0–3.25 ppm from the formed PAN block appeared. On the basis of corresponding integrals, the AN/LA and TPE/LA ratios were calculated (the method of calculation is explained in the SI). For the copolymer presented in Figure 4, these ratios were equal to 11.1 and 0.153, respectively, and in the starting reaction mixture, they were equal to 4.2 and 0.157, respectively. The change in the AN/LA ratio was due to the noticeable fractionation (approximately 60% was removed) of the solid product during its precipitation and the removal of unreacted PLA. The SEC curve of the polymerization product indicated an increase in molecular weight in comparison with the starting TPE-diET_PLA.

Signals corresponding to TPE units in the PLA chain in the range of 6.65–7.4 ppm were visible, although their shape (multiplicity) differed from those present in the spectrum of TPE-diET_PLA. New signals appeared at higher chemical shifts that resembled those characteristic of 4-hydroxybenzophenone phenyl protons, which suggested the presence of diphenyl methyl groups that were formed by the decomposition of TPE groups. Successive decomposition of the TPE groups with increasing conversion of the AN monomer was demonstrated by kinetic experiments. Figure 5 presents the ^{1}H NMR spectra of the reaction mixture recorded at different times of TPE-diET_PLA (M_n = 2200 1:1 wt. ratio of AN to TPE_PLA) heating in DMSO as a solvent.

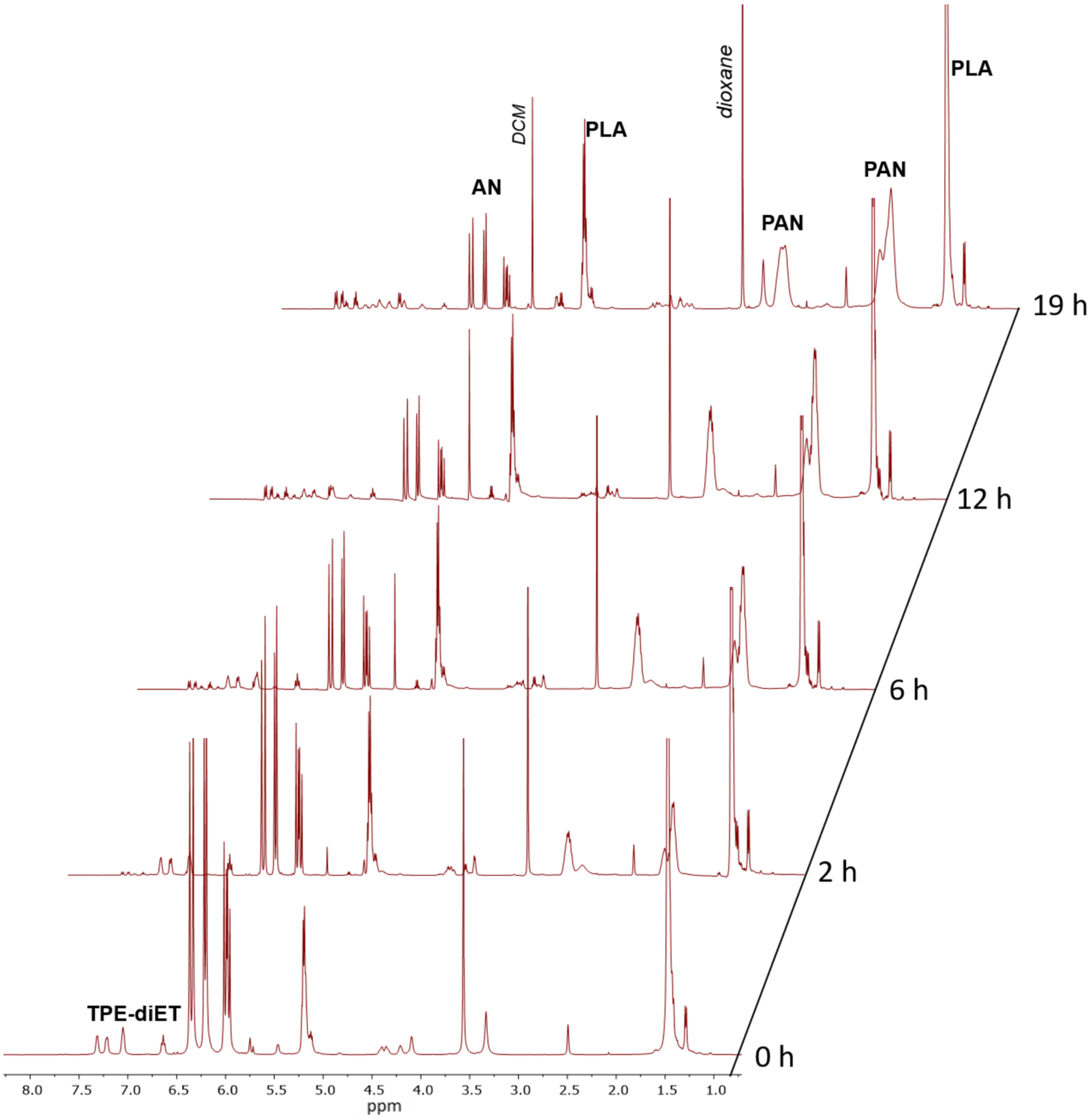

Figure 5. ^{1}H NMR spectra of the solution of TPE-diET_PLA reacting with acrylonitrile in DMSO-d_6 at 85 °C recorded at different times.

Figure 5 shows that the intensities of signals that corresponded to protons in the AN monomer in the range of 5.8–6.4 ppm decreased and the intensities of signals corresponding to formed PAN units increased with the heating time. As mentioned above, with increasing heating time, the successive decomposition of TPE groups was observed. Appropriate calculations (which are presented in the SI) allowed us to determine the AN conversion and percent of TPE group decomposition. Figure 6 presents kinetic plots for the AN polymerization in comparison with the decomposition of the TPE group.

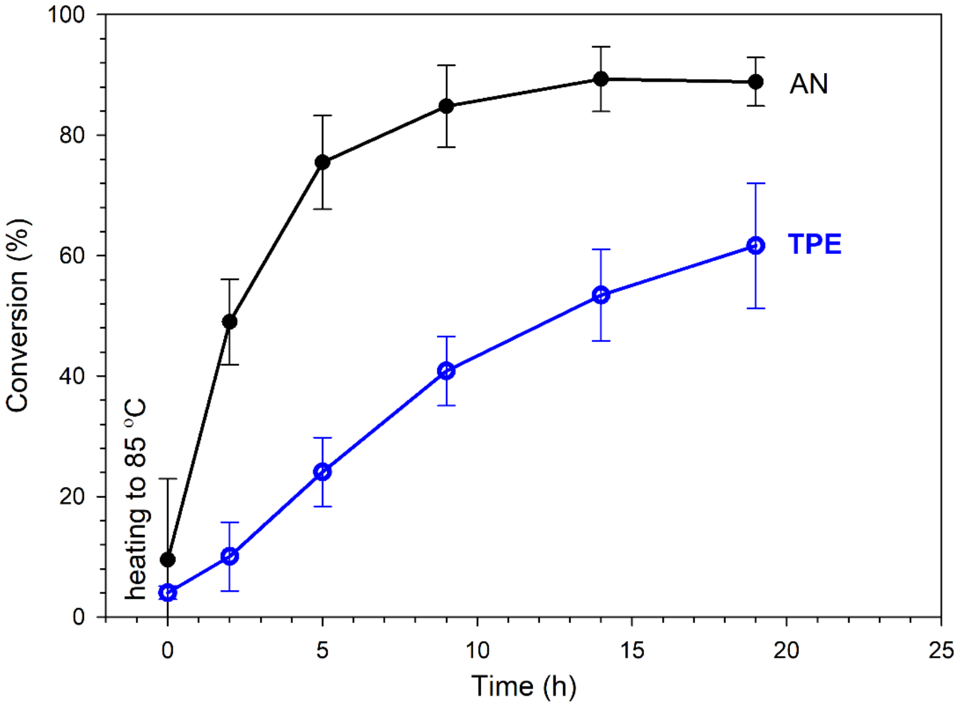

Figure 6. Conversion of AN and TPE groups decomposition as a function of heating time (reaction in an NMR tube in DMSO-d_6); plots based on average values of three measurements.

Irreversible TPE decomposition proceeded successively during heating along with initiation of the polymerization and consumption of the AN monomer. The conversion of AN almost stabilized after 15 h at a level of ~85% (in DMSO-d_6), which was when the irreversible decomposition of the TPE groups was ~60%. By prolonging the reaction time, further TPE decomposition could have been achieved; however, the reaction was stopped to avoid side reactions (which proceed with a high AN conversion, leading to a deteriorated quality of the product, as is shown later).

^{1}H NMR analysis of the reaction mixture and obtained product confirmed that the polymerization of AN was initiated by the TPE group present in the PLA chain. SEC analysis indicated the formation of a (co)polymer with a molecular weight higher than that of the initiating TPE-diET_PLA (shifting of the SEC curve, Figure 4) and similar to that calculated from the ^{1}H NMR spectrum with the assumption of a triblock copolymer structure (values shown in Table 1). However, some doubts related to the mechanism of vinyl monomer polymerization that was previously postulated by Braun (see Introduction, [13,14]) should be dispelled. Braun claimed that if TPED possessing tertiary hydroxyl groups is used as an initiator of unsaturated monomer polymerization, the growing polymer chain will not contain the TPED fragment as an end group. In our work, although the TPE group was linked to the PLA chain, it still contained tertiary -OH groups, and the same mechanism that was postulated by Braun could have occurred and led to a PAN homopolymer instead of the copolymer with PLA. These two mechanisms are presented in Figure 7.

Table 1. Polymerization of acrylonitrile at 85 °C for 24 h.

TPE_PLA		**Polymerization No.**	**AN/LA mol Ratio in Feed (wt. ratio)**	**Conversion of AN, %** [2]	**PLA-PAN-PLA Copolymers** [3]		
M_n [1] **g/mol**	**TPE/LA**				**AN/LA** [1]	**TPE/LA** [1]	**M_n**[1] **(SEC)** [4] **g/mol**
1400	0.157	1	4.2 (1)	73	11.1	0.153	5130 (4250)
2200	0.084	2	1.7 (0.5)	65	2.5	0.049	5760 (4580)
		3	3.2 (1)	69	3.45	0.060	5670 (4780)
		4	7.0 (2)	71	9.9	0.071	9370 (8500)
3300	0.054	5	3.5 (1)	62 81_4 days 89_7 days	2.3 N.d. [5] ″	0.050 N.d. [5] ″	6070 (5850) Bimodal SEC “

[1] The M_n of TPE_PLA (=TPE-diET_PLA), as well as the M_n, AN/LA, and TP/LA ratios in copolymers, were calculated on the basis of the intensity of appropriate signals in the ^{1}H NMR spectra of the precipitated products (the method of calculation is presented in SI). [2] Conversion was determined on the basis of the ^{1}H NMR spectrum of the reaction mixture. [3] PLA-PAN-PLA copolymers were analyzed after being precipitated to methanol, which resulted in the fractionation of the starting product; the precipitated polymer accounted for approximately 40% (No. 1), 65% (No. 3), and 50% (No. 5) of the starting product. [4] The approximate M_n from SEC analysis in DMF, shown for comparison, was calculated as M_n = M_n from SEC measurement with PS standards divided by 6.5 (for sample 1) or 6 (for samples 2–5). Factors "6.5" or "6" were found by comparing M_n's determined for HBP-diET_PLA in DCM and in DMF. [5] Not determined.

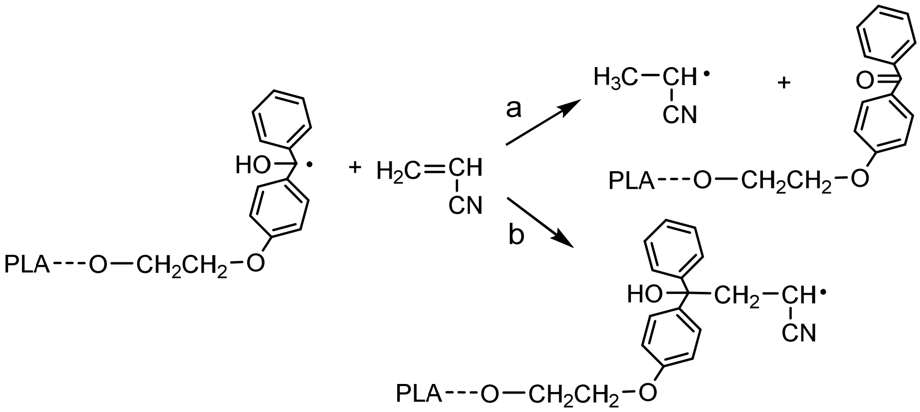

Figure 7. Two possible mechanisms for the initiation of AN polymerization by radicals formed from TPE-diET_PLA: (**a**) according to Braun vs. (**b**) proceeding by the addition of the (hyroxy)diphenylmethyl radical connected with the PLA chain to the AN monomer.

An analysis of the product microstructure based on a ^{13}C NMR spectrum provided further information about the polymerization mechanism. Additional polymerization of AN initiated with TPE_PLA 1400, with the AN/LA wt. ratio in the feed equal to 0.5, was performed, and the product was separated after 5 h by the evaporation of unreacted AN and solvents (this procedure allowed us to prevent the formed products from changing in the analyzed sample). Figure 8 presents ^{13}C NMR spectra for the polymerization product, together with the spectra for the initial PLAs for comparison. In the spectrum for the formed product (expected PLA/AN copolymer), a signal that was assigned to a quaternary carbon atom from the decomposed TPE unit attached to the AN unit at ~82 ppm was visible. On the other hand, the signal corresponding to the carbonyl carbon characteristic of the benzophenone moiety at ~195 ppm was not present. The mechanism of some vinyl monomers' polymerization initiated by TPED, suggested by Braun, should lead to the formation of AN homopolymer (without a TPE fragment) with simultaneous benzophenone formation. As a carbonyl group that corresponded to benzophenone was not formed in the reaction we studied, it was concluded that the polymerization did not proceed according to Braun's scheme but rather by the simple addition of the formed (TPE-diET_PLA)/2 radical to the AN monomer. The ^{13}C NMR analysis delivered unequivocal evidence that a block copolymer of PLA and PAN was formed, in which both blocks were linked through half of the TPE-diET unit. The most probable situation was that growing radicals recombined (or a growing radical combined with the (TPE-diET_PLA)/2 radical); thus, it was assumed that the triblock copolymer PLA-PAN-PLA was obtained.

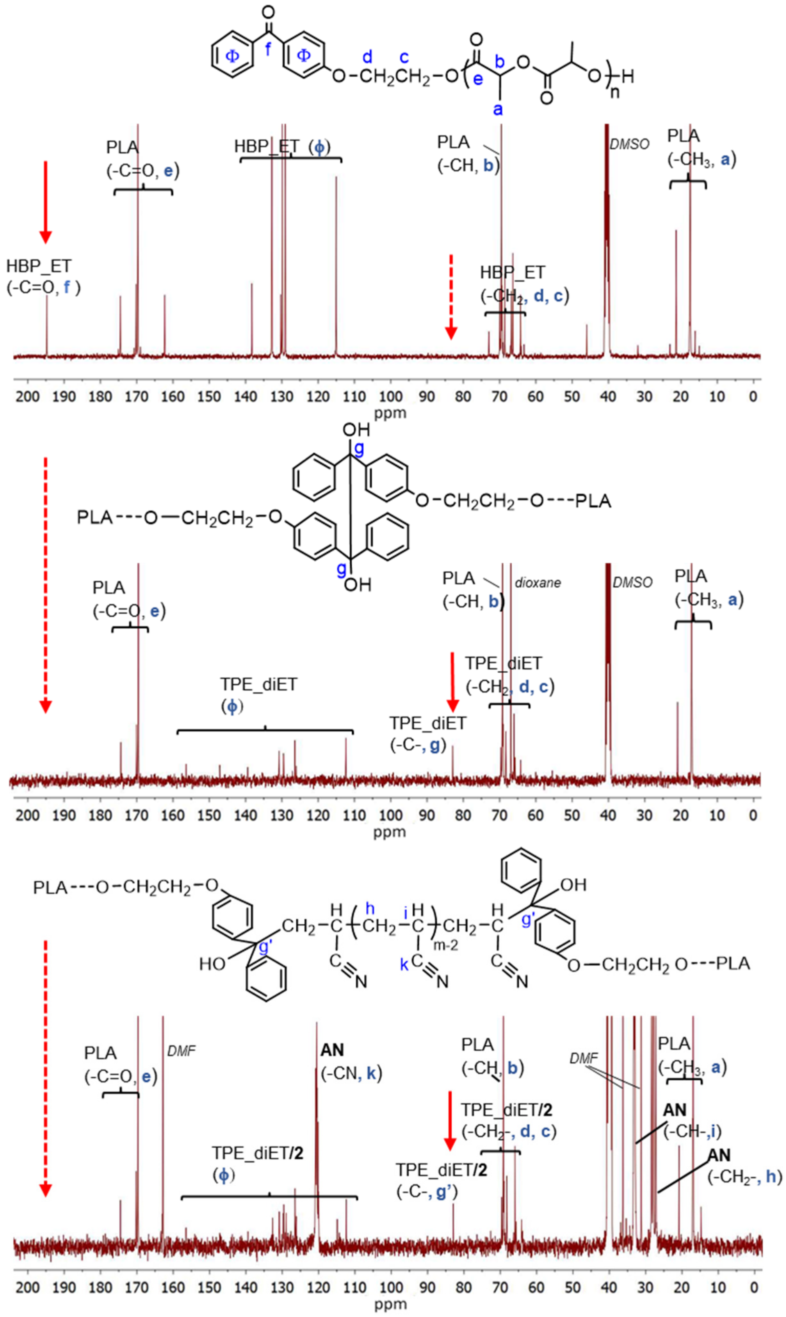

Figure 8. ^{13}C NMR spectra of HBP-ET_PLA (before coupling), TPE-diET_PLA (after coupling), and the product of the AN polymerization initiated with TPE-diET_PLA (TPE/PAN copolymer).

To show that it is possible to obtain PLA-PAN-PLA copolymers with varying lengths of PLA and PAN blocks by manipulating the molecular weight of the initial PLA and the AN to PLA ratio in the feed, several polymerizations were performed with three different TPE-diET_PLAs. ^{1}H NMR spectra of the products, as well as SEC traces, are shown in the Supporting Information (Figure S7), and the product composition and molecular weights are presented in Table 1.

The conversion of AN in the range of 62–73% was achieved within a 24 h reaction time. A prolongation in the reaction time results in a higher conversion, although the polymerization rate considerably decreases (this is shown by the kinetic experiment shown earlier in this contribution). The applied excess of AN with respect to the PLA polymer (No. 2–4 in Table 1) influences the length of the AN block. On the other hand, the ratio of AN to LA units may also be regulated by the molecular weight of the PLA containing TPE unit. In the case of reactions with the same excess of AN, a higher conversion was achieved when the TPE-diET_PLA with a lower M_n was used as a "macroiniferter", which may be explained by the better accessibility of the TPE group. However, it should be remembered that this ratio depends on the conversion of the AN monomer and product separation because its precipitation leads to the removal of unreacted PLA (only PLA was found in the solution after precipitation).

The TPE/LA ratio varied to a lesser extent and was close to the ratio in the initial TPE-diET_PLA (differences were due to polymer fractionation). The fact that the molecular weights of the obtained copolymers determined by SEC (with the awareness of the error resulting from the assumed method of counting) were close to those calculated from ^{1}H NMR spectra with the assumption of triblock copolymer formation supports the thesis that triblock copolymers, i.e., PLA-PAN-PLA, were formed by the recombination of two growing radicals, i.e., PLA-PAN●.

4. Conclusions

Failed initial attempts to introduce the TPE iniferter group into the PLA chain through the use of commercial TPED led us to develop a new synthetic methodology. This approach is based on the modification of 4-hydroxybenzophenone, the polymerization of lactide initiated by primary hydroxyl groups, and finally, the coupling of benzophenone groups that are placed at polymer chain ends. The expected structure of the resulting macroiniferter was confirmed by detailed analysis using NMR and FTIR spectroscopy and SEC. The application of the TPE-diET_PLA low-molecular-weight macroiniferter for the initiation of acrylonitrile polymerization resulted in a PLA-PAN-PLA triblock copolymer, which was demonstrated by ^{1}H and ^{13}C NMR as well as SEC analyses of the synthesized products. The acquisition of block copolymers confirmed the expected AN initiation mechanism, namely, through TPE dissociation (in the middle of the PLA chain) and then the addition of the resulting radicals to vinyl monomer molecules.

It was shown that the composition of copolymers was regulated by the manipulation of the macroiniferter length, substrate ratio, and polymerization conditions.

The presented approach may be applied for monomers other than those described in the present contribution; thus, it is a suitable method for the preparation of block copolymers from monomers polymerized by different mechanisms.

Supplementary Materials: The following supporting information can be downloaded at: https://www.mdpi.com/article/10.3390/polym14081529/s1, Figure S1. ^{1}H NMR spectrum ($CDCl_3$) and GC chromatogram for the synthesized HBP-ET. Figure S2: ^{1}H NMR spectra ($CDCl_3$) for HBP-ET_PLA, M_n=1100 and TPE-diET_PLA after coupling under UV radiation, M_n = 2200; PLAs formulas on the top; Figure S3: ^{1}H NMR spectra ($CDCl_3$) for HBP-ET_PLA, M_n = 1600 and TPE-diET_PLA after coupling under UV irradiation, M_n = 3300; Figure S4: ^{13}C NMR spectra for HBP-ET_PLA (M_n = 700) and TPE-diET_PLA (M_n = 1400) after the coupling reaction. The signal characteristic for carbonyl group of benzophenone moiety present in HBP-ET_PLA at ~195 ppm disappears after coupling and a new signal at ~82 ppm corresponding to quaternary carbon atom in TPE unit appears; Figure S5: ^{1}H^{13}C-HMBC NMR spectra for TPE-diET_PLA (M_n = 1400). An arrow indicates correlation between quaternary carbon atom and tertiary -OH group from TPE-diET unit; Figure S6: FTIR spectra for HBP-ET initiator, HBP-ET_PLA polymer (M_n = 700) and TPE-diET_PLA after coupling of HBP-ET_PLA (M_n = 1400); Figure S7: ^{1}H NMR spectra (DMSO-d6) and SEC curves (red line) for the products of reactions No: (a) 2, (b) 3, (c) 4, (d) 5 in Table 1 in the main text; "s" denotes solvent, assignments of other signals can be found in Figure 4 in the main text; black SEC line corresponds to starting TPE-diET_PLA; The expected structure of PLA-PAN-PLA copolymers on the top.

Author Contributions: Conceptualization, M.G., B.K., and M.B.; investigation, M.G.; methodology, M.G., B.K., and M.B.; supervision, B.K. and M.B.; writing—original draft, M.G. and M.B.; writing—review and editing, P.K. and M.B. All authors have read and agreed to the published version of the manuscript.

Funding: This work was supported by the National Science Centre, Poland, under Grant no. 2018/31/B/ST8/01969. Mateusz Grabowski acknowledges Bio-Med-Chem Doctoral School of the University of Lodz and Lodz Institutes of the Polish Academy of Sciences under which this study was conducted.

Institutional Review Board Statement: Not applicable.

Informed Consent Statement: Not applicable.

Data Availability Statement: The data presented in this study are available in the article text and Supplementary Material.

Conflicts of Interest: The authors declare no conflict of interest.

References

1. Farah, S.; Anderson, D.G.; Langer, R. Physical and mechanical properties of PLA, and their functions in widespread applications—A comprehensive review. *Adv. Drug Deliv. Rev.* **2016**, *107*, 367–392. [CrossRef] [PubMed]
2. Nagarajan, V.; Mohanty, A.K.; Misra, M. Perspective on Polylactic Acid (PLA) based Sustainable Materials for Durable Applications: Focus on Toughness and Heat Resistance. *ACS Sustain. Chem. Eng.* **2016**, *4*, 2899–2916. [CrossRef]
3. Pang, X.; Zhuang, X.; Tang, Z.; Chen, X. Polylactic acid (PLA): Research, development and industrialization. *Biotechnol. J.* **2010**, *5*, 1125–1136. [CrossRef] [PubMed]
4. Oh, J.K. Polylactide (PLA)-based amphiphilic block copolymers: Synthesis, self-assembly, and biomedical applications. *Soft Matter* **2011**, *7*, 5096–5108. [CrossRef]
5. Madhavan Nampoothiri, K.; Nair, N.R.; John, R.P. An overview of the recent developments in polylactide (PLA) research. *Bioresour. Technol.* **2010**, *101*, 8493–8501. [CrossRef] [PubMed]
6. Maharana, T.; Pattanaik, S.; Routaray, A.; Nath, N.; Sutar, A.K. Synthesis and characterization of poly(lactic acid) based graft copolymers. *React. Funct. Polym.* **2015**, *93*, 47–67. [CrossRef]
7. Puthumana, M.; Santhana Gopala Krishnan, P.; Nayak, S.K. Chemical modifications of PLA through copolymerization. *Int. J. Polym. Anal. Charact.* **2020**, *25*, 634–648. [CrossRef]
8. Becker, J.M.; Pounder, R.J.; Dove, A.P. Synthesis of poly(lactide)s with modified thermal and mechanical properties. *Macromol. Rapid Commun.* **2010**, *31*, 1923–1937. [CrossRef]
9. Yildirim, I.; Weber, C.; Schubert, U.S. Old meets new: Combination of PLA and RDRP to obtain sophisticated macromolecular architectures. *Prog. Polym. Sci.* **2018**, *76*, 111–150. [CrossRef]
10. Otsu, T. Iniferter concept and living radical polymerization. *J. Polym. Sci. Part A Polym. Chem.* **2000**, *38*, 2121–2136. [CrossRef]
11. Otsu, T.; Matsumoto, A.; Tazaki, T. Radical polymerization of methyl methacrylate with some 1,2-disubstituted tetraphenylethanes as thermal iniferters. *Polym. Bull.* **1987**, *17*, 323–330. [CrossRef]
12. Yao, X.Q.; Hou, X.J.; Wu, G.S.; Xu, Y.Y.; Xiang, H.W.; Jiao, H.; Li, Y.W. Estimation of C-C bond dissociation enthalpies of large aromatic hydrocarbon compounds using DFT methods. *J. Phys. Chem. A* **2002**, *106*, 7184–7189. [CrossRef]
13. Braun, D.; Becker, K.H. Aromatische Pinakole als Polymerisationsinitiatoren. *Die Angew. Makromol. Chemie* **1969**, *6*, 186–189. [CrossRef]
14. Braun, D.; Becker, K.H. Kinetik der Polymerisationsauslösung mit aromatischen pinakolen. *Die Makromol. Chemie* **1971**, *147*, 91–99. [CrossRef]
15. Btedzki, A.; Braun, D.; Menzel, W.; Titzschkau, K. Polymerizationsauslosung mit subsstituierten Ethanen. *Makromol. Chemie* **1983**, *294*, 287–294. [CrossRef]
16. Błedzki, A.; Braun, D.; Titzschkau, K. Polymerisationsauslösung mit substituierten ethanen, 6. Polymerisation von methylmethacrylat mit verschiedenen tetraphenylethanen. *Die Makromol. Chem.* **1983**, *184*, 745–754. [CrossRef]
17. Tharanikkarasu, K.; Radhakrishnan, G. A Novel Polyurethane Macroinitiator for Free Radical Polymerization. *Eur. Polym. J.* **1994**, *30*, 1351–1355. [CrossRef]
18. Tharanikkarasu, K.; Radhakrishnan, G. Tetraphenylethane Iniferters. II. Toluene Diisocyanate-Based Polyurethane Iniferter for "living Radical Polymerization of Acrylonitrile. *J. Polym. Sci. Part A Polym. Chem.* **1996**, *34*, 1723–1731. [CrossRef]
19. Tharanikkarasu, K.; Radhakrishnan, G. Tetraphenylethane iniferters. 3. "living" radical polymerization of methyl methacrylate using toluene-diisocyanate-based polyurethane iniferter. *J. Macromol. Sci. Part A Pure Appl. Chem.* **1996**, *A33*, 417–437. [CrossRef]
20. Tharanikkarasu, K.; Radhakrishnan, G. "Living" radical polymerization of styrene using tetraphenylethane-based polyurethane iniferter. *Polym. Int.* **1997**, *43*, 13–21. [CrossRef]
21. Tharanikkarasu, K.; Radhakrishnan, G. Tetraphenylethane iniferters: Polyurethane-polystyrene multiblock copolymers through "living" radical polymerization. *J. Appl. Polym. Sci.* **1997**, *66*, 1551–1560. [CrossRef]

22. Zhou, G.; Ma, C.; Zhang, G. Synthesis of polyurethane-g-poly(ethylene glycol) copolymers by macroiniferter and their protein resistance. *Polym. Chem.* **2011**, *2*, 1409–1414. [CrossRef]
23. Zhang, Y.; Wang, L.; Zhang, Z.; Zhang, Y.; Tuo, X. Synthesis and simultaneous self-assembly of multiblock fluorinated polyurethane in iniferter polymerization. *J. Polym. Sci. Part A Polym. Chem.* **2013**, *51*, 2161–2170. [CrossRef]
24. Grabowski, M.; Kost, B.; Gostyński, B.; Bednarek, M. Can tetraphenylethane (TPE) "iniferter" group be introduced into the polymer chain by coupling TPE diol with diisocyanate? *Polymer (Guildf).* **2022**, *246*, 124738. [CrossRef]
25. Muñiz, M.K. 3.14 The Pinacol Rearrangement. *Compr. Org. Synth. Second Ed.* **2014**, *3*, 741–756.
26. Zalibera, M.; Nesvadba, P.; Gescheidt, G. Reaction of benzopinacol with non-ionic bases: Reversing the pinacol coupling. *Org. Lett.* **2013**, *15*, 4627–4629. [CrossRef]
27. Tanimoto, S.; Toshimitsu, A. Synthesis of Ultraviolet Absorbers Having 2-Hydroxybenzophenone Moiety as the Functional Group. *Bull. Inst. Chem. Res., Kyoto Univ.* **1992**, *69*, 560–570.
28. Baśko, M.; Kubisa, P. Cationic polymerization of L,L-lactide. *J. Polym. Sci. Part A Polym. Chem.* **2010**, *48*, 2650–2658. [CrossRef]
29. Dashan, I.; Karaca, D.; Aydogan, B.; Temel, G. Preparation of single chain nanoparticles via photoinduced radical coupling process. *Eur. Polym. J.* **2019**, *113*, 183–191. [CrossRef]

polymers

MDPI

Supplementary Materials: A New Approach to The Synthesis of Polylactide/Polyacrylonitrile Block Copolymers

Mateusz Grabowski, Bartłomiej Kost, Przemysław Kubisa and Melania Bednarek

1. Benzophenone Derivative Containing Primary -OH Group (HBP-ET)

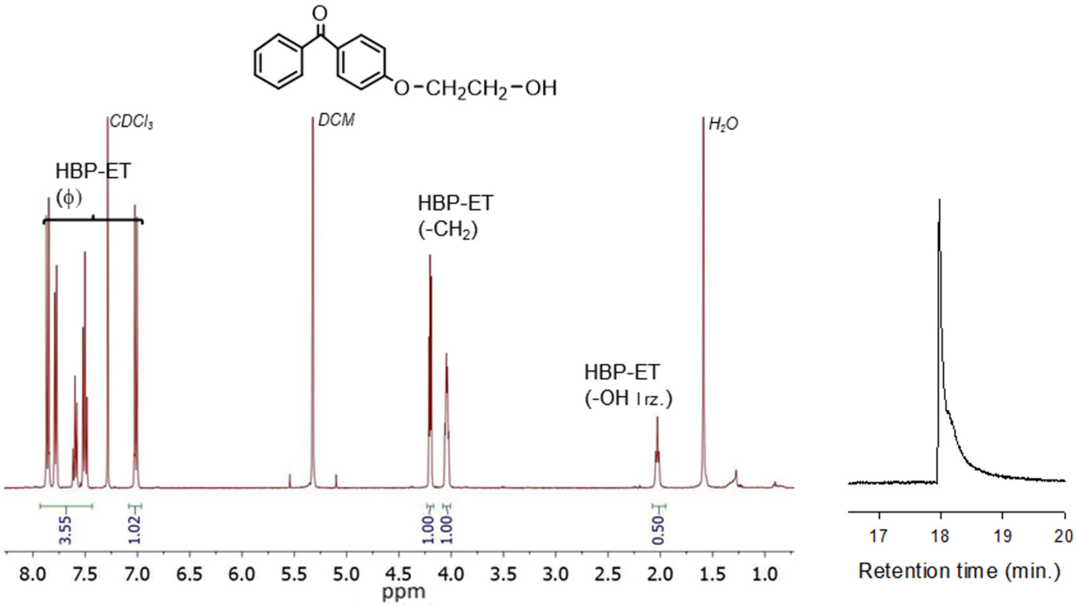

Figure S1. ^{1}H NMR spectrum ($CDCl_3$) and GC chromatogram for the synthesized HBP-ET.

2. PLAs Obtained by the Application Of HBP-ET as the Lactide Polymerization Initiator

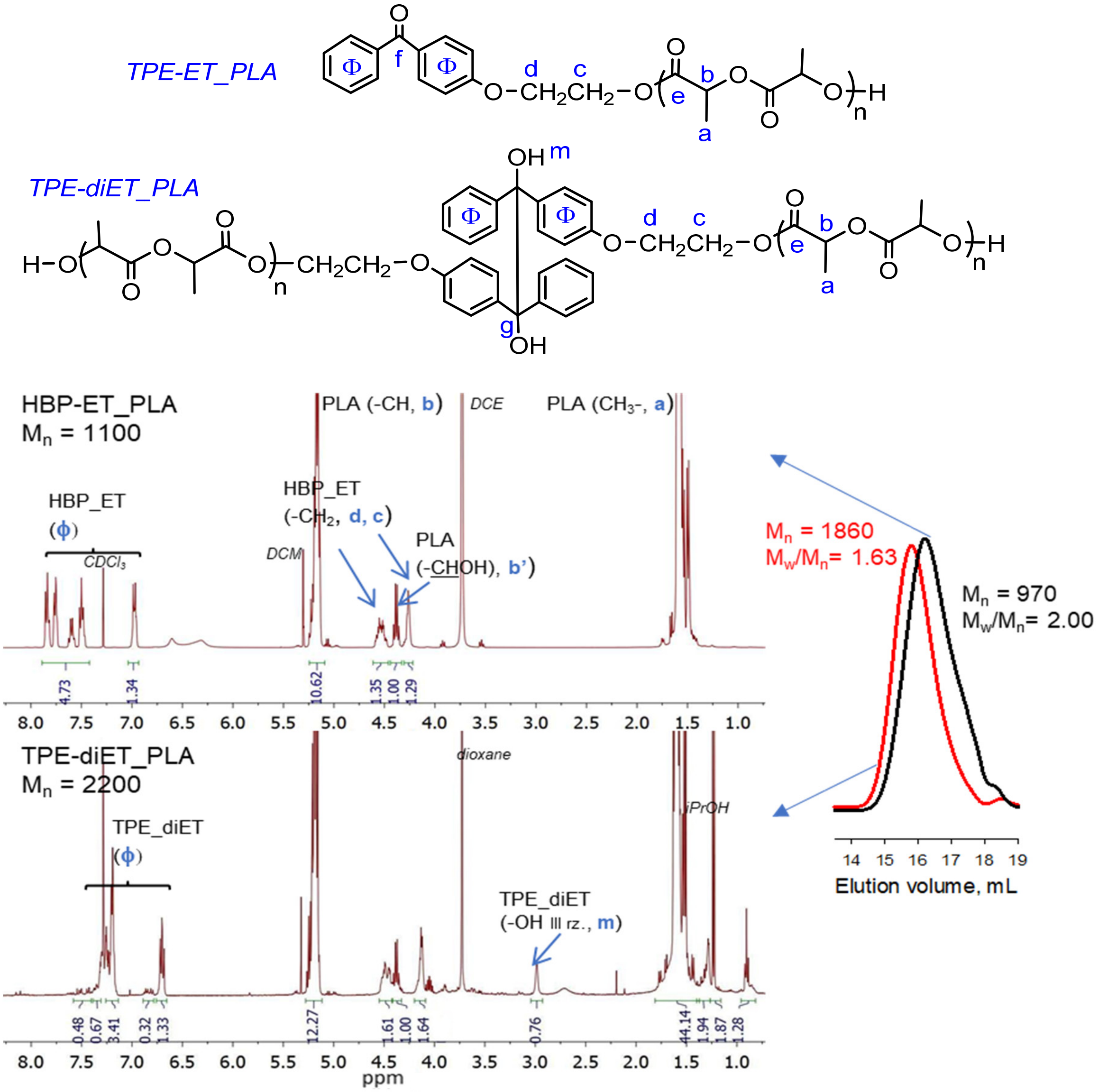

Figure S2. ^{1}H NMR spectra (CDCl$_3$) for HBP-ET_PLA, M_n=1100 and TPE-diET_PLA after coupling under UV radiation, M_n = 2200; PLAs formulas on the top.

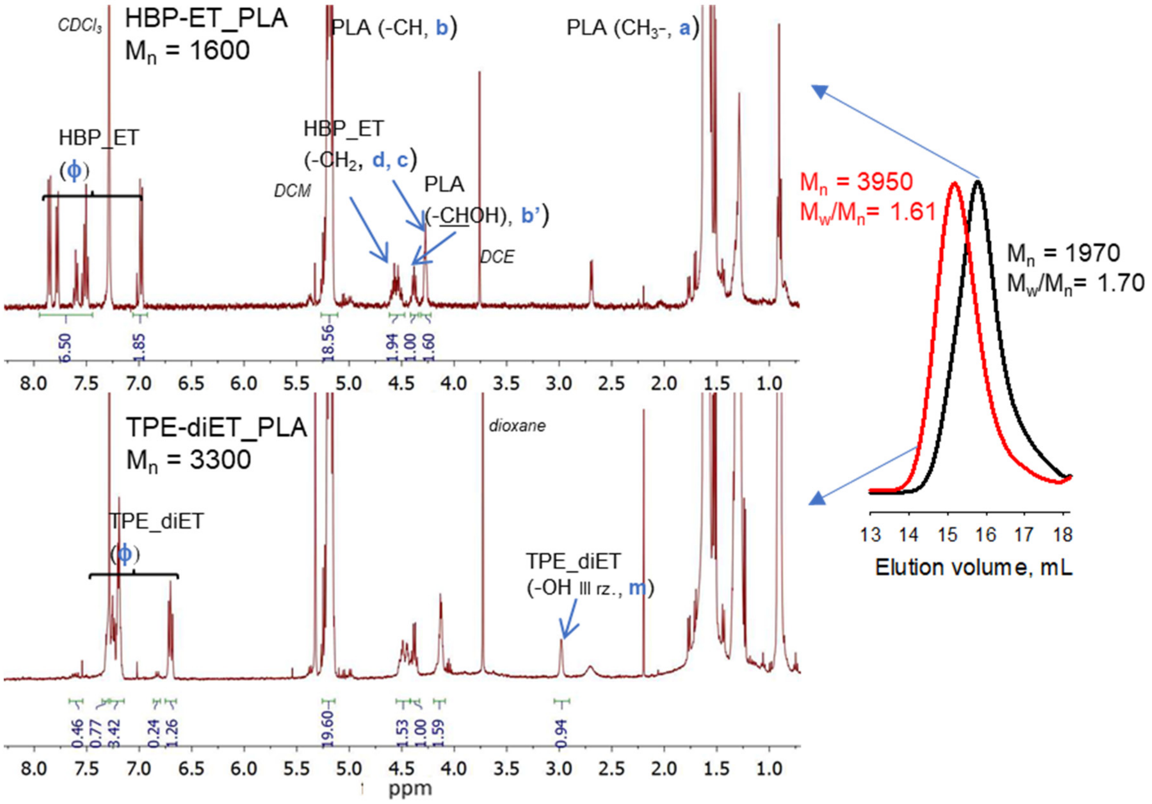

Figure S3. ^{1}H NMR spectra ($CDCl_3$) for HBP-ET_PLA, M_n=1600 and TPE-diET_PLA after coupling under UV irradiation, M_n = 3300.

Molecular weights of HBP-ET_PLA and TPE-diET_PLA polymers were calculated by the comparison of the intensities of signals corresponding to -<u>CH</u>(CH_3)-OH end groups at 4.3 ppm and corresponding to -<u>CH</u>(CH_3)- groups from PLA backbone at 5.2 ppm.

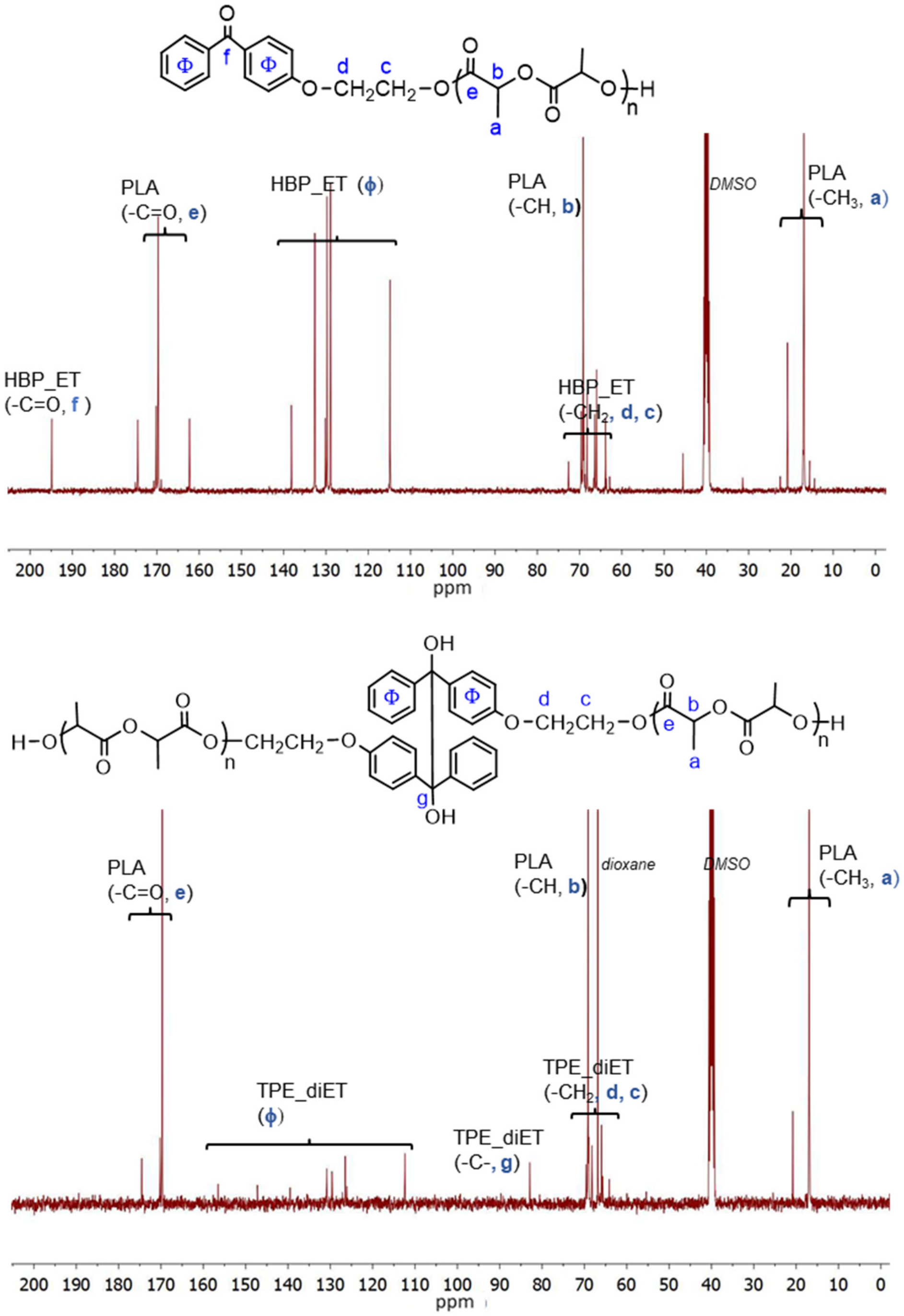

Figure S4. ^{13}C NMR spectra for HBP-ET_PLA (M_n = 700) and TPE-diET_PLA (M_n = 1400) after the coupling reaction. The signal characteristic for carbonyl group of benzophenone moiety present in HBP-ET_PLA at ~195 ppm disappears after coupling and a new signal at ~82 ppm corresponding to quaternary carbon atom in TPE unit appears.

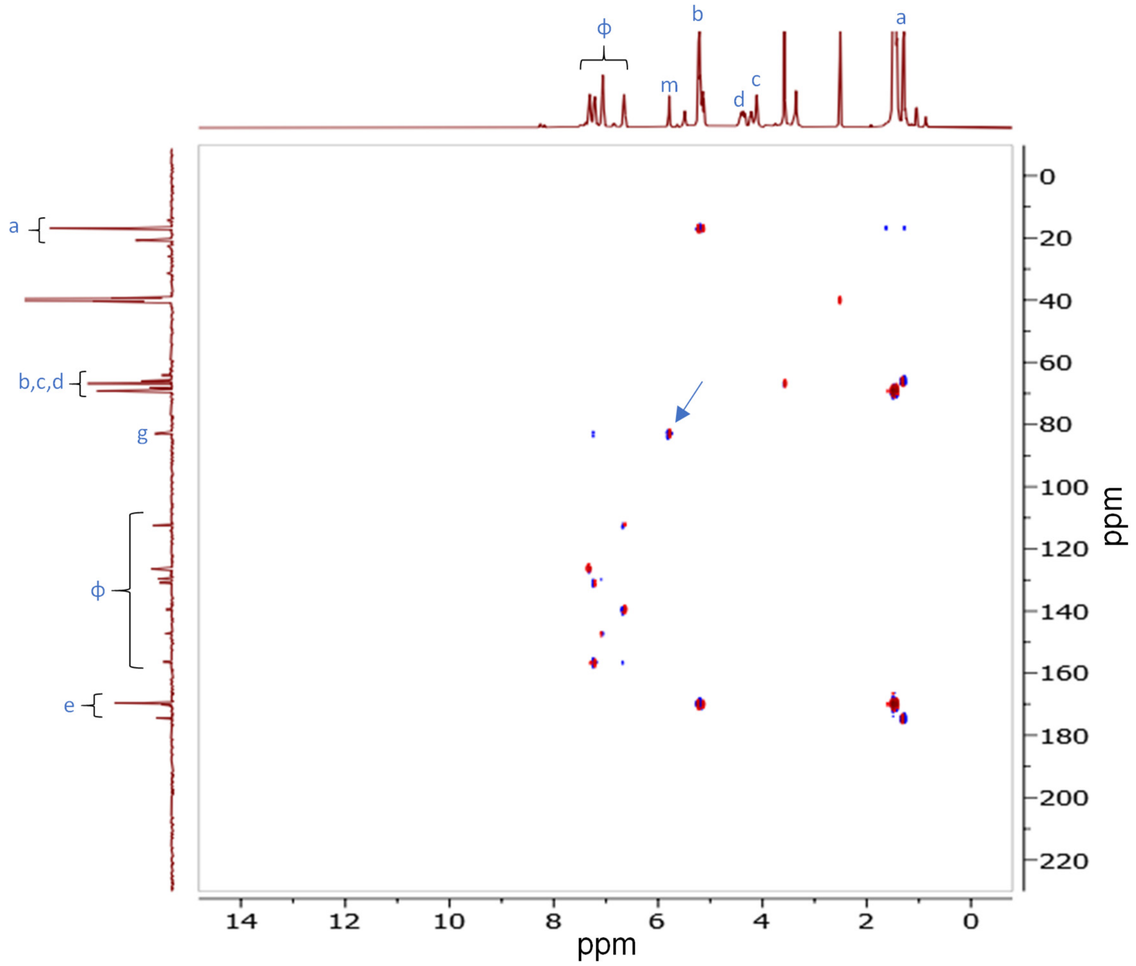

Figure S5. $^1H^{13}C$-HMBC NMR spectra for TPE-diET_PLA (M_n = 1400). An arrow indicates correlation between quaternary carbon atom and tertiary -OH group from TPE-diET unit.

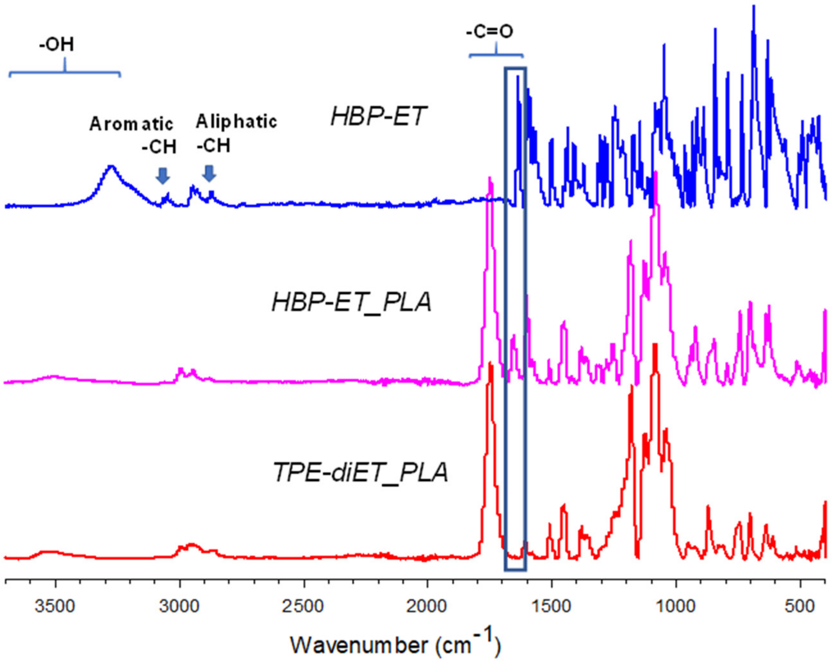

Figure S6. FTIR spectra for HBP-ET initiator, HBP-ET_PLA polymer (M_n = 700) and TPE-diET_PLA after coupling of HBP-ET_PLA (M_n = 1400).

It is visible that the signal corresponding to carbonyl group in HBP-ET at ~1650 cm^{-1} disappeared after coupling of HBP-ET_PLA leading to TPE-diET_PLA.

3. Conversion of Acrylonitrile for Performed Copolymer Syntheses and the Kinetic Experiment

Conversion of AN was calculated by the comparison of the intensities of signals corresponding to unsaturated groups at 5.8-6.4 ppm from AN monomer (3 protons) with the intensity of the well separated signal corresponding to methylene protons from PAN chain at 2.0-2.25 ppm (2 protons).

Decomposition percent of TPE groups (kinetic experiment) was calculated by the comparison of the intensities of signals in the range 6.6–7.8 ppm which remained after abstraction of signals at 6.65, 7.06, 7.25, and 7.36 ppm corresponding to initial TPE group, with the sum of intensities of all signals in the range 6.6–7.8 ppm.

4. Analysis of Acrylonitrile Polymerization Products

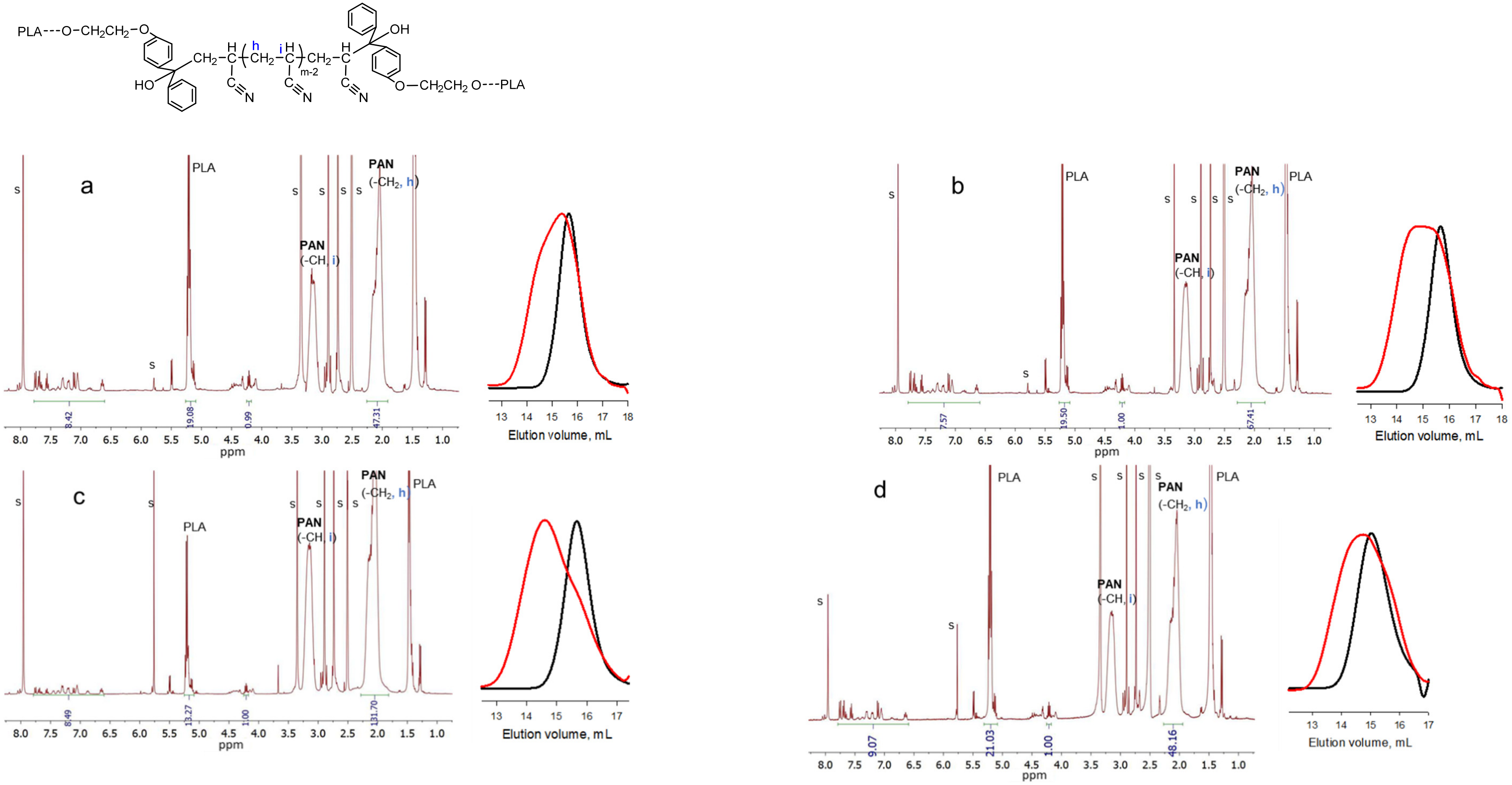

Figure S7. ^{1}H NMR spectra (DMSO-d6) and SEC curves (red line) for the products of reactions No: (**a**) 2, (**b**) 3, (**c**) 4, (**d**) 5 in Table 1 in the main text; "s" denotes solvent, assignments of other signals can be found in Fig. 4 in the main text; black SEC line corresponds to starting TPE-diET_PLA; The expected structure of PLA-PAN-PLA copolymers on the top.

Molecular weights of TPE-diET_PLA/PAN copolymers were calculated as follows:

1. $M_{PLA\ block}$ = $P_{n\ PLA}$ (intensity of the signal corresponding to -$\underline{CH}(CH_3)$- groups from PLA backbone at 5.2 ppm / intensity of the signal corresponding to -$\underline{CH}(CH_3)$-OH end groups at 4.3 ppm) × 144
2. $M_{PAN\ block}$ = $P_{n\ PAN}$ ($P_{n\ PLA}$ x AN/PLA ratio from Table 1) × 53
3. M_n of copolymer = $M_{PLA\ block}$ + $M_{PAN\ block}$ + 486 ($M_{TPE\text{-}diET}$)

Publikacja 3:

Mateusz Grabowski, Bartłomiej Kost, Agnieszka Bodzioch, Melania Bednarek. Functionalization of Polylactide with Multiple Tetraphenylethane Inifer Groups to Form PLA Block Copolymers with Vinyl Monomers. Int. J. Mol. Sci. 2023;24(1):19. doi:10.3390/ijms24010019

International Journal of
Molecular Sciences

Article

Functionalization of Polylactide with Multiple Tetraphenyethane Inifer Groups to Form PLA Block Copolymers with Vinyl Monomers

Mateusz Grabowski, Bartłomiej Kost, Agnieszka Bodzioch and Melania Bednarek *

Centre of Molecular and Macromolecular Studies, Polish Academy of Sciences, Sienkiewicza 112, 90-363 Lodz, Poland; mgrabowski@cbmm.lodz.pl (M.G.); kost@cbmm.lodz.pl (B.K.); agabodz@cbmm.lodz.pl (A.B.)
* Correspondence: bednarek@cbmm.lodz.pl

Abstract: In the present contribution, a new strategy for preparing block copolymers of polylactide (PLA), a bio-derived polymer of increasing importance, is described. The method should lead to multiblock copolymers of lactide with vinyl monomers (VM), i.e., monomers that polymerize according to different mechanisms, and is based on the introduction of multiple "inifer" (*INItiator/transFER agent*) groups into PLA's structure. As an "inifer" group, tetraphenylethane (TPE, known to easily thermally dissociate to radicals) was incorporated into PLA chains using diisocyanate. PLA that contained TPE groups (PLA-PU) was characterized, and its ability to form initiating radicals was demonstrated by ESR measurements. PLA-PU was used as a "macroinifer" for the polymerization of acrylonitrile and styrene upon moderate heating (85 °C) of the PLA-PU in the presence of monomers. The formation of block copolymers PLA/PVM was confirmed by ^{1}H NMR, DOSY NMR, and FTIR spectroscopies and the SEC method. The prepared copolymers showed only one glass transition in DSC curves with T_g values higher than those of PLA-PU.

Keywords: polylactide; block copolymer; tetraphenylethane; inifer; radical polymerization

Citation: Grabowski, M.; Kost, B.; Bodzioch, A.; Bednarek, M. Functionalization of Polylactide with Multiple Tetraphenyethane Inifer Groups to Form PLA Block Copolymers with Vinyl Monomers. *Int. J. Mol. Sci.* **2023**, *24*, 19. https://doi.org/10.3390/ijms24010019

Academic Editor: Ana María Díez-Pascual

Received: 24 November 2022
Revised: 14 December 2022
Accepted: 15 December 2022
Published: 20 December 2022

1. Introduction

Polylactide is one of the polymers under development that, originating from renewable resources, could replace petroleum-based polymers in some applications [1,2]. Concerning the various sophisticated applications, e.g., in biomedicine, but also in the production of commodity products, the tuning of material properties to meet application requirements is needed. One of the methods of modifying polymer properties is the introduction of other structural units into the polymer macromolecule. This can be achieved in different ways, one of which is copolymerization. Block copolymers are a combination of blocks of two or several homopolymers of different natures that provide new properties in comparison with individual homopolymers, and very often they can self-organize into interesting and sometimes very useful structures. Block copolymers can be synthesized via different approaches. The simplest method is successive polymerization if both blocks can by polymerized by the same mechanism. If, however, two blocks are to be prepared by different mechanisms, such as the copolymer polylactide/poly(vinyl monomer), then ring-opening polymerization has to be combined with known methods of radical polymerization including appropriate block(s) functionalization [3–5]. Thus, new combinations of known methods are being searched for and applied.

We have recently described the preparation of the triblock copolymer PLA/poly(acrylonitrile)/PLA [6] using the "macroinifer" (MI) concept [7]. The main step of this synthesis is the preparation of a PLA homopolymer containing a thermal "inifer" group in the middle of the PLA chain [6]. Tetraphenyletahane (TPE) was applied as the inifer, which is known as a group that undergoes dissociation into radicals under heating and as being able to initiate radical polymerization [8–11]. TPE was generated inside the PLA chain from benzophenone fragments [12,13] via a method we elaborated [6] (commercial benzopinacole could not be introduced via the initiation of lactide polymerization due to the insufficient reactivity of tertiary -OH groups, which was proven by us previously [13]). Using a PLA-TPE macroinifer, acrylonitrile (AN) was polymerized at 85 °C, resulting in the triblock copolymer. As was demonstrated, by varying the molecular weight of the initiating PLA-TPE and the initial AN/PLA-TPE ratio, the composition of the triblock copolymer could be regulated [6].

Following our earlier work, we decided to prepare multiblock copolymers of polylactide and selected poly(vinyl monomers) (PVM) while using the same TPE group as an inifer group but with the introduction of multiple TPE groups into a PLA-based polymer. This was achieved by coupling PLA-diol with TPE-containing diol using aliphatic diisocyanate. A similar approach has been used by other groups for the preparation of multiblock copolymers of poly(tetrahydrofuran), poly(propylene oxide), and poly(ε-caprolactone) with vinyl monomer blocks [14–19]. However, the authors used commercial diol containing TPE groups, i.e., tetraphenylethane diol (TPED, benzopinacol), for the coupling reaction. We found that the reaction of such a diol (TPED) with diisocyanate was doubtful due to the insufficient reactivity of the tertiary hydroxyl groups [20]. We also publish the results of experiments aiming to prove this fact, and we suggested replacing the commercial TPED with a derivative synthesized by us. This derivative was synthesized by coupling benzophenone functionalized with primary hydroxyl group [13].

Thus, in the present work, a TPE derivative containing primary hydroxyl groups (TPE-diET, the structure is shown in Figure 1) obtained from 4-hydroxyethoxybenzophenone was coupled with a PLA-diol using diisocyanate to obtain a PLA-based macroinifer. This macroinifer (PLA-PU) was used to polymerize radically acrylonitrile and styrene (ST) to produce multiblock copolymers via the insertion of vinyl monomer units in between TPE units in the PLA chain. The conditions required to achieve control over the synthesis of a polylactide with TPE groups and the course of the radical polymerization are elaborated, and the limitations for the molecular weight of the obtained PLA copolymer are discussed.

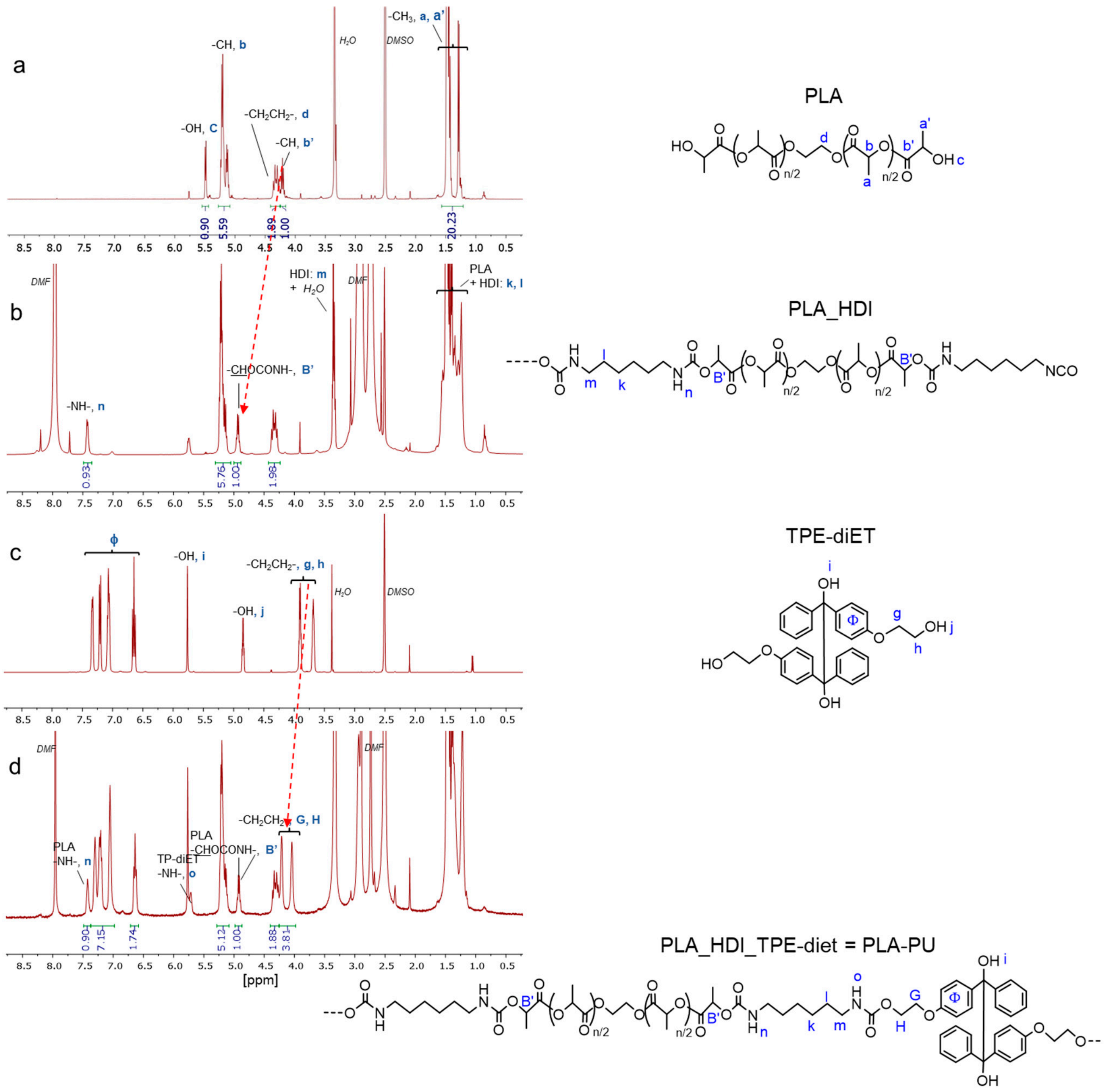

Figure 1. Tracking the formation of PLA-based polyurethane (PLA-PU) containing TPE groups by ^1H NMR analysis (DMSO-d_6). Red arrows indicate changes in the position of the terminal -<u>CH</u>OH (from PLA: (**a**,**b**)) or -<u>CH2CH2</u>OH (from TPE-diET: (**c**,**d**)).

2. Results and Discussion

2.1. Synthesis of Polylactide-Based Polymer Containing Multiple Tetraphenylethane Groups

A PLA-based polymer (polyester-urethane, PLA-PU) was synthesized by coupling PLA-diol with a low molecular weight diol containing TPE (TPE-diET) using hexamethyl-diisocyanante (HDI). First, polylactide diol was prepared via the cationic ring-opening polymerization of L-lactide using a difunctional initiator [21]. TPE-diET diol bearing primary -OH groups was synthesized according to the procedure described in our earlier article [13]. As a result of the preliminary experiments, DMF was chosen as a solvent that was able to solubilize all the substrates and products of polyurethane synthesis, and DBTDL was used as a catalyst for the formation of urethane linkages. It was important that the prepared PLA-based polymer had the assumed structure with TPE units covalently linked to the PLA chain. Thus, the synthesis was performed in two steps—first, PLA-diol was reacted with a two-fold excess of HDI in the presence of a catalyst at 40 °C, and next, after about 1.5 h, the TPE-diET was added to a small amount of solvent. The reaction was continued up to 24 h, and the product was analyzed at each reaction step by ^{1}H NMR of the reaction mixture. Finally, the product was precipitated two times before final analyses and further use. The success of coupling and the incorporation of TPE units in the polymer structure was confirmed by ^{1}H NMR and FTIR analyses. Corresponding spectra are shown in Figures 1 and S1.

In the ^{1}H NMR spectra, signals corresponding to all expected units from polylactide, TPE-diET, and HDI are present. Additionally the signal of the formed -NH- groups from urethane at 7.43 ppm appears after the addition of HDI and at 5.72 ppm after the addition of TPE-diET. Signals corresponding to -$\underline{CH}$OH PLA end groups and to -$\underline{CH_2CH_2}$OH groups in TPE-diET were shifted to new positions with higher chemical shift values after the reaction of -OH groups with diisocyanate (Figure 1).

In the IR spectra, the signals corresponding to -NH- groups at 3330 and 3400 cm^{-1}, to C=O groups from urethane at ~1730 cm^{-1}, and to -C-NH- at ~1630 cm^{-1} [22] are visible in addition to signals characteristic of PLA and TPE-diET (Figure S1). The obtained PLA-based polyurethane (PLA-PU) analyzed by SEC chromatography had a moderate molecular weight (its GPC curve is shown in Figure S1).

2.2. The Ability of TPE Groups inside PLA-Based Polyurethane to Form Radicals

Although, according to the above-cited literature, the -C(Ph)$_2$-C(Ph)$_2$- bond in a benzopinacole molecule can dissociate and initiate radical polymerization, it was not obvious that it could form radicals when present in a benzopinacole moiety (TPE-diET) placed in polylactide-based polyurethane. To check this, electron spin resonance (ESR) spectroscopy measurements were performed. PLA-PU with TPE inside was analyzed in the presence of TEMPO (2,2,6,6-tetramethylpiperidine-1-oxyl) radical able to capture -C(Ph)$_2$• radicals formed during heating. Figure 2 presents the ESR spectra recorded at different temperatures and the progress of the decomposition of TPE groups present in PLA-PU polymer with the temperature increase. The higher the temperature, the faster the decomposition of the TPE units (more formed radicals, and, consequently, more trapped radicals). It can be seen that above 75 °C, the rate of dissociation increases only slightly, and thus a temperature of 85 °C was selected in order to generate radicals at a sufficient rate while also limiting possible side reactions.

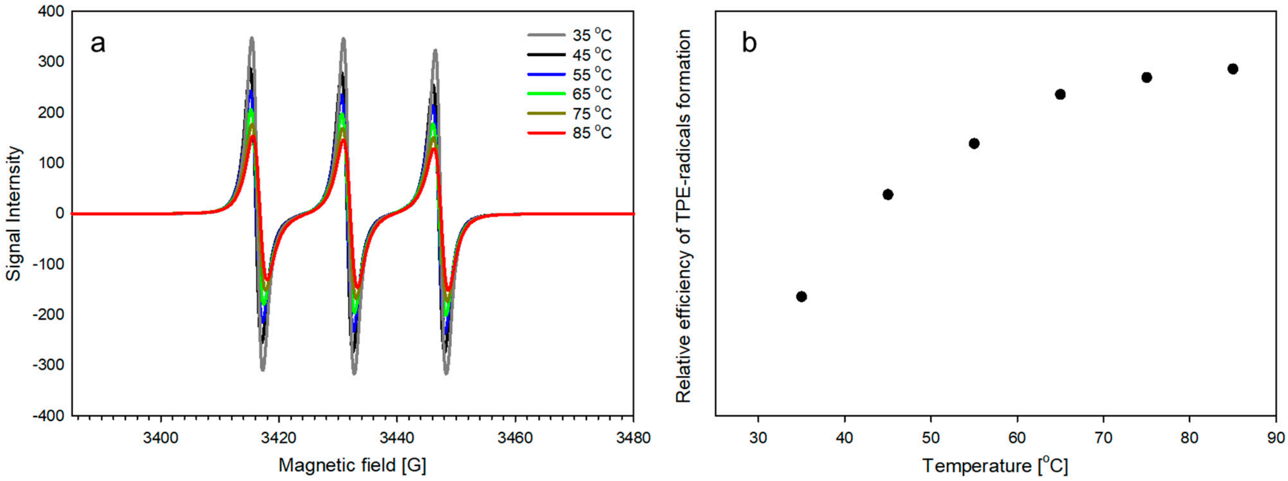

Figure 2. (**a**) ESR spectra of PLA-PU recorded at different temperatures in the presence of TEMPO. (**b**) Progress of the decomposition of TPE groups in a PLA-PU polymer with an increase in temperature (the relative concentration of radicals was calculated according to the method described in the SI using normalized intensities from ESR spectra, Figure S2, Equations (S1a,b)).

2.3. Polymerization of Acrylonitrile and Styrene Initiated with PLA-PU Containing TPE Groups

The anticipated formation of multiblock polylactide/poly(vinyl monomer) copolymers by the adaptation of the inifer concept [7] is presented schematically in Figure 3. In brief, assuming that, after the initiation of the radical polymerization of VM and several propagation steps, growing radicals will recombine, the introduction of VM blocks into PLA-based PU should proceed by the insertion of VM in the middle of the TPE groups present in PLA-PU.

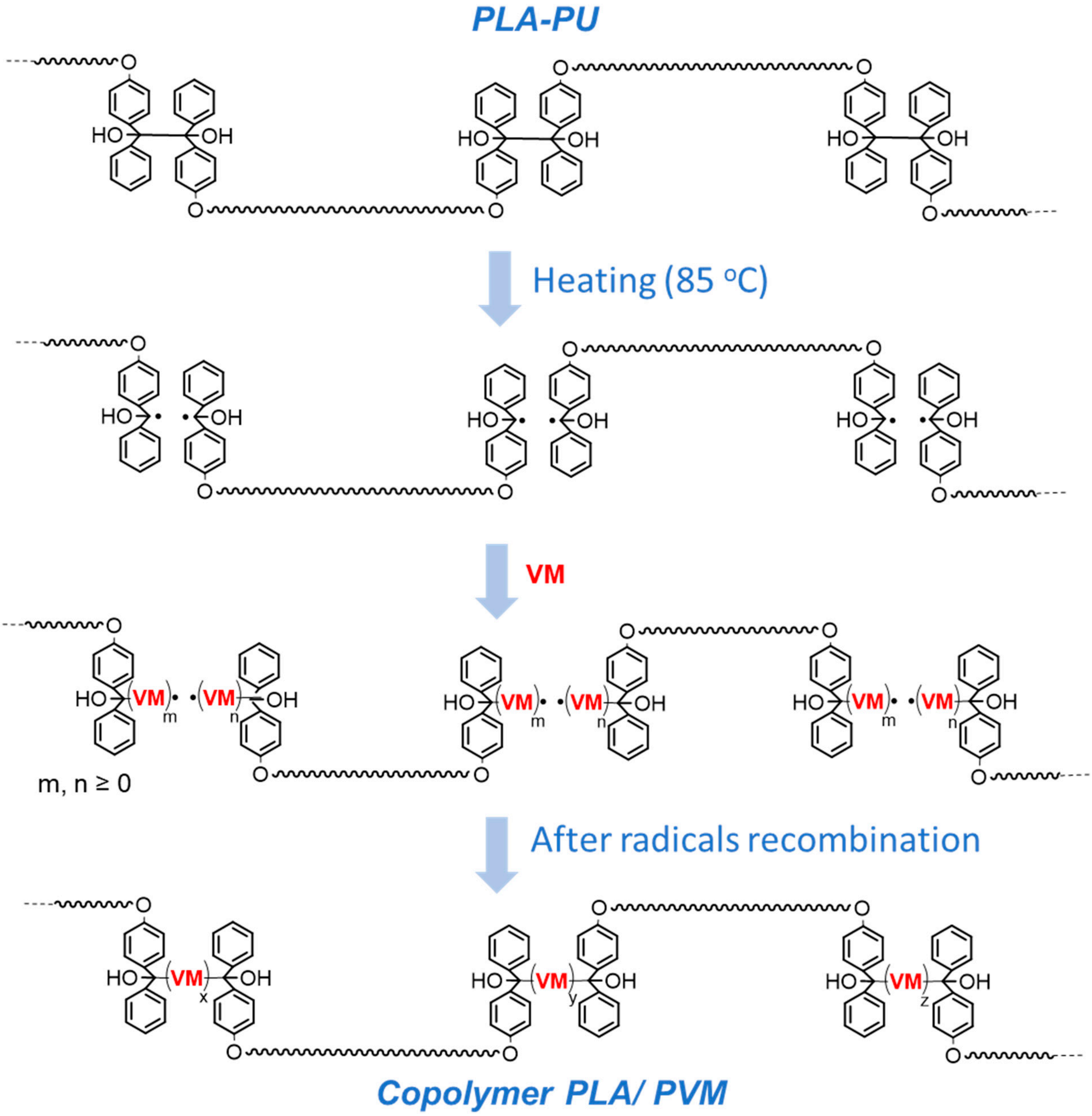

Figure 3. Schematic representation of the formation of a PLA/PVM copolymer using a PLA-PU macroinifer.

The idea presented in Figure 3 can be realized under one condition, i.e., when growing radicals are able to recombine. As is known from the literature, the termination of the polymerization of (meth)acrylates proceeds mainly by disproportionation [23,24], so in this case, there is a limited possibility to recombine the growing …PLA-…- $C(Ph)_2$-VM•

fragments that are formed after the dissociation of the TPE groups and the attachment of several VM units once again into one chain. The opposite is the case in the polymerization of styrene, where the recombination of styryl radicals dominates over their disproportionation [23]. Another vinyl monomer–acrylonitrile has been found to be capable of polymerizing with termination, mainly by recombination under appropriate conditions [25]. Considering this, in the present study, two vinyl monomers were chosen for the polymerization initiated by the PLA-PU macroinifer, i.e., acrylonitrile and styrene. Polymerizations were performed in two solvents with different polarities, DMF and anisole (the normalized solvent polarity parameter $E_T^N = 0.386$ for DMF and 0.198 for anisole [26]), by heating PLA-TPE macroinifer in the presence of a vinyl monomer to 85 °C. The dependence of the amount of VM incorporated in the copolymer on the initial VM/PLA ratio was shown in our previous work [6], and thus in this study, polymerizations were performed using the same mass of AN or ST with respect to the PLA-based macroinifer. The products isolated by the double precipitation of the reaction mixture were analyzed by the ^{1}H NMR, FTIR, and SEC methods (Figures 4, S3 and S4). In the ^{1}H NMR spectra of the copolymers prepared in DMA or anisole, the signals corresponding to AN or ST units were clearly visible. (Figure 4 presents exemplary spectra of the products of VM polymerization). By comparison with the intensities of the appropriate signals, the VM/LA ratio could be calculated.

The applied substrates for the vinyl monomer polymerization and characterization of the obtained products are presented in Table 1.

Table 1. Polymerization of VM with PLA-PU macroinifer (M_n = 37000, SEC), 85 °C, 24 h; the mass ratio of VM/PLA in the feed = 1.

Substrates				Conversion of VM [%]	PLA/PVM Copolymers [(a)]	
Vinyl Monomer, VM	Polymeriz. No	Mol Ratio of VM/LA in Feed	Solvent		Mol Ratio of VM/LA, ^{1}H NMR	M_n, SEC [(b)]
AN	1	4.8	DMF	85	7.0	n.d.
	2	4.8	Anisole	70	3.8	16,600
ST	3	2.5	DMF	37	0.4	n.d.
	4	2.5	DMF	45 (95 °C)	1.2	13,000
	6	2.5	Anisole	33	0.5	11,600

[(a)] Products analyzed after double precipitation (50–60% yield). [(b)] Calibration for polystyrene; M_n values should be treated with caution because polystyrene calibration could be inappropriate for the calculation of the M_n of a copolymer of LA with VM. The molecular weights determined for PLA with PST standards differ (sometimes significantly) from real values, thus different correcting factors are often applied [27]. n.d.—not determined.

Relatively high conversion of acrylonitrile was achieved in both solvents, DMF and anisole, during the applied polymerization time. It appeared, however, that the polymerization of styrene was not efficient at 85 °C (relatively low conversion), and thus it was also performed at 95 °C. As expected, a higher temperature promoted the decomposition of the TPE groups and, consequently, the conversion of styrene.

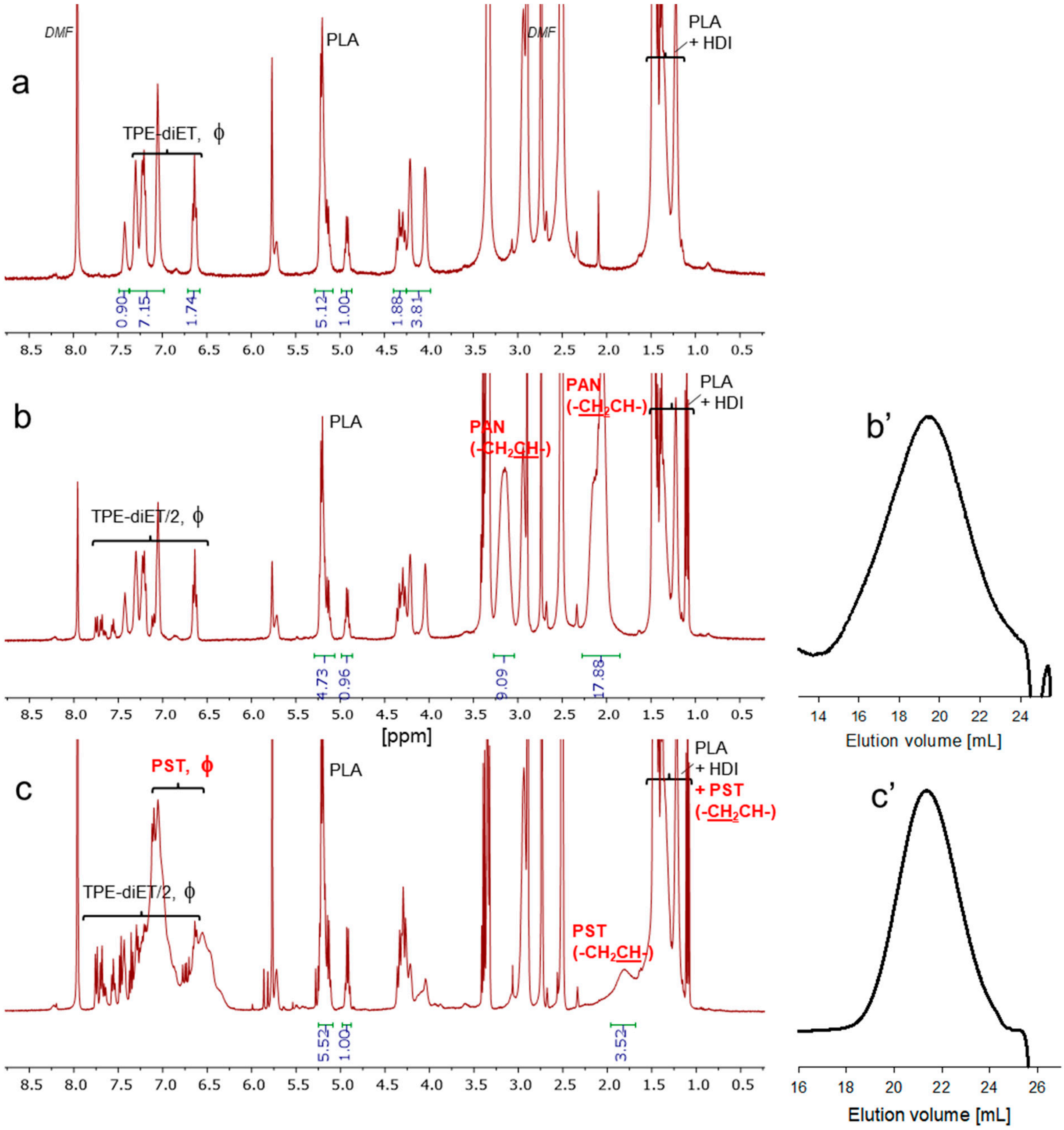

Figure 4. ^{1}H NMR spectra of the PLA-PU (**a**), PLA/PST (**b**), and PLA/PAN (**c**) copolymers prepared in DMF or anisole as a solvent; (**b′**,**c′**)—corresponding SEC curves.

The SEC analysis of the radical polymerization products provides two types of information. The first important observation is that all curves show a rather broad but definitely monomodal distribution, indicating the formation of copolymers (both monomeric units corresponding to lactide and vinyl monomer were detected by ^{1}H NMR spectroscopy). However, unexpectedly, when polystyrene calibration was applied (no reliable calibration for PLA/PVM copolymers is available), the obtained PLA/PVM copolymers had lower molecular weights than the initial PLA-PU (Table 1). Although the desired result is an increase in the molecular weight, a M_n value decrease is also explainable. First, different structural polymers were analyzed by SEC chromatography using unsuitable standards (polystyrene). Another possible reason for the observed decrease in the molecular weight is the sensitivity of polylactide to high temperature, and its possible degradation in the presence of small traces of catalyst and free -OH groups [28–30]. An additional experiment was performed where polyurethane prepared from PLA alone and HDI was heated for 24 h in DMF. It appeared that the molecular weight of PU dropped from 36,000 to 7000 as determined by SEC. In the ^{1}H NMR spectrum, new signals appeared corresponding to newly formed -OH groups (-$\underline{\text{CH}}$OH and -$\underline{\text{OH}}$). The results are presented in the SI (Figure S5). It is not excluded that DMF also contributed somehow to the PLA decomposition, because when the same PU prepared from PLA diol was heated in anisole, decomposition products were not detected in the ^{1}H NMR spectrum (although the M_n determined by SEC also decreased).

It should also be considered that a molecular weight decrease is a result of the incomplete recombination of growing -VM• radicals. If some growing radicals terminate by recombination and others by disproportionation, the products would be a mixture of multiblock copolymers of different lengths, which could explain the relatively broad dispersity observed by SEC. Because PLA-PU used as an inifer contains many TPE units, if the contribution of termination mechanism other than the recombination is not insignificant, the molecular weight of the final product may indeed be lower than that of the initial molecular weight of the PLA-PU.

Because the results obtained from the SEC analysis could not be treated as fully reliable, we searched for another method by which we could confirm the formation of copolymers. Such a possibility is offered by the application of diffusion-ordered spectroscopy (DOSY) NMR [31]. By this NMR method, each component in a mixture can be virtually separated based on its own diffusion coefficient. DOSY NMR appeared to be very useful to study the polymerization kinetics and determine the structure and molecular weight of the formed product [32–34]. Figure 5 presents DOSY maps (with ^{1}H NMR spectra on the top) obtained for the PLA-PU/PAN copolymer, the PLA-PU starting polymer, and the separately prepared PAN homopolymer. Similarly, in Figure 6, DOSY maps for the PLA-PU/PST copolymer, the PLA-PU, and the PST homopolymer are shown.

As can be seen in Figures 5 and 6 (and the data shown in Table S1), the diffusion coefficients for building blocks in pairs—PLA-PU, PAN ($D_{av.} = 1.26 \cdot 10^{-7}$ cm^2/s and $0.78 \cdot 10^{-7}$ cm^2/s, respectively) and PLA-PU, PST ($D_{av.} = 1.43 \cdot 10^{-7}$ cm^2/s and $7.47 \cdot 10^{-7}$ cm^2/s, respectively)—differ. Additionally, the values of the diffusion coefficients of the radical polymerization products are not the same as those characteristic of their building blocks (i.e., $D_{av} = 2.81 \cdot 10^{-7}$ cm^2/s for PLA-PU/PAN and $3.22 \cdot 10^{-7}$ cm^2/s for PLA-PU/PST), confirming the formation of the copolymer. It should be noted from the DOSY NMR spectra that the same diffusion coefficient for different structural components of PLA-PU means that the used macroinifer was pure (i.e., not contaminated with PLA diol or TPE-diET diol).

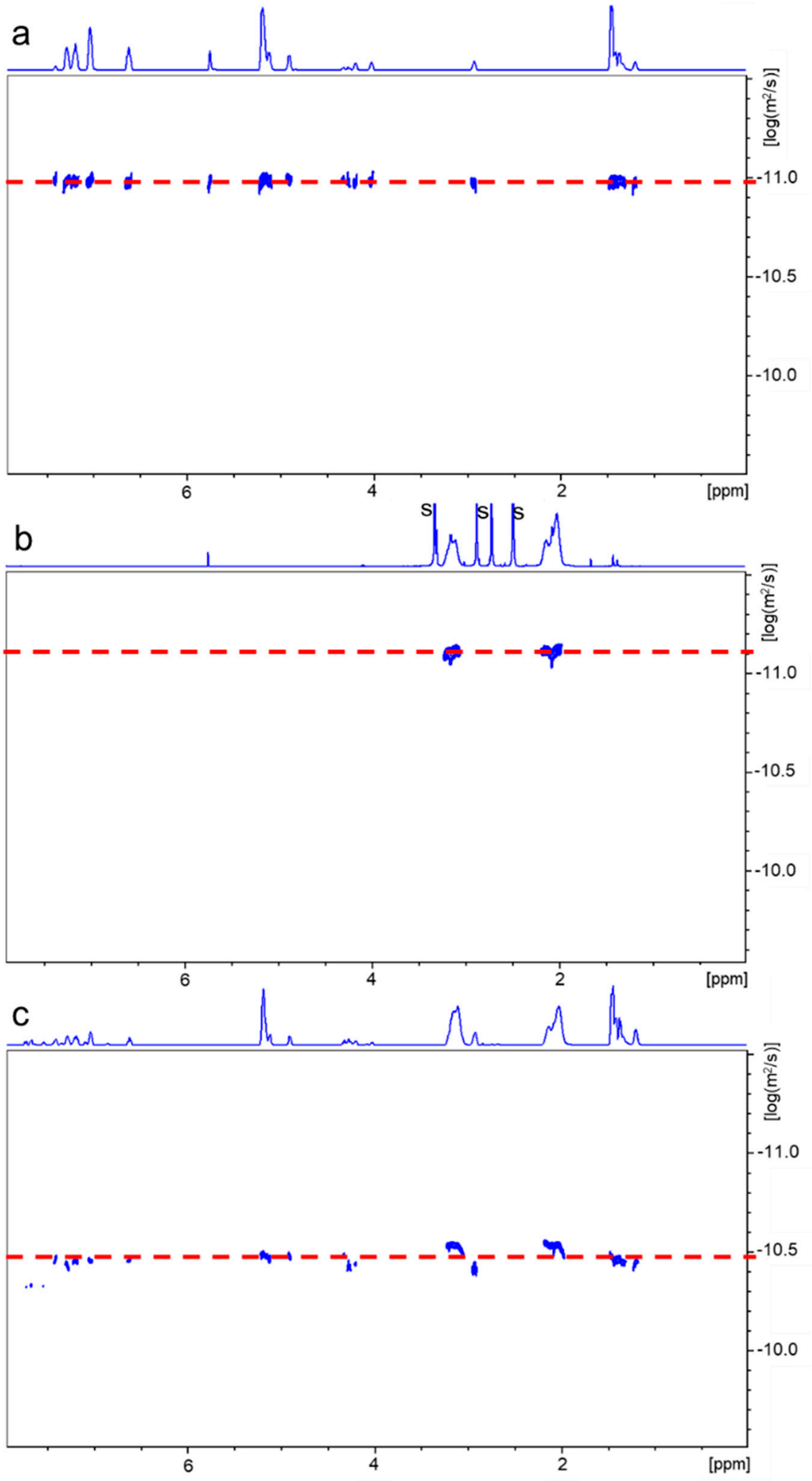

Figure 5. 2D DOSY NMR spectra of PLA-PU (**a**), PAN (**b**), and PLA/PAN copolymer (**c**) recorded in DMSO-d_6 (the area of the appearance of signals corresponding to the remaining solvents “s” is not shown).

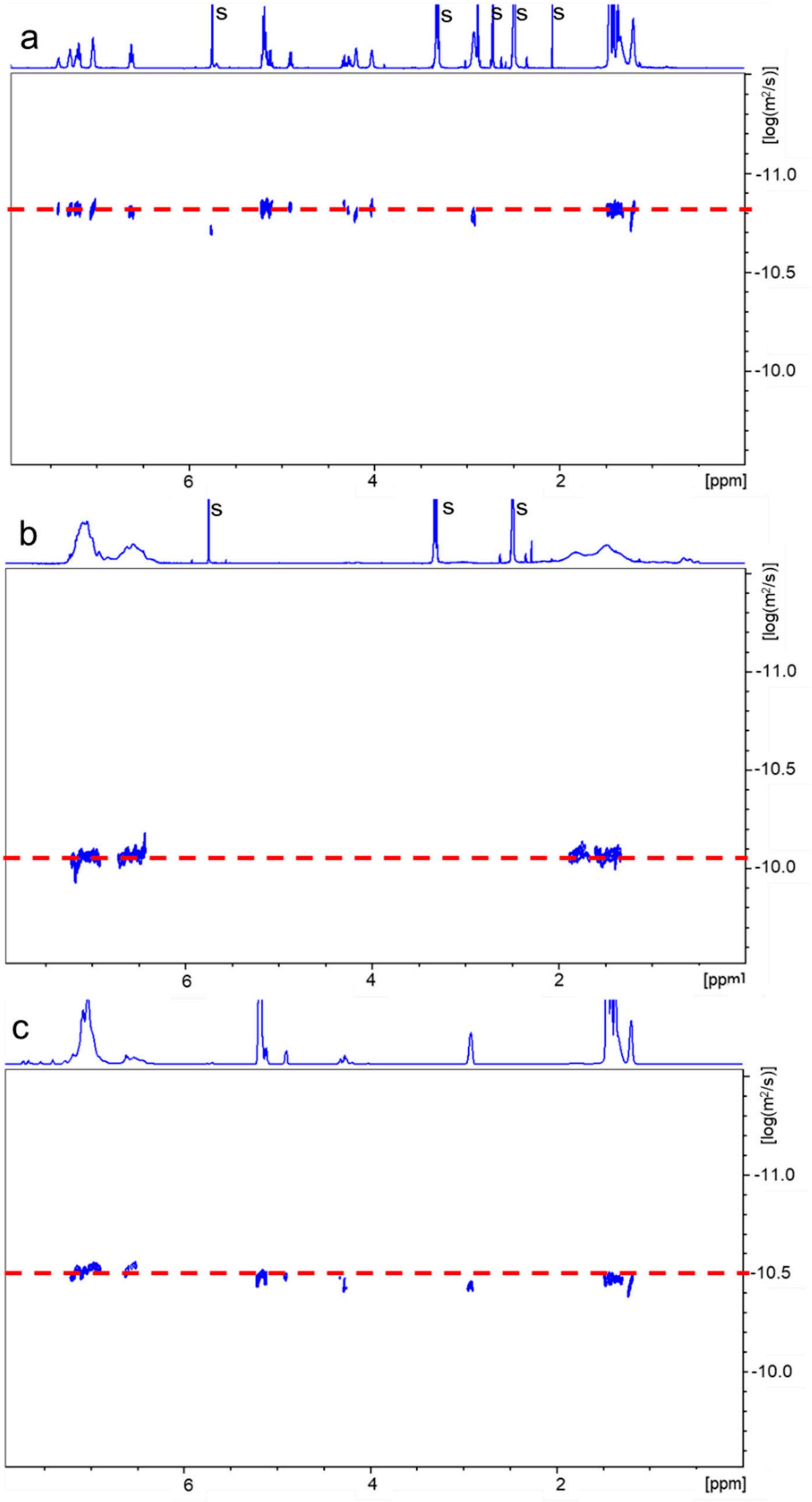

Figure 6. 2D DOSY NMR spectra of PLA-PU (**a**), PST (**b**), and PLA/PST copolymer (**c**) recorded in DMSO-d_6 (the area of the appearance of signals corresponding to the remaining solvents “s” is not shown).

An analysis of the products by DOSY NMR provides unequivocal proof that they are copolymers because signals of both PLA-PU and PVM blocks lie on the same diffusion line, showing that they are fragments of the same macromolecule. Moreover, in the spectra of the copolymers, there are no signals for which the diffusion coefficient would correspond to the diffusion coefficients of the starting PLA-PU or ST or AN homopolymers, which indicates the efficient initiation of VM polymerization by PLA-PU inifer and that the products are not contaminated by corresponding homopolymers.

The prepared PLA/PVM copolymers were also analyzed using the DSC method (Figure 7).

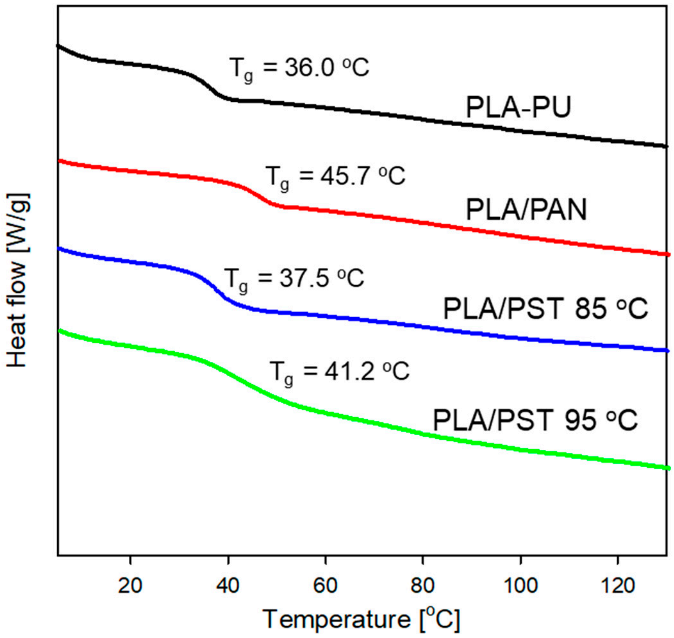

Figure 7. DSC curves for the PLA-PU macroinifer and the synthesized PLA/PAN copolymers: PLA/PAN, PLA/PST85, and PLA/PST95 (positions 2, 6, and 4 in Table 1, respectively). Fragments of DSC thermograms are shown where glass transitions could appear.

In the DSC curves of the copolymers, only one glass transition is visible, which means that there are no separated phases from the building blocks [35]. In the synthesized copolymers, both blocks are relatively short, and thus phase separation does not occur. On the other hand, the T_g values of the PLA/PAN and PLA/PST copolymers are different. They are higher than the T_g of the PLA-PU macroinifer. As the vinyl monomer fraction increases (polymerization of styrene performed at a higher temperature), the T_g value increases because the T_gs of the homopolymers of PAN and PST are higher (~96 °C [36] and ~100 °C [37], respectively, for polymers with an infinitive molecular weight). The DSC results also confirm the formation of the PLA/PVM copolymer.

3. Materials and Methods

3.1. Materials

L,L-Lactide from Purac was recrystallized from 2-propanol, sublimated, and stored under vacuum. The 2-bromoethanol (95%), 4-hydroxybenzophenone (HBP, 98%), hexamethylene diisocyanate (HDI, 99%), ethylene glycol (EG, 99.8%), which were all from Sigma-Aldrich (St.Luis, MO, USA/Steinheim, Germany), were used as received. Acrylonitrile (AN, 99%) was passed through an inhibitor removal column filled with silica gel and distilled under a vacuum. Styrene was purified with basic Al_2O_3 to remove the inhibitor and distilled under a vacuum. Trifluoromethanesulfonic acid (triflic acid, 99%) from Sigma-Aldrich was distilled under vacuum, and dibutyltin dilaurate (DBTDL, 98%) from

ABCR was used as received. Dichloroethane (DCE, pure p.a.), dimethylformamide (DMF, pure p.a.), and anisole (pure p.a.) from POCH (Gliwice, Poland) were dried over CaH_2, distilled before use, and stored over molecular sieves (4 Å). Chloroform (pure p.a.), 2-propanol (pure p.a.), ethanol (pure p.a.), diethyl ether (pure p.a.), and hexane (99%), all from POCH (Gliwice, Poland), were used as received. Potassium hydroxide (pure p.a.) was obtained from POCH (Gliwice, Poland), magnesium sulfate ($MgSO_4$, 99%) was obtained from Chempur (Piekary Slaskie, Poland), and both were used as received.

3.2. Synthesis of Polylactide Diol

Four grams (20 mmol) of L-lactide together with a stirring bar was placed in a Schlenk flask, which was evacuated for 0.5 h and then backfilled with N_2. Then, 9 mL of DCE was introduced through the rubber septum with a syringe, followed by the addition of ethylene glycol as an initiator (220 μL, 3.89 mmol) and triflic acid as a catalyst (100 μL, 1.13 mmol). Polymerization was performed at room temperature for 24 h. Then, the reaction mixture was neutralized by the addition of CaO, was filtered from the CaO, and was precipitated into hexane.

3.3. Synthesis of TPED Derivative Containing Primary Hydroxyl Groups (TPE-diET)

A total of 3.36 g (86 mmol) of potassium hydroxide was dissolved in 5 mL of distilled water in a beaker. Then, the solution was added to 10 g (50 mmol) of 4-hydroxybenzophenone in a round bottom flask. The resulting yellow reaction mixture was stirred at 70 °C until the HBP was dissolved. Next, 8 mL (108 mmol) of 2-bromoethanol was added via a syringe, and the stirring was continued for 24 h. The aqueous phase was subjected to extraction with chloroform, and the organic phase was extracted with distilled water 3 times. The combined organic extracts were dried with $MgSO_4$. The solvent was evaporated under a vacuum, and the resulting product was recrystallized by dissolving it in 4 mL of ethanol while heating. Then, excess diethyl ether was added and cooled down, which resulted in crystal growth. White crystals of HBP-ET were dried under vacuum and obtained with a yield of ~50%. In the next step, HBP-ET was placed into a quartz flask to which isopropanol (8 mL for every 1 g) was added. The flask was closed with a rubber septum and purged with nitrogen (with a needle) for 15 min. Then, the flask content was slightly heated until the mixture was dissolved. The homogenous solution was exposed to ultraviolet light (365 nm) for 24 h. The resulting white precipitate TPE-diET was then centrifuged from the rest of the reaction mixture and dried under vacuum (>99% pure, ^1H NMR, Figure 1).

3.4. Synthesis of PLA-Based Polyurethane (PLA-PU) Containing Multiple TPE-diET Groups

One gram of PLA-diol (1.18 mmol) was placed in a Schlenk flask that was evacuated for 0.5 h and then backfilled with N_2. Next, 5 mL of DMF was added and the mixture was stirred until the polymer dissolved. A total of 0.40 mL (2.48 mmol) of HDI was introduced through the rubber septum with a syringe followed by the addition of DBTDL (36 μL, 0.94 mmol) as a catalyst, and the flask was immersed in an oil bath preheated to 40 °C. After 1.5 h, when the conversion of PLA end groups was complete according to ^1H NMR, 0.46 g of TPE-diET dissolved in 1.5 mL of DMF was added through the rubber septum with a syringe. The mixture was stirred for 24 h total. Next, the reaction mixture was precipitated twice to cool diethyl ether. The resulting polymer was dried under a vacuum. The product was obtained with a yield of ~90%.

3.5. Polymerization of Acrylonitrile or Styrene using PLA-PU as a Macroinifer

The synthesis of the PLA/PAN or PLA/PST copolymer was performed as follows: PLA-PU (0.3 g) was placed in a Schlenk flask and vacuumed, and the flask was filled with nitrogen. Next, 3 mL of DMF (or anisole) was added through the rubber septum, the mixture was stirred until the polymer dissolved, and subsequently 0.32 mL of AN (0.3 g, 4.7

mmol) or 0.33 mL of ST (0.3 g, 2.9 mmol) was added to the reaction flask. The solution was degassed via three freeze–pump–thaw cycles. The flask was filled with nitrogen and heated in an oil bath at 85 °C for 24 h with stirring. The resulting polymer was precipitated twice to cold diethyl ether, decanted, and dried under reduced pressure.

3.6. Instrumental Methods

The ^{1}H NMR spectra of the synthetized–polymers were recorded in DMSO-d_6 (or $CDCl_3$) using a Bruker Avance 400 Neo instrument (Bruker, Billerica, MA, USA) operating at 400 MHz.

DOSY experiments were performed in DMSO-d_6 on a Bruker DRX500 spectrometer operating at 500 MHz (11.7 T).

Size exclusion chromatography (SEC) was performed in DMF as a solvent at 40 °C using a Wyatt (Dernbach, Germany) instrument equipped with two perfect separation solution (PSS) columns and one guard column (GRAM Linear, 10 µm, M_n between 800 and 1,000,000 Da) with a differential refractometer detector. The measurements were performed at a flow rate of 1 mL/min of the DMF eluent, containing 50 mmol LiBr (calibration with polystyrene standards). Alternatively, some analyses were performed using a Shimadzu Pump LC-20AD with a Shimadzu DGU-20A5 Degasser (Kioto, Japan) with a DMF flow rate of 0.8 mL·min^{-1} (polystyrene standards).

Electron spin resonance (ESR) spectra were recorded on an X-band EMX-Nano ESR spectrometer equipped with a nitrogen variable temperature unit on degassed DMF. The microwave power was set with the Power Sweep program below the saturation of the signal: power attenuation of 20 dB, modulation frequency of 100 kHz, modulation amplitude of 0.5 Gpp, and spectral width of 200 G. ESR spectra were recorded every 10 °C during the heating of the measuring tube over the range 35–85 °C with a tolerance of 2 °C. After reaching each measurement temperature, the system was stabilized for 30 s, during which time the spectrum was recorded.

Fourier transform infrared spectroscopy (FTIR) measurements were performed on a Thermo Scientific Nicolet 6700 instrument with an attenuated total reflectance (ATR) GoldenGate accessory (Waltham, MA, USA) and deuterated triglycine sulfate (DTGS) or mercury–cadmium–telluride (MCT) detectors. The spectra were obtained by adding 64 scans at a 2 cm^{-1} resolution.

Differential scanning calorimetry (DSC) analysis was performed at temperatures from 0 °C to 200 °C on a DSC 2500 TA Discovery system. The analyses were carried out in a nitrogen stream at heating and cooling rates of 10 °C min^{-1}.

UV coupling was performed in a photochemical reactor (RayonetRPR-200, Southern New England, Brandford, CT, USA) equipped with 12 UV lamps (λ = 365 nm) and a magnetic stirrer.

4. Conclusions

A polylactide-based macroinifer was successfully prepared via the introduction of a thermally dissociating tetraphenylethane group into a PLA chain byw coupling PLA diol with TPE-containing diol using diisocyanate. The coupling reaction was possible because the TPE derivative we synthesized contained primary hydroxyl groups. The coupling reaction appeared to be the most efficient for the two-step process performed with DMF as a solvent and DBTDL as a catalyst. The ability to form radicals upon heating of PLA-PU macroinifer containing multiple TPE groups was confirmed by ESR measurements. PLA-based macroinifer was applied to initiate the radical polymerization of acrylonitrile and styrene under heating at 85–95 °C. Although higher temperatures promote the TPE groups' decomposition to initiating radicals, it was found that 85 °C was sufficient to achieve up to 85% conversion of the monomer (used in the same mass amount as PLA-PU) over 24 h. The presence of new monomer units in the formed polymeric product was confirmed by ^{1}H NMR and FTIR spectroscopy. Moreover, the formation of the copolymer was unequivocally proven via DOSY NMR experiments. In the SEC curves, a decrease in the molecular weight could be assigned to the inadequate conditions of SEC analysis, the thermal instability of PLA chains, and the termination of growing radicals proceeding not only by recombination but partially by disproportionation. Despite the limitation on the value of the molecular weight of the obtained PLA/PVM copolymers, we proved that the described, relatively simple, method based on TPE inifer leads to copolymer formation. The study will be continued to elaborate conditions for the preparation of copolymers with higher molecular weights and higher block lengths, which could result in thermal property modification (e.g., an increase in the T_g value) or interesting morphologies (e.g., phase separation useful for obtaining porous materials).

Supplementary Materials: The following supporting information can be downloaded at: https://www.mdpi.com/article/10.3390/ijms24010019/s1. References [38,39] are cited in the supplementary materials.

Author Contributions: Conceptualization, M.G., B.K. and M.B.; investigation, M.G. and A.B.; methodology, M.G., B.K., A.B. and M.B; supervision, B.K. and M.B.; writing—original draft, M.G. and M.B.; writing—review and editing, M.B. All authors have read and agreed to the published version of the manuscript.

Funding: This work was supported by the National Science Centre in Poland, grant no. 2018/31/B/ST8/01969.

Institutional Review Board Statement: Not applicable.

Informed Consent Statement: Not applicable.

Data Availability Statement: Not applicable.

Acknowledgments: Mateusz Grabowski acknowledges Bio-Med-Chem Doctoral School of the University of Lodz and Lodz Institutes of the Polish Academy of Sciences under which this study was conducted. We would like to thank P. Kubisa for a helpful discussion of the results and for reviewing the manuscript.

Conflicts of Interest: The authors declare no conflicts of interest.

References

1. Farah, S.; Anderson, D.G.; Langer, R. Physical and mechanical properties of PLA, and their functions in widespread applications —A comprehensive review. *Adv. Drug Deliv. Rev.* **2016**, *107*, 367–392. https://doi.org/10.1016/j.addr.2016.06.012.
2. Nagarajan, V.; Mohanty, A.K.; Misra, M. Perspective on Polylactic Acid (PLA) based Sustainable Materials for Durable Applications: Focus on Toughness and Heat Resistance. *ACS Sustain. Chem. Eng.* **2016**, *4*, 2899–2916. https://doi.org/10.1021/acssuschemeng.6b00321.
3. Yildirim, I.; Weber, C.; Schubert, U.S. Old meets new: Combination of PLA and RDRP to obtain sophisticated macromolecular architectures. *Prog. Polym. Sci.* **2018**, *76*, 111–150. https://doi.org/10.1016/j.progpolymsci.2017.07.010.
4. Oh, J.K. Polylactide (PLA)-based amphiphilic block copolymers: Synthesis, self-assembly, and biomedical applications. *Soft Matter* **2011**, *7*, 5096–5108. https://doi.org/10.1039/c0sm01539c.
5. Dove, A.P. Controlled ring-opening polymerisation of cyclic esters: Polymer blocks in self-assembled nanostructures. *Chem. Commun.* **2008**, *48*, 6446. https://doi.org/10.1039/b813059k.
6. Grabowski, M.; Kost, B.; Kubisa, P.; Bednarek, M. A New Approach to The Synthesis of Polylactide/Polyacrylonitrile Block Copolymers. *Polymers* **2022**, *14*, 1529. https://doi.org/10.3390/polym14081529.
7. Otsu, T. Iniferter concept and living radical polymerization. *J. Polym. Sci. Part A Polym. Chem.* **2000**, *38*, 2121–2136. https://doi.org/10.1002/(SICI)1099-0518(20000615)38:12<2121::AID-POLA10>3.0.CO;2-X.
8. Braun, V.D.; Becker, K.H. Aromatische Pinakole als Polymerisationsinitiatoren. *Angew. Makromol. Chem.* **1969**, *6*, 186–189. https://doi.org/10.1002/apmc.1969.050060119.
9. Braun, D.; Becker, K.H. Kinetik der Polymerisationsauslösung mit aromatischen pinakolen. *Die Makromol. Chem.* **1971**, *147*, 91–99. https://doi.org/10.1002/macp.1971.021470108.
10. Błedzki, A.; Braun, D.; Menzel, W.; Titzschkau, K. Polymerisationsauslösung mit substituierten ethanen, 5. Polymerisation von verschiedenen methacrylmonomeren. *Die Makromol. Chem.* **1983**, *184*, 287–294. https://doi.org/10.1002/macp.1983.021840205.
11. Otsu, T.; Matsumoto, A.; Tazaki, T. Radical polymerization of methyl methacrylate with some 1,2-disubstituted tetraphenylethanes as thermal iniferters. *Polym. Bull.* **1987**, *17*, 323–330. https://doi.org/10.1007/BF00955715.
12. Furniss, B.; Hannaford, A.; Smith, P.; Tatchell, A. *Vogel's Textbook of Practical Organic Chemistry*; Longman Scientific & Technical, Longman House: London, UK, 1989.

13. Grabowski, M.; Kost, B.; Gostyński, B.; Bednarek, M. Can tetraphenylethane (TPE) "iniferter" groups be introduced into polymer chains by coupling TPE diol with diisocyanates? *Polymers* **2022**, *246*, 124738. https://doi.org/10.1016/j.polymer.2022.124738.
14. Zhou, G.; Ma, C.; Zhang, G. Synthesis of polyurethane-g-poly(ethylene glycol) copolymers by macroiniferter and their protein resistance. *Polym. Chem.* **2011**, *2*, 1409–1414. https://doi.org/10.1039/c1py00016k.
15. Zhang, Y.; Wang, L.; Zhang, Z.; Zhang, Y.; Tuo, X. Synthesis and simultaneous self-assembly of multiblock fluorinated polyurethane in iniferter polymerization. *J. Polym. Sci. Part A Polym. Chem.* **2013**, *51*, 2161–2170. https://doi.org/10.1002/pola.26619.
16. Tharanikkarasu, K.; Radhakrishnan, G. Tetraphenylethane iniferters: Polyurethane-polystyrene multiblock copolymers through "living" radical polymerization. *J. Appl. Polym. Sci.* **1997**, *66*, 1551–1560. https://doi.org/10.1002/(sici)1097-4628(19971121)66:8<1551::aid-app16>3.0.co;2-6.
17. Sundar, S.; Tharanikkarasu, K.; Dhathathreyan, A.; Radhakrishnan, G. Aqueous dispersions of poly(urethane-co-vinyl-pyridine) synthesised from polyurethane macroiniferter. *Colloid Polym. Sci.* **2002**, *280*, 915–921. https://doi.org/10.1007/s00396-002-0707-y.
18. Kim, B.K.; Tharanikkarasu, K.; Lee, J.S. Polyurethane-polymethacrylic acid multiblock copolymer dispersions through polyurethane macroiniferters. *Colloid Polym. Sci.* **1999**, *277*, 285–290. https://doi.org/10.1007/PL00013758.
19. Tharanikkarasu, K.; Kim, B.K. Modification of aqueous polyurethane dispersions via tetraphenylethane iniferters. *J. Appl. Polym. Sci.* **1999**, *73*, 2993–3000. https://doi.org/10.1002/(SICI)1097-4628(19990929)73:14<2993::AID-APP24>3.0.CO;2-B.
20. Ionescu, M. *Chemistry and Technology of Polyols for Polyurethanes*, 2nd ed.; Smithers Rapra Technology Ltd.: Shawbury, Shrewsbury, Shropshire, UK, 2016; Volume 2, ISBN 9781910242988.
21. Baśko, M.; Kubisa, P. Cationic polymerization of L,L-lactide. *J. Polym. Sci. Part A Polym. Chem.* **2010**, *48*, 2650–2658. https://doi.org/10.1002/pola.24048.
22. Nim, B.; Opaprakasit, P. Spectrochimica Acta Part A: Molecular and Biomolecular Spectroscopy Quantitative analyses of products from chemical recycling of polylactide (PLA) by alcoholysis with various alcohols and their applications as healable lactide-based polyurethanes. *Spectrochim. Acta Part A Mol. Biomol. Spectrosc.* **2021**, *255*, 119684. https://doi.org/10.1016/j.saa.2021.119684.
23. Nakamura, Y.; Yamago, S. Termination Mechanism in the Radical Polymerization of Methyl Methacrylate and Styrene Determined by the Reaction of Structurally Well-Defined Polymer End Radicals. *Macromolecules* **2015**, *48*, 6450–6456. https://doi.org/10.1021/acs.macromol.5b01532.
24. Ballard, N.; Hamzehlou, S.; Ruipérez, F.; Asua, J.M. On the Termination Mechanism in the Radical Polymerization of Acrylates. *Macromol. Rapid Commun.* **2016**, *37*, 1364–1368. https://doi.org/10.1002/marc.201600278.
25. Li, X.; Ogihara, T.; Kato, T.; Nakamura, Y.; Yamago, S. Evidence for Polarity-and Viscosity-Controlled Pathways in the Termination Reaction in the Radical Polymerization of Acrylonitrile. *Macromolecules* **2021**, *54*, 4497–4506. https://doi.org/10.1021/acs.macromol.1c00158.
26. Reichardt, C.; Welton, T. *Solvents and Solvent Effects in Organic Chemistry: Fourth Edition*, 2nd ed.; Verlag Chemie: Weinheim, Germany; Basel, Switzerland; Cambridge, UK; New York, NY, USA, 2010; ISBN 9783527324736.
27. Duda, A.; Penczek, S. Polymerization of ϵ-Caprolactone Initiated by Aluminum Isopropoxide Trimer and/or Tetramer. *Macromolecules* **1995**, *28*, 5981–5992. https://doi.org/10.1021/ma00122a001.
28. Lee, S.-H.; Hyun Kim, S.; Han, Y.-K.; Kim, Y.H. Synthesis and degradation of end-group-functionalized polylactide. *J. Polym. Sci. Part A Polym. Chem.* **2001**, *39*, 973–985. https://doi.org/10.1002/1099-0518(20010401)39:7<973::AID-POLA1073>3.0.CO;2-8.
29. Nishida, H.; Mori, T.; Hoshihara, S.; Fan, Y. Effect of tin on poly (l -lactic acid) pyrolysis. *Polym. Degrad. Stab.* **2003**, *81*, 515–523. https://doi.org/10.1016/S0141-3910(03)00152-6.
30. Wojtczak, E.; Kubisa, P.; Bednarek, M. Thermal stability of polylactide with different end-groups depending on the catalyst used for the polymerization. *Polym. Degrad. Stab.* **2018**, *151*, 100–104. https://doi.org/10.1016/j.polymdegradstab.2018.03.003.
31. Groves, P. Diffusion ordered spectroscopy (DOSY) as applied to polymers. *Polym. Chem.* **2017**, *8*, 6700–6708. https://doi.org/10.1039/C7PY01577A.
32. Li, W.; Chung, H.; Daeffler, C.; Johnson, J.A.; Grubbs, R.H. Application of 1H DOSY for facile measurement of polymer molecular weights. *Macromolecules* **2012**, *45*, 9595–9603. https://doi.org/10.1021/ma301666x.
33. Lewinski, P.; Sosnowski, S.; Kazmierski, S.; Penczek, S. Polymer Chemistry COMMUNICATION di ff usion-ordered spectroscopy (DOSY): A "One conversion , polymer structure, M n and M w. *Polym. Chem.* **2015**, *6*, 4353–4357. https://doi.org/10.1039/c5py00455a.
34. Cichoń, K.; Kost, B.; Basko, M. Synthesis and properties of ABA-triblock copolymers from polyester A-blocks and easily degradable polyacetal B-blocks. *Polym. Chem.* **2022**, *13*, 5243–5255. https://doi.org/10.1039/d2py00620k.
35. Daimon, H.; Okitsu, H.; Kumanotani, J. Glass transition behaviors of random and block copolymers and polymer blends of styrene and cyclododecyl acrylate. I. Glass transition temperatures. *Polym. J.* **1975**, *7*, 460–466. https://doi.org/10.1295/polymj.7.460.
36. Beevers, R.B. Dependence of the glass transition temperature of polyacrylonitrile on molecular weight. *J. Polym. Sci. Part A Gen. Pap.* **1964**, *2*, 5257–5265. https://doi.org/10.1002/pol.1964.100021221.
37. Rieger, J. The glass transition temperature of polystyrene. Results of a round robin test. *J. Therm. Anal.* **1996**, *46*, 965–972. https://doi.org/10.1007/BF01983614.
38. Available online: https://www.spectroscopyonline.com/view/the-infrared-spectra-of-polymers-iii-hydrocarbon-polymers (accessed on 20 November 2022).

39. Eren, O.; Ucar, N.; Onen, A.; Kizildag, N.; Karacan, I. Synergistic effect of polyaniline, nanosilver, and carbon nanotube mixtures on the structure and properties of polyacrylonitrile composite nanofiber. *J. Comp. Mat.* **2016**, *50*, 2073–2086.

SUPPORTING INFORMATION

Functionalization of Polylactide with Multiple Tetraphenyethane Inifer Groups to Form PLA Block Copolymers with Vinyl Monomers

*Mateusz Grabowski, Bartłomiej Kost, Agnieszka Bodzioch, Melania Bednarek**

Centre of Molecular and Macromolecular Studies, Polish Academy of Sciences, Sienkiewicza 112, 90-363 Lodz, Poland

1. Determination of molecular weights of synthesized PLA diols

Molecular weights of PLA polymers were calculated by the comparison of the intensities of signals (in DMSO-d_6) corresponding to -<u>CH</u>(CH_3)-OH end groups at 4.20 ppm and corresponding to -<u>CH</u>(CH_3)- groups from PLA backbone at 5.12 and 5.20 ppm (Figure 1 in the main text).

2. Analysis of PLA-based polyurethane (PLA-PU)

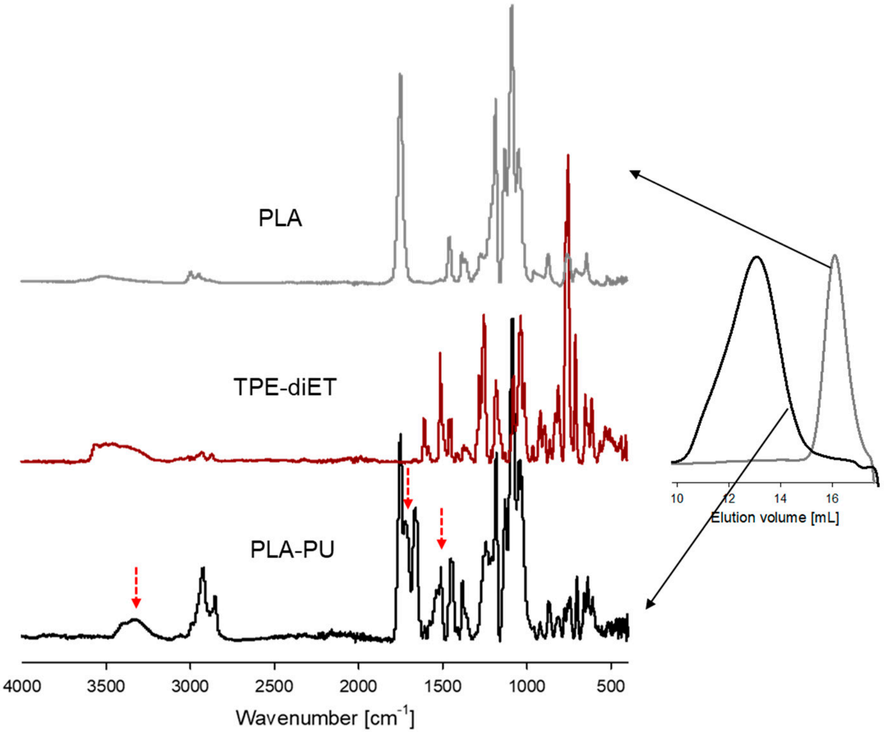

Figure S1. FTIR spectra of PLA-PU and the initial components (red arrows indicate newly formed urethane linkages) and SEC curves for starting PLA and PLA-PU (DMF as an eluent).

3. Calculation of the relative decomposition rate of TPE groups present in PLA-PU polymer on the basis of ESR spectra

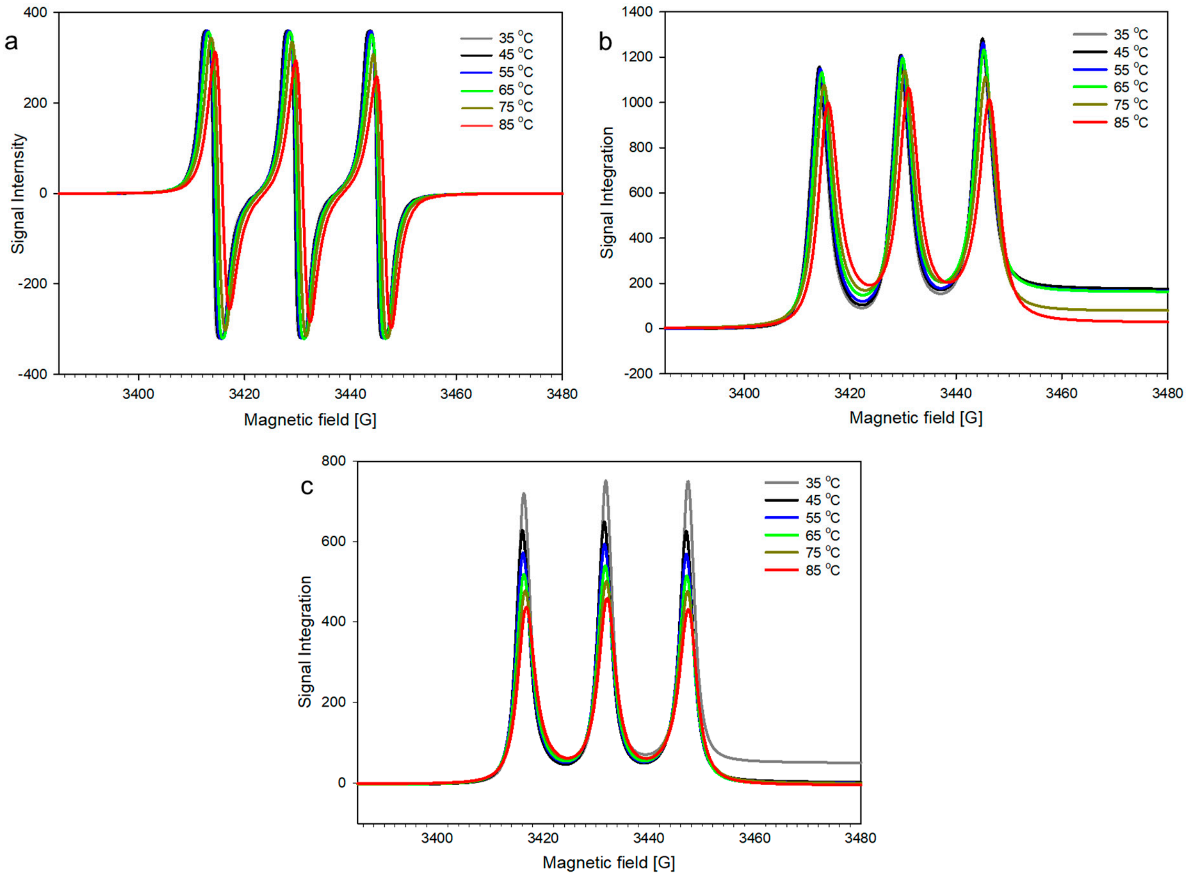

Figure S2. a) ESR spectra of TEMPO, b) normalized spectra for plots in Fig. S2a, c) normalized spectra for PLA-PU (+TEMPO) shown in Fig. 2a in the main text.

The concentration of the formed radicals was measured indirectly, by the measurement the concertation of TEMPO radicals which remained after catching …-TPE/2•. To calculate TPE decomposition ratio, the formula was applied:

$$Y= x_1(I_1 - I_2)/2x_2I_1 \quad \text{(S1a)}$$

x_1 – quantity of TEMPO (mols)

x_2 - quantity of TPE groups in PLA-PU (mols)

I_1 – integral area from the normalized absorption curve for TEMPO

I_2 – integral area from the normalized absorption curve for PLA-PU with TEMPO

Two solutions were prepared and ESR spectra for them were recorded at 35, 45, 55, 65, 75 °C:

1. 0.8 mg of TEMPO in 1 mL of DMF, i.e. 5.12 x10^{-3} mmol

2. 80 mg of PLA-PU + 0.8 mg of TEMPO in 1 mL of DMF, i.e. 46 x $x10^{-3}$ mmol + 5.12 $x10^{-3}$ mmol

After inserting the values into the equation (S1a):

$Y = 0.55(I_1 - I_2)/I_1$ (S1b)

ESR spectra presented in Fig. 2a for PU-PLA (with TEMPO) and Fig. S2a for TEMPO were transformed into normalized spectra presented in Fig. S2b and S2c using Origin Software (Integration of signals from the original ESR).

The I_1 and I_2 values were found from normalized spectra and were put into the equation 1b to find Y values at different temperatures. The dependence Y = f(T) is shown in Fig. 2b in the main text.

4. FTIR analyses of PLA/PST and PLA/PAN copolymers

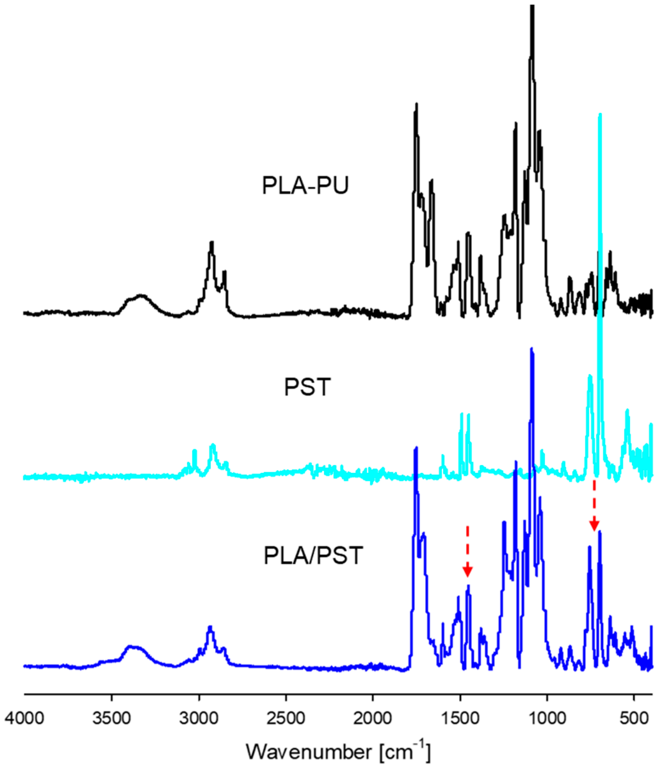

Figure S3. FTIR spectra of PLA-PU, additionally synthesized PST, and PLA/PST copolymer. Red arrows indicate the signals corresponding to aromatic ring (698 cm^{-1} and 1492 cm^{-1}) for PST [38].

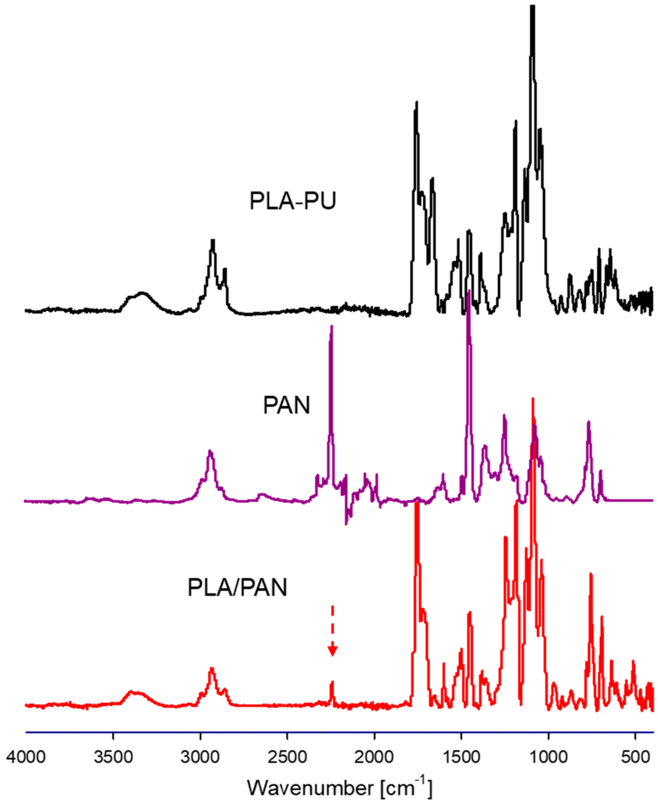

Figure S4. FTIR spectra of PLA-PU, additionally synthesized PAN, and PLA/PAN copolymer. Red arrows indicate the signal corresponding to nitrile group in PAN (2240 cm^{-1}) [39].

Homopolymers - PST and PAN for comparison in FTIR analyses were obtained via radical polymerizations of ST and AN correspondingly, initiated with AIBN.

5. The stability of PLA- based PU during heating

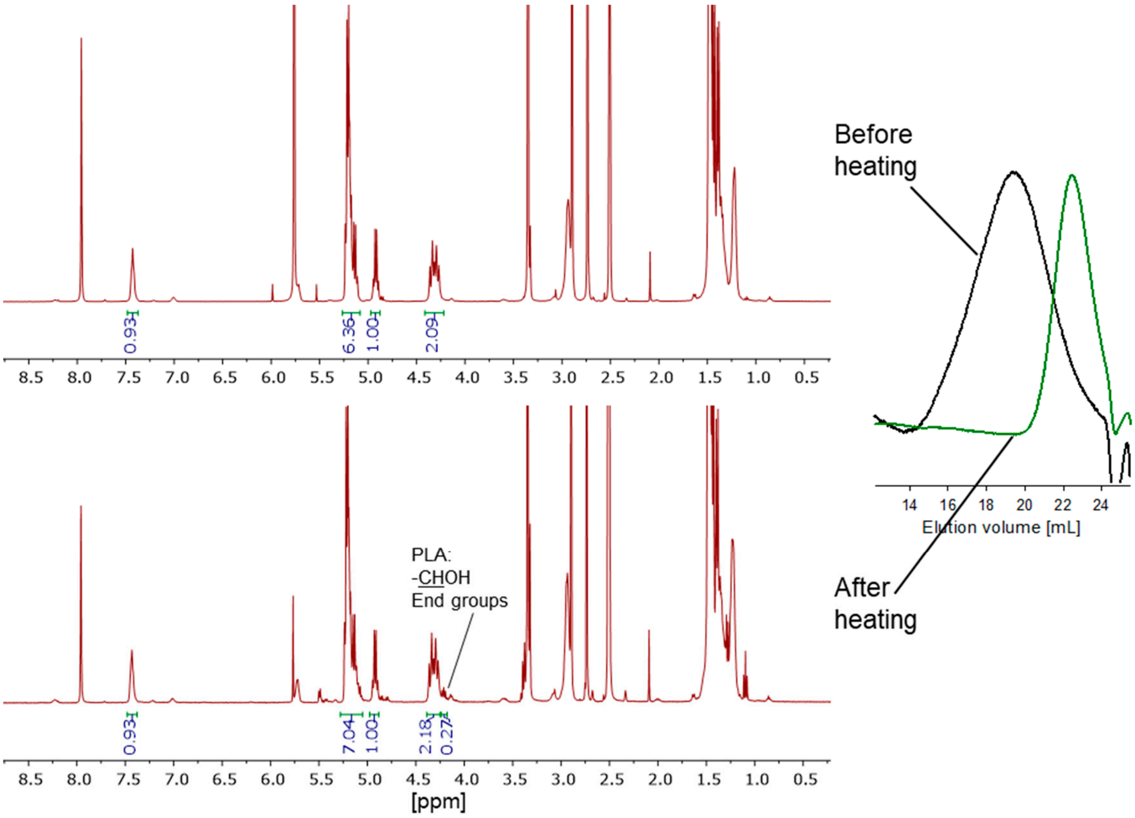

Figure S5 . ^{1}H NMR spectra of PLA-PU prepared without TPE-diET before and after heating in DMF at 85 °C for 24h and SEC curves for PU before and after heating (DMF as an eluent).

6. Diffusion coefficients of PLA-PU/PVM copolymers and corresponding homopolymers on the basis of DOSY NMR measurements

Table S1. The diffusion coefficients for groups in PLA/PVM copolymers and homopolymers corresponding to particular signals in ^{1}H NMR spectra shown in Fig. 5 and Fig. 6 in the main text.

PLA/PAN		PLA/PST	
Signal [ppm]	Diffusion coefficient x10^7, [cm^2/s]	Signal [ppm]	Diffusion coefficient x10^7, [cm^2/s]
PLA-PU		PLA-PU	
7.33-7.24	1.27	7.33-7.24	1.41
7.24-7.16	1.29	7.24-7.16	1.42

7.06-6.96	1.27	7.06-6.96	1.49
6.68-6.57	1.28	6.68-6.57	1.41
5.22-5.13	1.26	5.22-5.13	1.46
4.93-4.87	1.26	4.93-4.87	1.41
4.22-416	1.27	4.22-4.16	1.43
4.07-3.98	1.26	4.07-3.98	1.46
1.56-1.34	1.26	2.93-2.89	1.45
		1.56-1.34	1.40
PAN		PST	
3.16-3.09	0.78	7.25-6.88	7.44
2.14-2.06	0.78	6.88-6.31	7.47
		1.90-1.27	7.44
PLA-PU/PAN copol.		PLA-PU/PST copol	
7.76-7.02	2.80	7.75-7.62	3.25
6.89	2.83	7.56-7.41	3.20
6.64	2.82	7.23-6.30	3.21
5.22-5.13	2.81	5.22-5.13	3.21
4.93-4.87	2.78	4.93-4.87	3.18
4.38-4.16	2.80	4.22-416	3.27
3.22-3.05	2.85	2.95-2.89	3.25
2.20-1.90	2.86	1.56-1.34	3.26
1.51-1.41	2.76	1.21-1.19	3.25

Publikacja 4:

Mateusz Grabowski, Bartłomiej Kost, Mateusz Bartniak, Dorota Bociąga, Witold Szymański, Melania Bednarek. Copolymerization of lactide with functional epoxide as a way to the polymer network with dually active tetraphenylethane groups. *Polymer.* 2024;312:127673

Polymer 312 (2024) 127673

Contents lists available at ScienceDirect

Polymer

journal homepage: www.elsevier.com/locate/polymer

Copolymerization of lactide with functional epoxide as a way to the polymer network with dually active tetraphenylethane groups

Mateusz Grabowski [a,c], Bartłomiej Kost [a], Mateusz Bartniak [b], Dorota Bociaga [b], Witold Szymański [b], Melania Bednarek [a,*]

[a] Centre of Molecular and Macromolecular Studies, Polish Academy of Sciences, Sienkiewicza 112, 90-363 Lodz, Poland
[b] Institute of Materials Science and Engineering, Lodz University of Technology, Stefanowskiego 1/15, 90-537 Lodz, Poland
[c] BioMedChem Doctoral School of the University of Lodz and Lodz Institutes of the Polish Academy of Sciences, Matejki 21/23, 90-237 Lodz, Poland

ARTICLE INFO

Keywords:
Polylactide/poly(lactic acid)
Epoxy copolymer
Dynamic polymer network
Tetraphenylethane
Iniferter

ABSTRACT

A polylactide (PLA)-based network was prepared using functional PLA bearing pendant benzophenone (BP) groups capable of reacting between themselves. Benzophenone functional groups were introduced into PLA-based macromolecules through lactide cationic copolymerization with a pre-prepared epoxide derivative. A low molecular weight copolymer (M_n ~3000) with a low fraction of the epoxide (~20 mol.%) and on average of three pendant benzophenone groups was obtained. This copolymer was further coupled using aliphatic diisocyanate to achieve a threefold increase in molecular weight. The resulting copolymer was subjected to UV irradiation in solution to produce a crosslinked film through the linking reaction between benzophenone moieties, forming tetraphenylethane (TPE) thermally reversible groups as crosslinks. The PLA-based network with reversibly forming crosslinks was analyzed through rheology investigations, which indicated its dynamic character. Independently of the original method of preparing the dynamic network with not explored so far reversible groups, TPE groups were utilized as the initiating groups for the exemplary vinyl monomer polymerization, namely acrylonitrile. It was demonstrated that new polymer chains could be easily introduced inside the PLA-based polymer network through network heating in the presence of a vinyl monomer. This demonstrates the development of a new approach to PLA-based dynamic network modification, providing an additional possibility for the preparation of novel PLA-based materials.

1. Introduction

The growing demand for polymeric materials, driven by emerging applications, compels researchers to explore novel methods for their synthesis and modification. Recently, there has been significant emphasis on synthesizing polymers from renewable resources. Polylactide (PLA) obtained by ring-opening polymerization of lactide which can be received from corn, rice, potatoes, etc., has an established position among such polymers. The technology of its production is well developed nowadays and PLA has found an application in packaging, agriculture, and biomedicine and is further considered as a material for durable daily use items [1–3].

Although polylactide as a thermoplastic can replace some petroleum-based polymers in selected applications it provides worse thermal properties and shape stability [3,4]. To improve shape maintenance, crosslinking is often applied and crosslinked polylactide has been prepared using various methods [5–8] and its suitability for diverse applications has been investigated. Among the different crosslinking methods, chemical crosslinking at the material preparation stage can be found which generally relies on the chemical reaction between reactive groups present in a base polymer (prepolymer), or between groups present in prepolymer and additional coupling agent [7]. The coupling agent should be multifunctional when used for coupling a difunctional polymer or difunctional when used for coupling a multifunctional polymer. This type of crosslinked polymer preparation is naturally associated with the introduction of new chemical units into the polymer structure. Consequently, it leads to additional modifications in polymer properties, aside from those resulting from crosslinking. This approach offers numerous opportunities to create new materials with interesting properties.

A variety of methods exist for preparing polymers with specific end groups, including PLA [9–11]. Polylactides used for network

---

[*] Corresponding author.
E-mail address: melania.bednarek@cbmm.lodz.pl (M. Bednarek).

https://doi.org/10.1016/j.polymer.2024.127673
Received 25 June 2024; Received in revised form 6 September 2024; Accepted 26 September 2024
Available online 28 September 2024

preparation are usually functionalized with unsaturated groups at the chain ends [7,12,13] or with –OH groups [14]. PLA diols or –OH functionalized stars are coupled through reactions with different tri- or diisocyanates [7,14]. The latter method, leading to polyester-urethanes, was predominantly used in the past due to the interesting properties and usefulness of this type of material [15–17]. There are also examples of copolymerization of lactide with bicyclic monomers, such as bis-lactones and bis-carbonates [18,19], leading directly to network formation.

Copolymerization of lactide with other cyclic monomers may be a preliminary stage to crosslinked polymer if a cyclic monomer is substituted with a reactive functional group. Such copolymerization is an often applied method for introducing desired functionalities along inherently non-functional PLA chains [20–25]. The reaction between pendant functional groups should result in a crosslinked polymer.

We decided to use the above-mentioned method, i.e., the copolymerization of lactide with epoxide containing a reactive functional group to produce a crosslinked PLA-based material that incorporates reversibly dissociating groups in its structure. The group able to reversibly dissociate which we chose was the tetraphenylethane group (TPE). This group was previously applied as the initiating group for several vinyl monomer polymerizations [26–28]. Later, it was introduced into some polymer structures to form “macroiniferters” [29–32]. Our latest articles also contribute to these works resulting in the formation of well-defined polylactide/poly (vinyl monomer) copolymers [33,34]. Few articles appeared recently about the use of this group to create dynamic polymer networks [35–38] from which two concerned networks based on another polymer (polytetramethylene ether glycol) [35,36]. Moreover, the mentioned articles including our contributions [37,38], concern the synthesis of crosslinked polymers by coupling star PLAs as building blocks using diisocyanate.

In this work, we present another approach that relies on the reaction between linear PLA/(substituted epoxy) copolymer chains bearing pendant reactive groups, i.e. groups containing benzophenone (BP) moieties. Benzophenone is known as a substrate for the synthesis of benzopinacole (tetraphenylethanediol, TPED) at UV irradiation conditions [39]. Thus, the formation of covalent bonds between these pendant benzophenone groups is responsible for the formation of a crosslinked structure. Generated in this way TPE groups act as crosslinks. The idea of the dynamic network formation is presented schematically in Fig. 1.

The aim of this study was to explore how adding reversibly dissociating TPE groups to the PLA/(substituted epoxy) copolymer could modify the PLA-based material. We anticipated that this modification would lead to a dynamic PLA-based network capable of radical exchange reactions between TPE groups what would result in rheological properties advantageous for processing. Additionally, we aimed to investigate the potential for introducing third monomer units into the network structure by incorporating vinyl monomer (VM) units into the pre-prepared PLA/epoxy network. Our work focuses on demonstrating the possibilities resulting from the chosen synthesis path, rather than preparing materials with assumed properties.

2. Materials and methods

2.1. Materials

L,L-Lactide from Corbion was recrystallized from 2-propanol, sublimated, and stored under vacuum. 4-Hydroxybenzophenone (HBP, 98 %), hexamethylene diisocyanate (HDI, 99 %), anhydrous ethylene glycol (EG, 99.8 %), all from Sigma-Aldrich (St.Louis, MO, USA/Steinheim, Germany), were used as received. Epichlorohydrin (EPI, 99 %) from Pol-Aura was dried over CaH_2 and distilled before use. Acrylonitrile (AN, 99 %) was passed through an inhibitor removal column filled with silica gel and distilled under a vacuum. Trifluoromethanesulfonic acid (triflic acid, 99 %) from Sigma-Aldrich was distilled under vacuum, and dibutyltin dilaurate (DBTDL, 98 %) from ABCR was used as received. Dichloroethane (DCE, pure p.a.), and dimethylformamide (DMF, pure p.a.), from POCH (Gliwice, Poland) were dried over CaH_2, distilled before use, and stored over molecular sieves (4 Å). 2-Propanol (pure p.a.), hexane (99 %), diethyl ether (pure p.a.) all from POCH (Gliwice, Poland), were used as received. Potassium hydroxide (pure p.a.) was obtained from POCH (Gliwice, Poland) and used as received.

2.2. Synthesis of benzophenone substituted with epoxy group (BP_EP)

3.36 g (60 mmol) of potassium hydroxide was dissolved in 5 mL of distilled water in a beaker. Then, the solution was added to 10 g (50 mmol) of 4-hydroxybenzophenone in a round bottom flask. The

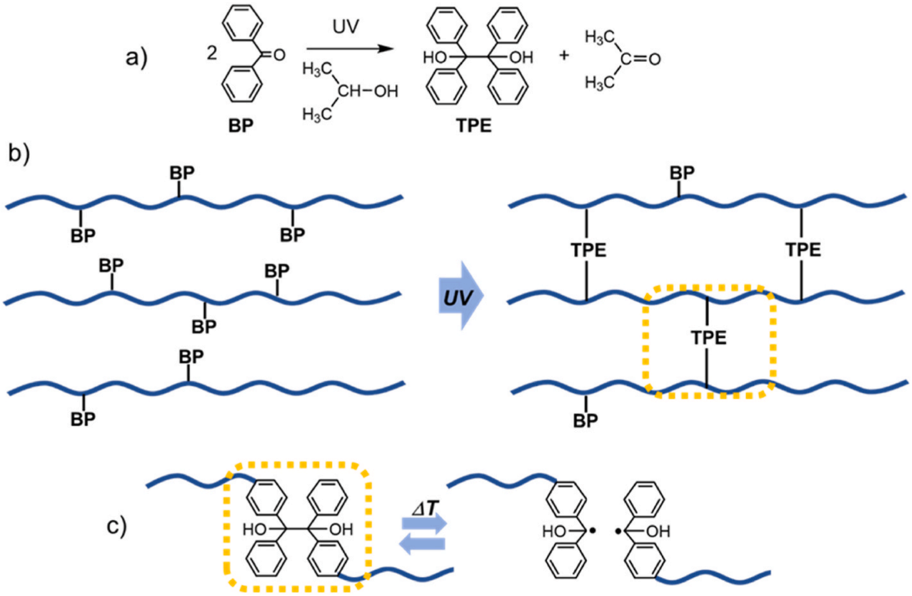

Fig. 1. Schematic representation of the formation of a reversible polymer network based on PLA: a) Formation of tetraphenylethane (TPE) groups via the UV-promoted reaction between two benzophenone molecules, (b) UV-promoted formation of the polymer network through coupling of linear chains bearing pendant BP groups, (c) Heat-promoted reversibility of network crosslinks.

resulting yellow reaction mixture was stirred at 70 °C until the HBP was dissolved, then 4.7 mL (5.5 g, 60 mmol) of ECH was added and the stirring was continued for 24 h. The resulting white precipitate was crystallized in the next step by dissolving it in 50 mL of isopropanol. White crystals of BP_EP were dried under vacuum and obtained with a yield of ~70 %.

^{1}H, $\mathrm{CDCl_3}$, 400 MHz, δ (ppm): 7.88–7.82 (2H, m, Ar), 7.78–7.74 (2H, m Ar), 7.61–7.56 (1H, m, Ar), 7.53–7.45 (2H, m, Ar), 7.05–6.98 (2H, m, Ar), 4.38–4.33 (1H, dd, epoxide ring, Ar-$\mathrm{OC\underline{H}_2CHCH_2O}$), 4.07–4.00 (1H, dd, Ar-$\mathrm{OC\underline{H}_2CHCH_2O}$), 3.41 (1H, m, epoxide ring, Ar-$\mathrm{OCH_2C\underline{H}}$-$\mathrm{CH_2O}$), 2.98 (1H, t, epoxide ring, Ar-$\mathrm{OCH_2CHC\underline{H}_2O}$, 2.81 (1H, dd, epoxide ring, Ar-$\mathrm{OCH_2CHC\underline{H}_2O}$).

^{13}C, $\mathrm{CDCl_3}$, 400 MHz, δ (ppm): 195.53 (1C, s, $\mathrm{C{=}O}$), 162.00 (1C,s $\mathrm{\underline{C}H{-}OCH_2CHCH_2O}$), 138.15 (1C, s, $\mathrm{C\underline{H}{-}C{=}O}$), 132.26 (1C, s, Ar), 132.01 (2C, s, Ar), 129.82 (1C, s, Ar), 129.70 (2C, s, Ar), 128.26 (2C, s, Ar), 68.83 (1C, s, epoxide ring, Ar-$\mathrm{O\underline{C}H_2CHCH_2O}$), 49.89 (1C, s, epoxide ring, Ar-$\mathrm{OCH_2\underline{C}HCH_2O}$), 44.66 (1C, s, epoxide ring, Ar-$\mathrm{OCH_2CH\underline{C}H_2O}$).

2.3. Synthesis of LA-co-BP_EP copolymer

4 g (27 mmol) of LA and 1.4 g of BP_EP (5.5 mmol) were placed in a Schlenk flask that was evacuated for 0.5 h and then backfilled with $\mathrm{N_2}$. Next, 9 mL of DCE was added and the mixture was stirred until the substrates dissolved. In the next step, 78 μL (1.37 mmol) of ethylene glycol as an initiator was added, followed by the addition of 50 μL (0.57 mmol) of triflic acid as a catalyst. Copolymerization was carried out at 50 °C for 72 h. Then, the reaction mixture was neutralized by the addition of ~1 g of CaO, then filtered from the CaO, and precipitated into hexane. The product was obtained with a yield of ~90 %.

^{1}H, $\mathrm{CDCl_3}$, 400 MHz, δ (ppm): 7.88–7.82 (2H, m, Ar), 7.78–7.74 (2H, m Ar), 7.61–7.56 (1H, m, Ar), 7.53–7.45 (2H, m, Ar), 7.05–6.98 (2H, m, Ar), 5.16 (1H,q, -$\mathrm{C\underline{H}(CH_3)}$-), 4.40–3.60 (10H, br, overlapping, -$\mathrm{OC\underline{H}_2}$-$\mathrm{C\underline{H}_2O}$- initiator, Ar-$\mathrm{OC\underline{H}_2C\underline{H}C\underline{H}_2O}$, -$\mathrm{C\underline{H}(CH_3)OH}$), 1.57 (3H, d, –CH ($\mathrm{C\underline{H}_3}$)O-), 1.49 (3H, d, –$\mathrm{CH(C\underline{H}_3)OH}$).

^{13}C, $\mathrm{CDCl_3}$, 400 MHz, δ (ppm): 195.53 (1C, s, $\mathrm{C{=}O}$), 174.96 (1C, s -$\mathrm{\underline{C}H(CH_3)OH}$), 169.36 (1C,s -$\mathrm{\underline{C}H(CH_3)O}$-, PLA), 162.00 (1C,s $\mathrm{\underline{C}H{-}OCH_2CHCH_2O}$), 138.15 (1C, s, $\mathrm{\underline{C}H{-}C{=}O}$), 132.26 (1C, s, Ar), 132.01 (2C, s, Ar), 129.82 (1C, s, Ar), 129.70 (2C, s, Ar), 114.26 (2C, s, Ar), 72.31 (1C, s, Ar-$\mathrm{OCH_2\underline{C}HCH_2O}$) 70.88 (2C, s, $\mathrm{O\underline{C}H_2\underline{C}H_2O}$- initiator, Ar-$\mathrm{OCH_2CH\underline{C}H_2O}$) 69.01 (1C, s -$\mathrm{\underline{C}H(CH_3)O}$-), 66.74 (-$\mathrm{\underline{C}H(CH_3)OH}$), 62.76 (1C, s, Ar-$\mathrm{O\underline{C}H_2CHCH_2O}$), 20.05 (1C, s –$\mathrm{CH(\underline{C}H_3)OH}$), 16.67 (1C, s –$\mathrm{CH(\underline{C}H_3)O}$-).

2.4. Coupling LA-co-BP_EP copolymer with HDI to (LA-co-BP_EP)HDI

The obtained copolymer was coupled using HDI. 2 g of LA-co-BP_EP was placed in a Schlenk flask that was evacuated and backfilled with $\mathrm{N_2}$. The copolymer was then dissolved in 8 mL of DCE, and the amount of 123 μL (0.77 mmol) of HDI was introduced through the rubber septum with a syringe followed by the addition of DBTDL (12 μL, 0.02 mmol) as a catalyst, and the flask was immersed in an oil bath preheated to 40 °C. The mixture was stirred for 24 h. Next, the reaction mixture was precipitated twice, first to hexane followed by the precipitation to diethyl ether. The resulting polymer was dried under a vacuum.

^{1}H, $\mathrm{CDCl_3}$, 400 MHz, δ (ppm): 7.88–7.82 (2H, m, Ar), 7.78–7.74 (2H, m Ar), 7.61–7.56 (1H, m, Ar), 7.53–7.45 (2H, m, Ar), 7.05–6.98 (2H, m, Ar), 5.16 (1H, q, -$\mathrm{C\underline{H}(CH_3)}$-, PLA), 5.10 (1H, br, -$\mathrm{C\underline{H}(CH_3)}$–*O*–C(O)NH-, PLA), 4.40–3.60 (10H, br, overlapping, -$\mathrm{OC\underline{H}_2C\underline{H}_2O}$- initiator, Ar-$\mathrm{OC\underline{H}_2CHC\underline{H}_2O}$, -$\mathrm{C\underline{H}(CH_3)OH}$), 3.15 (4H, d, –$\mathrm{CH(CH_3)}$-OC(O)–NH–$\mathrm{C\underline{H}_2CH_2CH_2CH_2CH_2CH_2}$- 1.57–1.19 (14 H, d, overlapping, –CH ($\mathrm{C\underline{H}_3}$)O-, –$\mathrm{CH(C\underline{H}_3)OH}$, $\mathrm{CH(CH_3)}$-OC(O)–NH–$\mathrm{CH_2C\underline{H}_2C\underline{H}_2C\underline{H}_2C\underline{H}_2C\underline{H}_2}$-).

2.5. Synthesis of PLA-TPE_EP network

0.3 g of (LA-co-BP_EP)HDI was placed in a Schlenk flask and vacuumed and the flask was filled with nitrogen. Next, 0.5 mL of nitrogen-purged isopropanol and 0.5 mL of nitrogen-purged dioxane were added through the rubber septum. The mixture was stirred until the copolymer dissolved. Next, the mixture was transferred using a syringe, to a 4 cm diameter Petri dish which was subsequently placed in a glass flask, filled with $\mathrm{N_2}$ and closed with a lid. The glass flask was placed in the UV chamber and exposed to ultraviolet light (365 nm) for 24 h. The resulting network was removed from the glass and dried in the vacuum oven at 50 °C overnight. The film was annealed at 100 °C for 1 h before analyses.

2.6. Polymerization of acrylonitrile using PLA-TPE_EP network as a macroiniferter

The synthesis of the PLA-TPE_EP/PAN network was performed as follows: PLA-TPE_EP (17.3 mg) was placed in a Schlenk flask and then vacuumed, and the flask was filled with nitrogen. Next, 2 mL of AN was added with a syringe through the rubber septum. The mixture was degassed by three freeze–pump–thaw cycles. The flask was filled with nitrogen and heated in an oil bath at 85 °C for 24 h with stirring. The resulting copolymer was removed from the Schlenk flask and washed with DMF to remove any traces of formed PAN homopolymer, followed by washing with diethyl ether to remove any remaining DMF. Finally it was dried under vacuum for 24 h.

2.7. Solubility and swelling tests

Samples of 7–15 mg of the network film were immersed in 5 mL of the solvent in a glass vial. The vial was then closed with a cap and kept for 24 h at room temperature, and for 1 h at 60 °C (in the case of $\mathrm{CHCl_3}$ and THF as solvents) or at 100 °C (in the case of DMF as a solvent). After the specified time, samples that were kept at room temperature were removed and weighed to determine the swelling ratio, which was calculated using the formula: swelling ratio (%) = $(m_{swollen} - m_{dry})/m_{dry}$ x 100 %. All samples were then dried in a vacuum oven for 24 h to determine the insoluble fraction.

2.8. Determination of gel content

A small part of the crosslinked polymer was refluxed in DCM in a Soxhlet apparatus for 4 h and then dried in a vacuum oven at 50 °C for 24 h. The gel content was determined gravimetrically and calculated as the ratio of the sample weight after extraction to its initial weight.

2.9. Tensile properties

The tensile test was carried out using a Linkam TST 350 mini tensile tester with a measuring range of force up to 200 N. The dog-bone shape samples with a measuring length of 12.5 mm, a width of 4.8–4.9 mm and a thickness of ~0.2 mm were cut from the network film. The test was carried out at room temperature. The deformation rate was 1.2 mm/min.

2.10. Rheological properties

The rheological measurements of the polymer network were performed using Physica MCR-702 rheometer (Anton Paar, Austria) connected to a Peltier heating/cooling fixture (MCR 180MD) and parallel-plate geometry (PP25). Samples in the form of discs with a diameter of 25 mm were analyzed. A constant 0.3 N force was applied. The recovery investigation was performed at 120 °C according to Refs. [37,40] The storage modulus was monitored during strain increasing up to 1000 %, and next modulus changes (a return to the previous value) were followed during applying 1 % strain. The shear-thinning investigation [37,41] was performed at a frequency of 1 Hz, and the strain deformation was changed repeatedly from 0.1 % to 100 %.

2.11. *Elastic modulus and hardness by nanoindentation*

Modulus and hardness of PLA-based network and networks with incorporated PAN were determined with a G-200 Nano Indenter (MTS Nano Instruments/KLA-Tencor Corporation; Milpitas, California, USA) equipped with NanoSuite 6.52.0 software. The data analysis with the Analyst program was based on Oliver and Pharr's approach [42]. The impressions (not less than ten indents per sample) were made with a Berkovich-type geometry indenter with a half angle equal to 65.3° and a declared by manufacturer roundness $r < 20$ nm. The studies were carried out using the CSM method (Continuous Stiffness Measurement) [43]. The CSM method is based on continuous measurement of the stiffness (S) during the material penetration to estimate hardness (H) and modulus of elasticity (E) of the material as a function of penetration depth ($h = 2000$ nm).

2.12. *Instrumental methods*

The ^{1}H NMR spectra of the synthesized polymers were recorded in a $CDCl_3$ solvent using a Bruker Avance 400 Neo instrument (Bruker, Billerica, MA, USA) operating at 400 MHz.

Diffusion Ordered Spectroscopy (DOSY) ^{1}H NMR measurements were carried out at 295 K on a Bruker Avance III 500 spectrometer equipped with automated tuned and matched (ATMA) 5 mm triple channel TBO (BB/H–F/D) probe head with actively shielded Z-gradients coil. For the ^{1}H DOSY measurements, each sample was stabilized at 295 K for at least 5 min before data accumulation, and the ^{1}H p/2 pulse length was checked and adjusted carefully for each sample. The standard Bruker pulse program dstebpgp3s was selected for measurements using double stimulated echo for convection compensation, Longitudinal Eddy Current Delay with bipolar gradient pulses for diffusion, and 3 spoil gradients. The gradient pulse (d) was set to 2 ms and the diffusion time (D) was set to 150 ms. The gradient spoil pulse was set to 0.6 ms, the eddy current delay was set to 5.0 ms, and the delay for gradient recovery was set to 0.2 ms. The d and D values were checked and adjusted for each sample to obtain appropriate signal attenuation across the DOSY measurement. The DOSY experiments were run in pseudo 2D mode with gradients varied linearly from 5 to 95 % in 16 steps with 16 scans per step. Spectra were processed by TopSpin 3.5pl6 software, supplied by the manufacturer. A 1-Hz line broadening Lorenzian function was applied, and each row was phased and baseline corrected before Fourier transformation in the F2 dimension. The diffusion coefficients for the resolved ^{1}H signals were extracted using the T1/T2 analyze module of the TopSpin program.

Size exclusion chromatography (SEC) was performed using an Agilent Pump 1100 Series with an Agilent G1379A Degasser, equipped with a set of two PLGel 5 μm MIXED-C columns. A Dawn Eos (Wyatt Technology Corporation) laser photometer (MALLS - Multiangle Light Laser Scattering) and a Wyatt Optilab Rex differential refractometer (RI) were used as detectors. Methylene chloride was used as an eluent at a flow rate of 0.8 mL/min at 25 °C.

Differential Scanning Calorimetry (DSC) analyses were performed using a DSC 2500 Discovery, TA Instruments, under a nitrogen atmosphere at temperatures ranging from 0 °C to 200 °C for (co)polymers at a heating and cooling rate of 10 °C min^{-1}. Both the temperature and heat flow were calibrated with indium.

Matrix-assisted laser desorption ionization-time of flight (MALDI TOF MS) experiments were performed using an Axima-Performance TOF spectrometer (Shimadzu Biotech, Manchester, UK) equipped with a nitrogen laser (337 nm). The pulsed extraction ion source accelerated the ions to a kinetic energy of 20 keV. Dithranol was used as a matrix and potassium trifluoroacetate was used as a cationating agent.

Fourier transform infrared spectroscopy (FTIR) measurements were performed on a Thermo Scientific Nicolet 6700 instrument with an attenuated total reflectance (ATR) GoldenGate accessory (Waltham, MA, USA) and deuterated triglycine sulfate (DTGS) or mercury–cadmium–telluride (MCT) detectors. The spectra were obtained by adding 64 scans at a 2 cm^{-1} resolution.

UV coupling was performed in a photochemical reactor (RayonetRPR-200, Southern New England, Brandford, CT, USA) equipped with 16 UV lamps ($\lambda = 365$ nm) and a magnetic stirrer.

3. Results and discussion

3.1. *Synthesis of LA-co-BP_EP copolymer*

Benzophenone side groups were previously introduced by copolymerization into different polymer chains as photoactive moieties generating radicals upon UV irradiation. These radicals were further active in the process of crosslinking or grafting other polymers [25,44]. Benzophenone radicals recombined then with radicals formed on polymer chains. In the present work benzophenone radicals were needed to generate TPE groups in between polymer chains.

LA-co-BP_EP copolymer was synthesized via cationic ring-opening copolymerization of L,L-lactide and BP_EP epoxy monomer using low molecular weight diol as an initiator and triflic acid as a catalyst. The copolymerization of LA with substituted epoxy monomers performed under acidic catalysis leads to copolymers with small molecular weight products [24]. First, the BP_EP monomer was produced via functionalization of HBP with an epoxy ring using epichlorohydrin in the Wiliamson ether synthesis reaction. The successful functionalization of 4-hydroxybenzophenone to BP_EP was confirmed by ^{1}H and ^{13}C NMR analyses (Figs. S1a and S1d). BP_EP containing epoxy ring was next used in copolymerization with L,L-lactide. The target copolymer should contain longer PLA fragments separated by units with side BP groups, which is why we used the initial epoxy/LA ratio = 0.2 and the target molecular weight was 3600. Preliminary experiments aimed at determining the copolymerization conditions showed that by increasing target molecular weight or epoxy/LA ratio, the worse control over M_n and copolymer composition was observed. Thus, for the present study, an epoxy/LA ratio equal to 0.2 and EG/LA equal to 0.05 were maintained.

Obtained LA-co-BP_EP copolymer was characterized by SEC, MALDI TOF, ^{1}H and ^{13}C NMR methods (see Fig. 2 and Figs. S1b, e, f). ^{1}H NMR analysis allowed for the determination of the copolymer molecular weight as well as copolymer composition. The calculated values were equal to $M_n = \sim 3000$ and BP_EP/LA = ~0.2 which means that one copolymer macromolecule contained 3 pendant BP groups on average. The expected structure of the LA-co-BP_EP copolymer was confirmed by MALDI TOF analysis (Fig. 2 and Fig. S2). In the MALDI TOF spectrum, the signals corresponding to macromolecules containing 1, 2 or 3 BP_EP

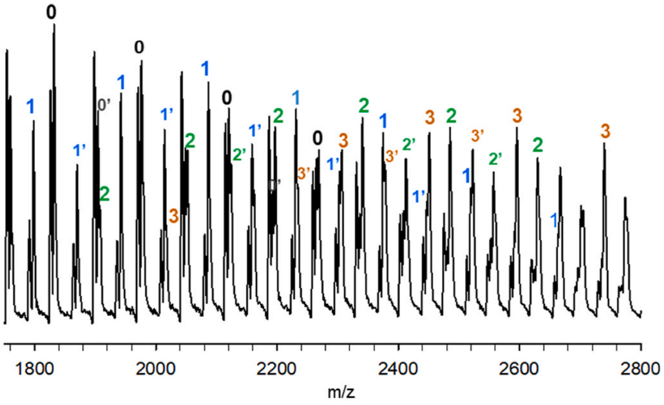

Fig. 2. Fragment of MALDI TOF spectrum of the obtained LA-co-BP_EP copolymer. Signal assignments: 0: $m/z = n \times M_{LA} + M_{EG} + M_{K+}$, 1: $m/z = n \times M_{LA} + M_{EG} + \mathbf{1M_{BP\_EP}} + M_{K+}$, 2: $m/z = n \times M_{LA} + M_{EG} + \mathbf{2M_{BP\_EP}} + M_{K+}$, 3: $m/z = n \times M_{LA} + M_{EG} + \mathbf{3M_{BP\_EP}} + M_{K}$. Series 1′, 2′, and 3′ correspond to macromolecules that underwent transesterification reactions.

units and several lactide units are nicely visible.

To achieve a higher number of pendant BP groups in one copolymer macromolecule, it was further coupled using hexamethylene diisocyanate. As a result, we produced a copolymer with a molecular weight $M_n = \sim 9000$ (determined by SEC, Fig. S1f) and 9 pendant BP groups on average which should result in good crosslinking ability. All expected signals corresponding to units of the coupled copolymer were detected in the ^{1}H NMR spectrum as shown in Fig. S1c. Additionally, the formation of the coupled copolymer as well as the copolymer before the coupling reaction was confirmed by DOSY NMR [45]. As seen on the DOSY maps with ^{1}H NMR spectra on the top (Fig. 3), the diffusion coefficients of every single building block of the copolymer are the same (the signals lie on the same line), showing that they are fragments of the same macromolecule. The reaction scheme leading to the coupled (LA-co-BP_EP)HDI copolymer is presented in Fig. 4.

3.2. Preparation of PLA-TPE_EP network by UV coupling of (LA-co-BP_EP)HDI copolymer

To obtain PLA-based network, prepared (LA-co-BP_EP)HDI copolymer was crosslinked via the reaction between pendant benzophenone groups that, subjected to UV irradiation in the presence of proton donor, led to the formation of tetraphenylethane diol (TPE) moiety in between copolymer chains (Fig. 1). By the deposition of the solution of (LA-co-BP_EP)HDI copolymer on the glass surface (Petri dish) and its irradiation by UV light, thin network film was obtained which was then dried in a vacuum at 50 °C and annealed at 100 °C. The obtained network contained over 95 % gel fraction and was not soluble in $CDCl_3$, THF, and DMF at room temperature. Solubility at higher temperatures did not exceed several percent. The results of solubility and swelling studies are shown in Table S1. The successful reaction between BP groups, leading to the formation of TPE groups and thus crosslinking, was confirmed by FTIR analysis of the network. In the IR spectrum a signal at 1650 cm^{-1} corresponding to a carbonyl group from benzophenone moiety in (LA-co-BP_EP)HDI copolymer, disappears (Fig. 5).

The prepared polymer network was analyzed by the DSC method. In the DSC curve only glass transition was observed with the T_g value equal to ~55 °C (Fig. 6a) which is about 12 °C higher than the T_g value of the starting (LA-co-BP_EP)HDI copolymer (Fig. S2). The absence of a melting peak indicates that the network with short monomer sequences is unable to crystallize. Thermogravimetric analysis (TGA) of the prepared polymer network demonstrated two-step decomposition starting from about 220 °C and with a maximum degradation rate at 280 °C (Fig. 6b and S7).

The mechanical properties of the prepared PLA-based network should depend on its composition. The presence of units of epoxide substituted with benzophenone moieties should change properties typical for networks constructed from PLA chains alone. The tensile test carried out on the PLA-TPE_EP network (Fig. 7) showed that it had noticeably reduced tensile strength in comparison with PLA materials. For example, PLA produced by NatureWorks under the tradename Ingeo™ - 3251D for injection molding has a tensile strength of 62 MPa [46], and crosslinked PLAs obtained by coupling star low molecular weight PLAs are characterized by tensile strength close to 50 MPa [47] or by slightly lower strength (between 20 and 45 MPa) if contain additional components [37]. Here, the tensile strength reached only 16 MPa and elongation at break is low as well, with ε_0 value comparable to that characteristic for commercial thermoplastic PLA. Despite this stiffness at room temperature, the network becomes elastic at elevated temperature and shows rheological properties that speak for its dynamic character which will be discussed in the following section.

3.3. Rheological properties of the prepared PLA-TPE_EP network and its dynamic character

To demonstrate the dynamic character of the obtained PLA-TPE_EP network, the rheological properties were investigated. An experiment (applied by other authors for the dynamic networks characterization [40]) was performed in which the network sample was subjected to high strain deformation of 1000 % in the shear mode, and next a constant strain of 1 % (at a frequency of 1 Hz) was applied and the relaxation modulus was followed as a function of time at a constant temperature of 120 °C (i.e., the temperature at which reversible dissociation of TPE moieties should be advanced [34]). The results of these measurements are presented in Fig. 8. Due to dynamic bond rearrangement at high temperatures, the complete recovery of mechanical properties of the network could be obtained.

Additionally, as convincing proof of the network's ability to recover its previous strength after the deformation the shear-thinning experiment was performed at 120 °C where strain deformations of 0.1 % and 100 % were applied repeatedly for the network sample [41]. As can be seen in Fig. 9, both storage and loss moduli change with the strain used, decreasing with large deformation. At low deformation, the storage modulus exceeds the loss modulus, while at high deformation it takes a lower value. However, after each large deformation, the moduli return to their previous values observed initially at small deformation. The reversible transformation from the solid-like (elastic) to liquid-like state for strain deformations of 0.1 % and 100 % occurs.

3.4. Using PLA-TPE_EP network as a macroiniferter for the vinyl monomer polymerization – the introduction of new monomer units into the network structure

In the previous sections, it was shown that the prepared network based on PLA containing TPE groups in its structure (located in the nodes of the polymer network), is a dynamic network capable of rearranging its structure. However, the reversible thermal dissociation of TPE groups to radicals, if it occurs in the presence of an unsaturated monomer, can lead to the initiation of polymerization of that monomer.

As it was mentioned in the Introduction, thermally dissociating TPE

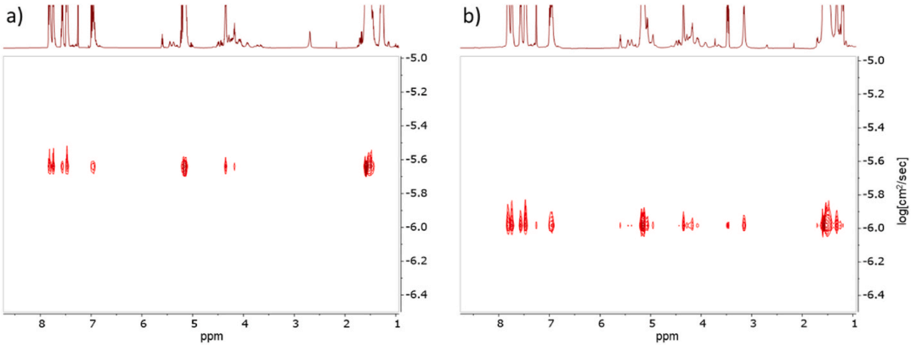

Fig. 3. DOSY ^{1}H NMR spectra of LA-co-BP_EP (a) and (LA-co-BP_EP)HDI copolymers (the area where signals corresponding to solvents appear is not shown).

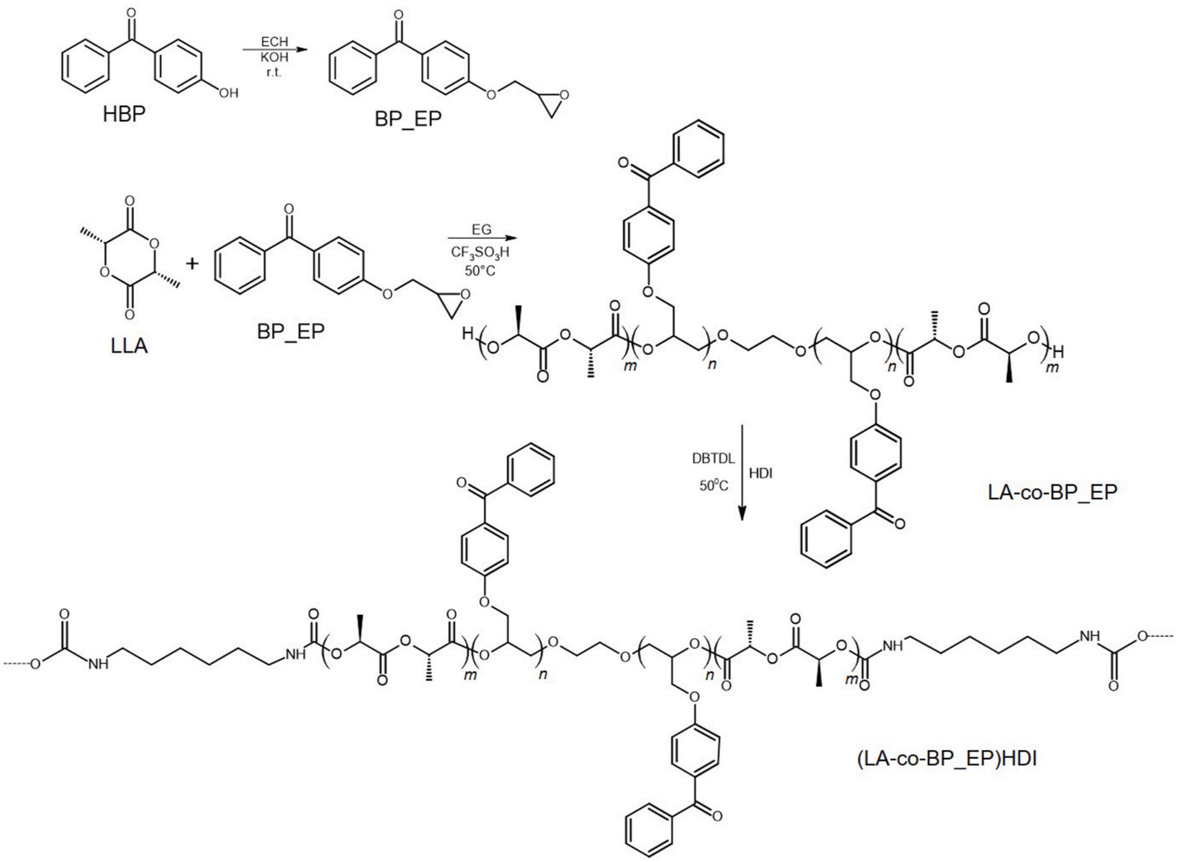

Fig. 4. Reaction scheme for the synthesis of (LA-co-BP_EP)HDI copolymer.

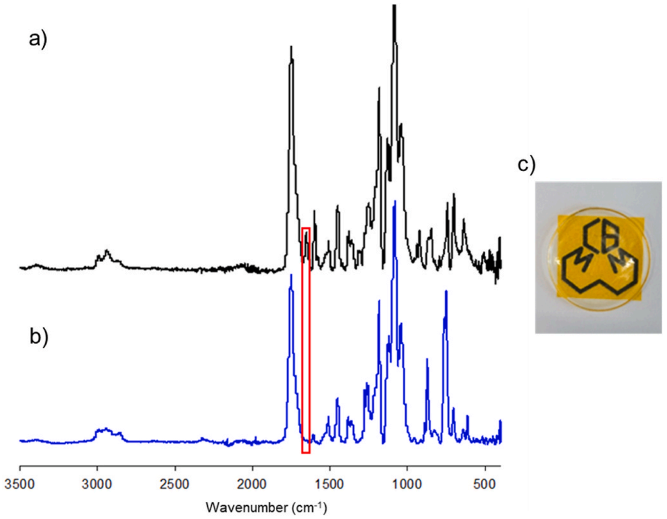

Fig. 5. FTIR spectra for (LA-co-BP_EP)HDI copolymer (a), PLA-TPE_EP network (b) and the photograph of the obtained network film (c).

groups incorporated into different polymer structures, mainly polyurethanes, were applied to initiate vinyl monomer polymerization [29–34]. We decided to initiate VM radical polymerization from a PLA-based network, i.e. synthesized in this work PLA-TPE_EP. Polymerization was performed by heating the network in the presence of acrylonitrile as VM at 85 °C. The temperature of 85 °C was chosen as it ensures effective dissociation of TPE groups [34]. Acrylonitrile was selected as a model vinyl monomer for two reasons. Firstly, its thermal polymerization can be disregarded at the temperature of 85 °C. Secondly, it is known that in its radical polymerization, chain termination mainly occurs through the recombination of propagated radicals, given the appropriate conditions [48]. This is an essential requirement for producing vinyl monomer chains that link two LA-co-BP_EP chains of the initial network. After 24 h of polymerization, the network was separated, washed with DMF and diethyl ether to remove unlinked PAN chains and then dried. For performed polymerization experiments, the increase of the sample weight by: 275 % (sample I) or 430 % (sample II), was observed. The higher increase in the sample mass (430 %) suggested the incorporation of AN into the network structure in the amount corresponding to the AN/LA molar ratio equal to ~20 (the way of calculation is explained in SI). The obtained product being a stiff transparent network (see Fig. S4 in SI) was not soluble in $CHCl_3$, THF and DMF solvents (Table S1) which indicates the incorporation of PAN chains in crosslinked structure by chemical bound. The FTIR spectroscopy confirmed the expected structure. In the FTIR spectrum of PLA-TPE_EP/PAN (Fig. 10), the absorption band at 2244 cm^{-1} corresponding to the stretching vibration of the nitrile groups $C\equiv N$ [49] can be easily detected apart from other signals overlapping with signals corresponding to the component groups of the initial PLA-TPE_EP network (bands at ~1450 cm^{-1} and ~2940 cm^{-1} corresponding to CH_2 groups, at ~1360 cm^{-1} corresponding to CH groups and additionally, signals corresponding to the cyclized PAN form at ~1600 cm^{-1} from $C{=}N$ and at ~1635 cm^{-1} from $C{=}C$ groups [50]. ^{13}C NMR in a solid state additionally confirmed the presence of AN units in the modified network (Fig. S5 in SI).

DSC analysis of the network after AN polymerization (Fig. 11a) shows quite different behavior of the material during heating compared to the initial network. It is difficult to identify the glass transition in the DSC thermogram of sample II which contains a large amount of AN units (20 times more AN units than LA units), a phenomenon often observed in PAN homopolymers [51]. The thermal stability of the network after

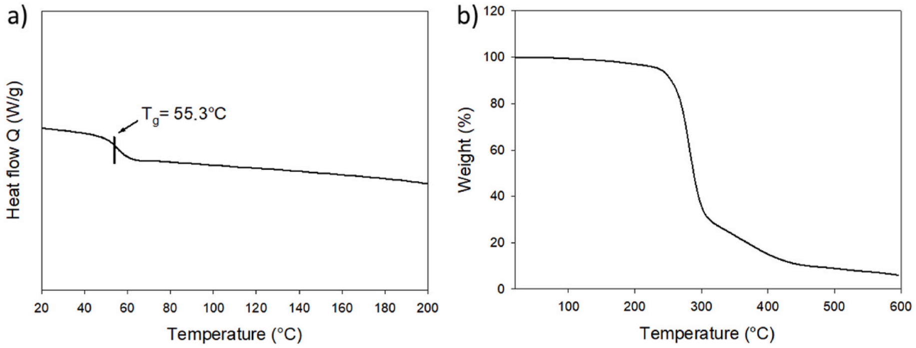

Fig. 6. DSC curve (2nd heating) (a) and TGA analysis of prepared PLA-TPE_EP network (b).

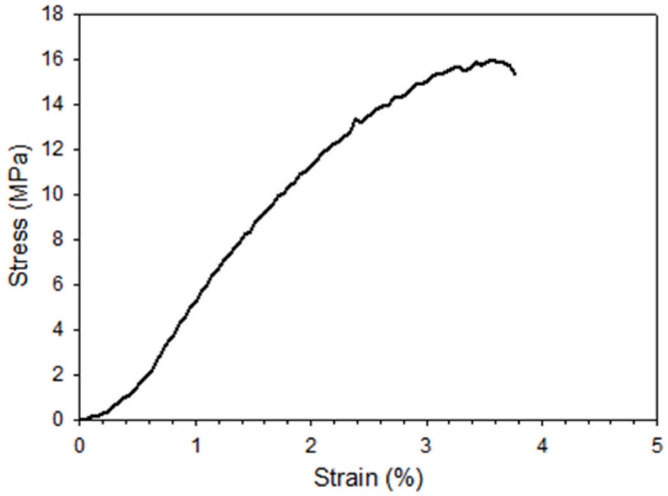

Fig. 7. Stress-strain curve for PLA-TPE_EP network (25 °C).

the incorporation of PAN fragments also varies from that of the initial network (Fig. 11b–S6 and S7). The material decomposition proceeds in several steps, with decomposition between 280 and 300 °C accounting for less than 9 % but most of the material degrades at higher temperatures, with the peak maximum at 436 °C. This is in contrast to the initial PLA-TPE_EP network where almost 70 % of the mass degraded up to 300 °C. Moreover, only 5–10 % of the residue is observed in the TGA curve of the original PLA-TPE_EP network after heating above 450 °C, while in the case of its copolymer with AN (sample II), approximately 58 % of the residue remains. This high residue in TGA analysis is characteristic of PAN that have undergone carbonization processes [52].

To further demonstrate that the introduction of PAN fragments into the PLA-TPE_EP network resulted in noticeable changes in network properties, elastic modulus and hardness of samples I and II were investigated using the nanoindentation method. The results presented in Fig. 12 show that both elastic modulus and hardness increase after the incorporation of PAN chains into PLA-based networks. Moreover, higher elastic modulus and hardness are observed with the incorporation of more AN units.

The same nanoindentation method allowed us to assess changes in modulus and hardness depending on the distance from the sample surface, up to 2 μm. It was found that both modulus and hardness only changed slightly (Fig. S8). The higher or lower values near the surface are likely due to the nanoindentation size effect [53].

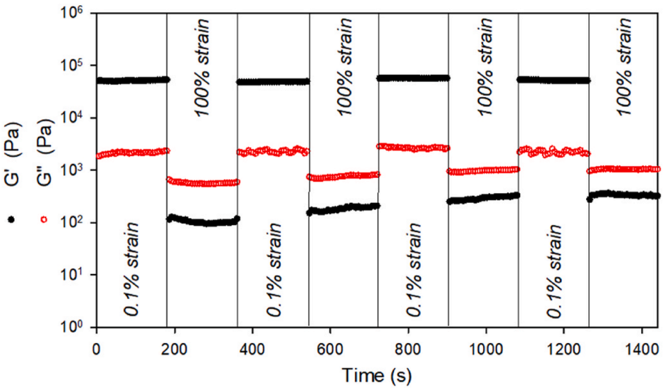

Fig. 9. The time dependence of storage and loss moduli for the PLA-TPE_EP network subjected to alternating small and large deformations; The measurement was performed at a constant temperature of 120 °C.

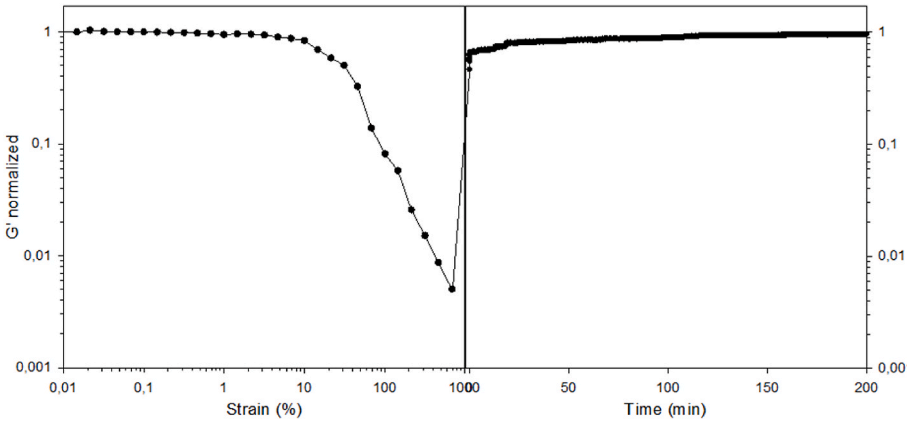

Fig. 8. Strain deformation dependence of the normalized storage modulus for the network PLA-TPE_EP; The measurement was performed at 120 °C.

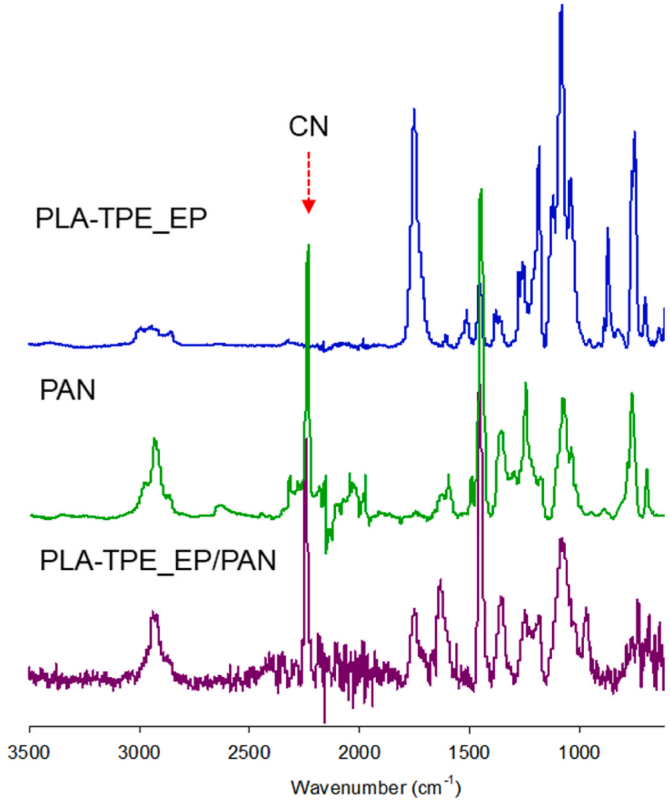

Fig. 10. FTIR spectra for PLA-TPE_EP initial network and the network PLA-TPE_EP/PAN (sample II) after polymerization of AN together with the spectrum of separately prepared PAN homopolymer for comparison (polymerization conditions are described in SI).

Summarizing this part, it should be stated that by the introduction of AN units into PLA-based networks, a combined network with high thermal stability, modulus, and hardness has been prepared.

4. Conclusions

A new epoxide monomer substituted with a benzophenone group (BP_EP) was successfully synthesized and used in ring-opening copolymerization with lactide, resulting in oligomeric copolymers with M_n of approximately 3000 bearing pendant benzophenone groups. In this manner, PLA-based oligodiols containing functional groups capable of further reactions were obtained (LA-co-BP_EP). The functionality of LA-co-BP_EP copolymer was increased to about 9 BP groups per macromolecule by coupling macromolecules using diisocyanate. Benzophenone functional groups have been used to link together polymer chains into the network according to a known UV-assisted reaction relying on the formation of tetraphenylethane (benzopinacole) moieties placed in crosslink points. The obtained copolymer network with high gel content of 95 %, prepared in the form of a polymer film, has a mechanical strength of 16 MPa as shown by the tensile test.

The presence of TPE groups in the network structure, which were capable of thermal reversible dissociation, offered expected additional possibilities. Rheology studies confirmed that the network was able to regain its mechanical strength after undergoing significant deformation, suggesting its processability.

In addition to its advantageous rheology, the network could be further modified by introducing new monomer units into its structure, specifically vinyl monomer that polymerizes according to the radical mechanism. DSC analyses of the modified networks containing acrylonitrile units indicate one-phase morphology, suggesting covalent linking of PAN chains with the network. The networks containing incorporated PAN showed a significant increase in thermal stability, modulus, and hardness. The simple method presented above for modifying the properties of PLA-based networks through the initiation of new monomer polymerization paves the way for new materials.

The results regarding both the dynamic nature of the network with TPE groups and the reactivity of TPE groups in initiating VM polymerization may expand the use of PLA-based materials by leveraging reversible covalent chemistry.

CRediT authorship contribution statement

Mateusz Grabowski: Writing – original draft, Methodology, Investigation. **Bartłomiej Kost:** Writing – review & editing, Methodology, Conceptualization. **Mateusz Bartniak:** Methodology, Investigation. **Dorota Bociaga:** Supervision. **Witold Szymański:** Methodology, Investigation. **Melania Bednarek:** Writing – review & editing, Writing –

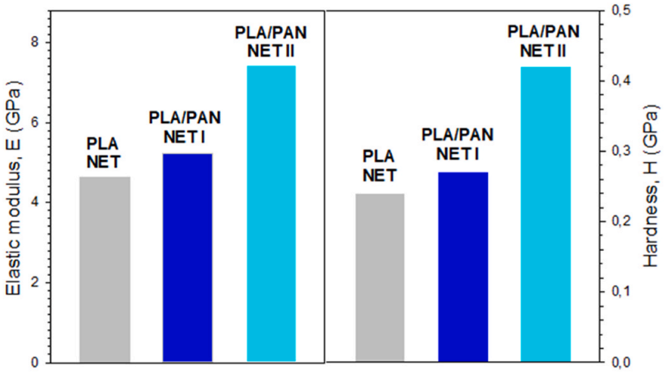

Fig. 12. Elastic modulus and hardness of PLA-TPE_EP and PLA-TPE_EP/PAN networks; E and H values presented in bar charts are average values calculated from the penetration depth from 200 to 2000 nm.

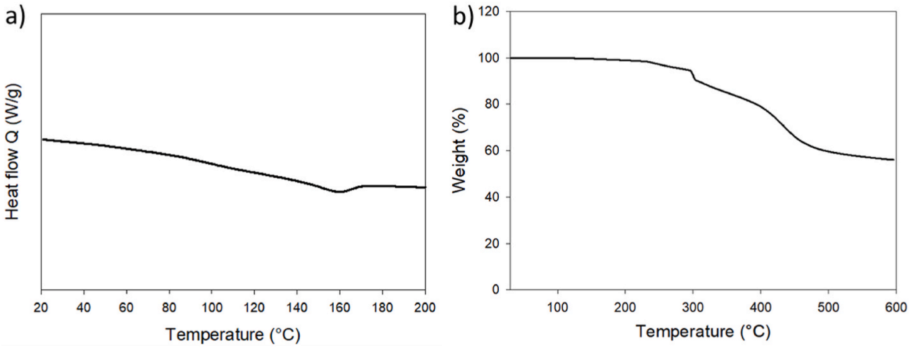

Fig. 11. DSC curve (2nd heating) (a) and TGA analysis (b) of the network incorporating PAN chains (PLA-TPE_EP/PAN – sample II).

original draft, Supervision, Methodology, Conceptualization.

Declaration of competing interest

The authors declare the following financial interests/personal relationships which may be considered as potential competing interests:

Melania Bednarek reports financial support was provided by National Science Centre Poland. If there are other authors, they declare that they have no known competing financial interests or personal relationships that could have appeared to influence the work reported in this paper.

Data availability

Data will be made available on request.

Acknowledgement

This work was supported by the National Science Centre in Poland under Grant no 2018/31/B/ST8/01969. The purchase of the Avance Neo 400 NMR spectrometer, used to obtain results included in this publication, was supported by the fundings from the EU Regional Operational Program of the Lodz Region, RPLD.01.01.00-10-0008/18.

The authors thank Andrzej Pawlak for performing a tensile test of the PLA-TPE_EP network.

Appendix A. Supplementary data

Supplementary data to this article can be found online at https://doi.org/10.1016/j.polymer.2024.127673.

References

[1] E. Balla, V. Daniilidis, G. Karlioti, T. Kalamas, M. Stefanidou, N.D. Bikiaris, A. Vlachopoulos, I. Koumentakou, D.N. Bikiaris, Poly(lactic acid): a versatile biobased polymer for the future with multifunctional properties - from monomer synthesis, polymerization techniques and molecular weight increase to PLA applications, Polymers 13 (2021) 1822, https://doi.org/10.3390/polym13111822.

[2] A. Jimenez, M. Peltzer, R. Ruseckaite, Poly(lactic acid) science and technology. Processing, properties. Additives and Applications, RSC, Cambridge, 2015.

[3] V. Nagarajan, A.K. Mohanty, M. Misra, Perspective on polylactic acid (PLA) based sustainable materials for durable applications: focus on toughness and heat resistance, ACS Sustain. Chem. Eng. 4 (2016) 2899–2916, https://doi.org/10.1021/acssuschemeng.6b00321.

[4] S. Farah, D.G. Anderson, R. Langer, Physical and mechanical properties of PLA, and their functions in widespread applications — a comprehensive review, Adv. Drug Deliv. Rev. 107 (2016) 367–392, https://doi.org/10.1016/j.addr.2016.06.012.

[5] S. lin Yang, Z.H. Wu, W. Yang, M.B. Yang, Thermal and mechanical properties of chemical crosslinked polylactide (PLA), Polym. Test. 27 (2008) 957–963, https://doi.org/10.1016/j.polymertesting.2008.08.009.

[6] Y. Hao, J. Chen, F. Wang, Y. Liu, X. Ai, H. Tian, Influence of crosslinking on rheological properties, ceystallization behavior and thermal stability of poly(lactic acid), Fibers Polym. 23 (2022) 1763–1769, https://doi.org/10.1007/s12221-022-4857-x.

[7] M. Bednarek, K. Borska, P. Kubisa, New polylactide-based materials by chemical crosslinking of PLA, Polym. Rev. 61 (2021) 493–519, https://doi.org/10.1080/15583724.2020.1855194.

[8] M. Bednarek, K. Borska, P. Kubisa, Crosslinking of polylactide by high energy irradiation and photo-curing, Molecules 25 (2020) 1–28, https://doi.org/10.3390/molecules25214919.

[9] R.P. Quirk, D.L. Pickel, 6.10 - Controlled End-Group Functionalization (Including Telechelics), Elsevier B.V., 2012, https://doi.org/10.1016/B978-0-444-53349-4.00168-0.

[10] D.J. Lunn, E.H. Discekici, J. Read de Alaniz, W.R. Gutekunst, C.J. Hawker, Established and emerging strategies for polymer chain-end modification, J. Polym. Sci. Part A Polym. Chem. 55 (2017) 2903–2914, https://doi.org/10.1002/pola.28575.

[11] M. Basko, M. Bednarek, Synthesis of functionalized polylactide by cationic activated monomer polymerization, React. Funct. Polym. 72 (2012) 213–220, https://doi.org/10.1016/j.reactfunctpolym.2012.02.003.

[12] R.F. Storey, S.C. Warren, C.J. Allison, A.D. Puckett, Methacrylate-endcapped poly (d,l-lactide- co-trimethylene carbonate) oligomers. Network formation by thermal free-radical curing, Polymer (Guildf). 38 (1997) 6295–6301.

[13] R. Sakai, B. John, M. Okamoto, J.V. Seppälä, J. Vaithilingam, H. Hussein, R. Goodridge, Fabrication of polylactide-based biodegradable thermoset scaffolds for tissue engineering applications, Macromol. Mater. Eng. 298 (2013) 45–52, https://doi.org/10.1002/mame.201100436.

[14] R.F. Storey, T.P. Hickey, Degradable polyurethane networks based on d,l-lactide, glycolide, ε-caprolactone, and trimethylene carbonate homopolyester and copolyester triols, Polymer (Guildf). 35 (1994) 830–838, https://doi.org/10.1016/0032-3861(94)90882-6.

[15] R. Storey, J. Wiggins, K. Mauritz, A. Puckett, Bioabsorbable composites. II: nontoxic, L-lysine - based poly(ester-urethane) matrix composites, Polym. Compos. 14 (1993) 17–25, https://doi.org/10.1002/pc.750140104.

[16] J.V. Seppälä, A.O. Helminen, H. Korhonen, Degradable polyesters through chain linking for packaging and biomedical applications, Macromol. Biosci. 4 (2004) 208–217, https://doi.org/10.1002/mabi.200300105.

[17] X. Xu, J.D. Skelly, J. Song, Chemically crosslinked amphiphilic degradable shape memory polymer nanocomposites with readily tuned physical, mechanical, and biological properties, ACS Appl. Mater. Interfaces 15 (2022) 2693–2704, https://doi.org/10.1021/acsami.2c19441.

[18] A.J. Nijenhuis, D.W. Grijpma, A.J. Pennings, Crosslinked poly (L-lactide) and poly (e-caprolactone), Polymer (Guildf). 37 (1996) 2783–2791.

[19] D.W. Grijpma, E. Kroeze, A.J. Nijenhuis, A.J. Pennings, Poly(l-lactide) crosslinked with spiro-bis-dimethylene-carbonate, Polymer (Guildf) 34 (1993) 1496–1503, https://doi.org/10.1016/0032-3861(93)90868-B.

[20] W.W. Gerhardt, D.E. Noga, K.I. Hardcastle, A.J. García, D.M. Collard, M. Weck, Functional lactide monomers: Methodology and polymerization, Biomacromolecules 7 (2006) 1735–1742, https://doi.org/10.1021/bm060024j.

[21] M. Heiny, V.P. Shastri, Cyclic comonomers for the synthesis of carboxylic acid and amine functionalized poly(L-lactic acid), Molecules 20 (2015) 4764–4779.

[22] D.E. Noga, T.A. Petrie, A. Kumar, M. Weck, A.J. García, D.M. Collard, Synthesis and modification of functional poly(lactide) copolymers: toward biofunctional materials, Biomacromolecules 9 (2008) 2056–2062, https://doi.org/10.1021/bm800292z.

[23] B. Saulnier, S. Ponsart, J. Coudane, H. Garreau, M. Vert, Lactic acid-based functionalized polymers via copolymerization and chemical modification, Macromol. Biosci. 4 (2004) 232–237, https://doi.org/10.1002/mabi.200300087.

[24] M. Bednarek, M. Basko, P. Kubisa, Functional polylactide by cationic ring-opening copolymerization of lactide with epoxides, React. Funct. Polym. 119 (2017) 9–19, https://doi.org/10.1016/j.reactfunctpolym.2017.07.008.

[25] S. Gazzotti, M.A. Ortenzi, H. Farina, A. Silvani, Synthesis of fluorine-containing, UV-responsive PLA-based materials by means of functionalized DOX monomer, Macromol. Chem. Phys. 223 (2022) 1–10, https://doi.org/10.1002/macp.202100436.

[26] D. Braun, K.H. Becker, Kinetik der Polymerisationsauslösung mit aromatischen pinakolen, Die Makromol, Chemie 147 (1971) 91–99, https://doi.org/10.1002/macp.1971.021470108.

[27] A. Błedzki, D. Braun, W. Menzel, K. Titzschkau, Polymerizationsauslosung mit subsstituierten Ethanen, Makromol. Chem. 294 (1983) 287–294.

[28] T. Otsu, A. Matsumoto, T. Tazaki, Radical polymerization of methyl methacrylate with some 1,2-disubstituted tetraphenylethanes as thermal iniferters, Polym. Bull. 17 (1987) 323–330, https://doi.org/10.1007/BF00955715.

[29] G. Zhou, C. Ma, G. Zhang, Synthesis of polyurethane-g-poly(ethylene glycol) copolymers by macroiniferter and their protein resistance, Polym. Chem. 2 (2011) 1409–1414, https://doi.org/10.1039/c1py00016k.

[30] K. Tharanikkarasu, G. Radhakrishnan, Tetraphenylethane iniferters. II. Toluene diisocyanate-based polyurethane iniferter for "living radical polymerization of acrylonitrile, J. Polym. Sci. Part A Polym. Chem. 34 (1996) 1723–1731.

[31] K. Tharanikkarasu, G. Radhakrishnan, Tetraphenylethane iniferters: polyurethane-polystyrene multiblock copolymers through "living" radical polymerization, J. Appl. Polym. Sci. 66 (1997) 1551–1560.

[32] B.K. Kim, K. Tharanikkarasu, J.S. Lee, Polyurethane-polymethacrylic acid multiblock copolymer dispersions through polyurethane macroiniferters, Colloid Polym. Sci. 277 (1999) 285–290, https://doi.org/10.1007/PL00013758.

[33] M. Grabowski, B. Kost, P. Kubisa, M. Bednarek, A new approach to the synthesis of polylactide/polyacrylonitrile block copolymers, Polymers 14 (2022) 1529, https://doi.org/10.3390/polym14081529Academic.

[34] M. Grabowski, B. Kost, A. Bodzioch, M. Bednarek, Functionalization of polylactide with multiple tetraphenyethane inifer groups to form PLA block copolymers with vinyl monomers, Int. J. Mol. Sci. 24 (2023) 19, https://doi.org/10.3390/ijms24010019.

[35] Z.P. Zhang, M.Z. Rong, M.Q. Zhang, Mechanically robust, self-healable, and highly stretchable "living" crosslinked polyurethane based on a reversible C–C bond, Adv. Funct. Mater. 28 (2018) 1706050, https://doi.org/10.1002/adfm.201706050.

[36] Y. Li, Z.P. Zhang, W.J. Mo, M.Z. Rong, M.Q. Zhang, D. Liu, Photo-induced topological self-reorganization and self-growth of polymer based on dynamic reversible aromatic pinacol units, Polymer (Guildf). 192 (2020) 122299, https://doi.org/10.1016/j.polymer.2020.122299.

[37] K. Borska, M. Bednarek, D. Gorgol, J. Osicka, M. Mrlik, Polylactide-based networks containing dynamic tetraphenylethane groups for 3D printed repairable and reprocessable constructs, React. Funct. Polym. 191 (2023) 105694, https://doi.org/10.1016/j.reactfunctpolym.2023.105694.

[38] M. Bednarek, M. Grabowski, M. Lipinska, A. Pawlak, Reversible polymer networks based on polylactide with tetraphenylethane thermally dissociating groups in crosslinks, Polym. Adv. Technol. (2024), https://doi.org/10.1002/pat.6390.

[39] B. Furniss, A. Hannaford, P. Smith, A. Tatchell, Vogel's Textbook of Practical Organic Chemistry, Longman Scientific & Technical, Longman House, London, 1989.

[40] N. Holten-Andersen, M.J. Harrington, H. Birkedal, B.P. Lee, P.B. Messersmith, K.Y. C. Lee, J.H. Waite, pH-induced metal-ligand cross-links inspired by mussel yield

self-healing polymer networks with near-covalent elastic moduli, Proc. Natl. Acad. Sci. U.S.A. 108 (2011) 2651–2655, https://doi.org/10.1073/pnas.1015862108.

[41] M.M. Lübtow, M. Mrlik, L. Hahn, A. Altmann, M. Beudert, T. Lühmann, R. Luxenhofer, Temperature-dependent rheological and viscoelastic investigation of a poly(2-methyl-2oxazoline)-b-poly(2-iso-butyl-2-oxazoline)-b-poly(2-methyl-2-oxazoline)-based thermogelling hydrogel, J. Funct. Biomater. 10 (2019) 36, https://doi.org/10.3390/jfb10030036.

[42] W.C. Oliver, G.M. Pharr, An improved technique for determining hardness and elastic modulus using load and displacement sensing indentation experiments experiments, J. Mater. Res. 7 (1992) 1564–1583.

[43] X. Li, B. Bhushan, A review of nanoindentation continuous stiffness measurement technique and its applications, Mater. Char. 48 (2002) 11–36, https://doi.org/10.1016/S1044-5803(02)00192-4.

[44] M. Körner, O. Prucker, J. Rühe, Kinetics of the generation of surface-attached polymer networks through C, H-insertion reactions, Macromolecules 49 (2016) 2438–2447, https://doi.org/10.1021/acs.macromol.5b02734.

[45] P. Groves, Diffusion ordered spectroscopy (DOSY) as applied to polymers, Polym. Chem. 8 (2017) 6700–6708, https://doi.org/10.1039/c7py01577a.

[46] NatureWorks, Ingeo TM Biopolymer 3251D Technical Data Sheet Injection Molding Process Guide, 2017.

[47] R.F. Storey, T.P. Hickey, Degradable polyurethane networks based on D,L-lactide, glycolide, ε-caprolactone, and trimethylene carbonate homopolyester and copolyester triols, Polymer (Guildf). 35 (1994) 830–838, https://doi.org/10.1016/0032-3861(94)90882-6.

[48] X. Li, T. Ogihara, T. Kato, Y. Nakamura, S. Yamago, Evidence for polarity- and viscosity-controlled pathways in the termination reaction in the radical polymerization of acrylonitrile. https://doi.org/10.1021/acs.macromol.1c00158, 2021.

[49] A. Jenab, R. Roghanian, N. Ghorbani, K. Ghaedi, G. Emtiazi, The efficacy of electrospun PAN/Kefiran nanofiber and kefir in mammalian cell culture: promotion of PC12 cell growth, anti-MCF7 breast cancer cells activities, and cytokine production of PBMC, Int. J. Nanomed. 15 (2020) 717–728, https://doi.org/10.2147/IJN.S232264.

[50] I. Karbownik, M. Fiedot, O. Rac, P. Suchorska-woźniak, H. Teterycz, Effect of doping polyacrylonitrile fibers on their structural and mechanical properties, Polymer (Guildf). 75 (2015) 97–108, https://doi.org/10.1016/j.polymer.2015.08.015.

[51] Y. Furushima, M. Nakada, H. Takahashi, K. Ishikiriyama, Study of melting and crystallization behavior of polyacrylonitrile using ultrafast differential scanning calorimetry, Polymer (Guildf). 55 (2014) 3075–3081, https://doi.org/10.1016/j.polymer.2014.05.015.

[52] Y. Cai, Q. Wang, Q. Wei, Q. You, F. Huang, L. Song, Y. Hu, W. Gao, Structure, thermal, and antibacterial properties of polyacrylonitrile/ferric chloride nanocomposite fibers by electrospinning, Int. J. Polym. Anal. Char. 15 (2010) 110–118, https://doi.org/10.1080/10236660903525083.

[53] C. Han, Indentation size effect in polymers, Adv. Mater. Sci. Res. 10 (2011) 393–413.

SUPPORTING INFORMATION

Copolymerization of lactide with functional epoxide as a way to the polymer network with dually active tetraphenylethane groups

Mateusz Grabowski[1,3], *Bartłomiej Kost*[1], *Mateusz Bartniak*[2], *Dorota Bociaga*[2], *Witold Szymański*[2], *Melania Bednarek*[1]*

[1] Centre of Molecular and Macromolecular Studies, Polish Academy of Sciences, Sienkiewicza 112, 90-363 Lodz, Poland

[2] Institute of Materials Science and Engineering, Lodz University of Technology, Stefanowskiego 1/15, 90-537 Lodz, Poland

[3] BioMedChem Doctoral School of the University of Lodz and Lodz Institutes of the Polish Academy of Sciences, Matejki 21/23, 90-237 Lodz, Poland

1. Analyzes of BP_EP and its copolymers with LA: LA-co-BP_EP and (LA-co-BP_EP)HDI

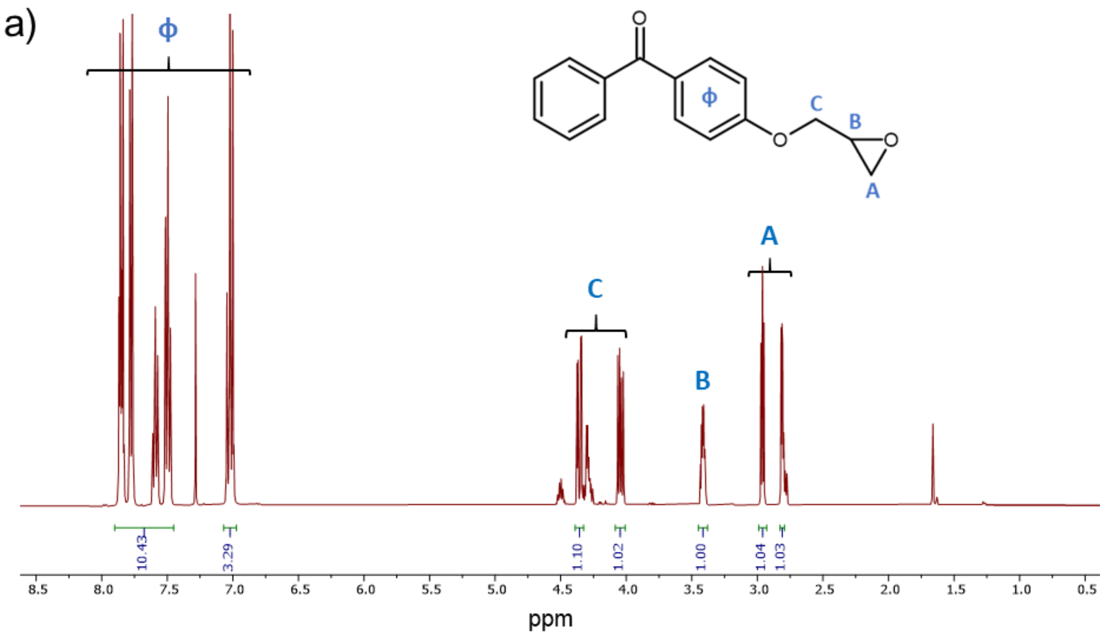

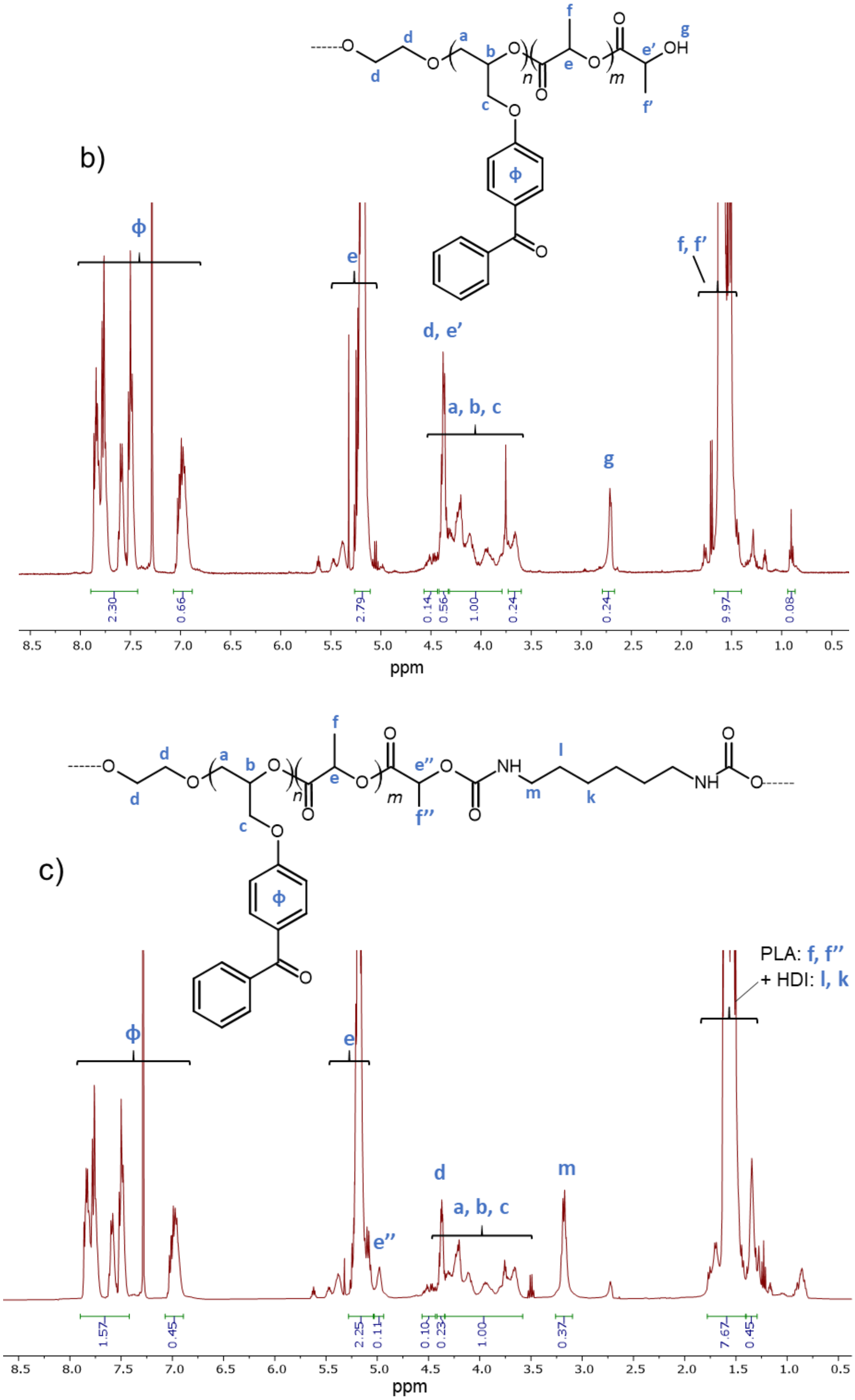
b)
f
g
OH
d
a
b
e'
n
e
m
f'
c
ϕ
ϕ
e
f, f'
d, e'
a, b, c
g
2.30
0.66
2.79
0.14
0.56
1.00
0.24
0.24
9.97
0.08
8.5 8.0 7.5 7.0 6.5 6.0 5.5 5.0 4.5 4.0 3.5 3.0 2.5 2.0 1.5 1.0 0.5
ppm
c)
f
d
a
b
e''
NH
l
NH
d
n
e
m
f''
m
k
c
ϕ
ϕ
e
PLA: f, f''
+ HDI: l, k
d
a, b, c
m
e''
1.57
0.45
2.25
0.11
0.10
0.23
1.00
0.37
7.67
0.45
8.5 8.0 7.5 7.0 6.5 6.0 5.5 5.0 4.5 4.0 3.5 3.0 2.5 2.0 1.5 1.0 0.5
ppm

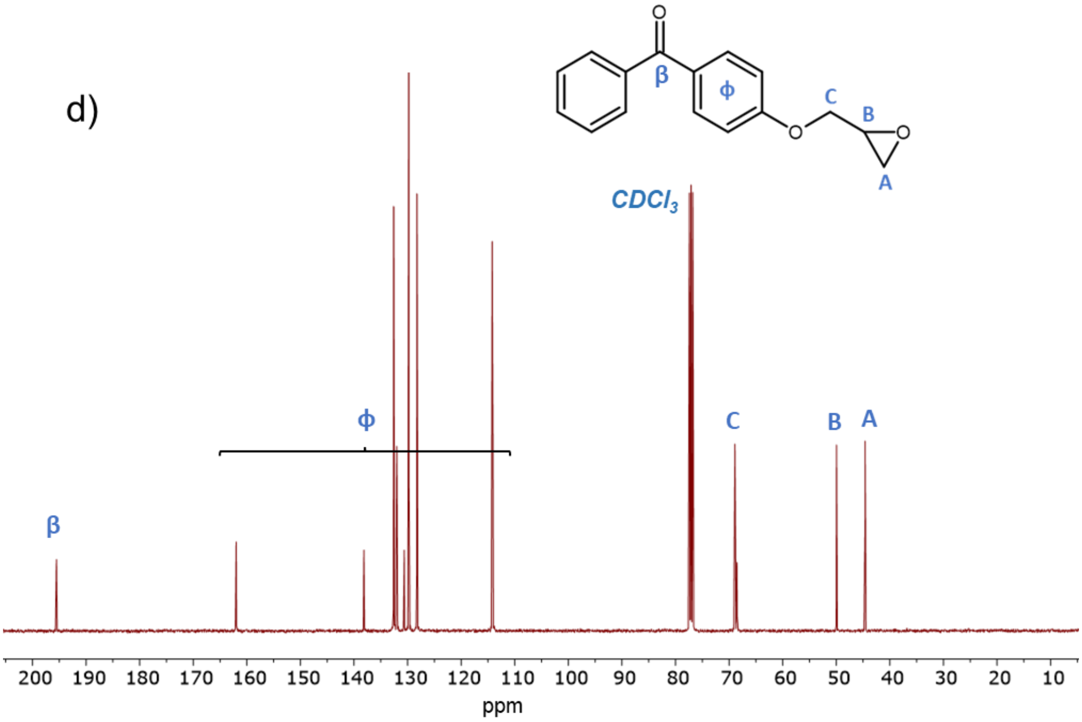
d)
β
ϕ
C
B
A
O
CDCl$_3$
ϕ
C
B
A
β
200 190 180 170 160 150 140 130 120 110 100 90 80 70 60 50 40 30 20 10
ppm

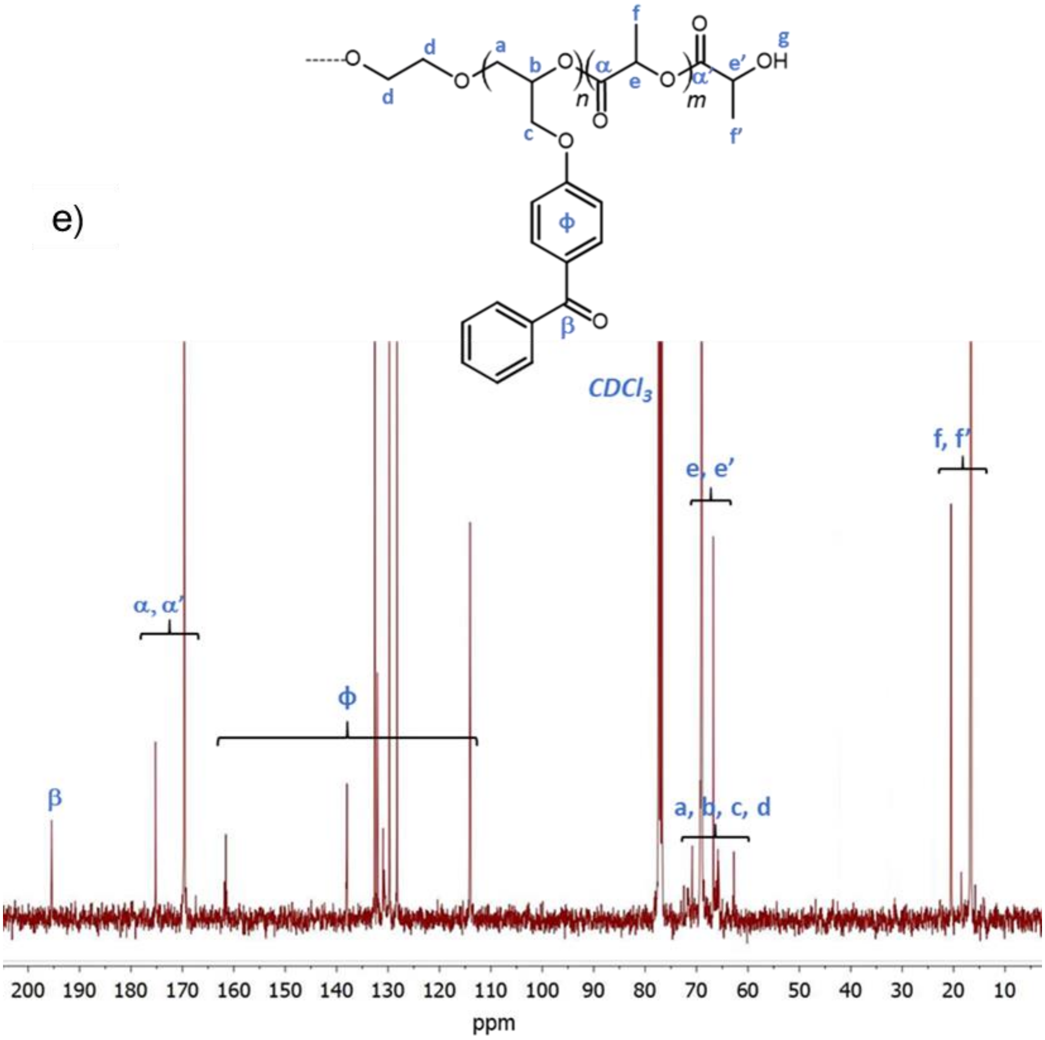
e)
d
a
b
α
f
e
α'
e'
g
OH
d
n
m
c
f'
ϕ
β
CDCl$_3$
f, f'
e, e'
α, α'
ϕ
β
a, b, c, d
200 190 180 170 160 150 140 130 120 110 100 90 80 70 60 50 40 30 20 10
ppm

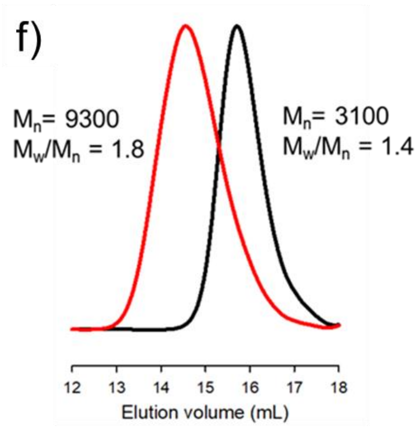

Figure S1. ^{1}H NMR spectra ($CDCl_3$) of BP_EP (a), LA copolymers: LA-co-BP_EP (b), (LA-co-BP_EP)HDI (c), ^{13}C NMR spectrum ($CDCl_3$) of BP_EP (d), ^{13}C NMR spectrum ($CDCl_3$) of LA-co-BP_EP (e) and SEC curves (f): LA-co-BP_EP – black line, (LA-co-BP_EP)HDI – red line.

In the ^{1}H NMR spectrum of BP_EP, signals corresponding to protons from phenyl rings in between 7.0 and 7.85 ppm are present, as well as signals from protons belonging to the epoxy ring and methylene group in the ranges 2.7- 3.45 and 4.0 – 4.45 ppm respectively. In the spectra of the synthetized copolymers, all signals corresponding to polylactide are present (at about 5.2 ppm corresponding to methine protons $-\underline{CH}(CH_3)-$ and at about 1.6 ppm corresponding to methyl group $-CH(\underline{CH_3})-$), also signals characteristic of protons from incorporated BP_EP groups are clearly visible in the range of 3.6 - 4.6 ppm and 6.85 -7.9 ppm. After coupling the obtained copolymer with HDI, the signals corresponding to PLA $-\underline{CH}OH$ end groups at 4.3 ppm are shifted to a new position at 4.9 ppm. SEC curves indicate monomodal molecular weights distributions and a shift in the direction of higher molecular weights after the coupling reaction. **The ratio of BP_EP/LA units in the copolymer** was calculated by comparing the intensity of the signal corresponding to $-\underline{CH}(CH_3)-$ groups in LA units (2 protons) at ~5.2 ppm with the intensity of the signals between 3.6 ppm and 4.6 ppm which, after abstraction of the signal at 4.3 ppm corresponding to LA end groups ($-\underline{CH}(CH_3)-OH$) and EG units, correspond to epoxy derivative (5 protons). BP_EP/LA ratio calculated on the basis of the presented in Fig. S1b spectrum = 0.19.

The M_n of LA-co-BP_EP was calculated as a sum of masses of LA and PB_EP units in one macromolecule. Firstly, $M_{n\ PLA} = DP_{n\ PLA}$ x 144 where DP_{nPLA} was calculated by the comparison of the intensities of signals corresponding to $-\underline{CH}(CH_3)-OH$ end groups at 4.3 ppm and corresponding to $-\underline{CH}(CH_3)-$ groups from PLA backbone at 5.2 ppm. The signal at 4.3 ppm is an overlapping signal corresponding to -<u>CH</u>(CH_3)-OH and -CH_2- groups of initiating EG. The fraction of the integration corresponding to PLA end groups is equal to 1/3 part of the total integration at 4.3 ppm. Secondly, $M_{n\ BP\_EP} = DP_{n\ BP\_EP} \times 254$ where $DP_{n\ BP\_EP} = DP_{n\ PLA} \times$ BP_EP/LA.

Thus, on the basis of presented in Fig. S1b spectrum, the calculation is as follows:
$DP_{n\ PLA}$ = [2.79 (2 protons) + (0.56/3)] : (0.56/3) (2 protons) = 15.6
$M_{n\ PLA}$ = 15.6 x 144 = 2250
$DP_{n\ BP\_EP}$ = 15.6 x 0.19 = 3.0
$M_{n\ BP\_EP}$ =3 x 254 = 760
$M_{n\ LA\text{-}co\text{-}BP\_EP} = M_{n\ PLA} + M_{n\ BP\_EP} + M_{EG}$ = 2250 + 760 + 62 = ~3070

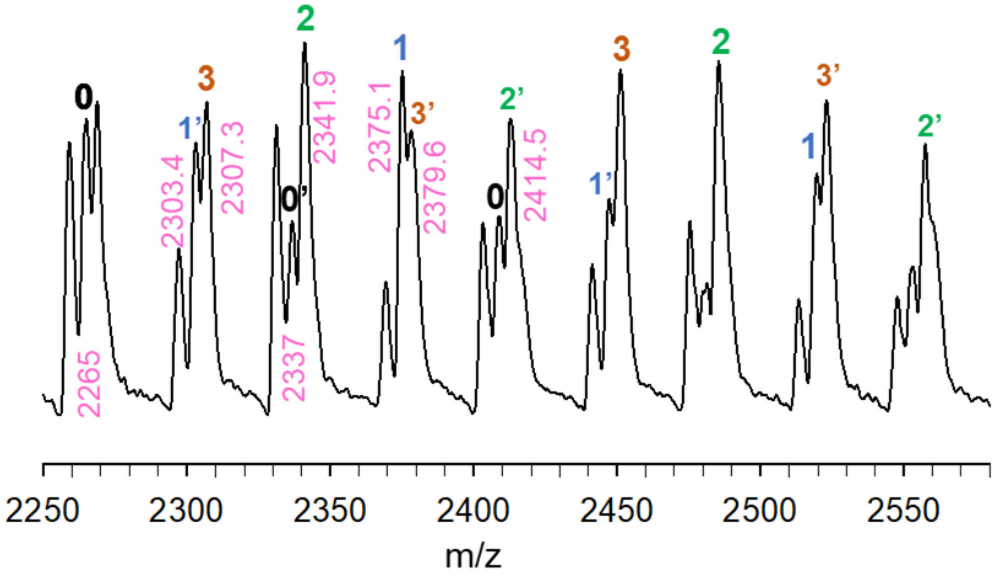

Figure S2. The expanded fragment of MALDI TOF spectrum of LA-co-BP_EP copolymer presented in Fig. 2 with signals assignments.

Calculations of masses for individual macromolecules belonging to series containing nLA units and not containing BP_EP unit (series 0) and containing 1, 2 or 3 BP_EP units (series 1, 2 or 3) and additionally for macromolecules which underwent transesterification reactions - series containing nLA/2 units and 0, 1, 2, 3 BP_EP units (series 0', 1', 2', 3'):
0: n=15: m/z = 15 x 144.14 + 62 + 39 = 2263.1 (signal at 2265 in the spectrum)
1: **n=14**: m/z = 14 x 144.14 + 62 + 254 + 39 = 2373.0 (signal 2375.1 in the spectrum)
2: **n = 12**: m/z = 12 x 144.14 + 62 + 2 x 254 +39 = 2338.7 (signal 2341.9 in the spectrum)
3: **n = 10**: m/z = 10 x 144.14 + 62 + 3 x 254 + 39 = 2304.4 (signal 2307.3 in the spectrum)

0': n = 31; m/z = 31 x 144.14/2 + 62 + 39 = 2335.2 (signal 2337 in the spectrum)

1': n = 27: m/z = 27 x 144.14/2 + 62 + 254 + 39 = 2300.9 (signal 2303.4 in the spectrum)

2': n = 25: m/z = 25 x 144.14/2 + 62 + 2 x 254 + 39 = 2410.8 (signal 2414.5 in the spectrum)

3': n =21: m/z = 21 x 144.14/2 + 62 + 3 x 254 + 39 = 2376.5 (signal 2379.6 in the spectrum)

(Differences of 2-3 mass units between the calculated and recorded values during measurement are due to imperfect calibration of the MALDI TOF instrument.)

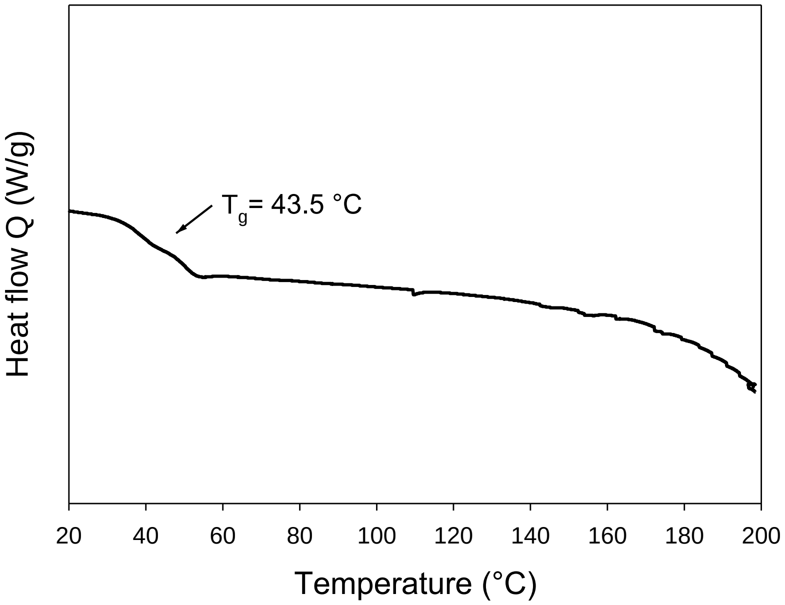

Figure S3. DSC analysis of (LA-co-BP_EP)HDI copolymer (2nd heating)

2. Characterization of PLA-TPE_EP/PAN modified network

Figure S4. Photograph of the piece of PLA-TPE_EP/PAN network, sample II (the weight increase by 430 %).

Table S1. Solubility and swelling of PLA-based networks in several solvents

Network	Solvent	Solubility at room temp., 24h %	Solubility at high temp., 1h %	Swelling at room temp. %
PLA-TPE_EP	$CHCl_3$	2	~0 [a)]	560
	THF	~0	3 [a)]	290
	DMF	1	8 [b)]	330
PLA-TPE_EP/PAN Sample I	$CHCl_3$	~0	3 [a)]	12
	THF	~0	1 [a)]	5
	DMF	~0	4 [b)]	140

[a)] Solubility at 60 ºC; [b)]Solubility at 100 ºC

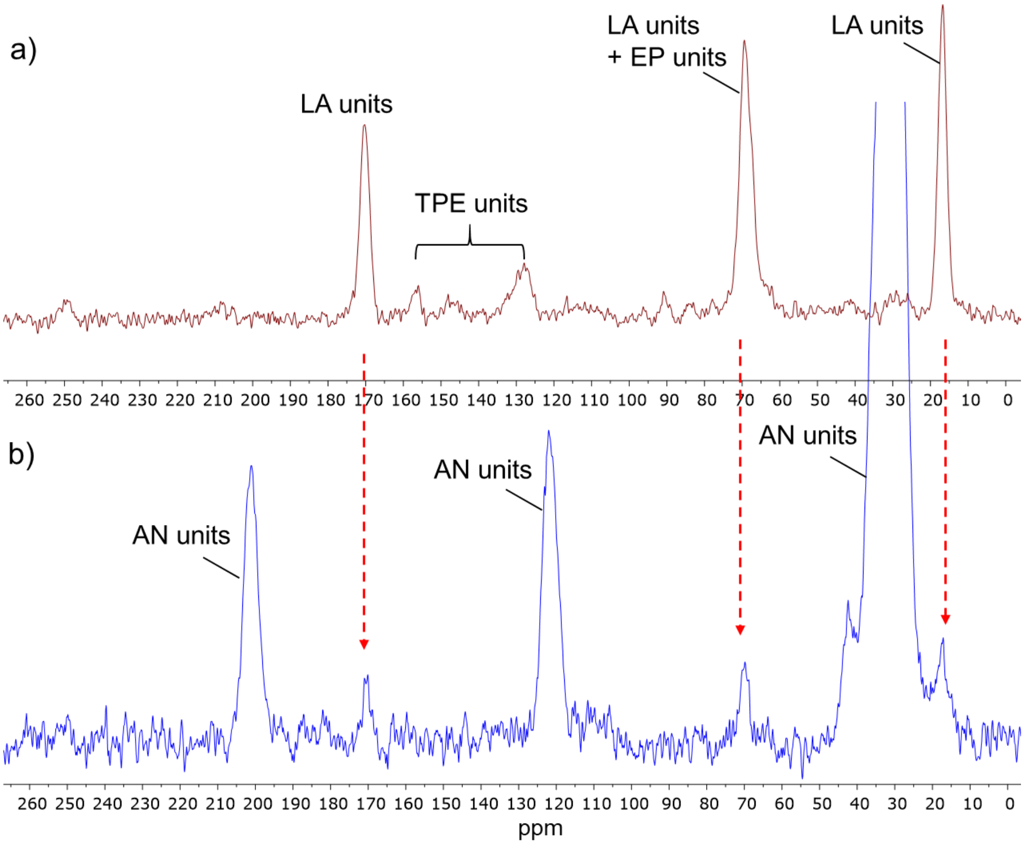

Figure S5. Solid-state ^{13}C NMR spectra of PLA-TPE_EP network (a) and PLA-TPE_EP/PAN network (b).[1]

Calculation of AN/LA ratio in the PLA-TPE_EP/PAN network (sample II)

The network was weighed before: m(PLA-TPE_EP), and after polymerization of AN: m(PLA-TPE_EP/PAN):

m(PLA-TPE_EP/PAN) = m(PLA-TPE_EP) + m(PAN)

It was assumed that the molar ratio LA/EP in copolymer and in obtained network after its coupling was the same and it was calculated on the basis on ^{1}H NMR spectrum of the copolymer that LA/EP = 5.

Excluding the HDI contribution, wt.% of LA in the initial network is equal to:

$\mathrm{wt\%(LA)} = [5x \cdot 144 / (1x \cdot 254 + 5x \cdot 144)] \cdot 100\% = 74\%$

x = number of EP mols

144 = molar mass of LA, 254 – molar mass of EP.

A mass of LA in the initial network is: m(LA) = 0.74 · m(PLA-TPE_EP). The same mass is in PLA-TPE_EP/PAN network.

<u>AN/LA mol ratio</u> = [m(PAN)/53] / [m(LA)/144], where 53 = molar mass of AN.

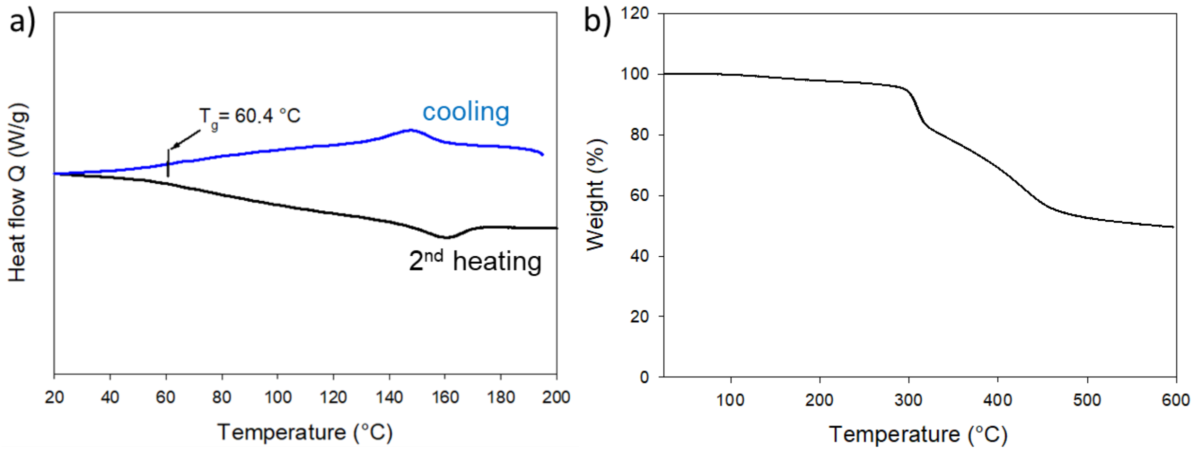

Figure S6. DSC curve (a) and TGA analysis (b) of the network PLA-TPE_EP/PAN, sample I (with less AN units incorporated).

In the DSC curve corresponding to the second heating, the glass transition cannot be observed but it can be detected in the cooling curve, with the T_g value equal to 60.4 ^{o}C i.e., 5 degree higher than that of initial network PLA-TPE_EP (T_g value of PAN determined by some authors is equal to ~85 °C in bulk.[2]

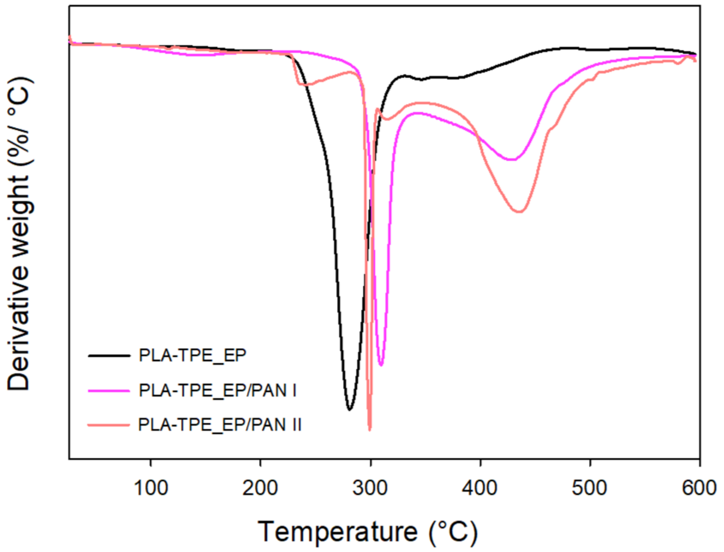

Figure S7. Derivative TGA curves for PLA-TPE_EP/PAN samples I and II and for the initial PLA-TPE_EP network.

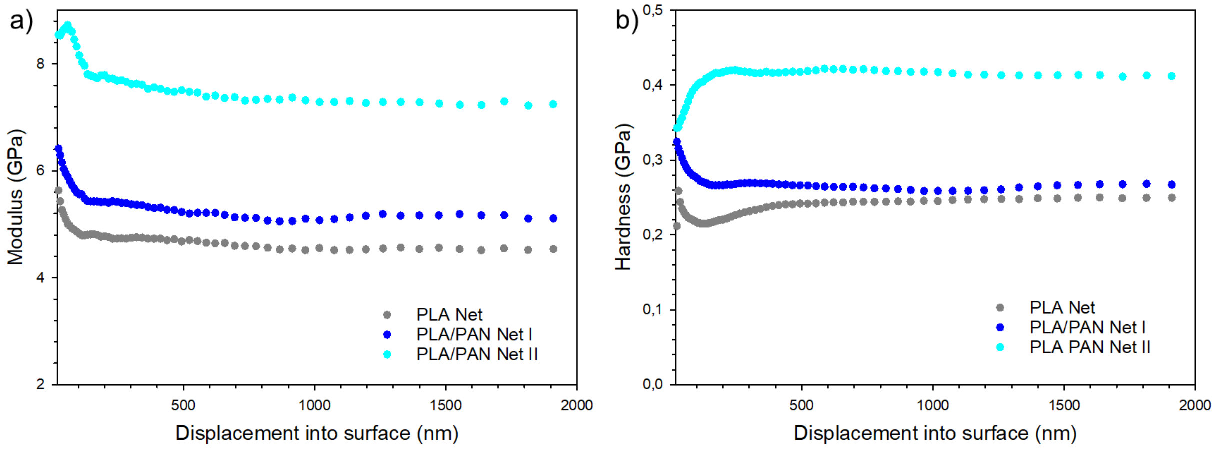

Figure S8. Elastic modulus and hardness of PLA-based networks in dependence on the distance from the surface.

Synthesis of poly(acrylonitrile) homopolymer

AN (0.8 g, 15 mmol) was placed in a Schlenk flask and 0.06 g (0.3 mmol) of AIBN was added. The solution was degassed via three freeze–pump–thaw cycles. The flask was filled with nitrogen and heated in an oil bath at 85 °C for 24 h with stirring. The precipitated PAN was washed with methanol three times, and dried for 48 h in vacuum.

References

[1] K. Ruhland, R. Frenzel, R. Horny, A. Nizamutdinova, L. van Wullen, J. Moosburger-Will, and S. Horn, Investigation of the chemical changes during thermal treatment of polyacrylonitrile and 15N-labelled polyacrylonitrile by means of in-situ FTIR and ^{15}N NMR spectroscopy, *Polym. Degrad. Stabil.* 2017, **146**, 298-316.

[2] W.S. Khan, M. Ceylan, A. Jabarrania, L. Saeednia, R. Asmatulu, Chemical and thermal investigations of electrospun polyacrylonitrile nanofibers incorporated with various nanoscale inclusions, *J. Therm. Eng*. 2017, **3**, 1375–1390.

Publikacja 5:

Melania Bednarek, Mateusz Grabowski, Magdalena Lipińska, Andrzej Pawlak. Reversible polymer networks based on polylactide with tetraphenylethane thermally dissociating groups in crosslinks. *Polym. Adv. Technol*. 2024;35(4):e6390. doi:10.1002/pat.6390

Received: 19 January 2024 | Revised: 21 March 2024 | Accepted: 23 March 2024

DOI: 10.1002/pat.6390

RESEARCH ARTICLE

polymers for advanced technologies WILEY

Reversible polymer networks based on polylactide with tetraphenylethane thermally dissociating groups in crosslinks

Melania Bednarek[1] | Mateusz Grabowski[1] | Magdalena Lipińska[2] | Andrzej Pawlak[1]

[1]Centre of Molecular and Macromolecular Studies, Polish Academy of Sciences, Lodz, Poland

[2]Institute of Polymer and Dye Technology, Lodz University of Technology, Lodz, Poland

Correspondence
Melania Bednarek, Centre of Molecular and Macromolecular Studies, Polish Academy of Sciences, Sienkiewicza 112, 90-363 Lodz, Poland.
Email: melania.bednarek@cbmm.lodz.pl

Funding information
Narodowe Centrum Nauki, Grant/Award Number: 2018/31/B/ST8/01969; EU Regional Operational Program of the Lodz Region, Grant/Award Number: RPLD.01.01.00-10-0008/18

Abstract

Polylactide (PLA)-based reversible/dynamic polymer networks were synthesized by coupling 4-arm PLA stars containing reversible tetraphenylethane (TPE) groups in the core using diisocyanate. Star-shaped PLAs with molecular weights of 3200 and 6400 g/mol were obtained by the original method involving UV coupling of linear PLAs containing benzophenone moieties in the chain middle. The efficient formation of networks with gel content close to 100% was confirmed by FTIR spectroscopy. Networks with different densities of reversible groups exhibited tensile strength in the range of 35–50 MPa. Their reversible character was demonstrated by stress relaxation measurements performed at different temperatures (120–150°C). The prepared networks were capable of very fast stress relaxation due to radical exchange reactions between TPE groups placed in crosslinks, in contrast to a reference network without TPE groups. It was shown in the repairing experiment that networks were capable of processing.

KEYWORDS

polylactide, reprocessability, reversible/dynamic polymer network, tetraphenylethane

1 | INTRODUCTION

Polylactide/poly (lactic acid) (PLA) a bio-based thermoplastic derived from renewable resources, currently holds an established technological position.[1–3] It is synthesized from lactic acid obtained by bacterial fermentation of corn, sugarcane, rice, potatoes, and so forth, making it annually available from renewable agricultural sources. PLA can be both chemically and mechanically recycled into virgin polymer for new applications. These multiple after-use options, combined with its production from renewable resources, position PLA as a leading biomaterial for the circular economy. Global PLA production in 2022 was approximately 350 kilotons and is expected to grow with the compound annual growth rate (CAGR) of 14% up to 2035.[4] In parallel with the increase in production and demand for polylactide products, efforts are underway to improve and modify its properties.

There are various methods described in a wide range of literature for modifying the properties of polylactide.[5–8] One method that improves the thermal and mechanical properties of polylactide is crosslinking. However, permanent crosslinking limits material processing. Introducing reversible covalent chemical bonds into the polymer network structure allows achieving both goals. Reversible/dynamic networks represent a rapidly developing area due to their numerous beneficial properties, such as shape memory, self-healing, and, most importantly, processing capacity. Various dynamic networks with different mechanisms of exchange between “reversible” bonds have been prepared and studied. This exchange is responsible for rearranging the network structure under appropriate stimuli, resulting in malleability during processing. Dynamic/reversible polymer networks are the subject of many articles.[9–14]

Dynamic polymer networks, including different reversible groups exchanging according to dissociative or associative mechanisms, have also been constructed based on PLA.[15–21] Our group has contributed

---

On the occasion of the 90th birthday of Professor Stanislaw Penczek.

to these works.[22,23] We demonstrated that by introducing thermally dissociating disulfide[22] or tetraphenylethane (TPE) groups[23] into the network structure, primarily consisting of linked PLA chains, we obtained a material with shape stability and the ability to repair and process, such as in 3D printing. TPE groups have not typically been explored to construct dynamic networks so far (only one group attempted to introduce them into a polymer based on poly(tetramethylene oxide)).[24]

The reversibility of TPE groups is related to the low energy of the $(Ph)_2C—C(Ph)_2$ bond (~200 kJ·mol^{-1}[25]) allowing easy thermal reversible dissociation to radicals. As proven in earlier work on PLA/Poly (vinyl monomer) copolymers,[26] this dissociation is more advanced at higher temperatures, and above 80°C the efficiency of the radicals formation stabilizes. The radicals placed on PLA macromolecules were reactive in further reactions. As we demonstrated in our previous work, networks containing TPE groups showed a dynamic nature,[22] similarly to networks with disulfide reversible groups, probably following a similar exchange mechanism.[22,23]

In this contribution, we describe the preparation of PLA-based networks by applying a novel approach, with the UV-promoted reaction as the main step, leading to networks containing reversible TPE groups in the network crosslinks. This is in contrast to previous networks where reversible groups were placed into linear fragments.[22,23] These different network structures are related to different methods of their synthesis and different starting components. Although both types of networks were prepared by coupling PLA star polymers using diisocyanate, in the previous method,[23] reversible TPE groups had to be introduced in the form of an additional low molecular weight diol, while in the present study, star PLA contained this group in the core, and such stars were linked to each other. PLA stars with the dynamic cores were, in turn, prepared by the original method relying on UV-promoted coupling of linear polymer chains containing benzophenone moieties in the middle.

Another network structure could result in different mechanical and rheological properties.

2 | EXPERIMENTAL PART

2.1 | Materials

L,L-Lactide from Corbion was recrystallized from 2-propanol, 4,4′-dihydroxybenzophenone (diHBP, 98%), hexamethylene diisocyanate (HDI, 99%, Sigma-Aldrich, St. Luis, MO, USA/Steinheim, Germany), trifluoromethanesulfonic acid (triflic acid, 99%, Sigma-Aldrich), dibutyltin dilaurate (DBTDL, 98%, ABCR) were used as received. Dichloroethane (DCE, pure p.a. from POCH, Gliwice, Poland) was dried over CaH_2, distilled before use, and stored over molecular sieves (4 Å). A 2-propanol (pure p.a.), hexane (99%), diethyl ether (99.5%), all from POCH, were used as received. Potassium hydroxide (pure p.a.) was obtained from POCH and used as received.

2.2 | Synthesis of di(hydroxyethyl)benzophenone

A 6.72 g (120 mmol) of potassium hydroxide was dissolved in 8 mL of distilled water in a beaker. The prepared solution was added to 10 g (467 mmol) of 4,4-dihydroxybenzophenone in a round bottom flask. The resulting yellow reaction mixture was stirred at 70°C until the diHBP dissolved. Next, 16 mL (226 mmol) of 2-bromoethanol was added with a syringe, and the stirring was continued for 24 h. The formed white precipitate was recrystallized by dissolving it in 700 mL of ethanol. White crystals of di(hydroxyethyl)benzophenone (diHEBP) were dried under vacuum and obtained with a yield of 80%.

2.3 | Synthesis of linear BP-PLA

Ring opening polymerization of L,L-LA was performed in bulk. A 4 g (27 mmol) of L,L-LA and 1.2 g (3.97 mmol) of diHEBP (amounts given for BP-PLA3, $M_n = 1400$) were evacuated for 1 h in a Schlenk flask equipped with a stirring bar and backfilled with N_2. The flask was immersed in an oil bath preheated to 110°C, after the monomer melted and the initiator dissolved, $Sn(Oct)_2$ (50 μL, 0.15 mmol) as a catalyst was added to the mixture. Polymerization was performed at 110°C for 24 h. After that time the reaction mixture was cooled down to room temperature, diluted with DCM, and precipitated to hexane (the polymeric product was obtained with a yield of 75%).

2.4 | Synthesis of star TPE-PLA

A 3.6 g of BP-PLA was placed into a quartz flask, to which 7.2 mL of dioxane and 15 mL of isopropanol were added. The flask was closed with a rubber septum and purged with nitrogen (with a needle) for 15 min. The mixture was stirred until the content dissolved. The homogenous solution was exposed to ultraviolet light (365 nm) while stirred for 24 h. Next, the solvents were evaporated, and the resulting coupled polymer was dried under vacuum.

2.5 | Synthesis of PLA network

A 0.6 g of star TPE-PLA was evacuated in a Schlenk flask equipped with a stirring bar, and next, it was backfilled with N_2. A 2 mL of DCE was added through the septum and after the polymer dissolution, HDI in the amount of 1.1:1 ratio of —NCO/—OH groups (70 μL in the case of using TPE-PLA3) and DBTDL (10 μL, 0.017 mmol) as a catalyst were introduced. The reaction mixture was stirred for 5 min at 40°C in an oil bath and subsequently transferred to a 6 cm diameter Petri dish. The dish was placed in a desiccator, which was filled with N_2 and heated to 40°C for 48 h. The resulting polymer network was dried in a vacuum oven overnight and annealed at 100°C for 1 h. The network's films were stored in a moisture-protected box.

2.6 | Determination of gel content

About 7 mg of the network film was refluxed in dichloromethane in a Soxhlet apparatus for 4 h and dried in a vacuum oven at 50°C for 24 h. The gel content was determined gravimetrically and calculated as the ratio of the sample weight after extraction to its initial weight.

2.7 | Tensile properties

Tensile tests were carried out using a Linkam TST 350 mini tensile tester with a measuring range of force up to 200 N. The dog-bone shape samples with a measuring length of 12.5 mm, a width of 4.8–4.9 mm and a thickness of 0.15–0.19 mm were cut from network films. The tests were carried out at room temperature. The deformation rate was 1.2 mm/min. Average values were calculated from measurements performed on three specimens.

2.8 | Rheological properties

Stress relaxation was studied with rheometer ARES G2 (TA Instruments, New Castel, DE, USA) equipped with steel parallel-plate geometry (diameter of 25 mm). All samples for testing were cut into discs with a diameter of 25 mm from films with a thickness of ~0.20 mm. The sample placed between two plates was first equilibrated at the chosen temperature for 20 min, at a normal force of 2 N, and then a 2% strain was applied. The development of the relaxation modulus over time during 60 min was recorded at temperatures 120, 130, 140, and 150°C. Measurement parameters were chosen on the basis of our previous experience with the analysis of relaxation times of similar PLA-based networks with reversible disulfide bonds that were preceded by frequency and strain sweep experiments.[22] To compare the degree of relaxation for various TPE-PLA networks the relaxation curves were normalized with respect to the initial stress.

2.9 | Instrumental methods

The ^{1}H NMR spectra of the synthesized polymers were recorded in a $CDCl_3$ solvent using a Bruker Avance 400 Neo instrument (Bruker, Billerica, MA, USA) operating at 400 MHz.

Size exclusion chromatography (SEC) was performed using an Agilent Pump 1100 Series with an Agilent G1379A Degasser, equipped with a set of two PLGel 5 μm MIXED-C columns. A Dawn Eos (Wyatt Technology Corporation) laser photometer (MALLS–multi-angle light scattering) and a Wyatt Optilab Rex differential refractometer (RI) were used as detectors. Dichloromethane was used as an eluent at a flow rate of 0.8 mL/min at 25°C.

Differential scanning calorimetry (DSC) analyses were performed using a DSC 2500 Discovery, TA Instruments, under a nitrogen atmosphere at temperatures ranging from 0 to 200°C for (co)polymers at a heating and cooling rate of 10°C min^{-1}. Both the temperature and heat flow were calibrated with indium.

Fourier transform infrared spectroscopy (FTIR) measurements were performed on a Thermo Scientific Nicolet 6700 instrument with an attenuated total reflectance (ATR) GoldenGate accessory (Waltham, MA, USA) and deuterated triglycine sulfate (DTGS) or mercury–cadmium–telluride (MCT) detectors. The spectra were obtained by adding 64 scans at a 2 cm^{-1} resolution.

UV coupling was performed in a photochemical reactor (RayonetRPR-200, Southern New England, Brandford, CT, USA) equipped with 16 UV lamps ($\lambda = 365$ nm) and a magnetic stirrer.

3 | RESULTS AND DISCUSSION

3.1 | Synthesis of star PLA-based polymers with TPE reversible groups in the core

A 4-arm star polylactides containing tetraphenylethane groups in the core were prepared in two steps. In the first step, linear PLAs were synthesized by the initiation of coordination-insertion L,L-lactide polymerization[27–29] using dihydroxysubstituted benzophenone (diHEBP) containing primary hydroxyl groups, which was previously obtained from the commercial 4,4′-dihydroxybenozophenone through its appropriate functionalization. The preparation procedure is described in Section 2, and the analysis of the functionalized product is presented in the Supporting Information (Figure S1). As a result of lactide polymerization initiated by diHEBP, PLAs containing benzophenone moiety in the middle of the chains were obtained. Next, these linear PLA macromolecules were transformed into 4-arm stars by coupling two chains together due to the formation of covalent bonds between benzophenone groups under UV irradiation, which is a known reaction of tetraphenylethane (benzopinacol) formation.[30] Figure 1 presents the reaction scheme.

According to the above procedure, two PLA-based star polymers with different molecular weights containing TPE groups in the cores were prepared and characterized (see Table 1). Additionally, the star polymer without TPE groups, with a core originating from di(trimethylolpropane), was synthesized for the preparation of the reference network.

The structures of the resultant PLA-based polymers were confirmed by ^{1}H NMR and FTIR spectra (Figure 2 and Figures S2, S3, S5). In the ^{1}H NMR spectrum of linear PLA (BP-PLA), signals corresponding to PLA units as well as phenyl and —CH_2— groups in the diHEBP initiator are visible in amounts corresponding to all macromolecules with BP units indicating quantitative initiation. A similar observation was made for the star TPE-PLA polymers obtained after the coupling reaction, with the difference that the signals corresponding to phenyl groups in TPE units are shifted to a new position, with small signals appearing additionally, likely corresponding to half of the macromolecule formed with BP unit at the end[32] (partially, not reacted BP-PLA).

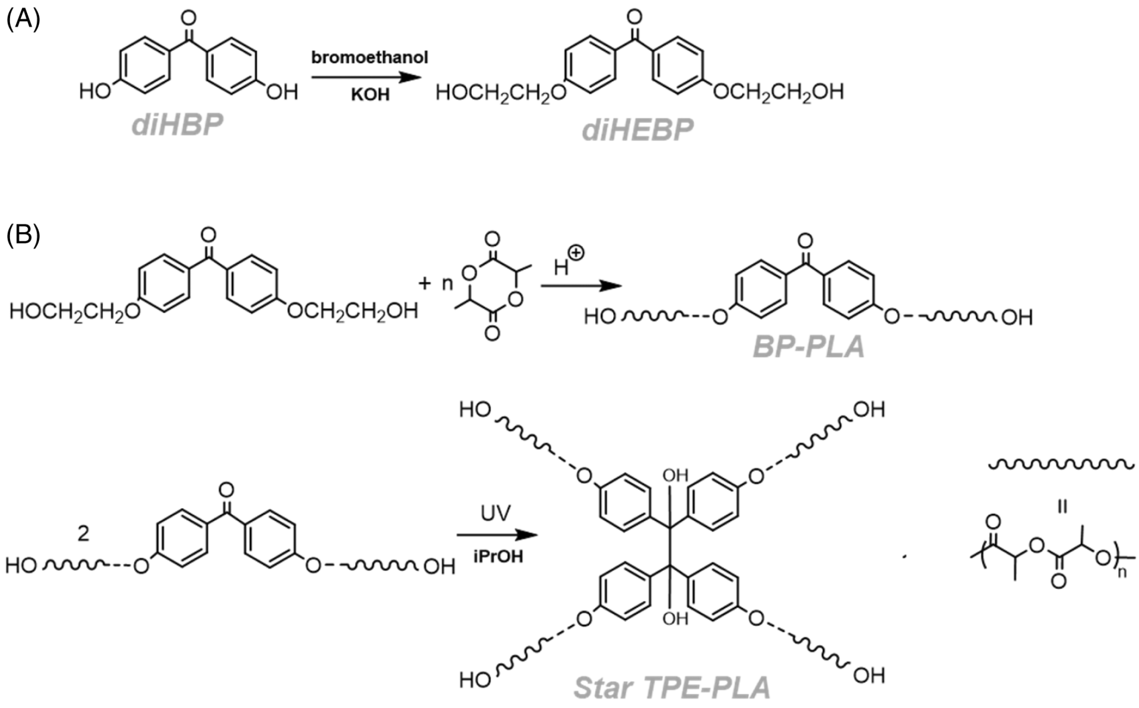

FIGURE 1 Reaction scheme for the synthesis of dihydroxybenzophenone containing primary —OH groups (A) and the synthesis of star TPE-PLA with TPE group in the core (B).

TABLE 1 Star polymers prepared for networks syntheses together with initial linear polymers (before coupling to stars).

	Linear BP-PLA		Star TPE-PLA	
Polymer acronym	M_n, ^{1}H NMR	M_n, SEC[a]	M_n, ^{1}H NMR	M_n, SEC[a]
TPE-PLA3	1600	3800	3200	6200
TPE-PLA6	3400	8000	6400	12,000
PLAref 2.5	-	-	2500	6000

[a] M_n values (SEC) were determined with polystyrene standards. For the calculation of trustworthy M_n, different coefficients are often used.[31]

3.2 | Synthesis of PLA-based networks by coupling PLA stars using diisocyanate

PLA-based networks were prepared by coupling PLA stars containing TPE groups in the core using aliphatic diisocyanate in the amount 1.1:1 in respect to PLA terminal (primary) —OH groups (—OH groups linked with the formed TPE groups are not reactive with diisocyanate at applied conditions[33]). The reaction was performed in DCE solution, which after dissolving all components was poured into a Petri dish to obtain a network film suitable for further analysis. The successful formation of networks was confirmed by FTIR analysis (Figure S5), and their appearance is presented in Figure S4. In FTIR spectra of all networks, signals corresponding to the formed urethane linkages can be observed along with signals characteristic of the initial star polymers. Networks were further investigated by means of gel content, DSC, and TGA analyses (Figures S6 and S7). The results are shown in Table 2.

As evident from the data in Table 2, networks with gel content close to 100% were obtained. Their glass transition temperatures do not differ much (up to 2°C) and are only slightly higher than those of the starting star polymers ($T_g = 40.8$°C for TPE-PLA3 and 44.2°C for TPE-PLA6). As evident from TGA curves, the main decomposition of networks starts from 200°C, but very slight decomposition up to ~4 wt.% can be observed between 100 and 200°C.

3.3 | Mechanical properties of PLA-based networks

All prepared networks were subjected to tensile tests to assess the difference in their mechanical performance. The results are shown in Figure 3.

Different behavior of networks in tensile tests is observed. The more densely crosslinked network, prepared from TPE-PLA3 shows greater tensile strength than that prepared from TPE-PLA6, which in turn, exhibits much greater elongation at break (24% versus ~11%). The reference network with a crosslinking density slightly higher than that of prepared from TPE-PLA3 shows even higher tensile strength.

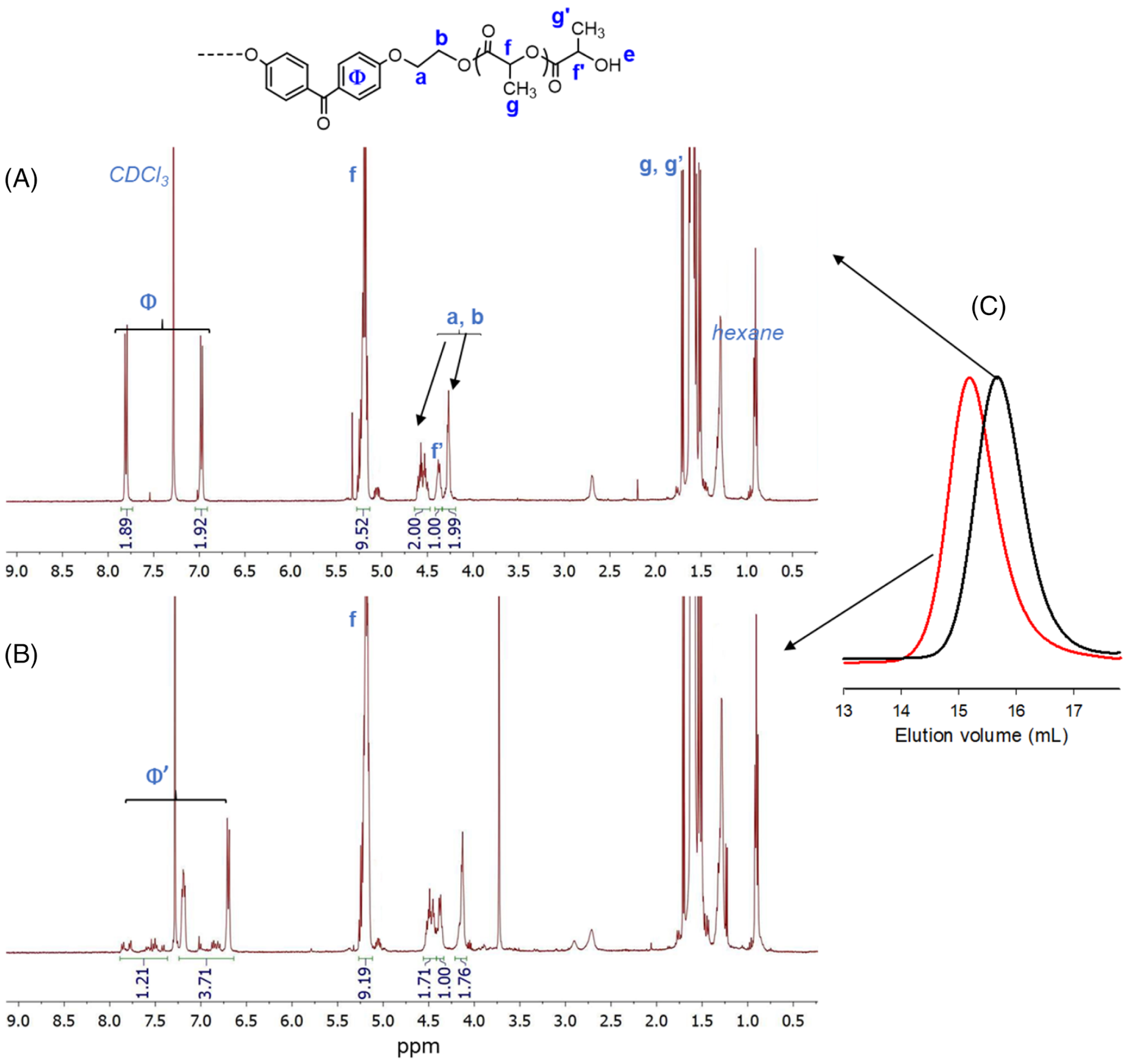

FIGURE 2 ^{1}H NMR spectra of BP-PLA (A) and TPE-PLA (B) polymers (TPE-PLA3) and SEC curves (C).

TABLE 2 Thermal properties of PLA-based networks.

Network from star PLA	Gel content %	T_g, DSC (°C)	$T_{\text{max d}}$[a], TGA (°C)
TPE-PLA3	99	49.9	238.5
TPE-PLA6	99	48.2	246.0
PLAref 2.5	99	50.3	224.7

[a] $T_{\text{max d}}$, = Temperature of the maximum decomposition (from derivative curves shown in Figure S7b).

3.4 | Rheological properties of PLA-based networks with reversible TPE groups in their crosslinks

To detect the dynamic character of PLA-based networks with thermally labile crosslinks constituted of TPE groups, the relaxation measurements were performed at different temperatures. Although the decomposition of the TPE group into radicals begins at lower temperatures, the measurement was deliberately carried out at higher temperatures to also enable the breaking of hydrogen bonds between urethane groups.[22] The results are shown in Figure 4.

As evident from the plots presented in Figure 4, networks relax their stress in a very short time, which can be ascribed to very fast reversible dissociation of TPE groups to radicals. Fast relaxation was also observed for other dynamic groups such as, for example, siloxane or disulfide groups.[34–36] Different relaxation behaviors of networks with TPE groups can be noticed depending on crosslinking density and the length of PLA chains. The temperature has a noticeable effect on the relaxation time of loosely crosslinked polymer TPE-PLA6 but a smaller effect on densely crosslinked polymer TPE-PLA3. The network prepared from TPE-PLA6 has sufficiently long PLA chains between crosslinks the movements, of which enable total relaxation within 1–

1000 s depending on temperature. We compared τ^* values, that is, times, at which 63% of the initial stress is relaxed, usually determined to characterize viscoelastic properties of different dynamic networks such as vitrimers[37] but also networks relaxing according to dissociative mechanism.[38,39] For our networks, τ^* values (determined at relatively high temperatures and chosen measurement conditions) were much below 1 s. This very fast relaxation is due mainly to fast radical exchange reactions between TPE groups placed in crosslinks of networks. With the temperature increase, the balance between the forms of the TPE group dissociated into radicals and the recombinant ones are probably shifted toward the dissociated forms, which would support a partially dissociative mechanism of exchange between TPE groups.

In the more dense network, prepared from TPE-PLA3, the relaxation isn't complete within 1000 s of the measurement and after fast relaxation in the initial stage (attributed to the radical exchange), it stops, probably, due to limited chain mobility.[40] Additionally, in the more densely crosslinked network, there are more urethane linkages. It is known that polyurethanes are able to relax their stress due to reversible urethane formation, but in a much longer time and at higher temperatures.[40] Therefore, in Figure 4B we can notice a further slow decrease of the normalized relaxation modulus at the end of the measurement duration.

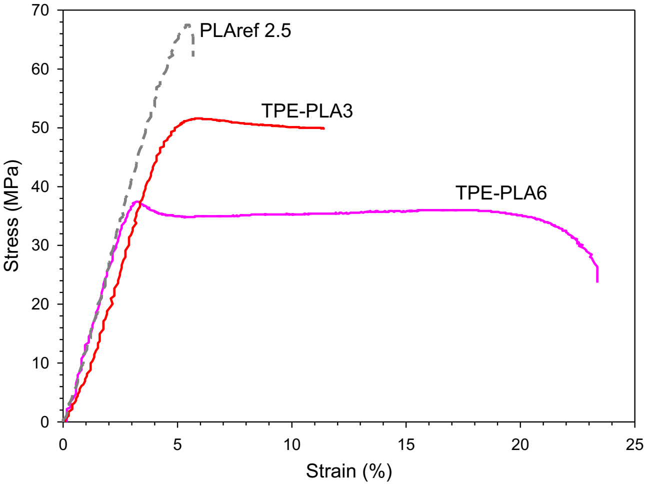

FIGURE 3 Stress–strain curves for networks prepared from TPE-PLA3 and TPE-PLA6 and for reference network PLAref 2.5 prepared without TPE groups.

Next, we compared the relaxation of the above-discussed networks containing reversible TPE groups with the relaxation of the reference network without TPE units, prepared from the star PLA by coupling with diisocyanate, with $M_n \sim 2500$ g/mol, which is comparable to TPE-PLA3. Contrary to networks with TPE groups, the fast initial relaxation (within seconds) was not observed, only slow relaxation starting before 1000 s assigned to reversible urethane linkages formation (Figure S8). In the case of the reference network, the relaxation doesn't reach 63% within the measurement time.

The measurements of the stress relaxations at different temperatures allowed us to calculate the average activation energy E_a for TPE-PLA6 and TPE-PLA3 according to the Arrhenius equation,[37] as shown in SI (Figure S9). A small deviation from the linearity of Arrhenius dependence may indicate a change in the overall relaxation mechanism, that is, a change in the relative contributions of various mechanisms, predominantly related to the exchange between TPE groups (such as the mechanism analogous to metathesis of disulfide groups,[41] the dissociative and associative mechanisms) but also the reverse reaction of the urethane group formation. The average E_a values for TPE-PLA6 and TPE-PLA3 were equal to 100 and 83 kJ/mol, respectively.

The ability of PLA-based networks containing TPE groups to rearrange their structure under heating was additionally confirmed by the repair experiment performed with both networks. The rectangular sample was cut into two parts from the network film, next, the parts were joined together with overlapping ends and heated at 150°C for 40 min or 1 h under relatively low weight pressure (~70 kPa). After

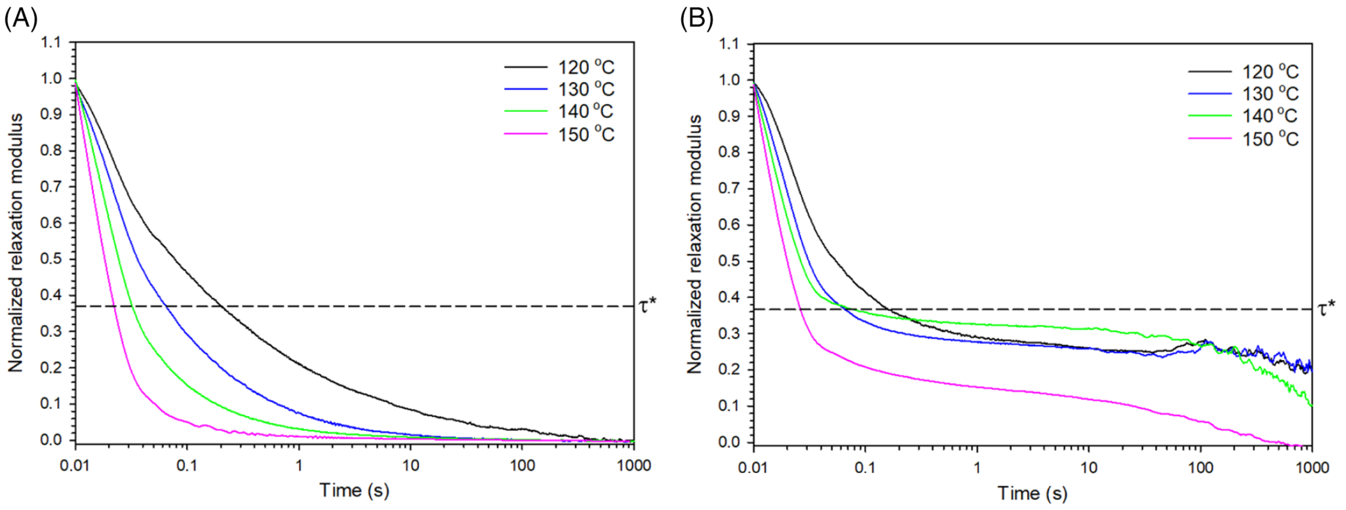

FIGURE 4 Normalized stress relaxation of TPE-PLA6 (A) and TPE-PLA3 (B) at different temperatures.

this treatment, the two parts were joined together forming a film with uniform thickness as shown in Figure S10. Tensile test performed with the repaired network from TPE-PLA6 star, that is, the network with longer PLA chains enabling better sequential movements upon heating (see Figure S11), showed satisfying mechanical strength, that is, after the repairing procedure, the network was characterized by the even higher tensile strength (with noticeably lower elongation at break), which is often observed for different types of reversible polymer networks.[24,42,43]

4 | CONCLUSIONS

An original approach involving the introduction of a benzophenone moiety in the middle of polylactide chains enabled the synthesis of PLA star polymers with $M_n = 3200$ and 6400 g/mol with thermally reversible tetraphenylethane groups in the core. The coupling of these star polymers using diisocyanate efficiently led to the formation of polymer networks (~99% gel content) containing reversible groups in the crosslinks. Different crosslinking densities resulted in varying mechanical properties of the prepared polymer networks, with tensile strength between 35 and 50 MPa and elongation at break in the range of 11.5%–23.5%. Rheological studies allowed us to demonstrate the dynamic nature of the produced PLA-based networks. Specifically, an investigation of networks stress relaxation performed at different temperatures (between 120 and 150°C) showed that both networks relax their initial stress very fast, (within seconds). For the less densely crosslinked network (with longer chains allowing more free movements), total stress relaxation is achieved within 8 min at 120°C and over 1 s at 150°C. In the densely crosslinked network, further stress relaxation occurs only after a longer time, suggesting the participation of urethane exchange in the total relaxation process. Finally, it was shown that prepared PLA-based networks containing thermally reversible TPE groups in crosslinks were capable of processing.

ACKNOWLEDGMENTS

This work was supported by the National Science Centre in Poland under Grant no 2018/31/B/ST8/01969. The purchase of the Avance Neo 400 NMR spectrometer, used to obtain results included in this publication, was supported by the funding from the EU Regional Operational Program of the Lodz Region, RPLD.01.01.00-10-0008/18. Mateusz Grabowski acknowledges Bio-Med-Chem Doctoral School of the University of Lodz and Lodz Institutes of the Polish Academy of Sciences.

CONFLICT OF INTEREST STATEMENT

The authors declare no conflict of interest.

DATA AVAILABILITY STATEMENT

The data that support the findings of this study are available from the corresponding author upon reasonable request.

ORCID

Melania Bednarek https://orcid.org/0000-0003-1445-9878
Magdalena Lipińska https://orcid.org/0000-0002-6581-5126

REFERENCES

1. Auras R, Lim L-T, Selke S, Tsuji H. In: Auras R, Lim L-T, Selke S, Tsuji H, eds. *Poly(Lactic Acid): Synthesis, Structures, Properties, Processing, and Applications*. John Wiley & Sons; 2010.
2. Sin LT, Rahmat AR, Rahman WA. Overview of poly(lactic acid). In: Sin LT, Rahmat AR, Rahman WA, eds. *Polylactic Acid PLA Biopolymer Technology and Application*. First ed. Elsevier; 2012.
3. Slomkowski S, Penczek S, Duda A. Polylactides-an overview. *Polym Adv Technol*. 2014;25(5):436-447. doi:10.1002/pat.3281
4. ChemAnalyst. Decode the Future of Polylactic Acid. https://www.chemanalyst.com/industry-report/polylactic-acid-pla-market-673
5. Balla E, Daniilidis V, Karlioti G, et al. Poly(lactic acid): a versatile biobased polymer for the future with multifunctional properties–from monomer synthesis, polymerization techniques and molecular weight increase to PLA applications. *Polymers (Basel)*. 2021;13:1822. doi:10.3390/polym13111822
6. Jimenez A, Peltzer M, Ruseckaite R. Poly(lactic acid) science and technology. *Processing, Properties, Additives and Applications*. RSC; 2015.
7. Nagarajan V, Mohanty AK, Misra M. Perspective on polylactic acid (PLA) based sustainable materials for durable applications: focus on toughness and heat resistance. *ACS Sustain Chem Eng*. 2016;4:2899-2916. doi:10.1021/acssuschemeng.6b00321
8. Rasal RM, Janorkar AV, Hirt DE. Poly(lactic acid) modifications. *Prog Polym Sci*. 2010;35(3):338-356. doi:10.1016/j.progpolymsci.2009.12.003
9. Bowman CN, Kloxin CJ. Covalent adaptable networks: reversible bond structures incorporated in polymer networks. *Angew Chemie–Int Ed*. 2012;51(18):4272-4274. doi:10.1002/anie.201200708
10. Denissen W, Winne JM, Du Prez FE. Vitrimers: permanent organic networks with glass-like fluidity. *Chem Sci*. 2016;7(1):30-38. doi:10.1039/c5sc02223a
11. Ma S, Webster DC. Degradable thermosets based on labile bonds or linkages: a review. *Prog Polym Sci*. 2018;76:65-110. doi:10.1016/j.progpolymsci.2017.07.008
12. Fortman DJ, Brutman JP, De Hoe GX, Snyder RL, Dichtel WR, Hillmyer MA. Approaches to sustainable and continually recyclable cross-linked polymers. *ACS Sustain Chem Eng*. 2018;6(9):11145-11159. doi:10.1021/acssuschemeng.8b02355
13. Zheng N, Xu Y, Zhao Q, Xie T. Dynamic covalent polymer networks: a molecular platform for designing functions beyond chemical recycling and self-healing. *Chem Rev*. 2021;121(3):1716-1745. doi:10.1021/acs.chemrev.0c00938
14. Jin Y, Lei Z, Taynton P, Huang S, Zhang W. Malleable and recyclable thermosets: the next generation of plastics. *Matter*. 2019;1(6):1456-1493. doi:10.1016/j.matt.2019.09.004
15. Inoue Kazuhiko YM, Masatoshi I. Recyclable shape-memory polymer: poly(lactic acid) crosslinked by a thermoreversible Diels–Alder reaction. *J Appl Polym Sci*. 2009;12:876-885.
16. Djidi D, Mignard N, Taha M. Thermosensitive polylactic-acid-based networks. *Ind Crops Prod*. 2015;72:220-230. doi:10.1016/j.indcrop.2014.09.035
17. Nagata M, Sato Y. Synthesis and properties of photocurable biodegradable multiblock copolymers based on poly(ε-Caprolactone) and poly(L-Lactide) segments. *J. Polym. Sci. Part A Polym Chem*. 2005;43(11):2426-2439. doi:10.1002/pola.20718
18. Wu L, Jin C, Sun X. Synthesis, properties, and light-induced shape memory effect of multiblock polyesterurethanes containing biodegradable segments and pendant cinnamamide groups. *Biomacromolecules*. 2011;12(1):235-241. doi:10.1021/bm1012162

19. Brutman JP, Delgado PA, Hillmyer MA. Polylactide vitrimers. *ACS Macro Lett*. 2014;3(7):607-610. doi:10.1021/mz500269w
20. Ussama W, Shibata M. Self-healing disulfide-containing polyester-urethane networks composed of 6-armed star-shaped oligolactide and oligocaprolactone segments. *J Polym Res*. 2021;28(1):5. doi:10.1007/s10965-020-02360-6
21. Bednarek M, Kubisa P. Reversible networks of degradable polyesters containing weak covalent bonds. *Polym Chem*. 2019;10(15):1848-1872. doi:10.1039/c8py01731j
22. Borska K, Bednarek M, Pawlak A. Reprocessable polylactide-based networks containing urethane and disulfide linkages. *Eur Polym J*. 2021;156:110636. doi:10.1016/j.eurpolymj.2021.110636
23. Borska K, Bednarek M, Gorgol D, Osicka J, Mrlik M. Polylactide-based networks containing dynamic tetraphenylethane groups for 3D printed repairable and reprocessable constructs. *React Funct Polym*. 2023;191(August):105694. doi:10.1016/j.reactfunctpolym.2023.105694
24. Zhang ZP, Rong MZ, Zhang MQ. Mechanically robust, self-healable, and highly stretchable "living" crosslinked polyurethane based on a reversible C-C bond. *Adv Funct Mater*. 2018;28(11):1706050. doi:10.1002/adfm.201706050
25. Yao XQ, Hou XJ, Wu GS, et al. Estimation of C-C bond dissociation enthalpies of large aromatic hydrocarbon compounds using DFT methods. *J Phys Chem A*. 2002;106(31):7184-7189. doi:10.1021/jp020607x
26. Grabowski M, Kost B, Bodzioch A, Bednarek M. Functionalization of Polylactide with multiple tetraphenyethane Inifer groups to form PLA block copolymers with vinyl monomers. *Int J Mol Sci*. 2023;24(1):19. doi:10.3390/ijms24010019
27. Penczek S, Duda A, Kowalski A, Liniszowski J, Majerska K, Biela T. On the mechanism of polymerization of cyclic esters induced by tin(II) Octoate. *Macromol Symp*. 2000;157:61-70.
28. Kowalski A, Duda A, Penczek S. Kinetics and mechanism of cyclic esters polymerization initiated with tin(II) Octoate. 3. polymerization of L,L-Dilactide. *Macromolecules*. 2000;33(20):7359-7370. doi:10.1021/ma000125o
29. Kowalski A, Libiszowski J, Majerska K, Duda A, Penczek S. Kinetics and mechanism of ε-Caprolactone and l,l-Lactide polymerization coinitiated with zinc octoate or aluminum acetylacetonate: the next proofs for the general alkoxide mechanism and synthetic applications. *Polymer (Guildf)*. 2007;48(14):3952-3960. doi:10.1016/j.polymer.2007.05.007
30. Furniss B, Hannaford A, Smith P, Tatchell A. *Vogel's Textbook of Practical Organic Chemistry*. Longman Scientific & Technical; 1989.
31. Kost B, Socka M, Cichon K, Brzezinski M, Basko M, Biela T. Molar mass determination via linear regression from SEC measurements: the case of polylactide, polycaprolactone and poly(2,-2-Dimethylthrimethylene carbonate). *Polym Adv Technol*. 2024;45(1):e6296.
32. Grabowski M, Kost B, Kubisa P, Bednarek M. A new approach to the synthesis of polylactide/polyacrylonitrile block copolymers. *Polymers (Basel)*. 2022;14:1529. doi:10.3390/polym14081529
33. Bednarek M, Grabowski M. Can tetraphenylethane (TPE) "Iniferter" groups be introduced into polymer chains by coupling TPE diol with diisocyanates? *Polymer (Guildf)*. 2021;2022(246):124738. doi:10.1016/j.polymer.2022.124738
34. Debsharma T, Amfilochiou V, Wróblewska AA, De Baere I, Van Paepegem W, Du Prez FE. Fast dynamic siloxane exchange mechanism for reshapable vitrimer composites. *J Am Chem Soc*. 2022;144(27):12280-12289. doi:10.1021/jacs.2c03518
35. Xu X, Ma S, Feng H, et al. Dissociate transfer exchange of tandem dynamic bonds endows covalent adaptable networks with fast reprocessability and high performance. *Polym Chem*. 2021;12(36):5217-5228. doi:10.1039/d1py01045j
36. Yuan WQ, Liu GL, Huang C, Li YD, Zeng JB. Highly stretchable, recyclable, and fast room temperature self-healable biobased elastomers using polycondensation. *Macromolecules*. 2020;53(22):9847-9858. doi:10.1021/acs.macromol.0c01665
37. Capelot M, Unterlass MM, Tournilhac F, Leibler L. Catalytic control of the vitrimer glass transition. *ACS Macro Lett*. 2012;1(7):789-792. doi:10.1021/mz300239f
38. Chakma P, Morley CN, Sparks JL, Konkolewicz D. Exploring how vitrimer-like properties can be achieved from dissociative exchange in anilinium salts. *Macromolecules*. 2020;53(4):1233-1244. doi:10.1021/acs.macromol.0c00120
39. Zhu S, Wang Y, Qin J, et al. Hemiaminal dynamic covalent networks with rapid stress relaxation, reprocessability and degradability endowed by the synergy of disulfide and hemiaminal bonds. *RSC Adv*. 2023;13(41):28658-28665. doi:10.1039/d3ra05413f
40. Brutman JP, Fortman DJ, De Hoe GX, Dichtel WR, Hillmyer MA. Mechanistic study of stress relaxation in urethane-containing polymer networks. *J Phys Chem B*. 2019;123(6):1432-1441. doi:10.1021/acs.jpcb.8b11489
41. Rekondo A, Martin R, Ruiz De Luzuriaga A, Cabañero G, Grande HJ, Odriozola I. Catalyst-free room-temperature self-healing elastomers based on aromatic disulfide metathesis. *Mater Horizons*. 2014;1(2):237-240. doi:10.1039/c3mh00061c
42. Altuna FI, Pettarin V, Williams RJJ. Self-healable polymer networks based on the cross-linking of epoxidised soybean oil by an aqueous citric acid solution. *Green Chem*. 2013;15(12):3360-3366. doi:10.1039/c3gc41384e
43. Denissen W, Rivero G, Nicolaÿ R, Leibler L, Winne JM, Du Prez FE. Vinylogous urethane vitrimers. *Adv Funct Mater*. 2015;25(16):2451-2457. doi:10.1002/adfm.201404553

SUPPORTING INFORMATION

Additional supporting information can be found online in the Supporting Information section at the end of this article.

How to cite this article: Bednarek M, Grabowski M, Lipińska M, Pawlak A. Reversible polymer networks based on polylactide with tetraphenylethane thermally dissociating groups in crosslinks. *Polym Adv Technol*. 2024;35(4):e6390. doi:10.1002/pat.6390

SUPPORTING INFORMATION

Reversible polymer networks based on polylactide with tetraphenylethane thermally dissociating groups in crosslinks

Melania Bednarek1)*, Mateusz Grabowski1), Magdalena Lipińska2), Andrzej Pawlak1)

1) Centre of Molecular and Macromolecular Studies, Polish Academy of Sciences, Sienkiewicza 112, 90-363 Lodz, Poland

2) Institute of Polymer and Dye Technology, Lodz University of Technology, Stefanowskiego 16, 90-537, Lodz, Poland

1. Functionalization of 4,4’-dihydroxybenzophenone

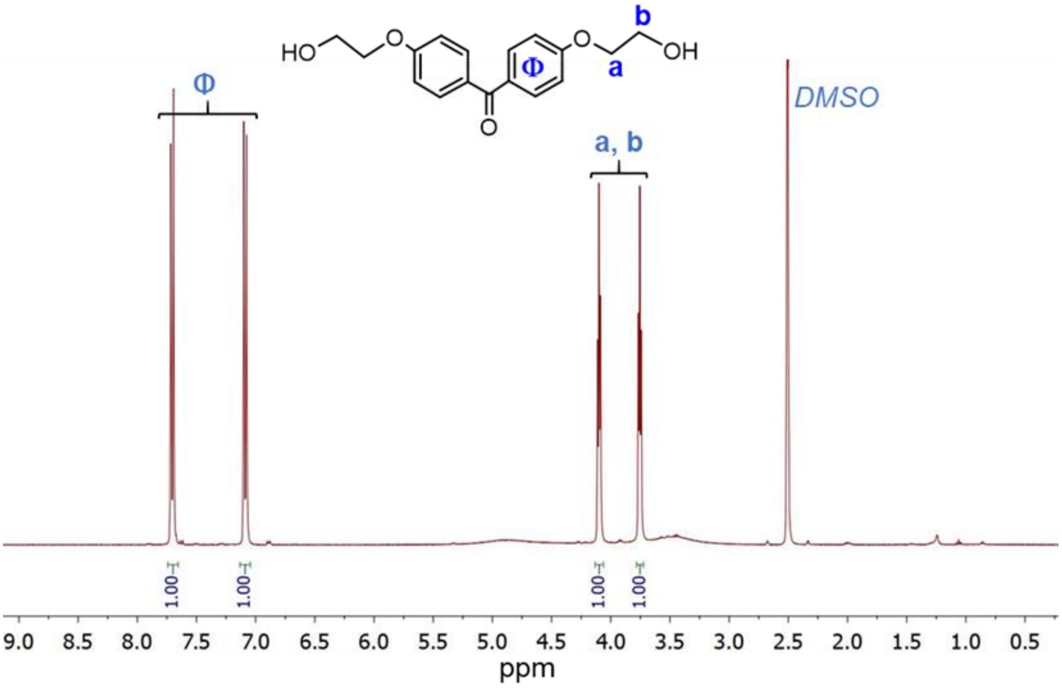

Figure S1. ^{1}H NMR (DMSO) of synthesized diHEBP.

2. Analyses of prepared star polymers

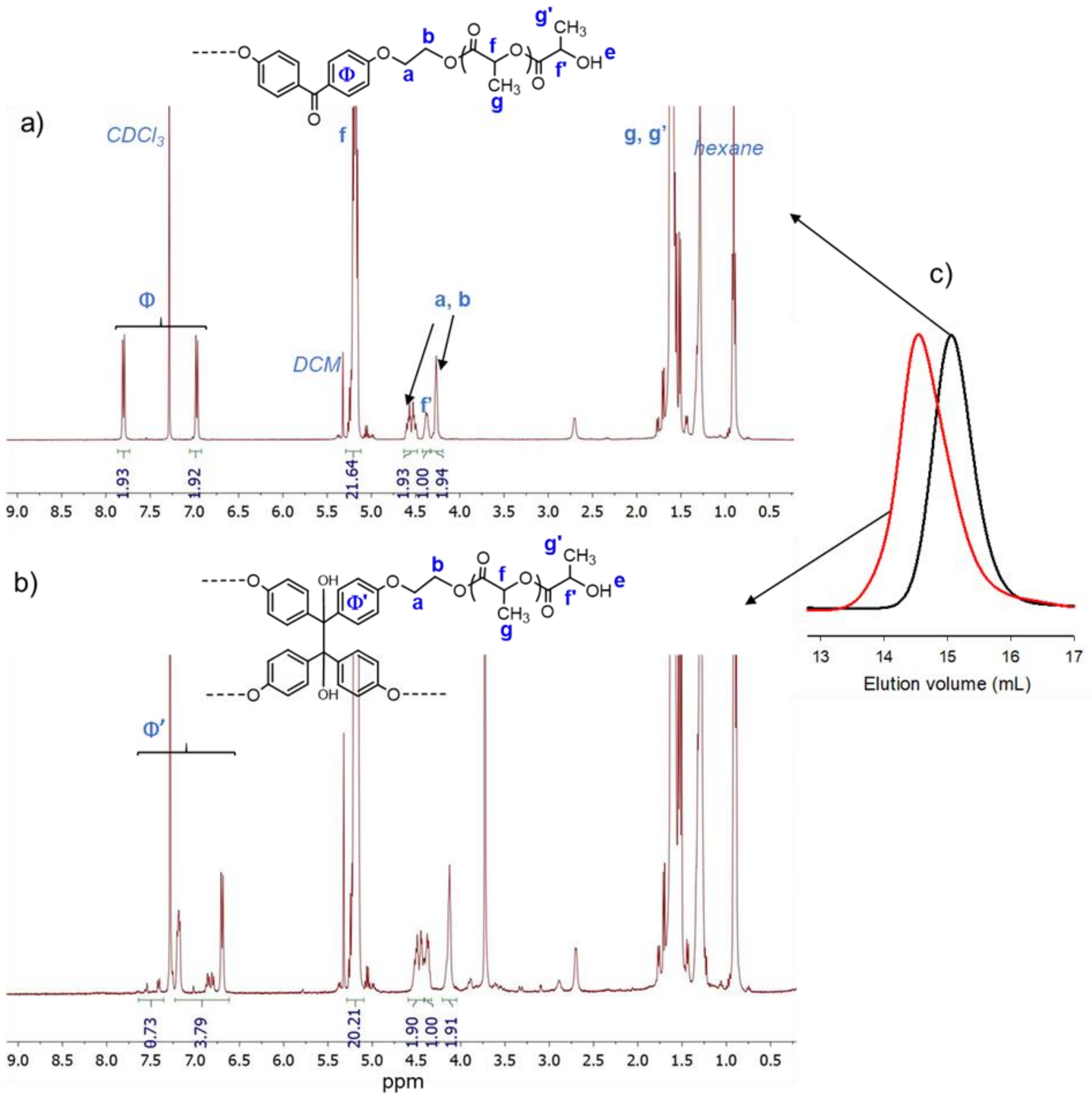

Figure S2. ^{1}H NMR spectra ($CDCl_3$) of BP-PLA6 (a) and TPE-PLA6 (b) polymers and SEC curves (c).

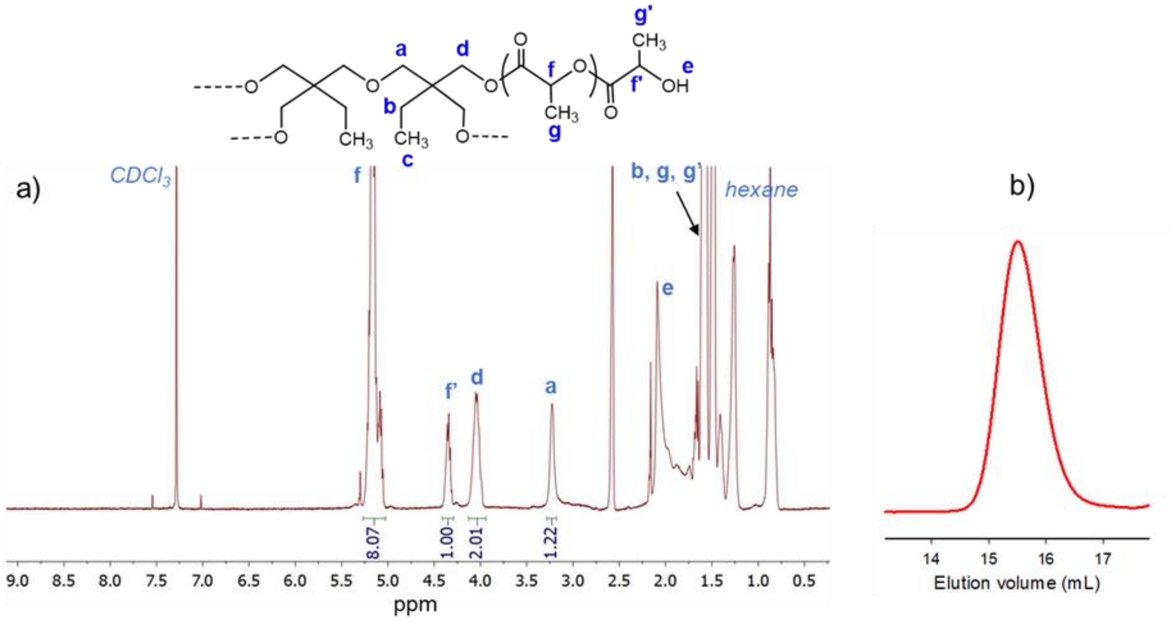

Figure S3. ^{1}H NMR spectrum ($CDCl_3$) of PLA reference star polymer (a) and SEC curve (b).

3. Analyses of prepared PLA-based networks

TPE-PLA3 TPE-PLA6 PLAref

Figure S4. Appearance of PLA network films.

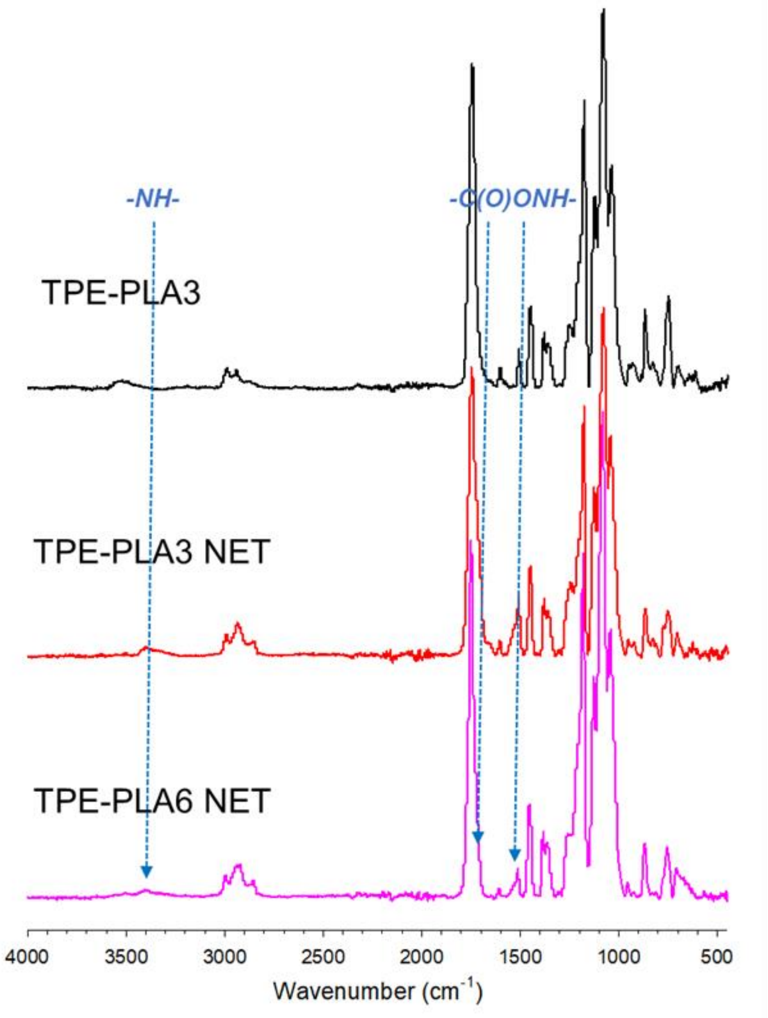

Figure S5. FTIR spectra of starting TPE-PLA star polymer and prepared networks TPE-PLA3 and TPE-PLA6; Blue arrows indicate the presence of the formed urethane groups in the networks.

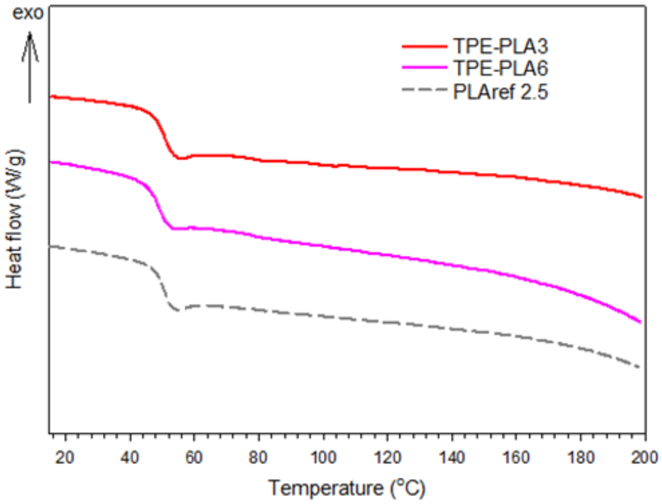

Figure S6. DSC curves for prepared PLA networks.

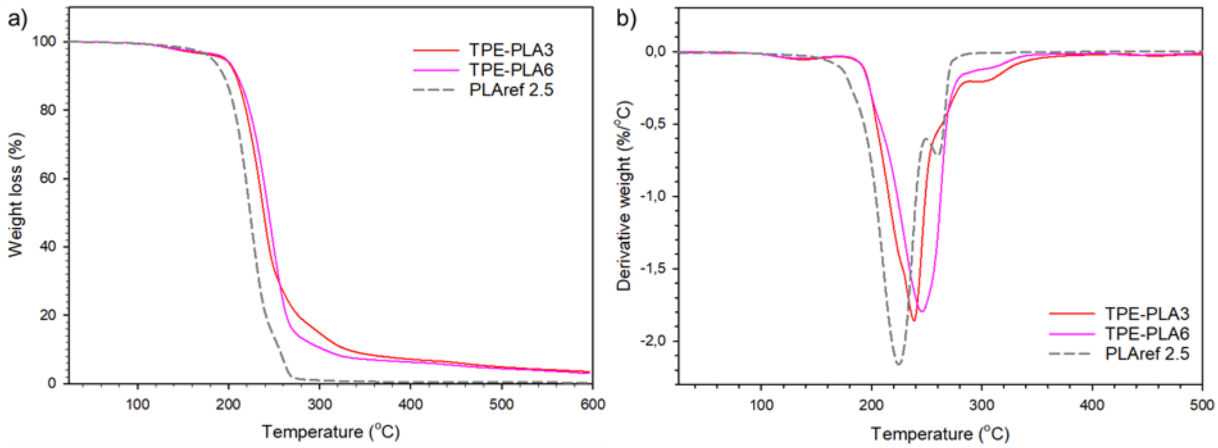

Figure S7. TGA curves (a) and derivative curves (b) for prepared PLA networks.

4. Dynamic character of TPE-PLA networks

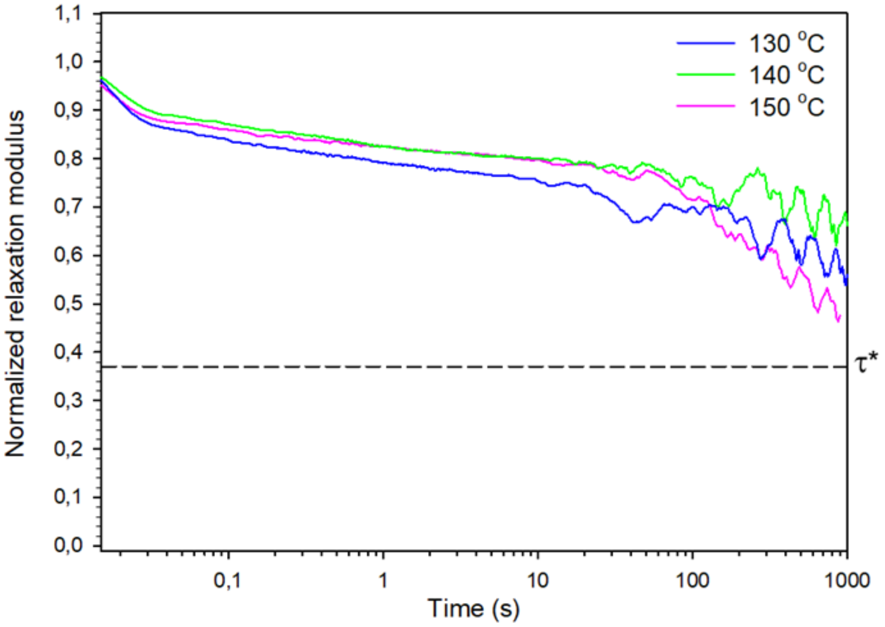

Figure S8. Normalized stress relaxation of PLAref 2.5 at different temperatures.

Calculation of activation energy for the stress relaxation of TPE-PLA networks

Relaxation times τ* follow an Arrhenius law with the temperature $\tau(T) = \tau_0 \exp(Ea/RT)$. The τ* values are determined as the time necessary to relax 63% of the initial stress from the plots of the time dependence of the normalized relaxation modulus.

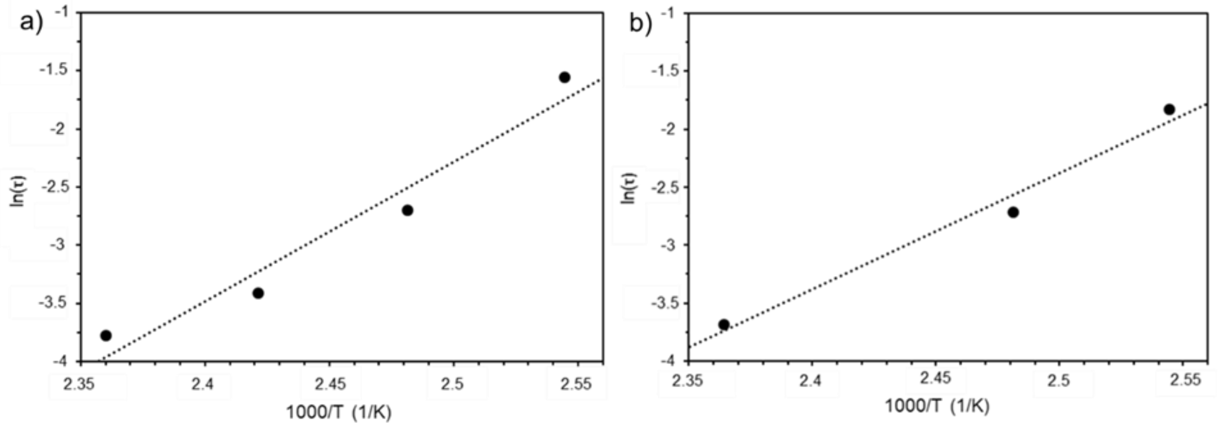

Figure S9. Dependence of lnτ = f(1/T) for networks: TPE-PLA6, (a) and TPE-PLA3 (b); E_a values read from the slope of regression lines are 100 kJ/mol and 83 kJ/mol respectively (R^2 = 0.95 (a), 0.98 (b)).

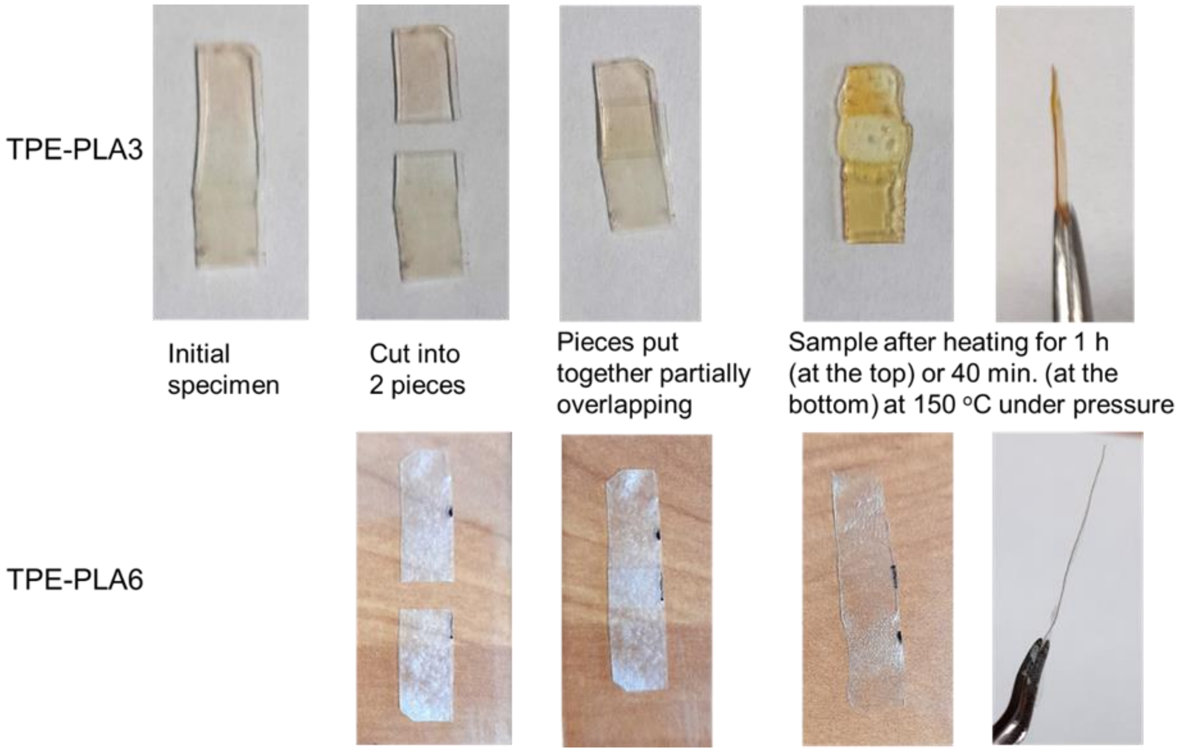

Figure S10. Repairing experiment performed with networks prepared from TPE-PLA3 and TPE-PLA6 star polymers.

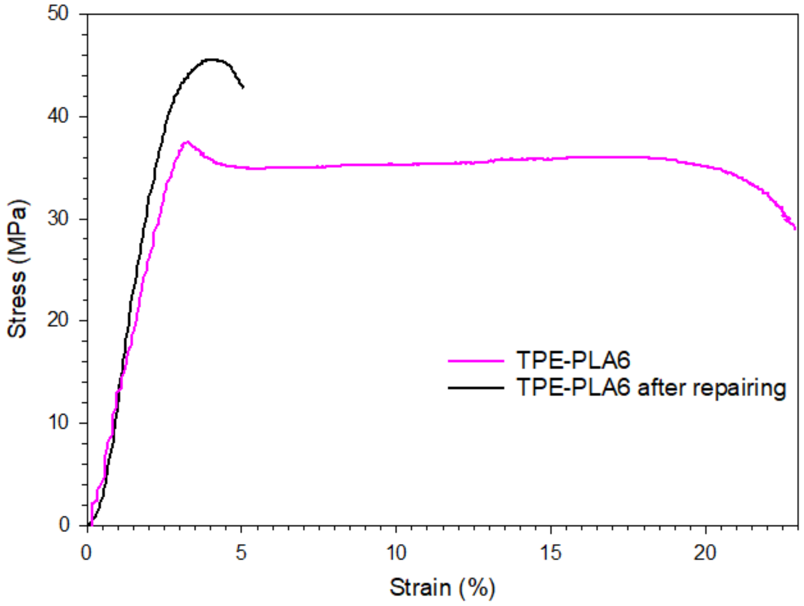

Figure S11. Mechanical strength of the network as-prepared and after repairing.

Publikacja 6:

Melania Bednarek, Mateusz Grabowski. Polylactide/poly(vinyl monomer) block copolymers for specific applications. *Polymer Reviews*. 2024;64(3):898-938.
doi:10.1080/15583724.2024.2310105

POLYMER REVIEWS
https://doi.org/10.1080/15583724.2024.2310105

Taylor & Francis
Taylor & Francis Group

REVIEW ARTICLE

Polylactide/poly(vinyl monomer) block copolymers for specific applications

Melania Bednarek and Mateusz Grabowski

Centre of Molecular and Macromolecular Studies, Polish Academy of Sciences, Lodz, Poland

ABSTRACT
In recent years, there has been continuous growth in the market for polylactide/poly(lactic acid) (PLA) which can be attributed to the increasing preference for environmentally friendly products derived from renewable resources. Apart from its established biomedical applications, polylactide is being considered as a replacement for petroleum-based polymers in various industries, including packaging, electronics, automotive, and textiles. However, PLA modification is necessary to meet the properties of common thermoplastics for target applications. One of the modification methods involves the synthesis of PLA block copolymers, including widely exploited polymers of vinyl monomers (PVM). This review article covers a wide range of applications suggested for PLA/PVM block copolymers as discussed in recent articles. A brief overview of the synthesis methods for PLA/PVM block copolymers is provided. The tendency of block copolymers to self-assemble, leading to specific morphologies, is discussed, and applications that take advantage of this behavior, such as polymeric micelles or porous materials, are highlighted. Examples of using micelles for the delivery of biologically active compounds are presented. Other biomedical applications, such as materials for tissue engineering and medical devices, are also discussed. Finally, the article covers materials for common plastic applications obtained through reactive blending/extrusion, which produces PLA/PVM copolymers *in situ*.

ARTICLE HISTORY
Received 24 July 2023
Accepted 9 January 2024

KEYWORDS
Polylactide; poly(lactic acid); copolymers; vinyl monomers; application

1. Introduction

The mechanical properties of polylactide/poly(lactic acid), degradable and biocompatible polyester received from renewable resources such as corn, sugarcane, and rice, are comparable to widely used petroleum-based polymers like polystyrene or poly(ethylene terephthalate).[1] PLA can be easily processed using standard equipment through methods like thermoforming, injection molding, blow molding, film extrusion, or fiber spinning. Due to its favorable characteristics and environmental concerns, PLA is considered as a potential replacement for petroleum-based plastics in the production of various consumer goods, in addition to its existing applications in packaging, agriculture, and biomedicine.[2–5]

CONTACT Melania Bednarek melania.bednarek@cbmm.lodz.pl Centre of Molecular and Macromolecular Studies, Polish Academy of Sciences, Sienkiewicza 112, Lodz 90-363, Poland.

However, as a thermoplastic, PLA has certain disadvantages, such as stiffness and brittleness at room temperature because of its high T_g value (55–65 °C), poor thermal stability, slow crystallization, and low hydrophilicity, which is a crucial factor in biomedical applications. To address these limitations, various methods for modifying PLA properties, focused on specific applications, have been developed including crosslinking, plasticization, addition of fillers, heterogenous nucleation but also copolymerization, and blending with other polymers. There is a broad literature concerning methods of the synthesis of polylactide, its physical properties and these properties modification[2–4,6,7] thus, this general information will be omitted in the present contribution. To summarize shortly, the main goal of the modifications is to improve thermal and mechanical performance, as well as enhance the hydrophilicity of inherently hydrophobic PLA. Enhanced thermal and mechanical strength are essential *e.g.*, in packaging, preparation of PLA fibers and filaments for 3D printing, and production of different daily use objects.[2,4,5] Hydrophilicity is important in different biomedical applications including implants, stiff or soft (often in the form of hydrogels), and drug delivery systems, also in the form of hydrogels and membranes but predominantly in the form of nano(micro)particles.[8–11] Increased hydrophilicity can be achieved through the preparation of block copolymers, a special type of copolymers. Block amphiphilic copolymers can self-assemble into micelles under appropriate solvent and temperature conditions,[12] offering the possibility of obtaining various nano- and microparticles. However, not only amphiphilic block copolymers exhibit self-organization tendencies. Two (or more) blocks of different nature form separate phases in a solid state and their macromolecules very often self-organize to interesting morphologies[13] which can be highly beneficial.

Considering the aforementioned factors, there is a continued need for the development and improvement of materials based on polylactide, including those composed of block copolymers. On the other hand, advances in reversible deactivation radical polymerization (RDRP) techniques[14] allowed researchers to extend the range of monomers used beyond cyclic monomers which polymers are typically combined with PLA (both blocks synthesized by the same polymerization mechanism). Copolymers of lactide with vinyl monomers (VM) require a combination of distinct chemical processes namely, ring-opening (ROP) and radical polymerization (RP). Numerous researchers have investigated such methods and reported their results, also in review articles.[15,16] However, these sources do not provide information about the areas in which prepared copolymers could be useful. Therefore, we decided to compile information about synthesized copolymers with their suggested or developing/implemented applications. This compilation can assist researchers in improving materials for specific applications and aid those seeking applications for newly synthesized copolymers with interesting properties.

2. Overview of general methods for the synthesis of PLA/PVM block copolymers. Polymerized vinyl monomers

Although, as it was stated, diverse strategies for polyester/poly(vinyl monomer) block copolymers syntheses have been discussed in numerous reviews[10,15–19] we decided to provide a brief summary of these methods and present representative examples of prepared copolymers (refer to Table 1 and Fig. 1).

Table 1. Vinyl (unsaturated) monomers used for the synthesis of PLA block copolymers by different methods.

Monomer		Synthesis method	Type of copolymer	Reference
Methacrylates	MMA	Dual Initiator, ATRP one pot	Linear AB	[21]
		Dual Initiator, ATRP first	Linear ABC	[22]
		Dual Initiator, ROP first, ATRP next	Linear AB	[23]
		PLA MI for ATRP	Linear AB	[24]
		PLA MI for ATRP	Star AB	[25]
		Dual/Inifer, ROP first and click with other polymers	Miktoarm star	[26]
		Dual/Inifer, ROP and RAFT, one pot	Linear AB	[27]
	n-BMA	Functionalization of PLA and PBMA with norbornene, ROMP of macromonomers	Comb/Brush	[28]
	t-BMA	Dual/Inifer, one pot, simultaneous ROP and RAFT	Linear AB	[27]
	HEMA	Dual Initiator for ROP and ATRP, one pot	Linear AB	[29]
		Dual/Inifer, RAFT first, ROP next	Linear AB-C	[30]
		PLA functionalization for RAFT	Linear A-BC	[31]
		ATRP first, grafting from to attach PLA, ATRP from end-funcionalized PHEMA	Comb	[32]
		ATRP first, partial functionalization of -OH, next ROP and ATRP	Comb, BC from A	[33]
	PEG_MA (PEGMA)	Dual Initiator, ROP first, ATRP next	Linear AB	[34]
	DMAEMA,	Dual Initiator, ROP first, ATRP next	Linear AB	[35]
	DEAEMA	Dual Initiator for ROP and ATRP, one pot	Linear AB	[36]
		Dual/Inifer, RAFT first, ROP next	Linear AB	[30]
		Dual/Inifer, ROP first, RAFT next	Linear AB	[37]
		Dual/Inifer, one pot, ROP first, RAFT next	Linear AB	[38]
		Star PLA functionalization, ATRP of DEAEMA initiated with PEG, functionalization, click	Star ABC with dendritic core	[39]
	GMA	PLA functionalization, next ATRP	Linear AB	[40]
		AIBN first, next ROP and click C	Grafted AB-C	[41]
		AIBN for AB grafted with PEG, next functionalization for ST graft	Doubly grafted AB-C, next D, bottlebrush	[42]
		Dual Initiator, ATRP first, ROP next and again ATRP	AB-C comb	[43]
		Dual/Inifer, RAFT first	ABC miktoarm star	[44]
		Dual/Inifer, one pot, ROP first	AB comb	[45]
		Dual/Inifer, one pot, simultaneous	AB comb	[38]
	MPC	Dual/inifer, one pot, ROP first	AB linear	[46]
		Direct end-capping of PLA to initiate ATRP		[47]
	NMAS	Dual/Inifer, ROP first, RAFT of NMAS and MPC	Linear A-BC	[48]
Acrylates	MA	Dual/Inifer, ROP first and click with other polymers	Miktoarm star	[26]
	n-BA	RAFT of n-BA, click with PLA	Miktoarm star AB	[49]
	t-BA	Dual Initiator, ROP first, ATRP next	Linear AB	[50]
		PLA functionalization, next ATRP	Linear ABA	[51]
	HEA	Dual/Inifer, ROP first	Linear A-BC	[52]
		PLA functionalization, next RAFT	Linear A-BC	[31]
	PEG-A	RAFT of PEG-A, functionalization and click with functionalized PLA	Miktoarm star AB	[49]
	DMAEA	Dual/Inifer, ROP first	Linear AB	[37]
	NAS	PLA functionalization, next NMP of NAS and NVP	Linear A-BC	[53]
	AA (protected)	Dual/Inifer, ROP first	Linear AB	[37,54]
Acrylamides	AAm	ATRP of AAm from PEG-Br, ROP of LA and click	Linear ABC	[55]
	DMA	Dual/Inifer, RAFT first, ROP next	Linear AB-C	[56]
	NIPAM	Dual/Inifer, RAFT first, ROP next	Linear AB-C	[56]
		Dual/Inifer, ROP first, next RAFT	Linear AB	[57,58]
		Dual/Inifer, one pot simultaneous	Linear AB	[27]

(*continued*)

Table 1. Continued.

Monomer		Synthesis method	Type of copolymer	Reference
		Dual Initiator, NMP first, ROP next	Linear AB	[59]
		PLA functionalization, next ATRP	ABA	[60]
		PLA functionalization, next RAFT	Star POSS-AB	[61]
		RAFT of NIPAM, click with PLA	Miktoarm star AB	[49]
	AEA-boc	Dual/Inifer, ROP first, RAFT next	Linear AB	[62]
	HPMA	Dual/Inifer, ROP first, next RAFT	Linear AB	[63]
S,		Dual Initiator, ATRP first	Linear AB	[64]
FS		Dual Initiator, ATRP first	Linear and star ABC	[22]
		Dual Initiator, ROP first, ATRP next	Linear AB and ABC	[50]
		Dual Initiator, one pot ATRP and ROP simultaneous	Linear AB	[65]
		Dual/Inifer, RAFT first	Linear ABC	[66]
		Dual/Inifer, one pot RAFT and ROP simultaneous	Linear AB	[27]
		Dual Initiator, NMP first	Linear AB	[67,68]
		Dual Initiator, ROP first, NMP next	Linear AB and ABC	[69]
		PLA functionalization, ATRP next	Linear AB	[25]
		PLA functionalization, RAFT next	Linear ABC	[70]
		PLA functionalization, next RAFT	Linear AB and star AB	[71]
		PLA functionalization, next RAFT of FS	Linear AB	[72]
		ATRP of HEMA, next partial functionalization, grafting PLA, PS	Comb	[33]
AN		Dual Initiator, ROP first, ATRP next	Linear AB	[73]
		Dual/Inifer, ROP first	Linear ABA	[74]
VP		Dual/Initiator, ROP first, ATRP next	Linear AB	[75]
NVP		Dual/Inifer, one pot simultaneous	Linear AB	[76]
		PLA functionalization, next RAFT	Linear AB and star AB	[77,78]
VAc/VA		PLA-alkyne, RAFT of VAc, hydrolysis, click	Linear AB	[79]
IB		Anionic of IB, functionalization, ROP coordination of LA	ABA (and $(AB)_n$ by using diisocyanate)	[80]
		Sequential anionic	ABA	[20]
IP		Anionic of IP, functionalization, ROP coordination of LA	ABA	[81]
		RAFT of IP, HEMA and HEA, ROP of LA (TBD as catalyst)	ABC-D	[82]

MMA: methyl methacrylate; n-BMA: n-butyl methacrylate; t-BMA: tert-butyl methacrylate; HEMA: hydroxyethyl methacrylate; PEG_MA: polyethylene glycol methacrylate; DMAEMA - 2-(N,N-dimethylamino)ethyl methacrylate; DEAEMA - 2-(N,N-diethylamino)ethyl methacrylate; GMA: glycidyl methacrylate; MPC: methacryloyloxyethyl phosphorylcholine; NMAS - N-methacryloxysuccinimide; MA: methyl acrylate; n-BA: n-butyl acrylate; t-BA: tert-butyl acrylate; HEA: 2-hydroxyethyl acrylate; PEG_A: polyethylene glycol acrylate; DMAEA -2-(N,N-dimethylamino)ethyl acrylate; NAS: N-acryloxysuccinimide; AA: acrylic acid; AAm: acrylamide; DMA: N,N-dimethylacrylamide; NIPAM: N-isopropylacrylamide; AEA-boc: protected acrylamidoethylamine; HPMA: N-(2-hydroxypropyl)methacrylamide; S: styrene; FS -fluorostyrene; AN: acrylonitrile; VP: vinylpyridine; NVP: N-vinylpyrrolidone; VAc: vinyl acetate; VA: vinyl alcohol; IB:isobuten; IP: isoprene; ATRP: atom transfer radical polymerization; RAFT: reversible addition-fragmentation chain-transfer; NMP: nitroxide-mediated polymerization; ROMP: ring opening metathesis polymerization. POSS: Polyhedral oligomeric silsesquioxane; TBD: 1,5,7-Triazabicyclodec-5-ene.

The elaborated methods can be categorized into several groups:

1. Application of dual initiators for ROP and RDRP.
2. Preparation of the first block followed by transforming the chain end(s) into initiating group(s) for the polymerization of monomer forming the second block.
3. Synthesis of graft/comb copolymers by utilizing existing pendant groups from the first block as initiating groups for the polymerization of the new monomer.
4. Coupling of two preformed blocks containing end groups able to react.

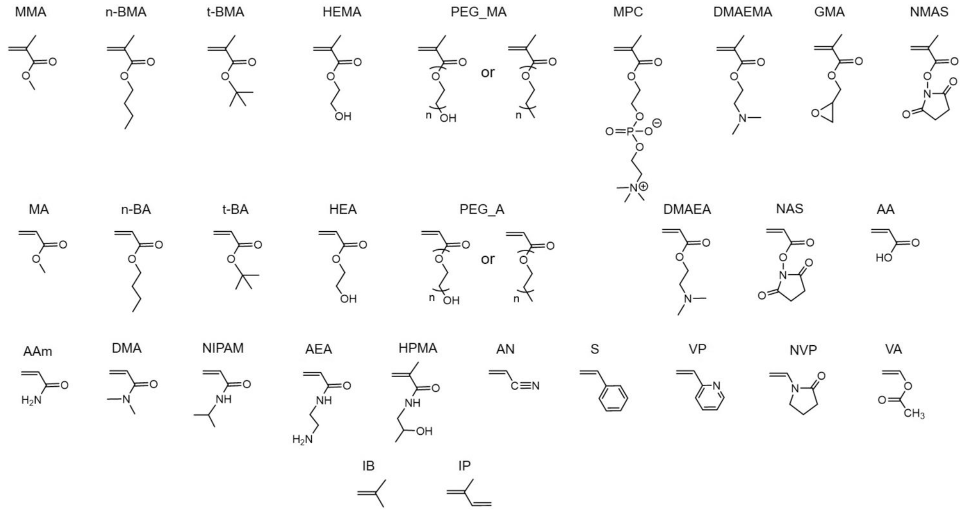

Figure 1. Structures of vinyl/unsaturated monomers used for the preparation of block copolymers with PLA.

An additional approach involves performing successive polymerizations, such as ROP of lactide followed by polymerization of unsaturated monomers using anionic catalysts for both stages. This method has been applied in the synthesis of copolymer PLA-b-poly(isobutene).[20]

The easiest method for synthesizing block copolymers from monomers that polymerize through different mechanisms is the use of dual initiators that contain initiating groups for both, ROP and radical polymerization. However, it should be noted that not all initiating groups for one mechanism remain stable when polymerization according to the other mechanism proceeds. Fortunately, ATRP, RAFT, and NMP polymerizations are tolerant to hydroxyl groups, and dual initiators containing – OH group and group initiating radical polymerization have often been applied also for PLA copolymers (although thioester groups for RAFT polymerization act as "inifers" rather than just initiating groups). Synthesis of block copolymers with the application of dual initiators may be achieved through ROP, or RDRP first methods, or as one-pot process.[15] It seems however, that better control over the entire process can be achieved through successive polymerizations. Most ROPs are performed using tin octoate as a catalyst. When the PLA block is formed simultaneously with the block formed by ATRP, the catalyst is present in the reaction medium and may interfere with the control of ATRP. Therefore, it is generally preferable to first perform ATRP polymerization followed by ROP of lactide.

Similarly, when using RAFT inifers containing -OH groups, the vinyl monomer is polymerized first followed by the lactide polymerization from formed macroinitiators.[15] In the alternative PLA first method, the stability of the PLA chain during radical polymerization must be considered. NMP dual initiators have been applied for both ROP and NMP first approaches[15] however, it should be remembered that NMP requires relatively high temperatures (over 110 °C) to cleave the carbon-oxygen bond. Quite recently, there have been a report on the use of a completely new double initiator/inifer, namely the tetraphenylethanediol (TPE) derivative.[74] Since TPE group can dissociate under moderate heating and initiate radical polymerization of an unsaturated monomer, the triblock copolymers PLA/P(acrylonitrile) were easily obtained by initiating LA polymerization using TPE-containing diol and subsequently heating the PLA macroinifer in the presence of AN monomer.

As it was written, another approach to PLA block copolymers involves the transformation of end groups of the first block to initiating groups for the polymerization of the second monomer. Polylactide as a first block possesses hydroxyl end groups that can be transformed *in situ* into groups initiating radical polymerization by quenching lactide polymerization with the appropriate compound or initiating groups may be introduced by post-polymerization functionalization. This is typically achieved through esterification with the appropriate acyl chloride/bromide allowing for the introduction of initiating groups for ATRP, RAFT, and NMP. Linear diblock, triblock, or star copolymers were prepared by this approach.[15]

Another versatile method involves coupling previously formed blocks containing reactive end groups using well-known click reactions such as alkyne/azide or alkyne(alkene)/thiol. In the case of PLA-based copolymers, this strategy was applied for coupling different blocks.[39,49]

Polymerization of lactide from PVM (obtained by any from RDRP methods) bearing pendant hydroxyl groups leads to graft/comb copolymers. Alternatively, comb copolymer with PLA side chains may be obtained by initially preparing PLA macromonomer (through the initiation of ROP using a compound with an unsaturated group or post-polymerization functionalization with this group) and subsequently polymerizing, or preferably copolymerizing, the obtained macromonomers using any RDRP technique.

3. Nanostructures obtained from PLA/PVM block copolymers self-organization

Block copolymers composed of different in-nature polymers exhibit a tendency to self-organize, both in solution, and in the solid state.[12,13,83,84] The self-organization of PLA copolymers in solution has shown the most significant application effects. Typically, hydrophobic PLA is combined with different hydrophilic blocks, primarily for biomedical and pharmaceutical applications. Amphiphilic block copolymers have the ability to self-assemble in solution, forming micelles of different shapes and sizes, and a significant number of articles have been published on this topic.[17,84–89] The self-assembly into micelles provides a basis for various drug delivery systems (DDS) based on PLA such as liquid micellar systems with entrapped biologically active compound or solid micro/nanoparticles.[10,16,90–100] The second, hydrophilic building block for amphiphilic PLA block copolymers is typically made of poly(ethylene glycol) (obtained, similarly to PLA, through ROP polymerization),[101] polysaccharides, polypeptides, polyurethanes,[10] or can be synthesized through radical polymerization using monomers such as some (meth)acrylates or other vinyl monomers.[10] In water, amphiphilic copolymers self-organize in a way that the water-soluble blocks are solvated in the aqueous phase while the hydrophobic PLA blocks are protected in the core of the aggregate. Various morphologies can be observed, including spherical micelles (with more than 50% hydrophilic part), cylindrical, worm-like micelles (40–50% hydrophilic part) and bilayer spherical polymersomes (25–40% hydrophilic part)[17] (Fig. 2).

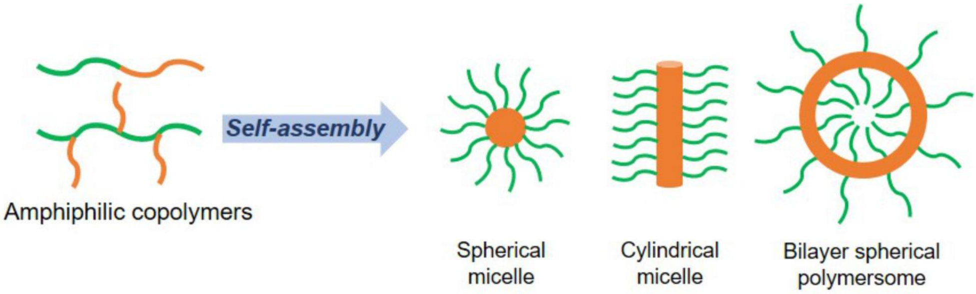

Figure 2. Self-organization of amphiphilic block copolymers in solution.

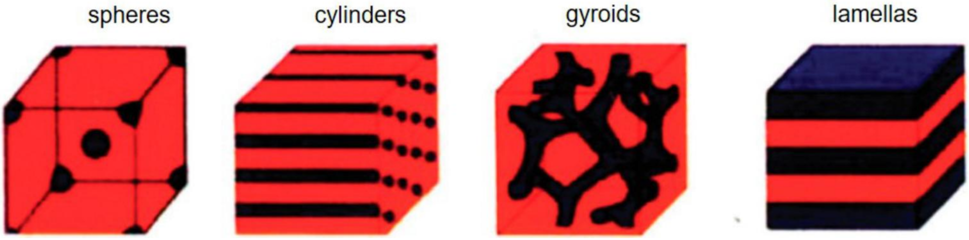

Figure 3. Morphological forms of AB diblock copolymers depending on their composition.[84] Adapted with permission from MDPI, 2017.

The specific morphology depends on the relative proportion of hydrophobic and hydrophilic portion while the size of the aggregates is influenced by the molecular weight of the copolymer. These aggregate forms have also been reported in the literature on amphiphilic PLA copolymers.[10,16,17]

In the solid state, the chemical incompatibility of blocks acts as a driving force for the phase separation and self-assembly into various morphologies.[83,84,102–104] Theoretical frameworks developed for non-crystalline diblock copolymers distinguish morphologies such as spheres, cylinders, gyroids, and lamellas (refer to Fig. 3). The equilibrium morphologies of triblock copolymers exhibit even greater diversity.

The observed morphology depends on several parameters, including the volume fraction of both blocks, the Flory–Huggins interaction parameter for the monomers pair, and the degree of polymerization.[84] Therefore, by manipulating these parameters, control over the morphology can be achieved. The specific morphology of copolymers in bulk and thin films can be, in turn, useful for certain applications *e.g.*, for the preparation of porous materials.

3.1. Self-organization of PLA amphiphilic block copolymers in solution and their application as drug delivery systems and imaging agents

As previously mentioned, amphiphilic block copolymers composed of hydrophobic PLA and a hydrophilic second block can aggregate into micelles in a water environment.[10,16,17] When the aggregation occurs in the presence of the biologically active compound, it becomes entrapped within the formed micelles. Micellar nanoparticles are typically separated through solvent evaporation or evaporation/extraction methods.[105]

Micelles prepared from amphiphilic copolymers are often thermo- and/or pH-responsive. This facilitates the release of the encapsulated compound. The thermoresponsiveness of micelles is associated with their lower critical solution temperature (LCST), which marks the point of transition from a coil-to-globule state. This temperature can be adjusted by altering the composition of the amphiphilic copolymer. The drug release from thermoresponsive polymeric micelles is governed by temperature-induced changes in their structure, analogous to how changes in pH lead to alterations in the structure of pH-sensitive micelles.

Sometimes the entrapped compound is covalently linked to PLA copolymer to enhance encapsulation efficiency. However, in such cases, the detachment mechanism should be accessible, typically through the presence of an appropriate stimuli-responsive linkage, such as disulfide.[106,107] Micelles prepared from amphiphilic PLA copolymers are among the variety of different drug delivery systems (DDS) based on PLA, including those prepared solely from PLA or its copolymers with another hydrophobic block.[108,109] Drug delivery systems generally provide control over drug delivery, usually provide delivery for a prolonged time, enable targeted delivery, reduce drug toxicity, and protect encapsulated agents against oxidation, among other benefits. Nanocarriers allow for overcoming cellular barriers in the delivery of various hydrophobic drugs such as nucleic acids and proteins.[110] Polymer micelles, in comparison with small surfactants, have low critical micelle concentration (CMC), providing them with strong resistance to dilution and stability in bloodstream during delivery.[110] This property is crucial for targeted drug release.[91,110]

A variety of PLA/poly(vinyl monomer) copolymers have been prepared for micellization study and the encapsulation of pharmaceutical agents was attempted.[10,16,17,100,107] PLA as a hydrophobic block arranges into a micelle core and a hydrophilic block forms the corona. The hydrophilic block of the corona was prepared from such monomers as PEGMA/OEGMA (oligoethylene glycol methacrylate), AAm, DMAEA, NIPAM and to a lesser extent, NVP, MPC, HPMA, GMA, and others using various RDRP methods described in Section 2.

The hydrophobic polylactide core enables the entrapment of different hydrophobic biologically active compounds, and the successful encapsulation of various drugs (mainly anticancer and nucleic acids but also immune-sensitive and others) has been performed. The therapeutic agent was often accompanied by the imaging agent. The role of the micelle corona can vary. Its primary function is to protect the nanocarrier from capture by macrophages, thereby increasing its circulation lifetime in the bloodstream. This role is fulfilled by the PEG block, and in early and most works, this block was linked to the PLA block through the initiation of LA polymerization by the PEG macroinitiator. But the PEG chain was also linked to the PLA block as a side chain, by radical polymerization of PEG-(meth)acrylate (PEGMA).[111–117] Copolymers of other vinyl monomers, *i.e.*, N-vinylpyrrolidone (NVP) or 2-(methacryloyloxy)ethyl phosphorylcholine (MPC), can replace PEG which is found to cause hypersensitivity reactions linked to anti-PEG antibody production.[118] For example, the polymerization of MPC and subsequent coupling with PLA chain through click reactions has resulted in micelles with super hydrophilic surface resisted to nonspecific protein adsorption.[119] The highly hydrophilic block has also been synthesized *via* radical polymerization of (2-hydroxypropyl)methacrylamide (HPMA)[63] and others.[16]

The hydrophilic corona of PLA-based micelles can also exhibit pH-sensitive behavior, leading to pH-responsive micelles. Thus, hydrophilic block prepared from monomers with acidic or basic functions, such as (meth)acrylic acid ((M)AA), dimethylaminoethyl methacrylate (DMAEMA), aminoethyl(meth)acrylamide (AE(M)A), and vinyl imidazole (VIM) exhibit pH-responsive behavior, allowing for triggered drug release.[16]

Another interesting type of PLA-based micelles is the one prepared with glycopolymers where the (meth)acrylate derivative of monosaccharide sugar was radically polymerized.[120] These nanocarriers are focused on targeted delivery, primarily due to the presence of many active sites that promote the binding of carbohydrates to their receptors on cells.

Of course, the combination of the mentioned above monomers was often used to achieve several effects simultaneously, and different functional groups are employed to bound and to enable the release of the drug.

In appearing articles on PLA/PVM amphiphilic copolymers, some researchers only suggested the application of prepared by them micelles as drug carriers, however, there is a large group of papers describing the study of the encapsulation of the particular pharmaceutical agent as well as its release and a nice review on this topic has come up recently.[16] Table 2 presents examples of the suggested or investigated applications of different prepared drug carriers based on amphiphilic PLA/PVM copolymers that are described in the literature. However, it is important to note that most of the developed drug delivery systems and commercialized products are based on PLA alone or PLA/PEG and PLA/PGA (polyglycolic acid) copolymers.[95]

3.2. Self-organization of PLA block copolymers in the solid state

3.2.1. Porous materials

Nanostructured block copolymers are often precursors of porous materials. When two blocks are characterized by contrasted degradability, the selective removal of one of them is a convenient way to achieve controlled porosity of the intended material.[65,140] In the case of PLA block copolymers with separated phases in the solid state, the PLA block is typically removed (referred to as the "sacrificial block"), and the resulting material is constructed from another polymer. Although the final product does not contain polylactide, we include PLA/PVM copolymers leading to such materials in this review due to their potential great utility.

Various polymers have been applied as the block intended to form the final porous material, with polystyrene being particularly useful as a material for applications such as separation membranes, heterogenous catalysis, or template-assisted synthesis of nanomaterials.[65,140–144] Mesoporous materials obtained from PLA/PS block copolymers have been prepared and intensively studied by the Hillmyer group and described in a series of articles.[72,140,143–159] The authors introduced sometimes additional block of another monomer to achieve specific properties. Di(tri)block copolymers were typically synthesized by initiating the anionic polymerization of styrene, followed by the transformation of the end group of the first block into an –OH group, which initiates the ROP of lactide catalyzed by triethyl aluminum. Alternatively, a PLA macroinitiator was prepared first, followed by radical polymerization of styrene or styrene with other

Table 2. Drug carriers based on PLA/PVM copolymers.

Vinyl monomer	Copolymer structure	Designed for drug delivery/imaging	Drug release/micelles disintegration (degradation)[a]	Reference
OEGMA/ PEGMA	POEGMA-PLA-POEGMA	Curcumin	–	[111]
	PLA-POEGMA	Imaging dye-DIL, curcumin	38% in 10 h and ∼70% of curcumin in 100 h for 5% loaded particles in a buffer (a profile similar to PLGA copolymers).	[112]
	PLAstar-CAPMA-POEGMA	Camptothecin cov.	Near zero-order release due to the degradation; 74–95% of camptothecin at pH = 7.4 in 42 d depending on copolymer composition.	[113]
	PLA_SS_PEGMA polymersomes	FA cov., DOX	82% at pH = 5 and 65% at pH = 7.4 with the addition of glutathione in 70 h.	[114]
	POEGMA-PLA_SS_PLA-POEGMA	DOX	At pH = 7, in the presence of dithiothreitol, the M_n of copolymer decreased two times in 50 h.	[115]
	PEG(FA)_SS_OEGMA-P(HEMAgLA)	FA cov., DOX	59% at pH = 5 and 46% at pH = 7.4 in 24 h; with the addition of dithiothreitol: 71% at pH =7.4.	[116]
	(POEGMA-NAS)-PLA	Paclitaxel	50% at pH = 5 and 35% at pH = 7.4 in 5 days; with glutathione: 65%.	[117]
NVP	PLA-PNVP	Propofol	–	[121]
	PNVP-PLA-PNVP	DOX	15% at pH = 7.4 in 48 h.	[122]
	Star PLA-PNVP	Methotrexate	∼20% at pH = 7.4 and ∼40% at pH = 5 in 24 h.	[78]
	PLA-b-P(NAS-co-NVP) with lectin	Imiquimod	∼55% at pH= 7.4 and ∼70% at pH = 5 in 2 h and ∼100% in 50 h.	[53]
	PLA-b-P(NAS-co-NVP), capsin protein	Imiquimod	Over 90 % at pH = 7.4 and ∼100% at pH = 5 in 7 h.	[123]
	PLA-b-P(NAS-co-NVP), peptide	mRNA	–	[124]
MPC	(PLA-PMPC$_3$)$_3$	Paclitaxel	Almost sustainable release of 50% during 20 h and ∼80% in 3 d at pH = 7.4.	[119]
	PLA-P(MPC-NMAS) cov. Cysteine	Rhodamine B	Release of rhodamine in 89 days was two times higher at pH =2 than at p = 7.4.	[48]
HPMA	PLA-PHMPA	Paclitaxel	Almost zero-order release; 80% in 120 h at pH = 7.4; 50% of copolymer degrades in 1 h at pH = 5.2.	[63,125]
GMA	PLA-PGMA	Naproxen	40% at pH = 7.4 in 48 h.	[40]
(M)AA (PtBA/PtBMA)	PLA-PMAA-PEGMA	Nifedipine	96-100% at pH = 7.4 and 66–73% at pH = 1.2 in 24 h.	[43]
	PEG-(PtBA-g-PLA) brush	DOX	Reduced burst release; 26.5% during 12 h and ∼65% in 96 h at pH = 5.	[126]
	PLGA-PAA	DOX, Hydroxytyrosol	78% or 70% of DOX while 96% or 85% of hydroxytyrosol at pH = 5.4 or 7.4 respectively in 72 h.	[127]
Aam	PEG-PAAm-PLA	Pyrene	82% at pH = 7.4 and 27% at pH = 1.2 in 72 h.	[55]
DMAEMA	PLA-PDMAEMA	Dipyridamole	–	[128]
	CD_PLA-PDMAEMA-PEtOxMA)$_{21}$_gold NP	DOX, tomographic imaging	18% at pH = 7.4, 56% at pH = 6.5 and 88% at pH = 5 in 102 h.	[129]
	(PLA-PDMAEMA$_3$)$_{1\text{-}3}$	DOX, microRNA	88–100% of DOX at pH = 7.4 in 24 h.	[130]
AEA	PAEA-PDLLA	Nucleic acids (siRNA, DNA)	More efficient release of DNA at pH = 5 than at pH = 7.4.	[62,131]

(*continued*)

Table 2. Continued.

Vinyl monomer	Copolymer structure	Designed for drug delivery/imaging	Drug release/micelles disintegration (degradation)[a]	Refe rence
NIPAM	P(NIPAM-DMA)-PLA	Paclitaxel	Micelles with paclitaxel almost stable at pH = 7.4 in 10 d and completely disintegrated at pH = 5 in 5 d.	[56]
	P(NIPAM-DMA)-PLLA-P(NIPAM-DMA)	Amphotericin B	55–70% at 37°C and 58–93% at 40°C in 10 d in water.	[132]
	P(NIPAM-DMA)-PLLA-P(NIPAM-DMA)	Curcumin	For 6% drug loading, 84% at 37°C and 92% at 40°C at pH = 7.4 in 30 d.	[133]
	PEG-P(HEMA-PLA)-PNIPAM	DOX	30% at 37 °C and 26% at 25 °C at pH = 7.4 in 72 h.	[134]
	PLA-PNIPAM-PLA	Adriamycin	62% at 37°C and 45% at 20°C at pH = 7.4 in 50 h (unchanged up to 160 h of the study)	[135]
	starPLA-PNIPAM with porphyrine core	PD therapy	–	[136]
VIM	P(VCL-VIM)-g-PLA	protoporphyrin – PD therapy	7% at pH = 7.4 and 50% at pH = 5 in 72 h.	[137]
Sugar-(meth)acrylate	PLA-HEA_Fru-CEA	RAPTA C	–	[138]
	PLA-P(LAMA) porphyrine core	PD therapy	–	[139]
	PMAGP-PLA-PMAGP	Paclitaxel	65% at pH = 7.4, 79% at pH = 5 and 83% at pH = 4 in 100 h.	[120]

CAPMA: captothecin methacrylate; -SS: disulfide group; DIL: 1,1′-dioctadecyl-3,3,3′,3′-tetramethylindo-carbocyanine perchlorate; cov.: covalently bound; FA: folic acid; DOX: doxorubicin; PLGA: poly(lactide-co-glicolide); NMAS: N-methacryloxysuccinimide; VCL: vinylcalrolactam; PLLA: poly(L,L-lactide); PDLLA: poly(D,L-lactide); APD: phodynamic therapy; CD: cyclodextrin; Ox: oxazoline; EtOxMa: [oligo(2-ethyl-2-oxazoline)methacrylate]; RAPTA C: drug for breast cancer therapy, (dichlororuthenium (II) (p-cymene) (1,3,5-triaza-7-phosphaadamantane); FRU: D-fructose; CEA: chloroethyl acrylate; P(LAMA): poly(lactobionamidoethyl methacrylate); PMAGP: poly(6-O-methacryloyl-α-D-galactopyranose).

The meaning of other abbreviations is the same as for Table 1 ("P" before the monomer name means "poly", *e.g.*, PEGMA = poly(ethylene glycol methacrylate)).

[a] The release study was conducted at 37 °C for most drug carriers. In the case of thermoresponsive micelles, the release study was frequently performed both below and above LCST. In most cases, a burst release of the drug was observed, except for the release of covalently linked drugs, which occurs due to the dissociation of a specific bond and/or slow degradation of PLA.

monomers. The separated phases were oriented by forcing copolymer through a hollow tube at elevated temperatures. In all cases, porous material was obtained by etching PLA block from copolymer monolith (hydrolysis under alkaline conditions).[145,146] Porous materials with narrow pore size distributions (cylinder diameter in the range of 15–45 nm depending on copolymer molecular weight) and with hydroxyl functional groups on the walls of the pores were prepared as shown in Fig. 4. The authors studied the porosity and the liquid permeability of obtained material and demonstrated the ability to regulate pore sizes, making this material suitable for nanomaterial synthesis, catalyst supports, and advanced separations.

PLA/PS block copolymers have also been utilized by other research groups for the preparation of porous materials. Gorzolnik *et al.*[65] and Grande *et al.*[141] reported on the preparation of mesoporous polystyrene membranes through the synthesis of PS/PLA diblock copolymers with a carboxyl group at the junction between both blocks followed by the hydrolysis of PLA block in the oriented copolymer. The copolymer was prepared using a dual initiator for ROP and ATRP polymerizations. The separated phases with PLA-forming cylinders, were oriented by using shear forces, and PLA phase was removed by hydrolysis under alkaline conditions. The porosity of the resulting PS material containing carboxyl groups on the pore walls, was investigated for catalysis and

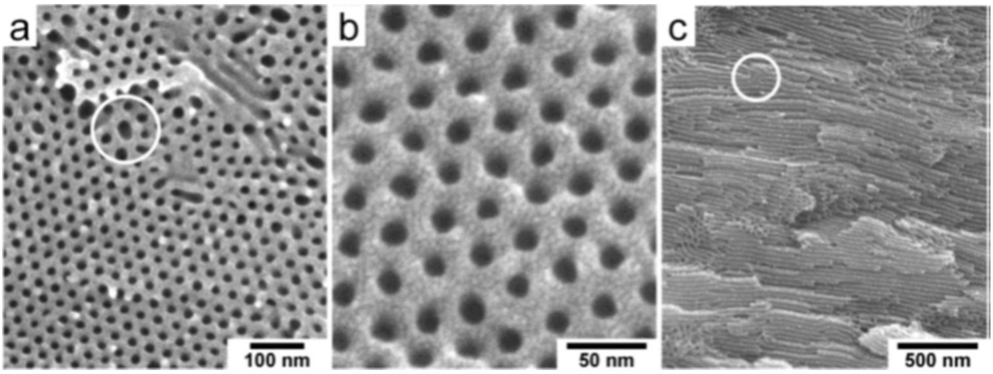

Figure 4. SEM pictures of porous material obtained using PLA/PS copolymer with M_n ~37,000 g·mol^{-1} and mol fraction of PLA = 0.38: (a,b) view perpendicular to the cylinder axes, (c) view parallel to the cylinder axes. (Circles show defects).[146] Reproduced with permission from ACS, 2002.

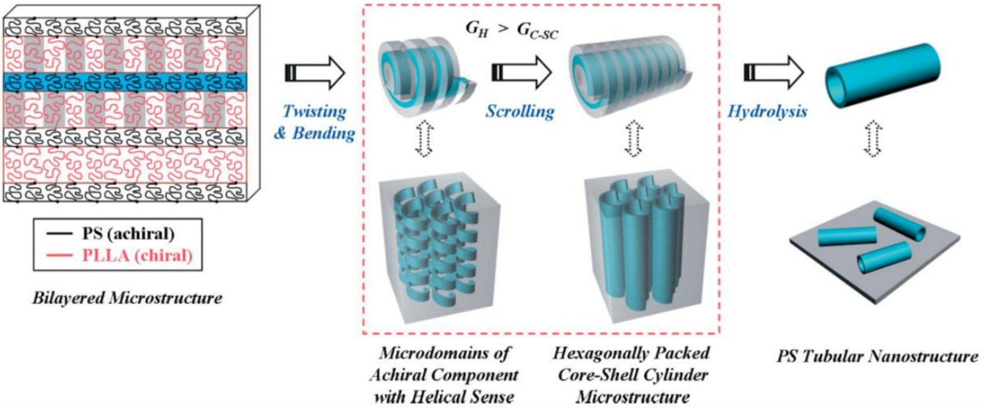

Figure 5. Visualization of the formation of PS tubular nanostructures by hydrolysis of PLLA in core-shell cylinder microstructure which was formed due to chirality-driven twisting and bending of the bilayered microstructure; G_H: Gibbs' free energy of the helix; $G_{C\text{-}SC}$: Gibbs' free energy of the core-shell cylinder.[161] Reproduced with permission from Wiley, 2006.

filtration applications. PLA/PS block copolymers were also prepared by Bolton *et al.*[160] however, with bottle-brush structure with PLA and PS as side chains. Again, these block copolymers self-assembled into a cylindrical morphology but this time, with large domain spacings. PLA cylinders were selectively etched out (at acidic conditions) of the shear-aligned polymer monoliths to generate nanoporous materials with a large cylindrical pore diameter of 55 nm. The remaining backbone inside the pores acted as a hydrophilic coating, resulting in efficient water uptake. The described method expanded the range of available pore sizes for nanoporous materials which the authors suggested could be utilized for nanofiltration. The interesting morphology of diblock PLA/PS copolymers was observed by Ho *et al.*[161] *i.e.*, hexagonally packed nanohelical microstructure when using chiral PLLA and appropriate PLA and PS proportion. A core-shell cylindrical microstructure with PST as cylinders, was formed as depicted in Fig. 5. The tubular structure obtained, after removing of PLA matrix, could be useful as drug carriers, nanocables, and nanoreactors for templating inorganic materials (metals, silica and metal oxides).

Hillmyer group expanded their research on porous materials beyond diblock PLA/PS copolymers. They prepared porous monoliths from ordered poly(cyclohexylethylene)-polylactide (PCHE-PLA) diblock copolymers starting with the dehydrogenation of polystyrene.[147] It appeared that the obtained nanoporous material (also with the possibility of the pores regulation) exhibited a higher softening temperature and resistance to solvents that dissolved analogous PS monoliths what is very important for the intended applications. Furthermore, they developed porous materials based on triblock copolymers, specifically polystyrene-polydimethylacrylamide-polylactide (PS-PDMA-PLA) which also self-assembled into a cylindrical morphology.[148–150] This allowed for control over the properties of the pores surface. In the material prepared from ABC copolymer, the A block constituted the matrix, C block was the removable minor component, and B block provided the functionality on the surface of the pores. The resulting nanoporous PS-based material with hydrophilic pores environment (due to the presence of PDMA block) appeared to efficiently uptake water making it potentially useful for biocatalysis, water purification, and biomolecule separations.[140,150] Moreover, controlled hydrolysis of PDMA fragments, and subsequent modification of the acidic groups on the pore surface could allow for the attachment of different functional groups further expanding the range of applications.[149] Porous membranes (thin films) were also prepared from polystyrene/polyisoprene/PLA copolymers (PS/PI/PLA) with cylindrical morphology, after removing of PLA block. In this case, PS/PI blocks were prepared *via* anionic polymerization.[151]

By incorporating multifunctional monomer as a third component of triblock copolymer, Hillmyer group prepared materials with percolating mesopores. The phase separation was polymerization-induced. Thus, polylactide with a trithiocarbonate chain transfer agent at one chain end (PLA-CTA) was chosen as the chemically etchable block, and styrene/divinylbenzene (S/DVB) mixture as the crosslinkable agent. The resulting microphase separation was kinetically trapped in this case. The removal of the etchable PLA generated percolating nanopores in a crosslinked matrix.[152,153] According to the authors, materials with percolating mesopores and rapid mass transport were attractive for applications such as catalysis, nanotemplating, and separations. This type of polymerization was further termed "polymerization-induced microphase separation" (PIMS) by the authors, and considered as leading to materials with meso and/or micro pores by using differently substituted styrenic monomers[154] (Fig. 6).

In a similar manner to the examples mentioned above, phase separation was achieved in the case of polyactide-b-poly(styrene-s-butadiene) [PLA-b-P(S-s-B)] which was radically cured in the disordered state.[155] Percolating mesopores were also observed in the case of copolymer composed of etchable polylactide and a crosslinkable block formed from a statistical copolymer of styrene and glycidyl methacrylate [PLA-b-P(S-s-GMA)].[156] Other porous membranes with the increased hydrophilicity were prepared from triblock copolymers, specifically polylactide-*b*-poly(oligoethylene glycol methyl ether methacrylate)-*b*-poly(styrene-*s*-methyl methacrylate) (PLA-POEGMA-PSMMA), where PLA served as the etchable pore-forming block, POEGMA as the hydrophilic pore-lining block, and PSMMA as the matrix block.[157]

As evident from the literature examples provided above, PS-based porous materials with tunable pore size (prepared also as double-layered films) were primarily designed for water purification membranes and were often studied on water permeability and size selectivity.[144,155,159,162]

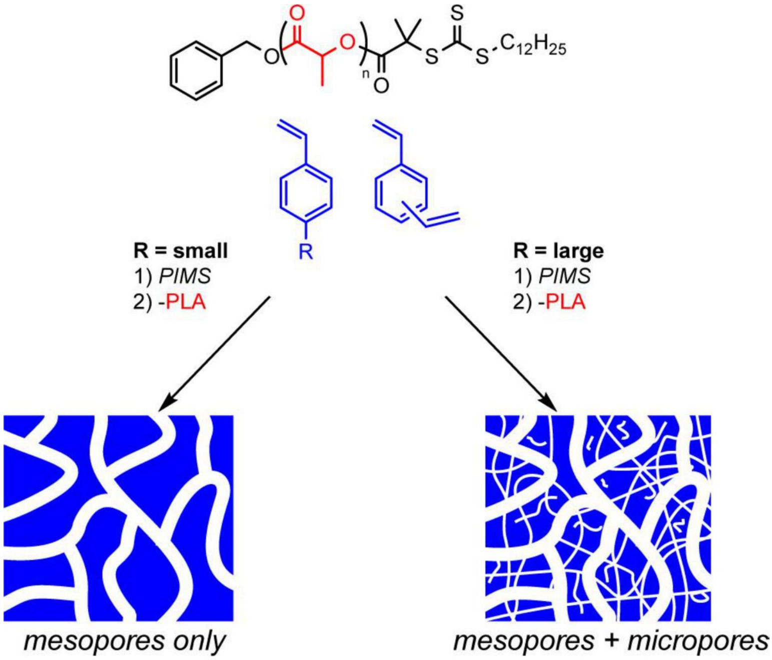

Figure 6. Preparation of nanoporous polymer monoliths *via* the PIMS method and subsequent etching of PLA. On the left: mesopores as a result of the application of small, lower T_g styrenic monomers. On the right: meso- and micropores (due of poor chain packing in the kinetically trapped state) in the case of using sterically bulky, high-T_g styrenic monomers.[154] Reproduced with permission from ACS, 2017.

Another interesting postulated application was the use of these materials as frits in the fabrication of aqueous reference electrodes. For this purpose, monoliths were prepared from a bicontinuous, microphase-separated, and crosslinked block polymer precursor, *i.e.*, polylactide-b-poly(isoprene)-b-poly(styrene-co-divinylbenzene) [PLA-b-PI-b-P(S-co-DVB)].[158]

The application as a template was intendent for nanostructured films prepared from poly(lactide)-b-poly(4-fluorostyrene) (PLA-b-PFS) copolymers.[72] A thin film of PLA-b-FST was deposit on gold-coated silicon/silicon oxide substrates, aligned using an electric field and subjected to mild degradation of the PLA phase which resulted in the formation of nanoporous PFT templates. Subsequently, nanowires were grown electrochemically within these templates using a $CuSO_4$ solution, followed by the templates dissolution/degradation (see Fig. 7). The authors suggest that this method could be employed as a nanoscale templating technique for conjugated polymers in photovoltaic applications.

The same group used PLA copolymer with another styrenic monomer, that is styrene substituted with trifenylamine group (PSTPA) to prepare a mesoporous hole-conducting polymer matrix after selective etching of the minority PLA domains. The pore cylindrical structure was replicated electrochemically in platinum, with a view of producing nano-organized heterojunction structures for solar cells.[163]

A similar templating function of etched PLA/PS copolymer was reported by Lo *et al.*[164] who used prepared PS film with cylindrical pores to fill in with semiconductor material, specifically CdS. Through a suitable templating process, they were able to

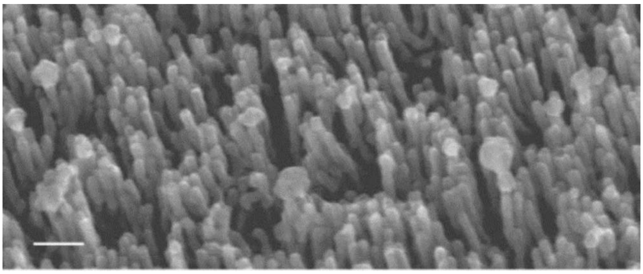

Figure 7. SEM image of freestanding, electrodeposited nanowires following UV degradation of the PFS matrix. The PFS-PLA template was aligned using an electric field. The scale bar represents 100 nm.[72] Reproduced with permission from RSC, 2007.

reduce the amount of CdS while enhancing the emission intensity. This was confirmed by UV absorption measurements and the photoluminescence of the templated CdS nanocrystals.

In applications as filtrating membranes with good selectivity, as well as in other applications, control over pore shape and size is crucial. The shape of the pores depends on the obtained morphology of di(tri)-block copolymers discussed at the beginning of Section 3. Among existing thermodynamically stable morphologies, cylindrical and gyroid (bicontinuous) morphologies are particularly advantageous for transport. Therefore, intentionally designing appropriate volume proportions of individual copolymer blocks is necessary to obtain these morphologies (Theoretically developed phase diagrams are very helpful in this regard).[83] The size of the separated domains and, consequently, the size of pores obtained after etching depends on the molecular weight of the copolymer blocks. The cylindrical morphology requires prior cylinders alignment (in the case of thin films – perpendicular to the film surface) in order to obtain liquid permeability. This alignment in thin films is achieved through the careful selection of coating parameters.[159] Gyroid morphologies, which naturally possess interconnected domains, eliminate the need for the alignment process. In addition to equilibrium ordered morphologies, recent works presented in this review have focused on kinetically trapped morphologies, which enable the use of a wider range of block copolymer compositions and result in narrower pore size distributions compared to those obtained under equilibrium conditions. To trap this non-equilibrium state, the matrix polymer is often crosslinked.[152–154] This, in turn, requires the introduction of an additional crosslinking monomer into the initial copolymer preparation. Thus, the amount of crosslinker used also determines the trapped morphology and the shape and size of the resulting pores. These materials, after etching the removable PLA, are crosslinked, enhancing their resistance to temperature and solvents. Efficient methods for selective etching of the sacrificial block (in this case, the PLA block) have been developed, allowing for the maintenance of pore shape and size.[146]

3.2.2. Photonic crystals and others

Brush block copolymers consisting of polystyrene and polylactide arms, with high molecular weights (up to 63,000,000 $g{\cdot}mol^{-1}$) synthesized by Runge *et al.*[165]

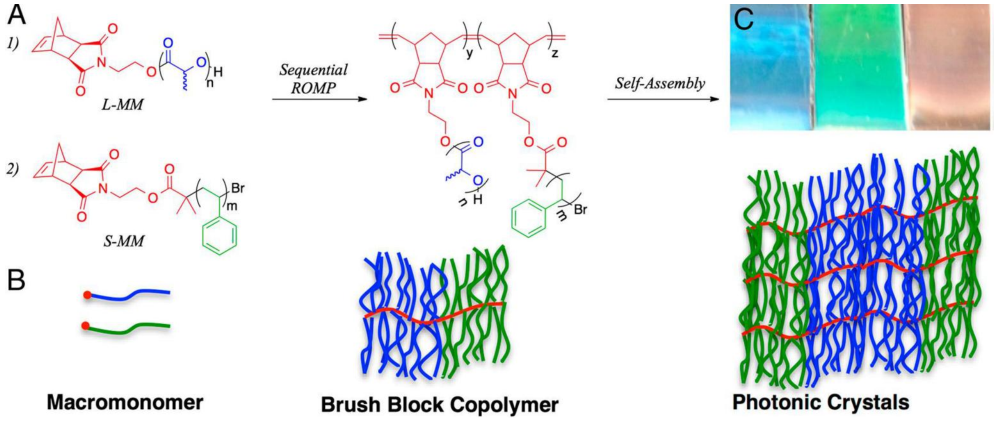

Figure 8. (a) Styrene and lactide-based macromonomers were sequentially polymerized by ROMP to brush block copolymers. (b) A schematic representation of the assembly of copolymers into ordered lamellar nanostructures. (c) Appearance of copolymer depending on different annealing techniques.[166] Reproduced with permission from PNAS, 2012.

were capable of assembling in the solid state with domain sizes exceeding 100 nm. Because the authors observed the change of the color of copolymer material before and after assembling (from white to blue), they postulated its utility as photonic crystals. An interesting application of PLA/PS brush block copolymers was suggested by Grubbs group.[166] They prepared norbornene-functionalized polylactide and polystyrene macromonomers which were subsequently copolymerized by ring-opening metathesis polymerization (ROMP). The obtained copolymers spontaneously assembled into large ordered nanostructures (>100 nm) resembling pseudo-1D photonic crystals (Fig. 8). The annealing of the polymer powders under compression appeared to be the efficient assembly technique. The authors propose that the prepared self-assembling copolymers have potential as building materials that reflect near-infrared (NIR) radiation, thereby inhibiting the thermalization of NIR radiation in urban environments.

In another study, by Dirany *et al.*[64] PLA/PS block copolymers self-assembling into cylindrical structures in thin films were also suggested as a material for nanolithography. The authors determined drying conditions as well as copolymer composition to achieve desired cylindrical morphology of the film deposited by spin coating on Si substrate.

4. Materials for tissue engineering and other biomedical applications

As discussed in the previous Section 3.1, a wide area of the application of PLA/PVM block copolymers is biomedicine, where the self-organization of amphiphilic copolymers in solution was used to produce the variety of drug nanocarriers. However, drug delivery systems include also injectable hydrogels that play a complex role in tissue engineering. Other biomedical applications of materials based on PLA/PVM copolymers such as mats, scaffolds, stents, etc. have also been developed and described in the literature,[10,167–169] although there are not many examples of the combination of polylactide with vinyl monomer polymers. It is copolymers composed of PLA and blocks prepared from other cyclic monomers such as glycolide (GA), ε-caprolactone (CL), cyclic carbonates, and PEG that have been predominantly used in tissue engineering. The application of these copolymers in tissue engineering has been suggested in numerous articles[11,167,170–174] and they have also been subject of different patents.[175] Polyesters (polycarbonates) have been the most commonly used for biomedical applications primarily because of their ability to degrade in the physiological environment due to the presence of ester (carbonate) bonds. Poly(vinyl monomers) are not degradable (although some efforts are made to achieve their partial degradation[176]; however, their other features are valuable, as will be discussed later in the text, and only those that are biocompatible are utilized. In the case of copolymers of polylactide with poly(vinyl monomers), monomers like acrylic acid, HEMA, OEGMA, NIPAM, and *N*-(meth)acryloxysuccinimide (NAS, NMAS, allowing for the linking of biologically active compounds) have been utilized. These synthesized copolymers introduce hydrophilicity, and when they contain a poly(*N*-isopropylacrylamide) (PNIPAM) block, they are capable of forming thermoresponsive gels due to the sol-gel behavior of PNIPAM.[177]

4.1. Hydrogels for injectable scaffolds

The injectable thermoresponsive hydrogels are liquid at room temperature (sol-gel transition occurs at lower critical solution temperature LCST, which is below 37 °C) but become solid scaffolds at body temperature. This property is crucial in implantation procedures as it allows for less invasive delivery compared to pre-formed implants, avoiding the need for large incisions. Injectable hydrogels serve the purpose of providing tissue mechanical support as well as facilitating drug and cell delivery. PNIPAM, which displays an LCST at 32 °C, is the most commonly employed thermoresponsive polymer. It is often combined with blocks of other vinyl monomers, either more hydrophilic or hydrophobic, to modify the LCST.[177,178]

Various combinations of PLA and PNIPAM, along with other vinyl monomer units, have been explored. Ma and Nelson[178] copolymerized PLA-methacrylate with NIPAM and HEMA yielding mechanically strong hydrogel with tensile strengths of up to100 kPa. This material was not toxic to muscle cells and underwent complete degradation in PBS over a period of 6–7 months at 37 °C. The authors suggest that the prepared material could find applications in regenerative medicine, such as ventricular bulking after myocardial infarction. In another study, the same authors introduced a new component to thermoresponsive copolymer, namely *N*-methacryloxysuccinimide (NMAS) which units were able to bind model protein – BSA.[177] Release studies demonstrated prolonged bioactivity of the protein, aligning with the tissue remodeling period. Independently of protein conjugated with polymer, the authors embedded particles containing proteins inside gel material. Another similar material, prepared with *N*-acryloxysuccinimide (NAS) instead of NMAS and additionally acrylic acid was covalently linked with type I collagen[179] to enhance muscle cell adhesion to hydrogel and cells viability. The copolymer material was susceptible to hydrolysis (enhanced due to the introduction of acrylic acid units) forming nontoxic degradation products. The authors propose that thermoresponsive hydrogels prepared by them could be used as

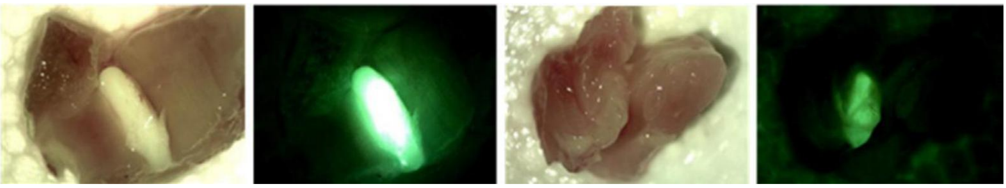

Figure 9. Bright field and fluorescent images of excised rat leg muscles injected with hydrogels PLA-MA/NIPAM/HEMA/MAA: excised on the same day of injection (on the left) and excised 21 d after injection (on the right). The white mass and green fluorescence indicate the hydrogel.[180] Adapted with permission from Elsevier, 2015.

delivery systems for cells or pharmaceutical agents in various tissue engineering applications. Zhu *et al.* also prepared an easy degradable copolymer by copolymerization of PLA-methacrylate with NIPAM, HEMA, and MAA (methacrylic acid).[180] The authors studied the cytotoxicity of degradation products (*in vitro* and *in vivo*) by measuring the relative metabolic activity of rat vascular smooth muscle cells. The results indicated the increase in the overall metabolic activity of the cultures over the course of 7 d, suggesting cell proliferation. The hydrogels solidified immediately upon injection into the muscles, forming distinct volumes. Figure 9 illustrates the effect of hydrogel degradation and absorption.

In another study, copolymers of HEMA-PLA, NIPAM, OEGMA, and NAS were synthesized.[181] Similar to the previously described examples, pendant succinimide groups were used to bind various proteins, such as α-elastin with primary amine groups. The hydrogels were formed from this copolymer at 37 °C and they were highly stable in the physiological environment. Furthermore, more than 80% of dermal fibroblast cells encapsulated in these hydrogels which were mechanically stronger compared to other hydrogels, remained viable, and the number of encapsulated cells increased for at least 5 days. These findings highlight the potential utility of hydrogel-elastin material as attractive in tissue engineering.

4.2. Solid scaffolds/implants and materials for contact with living tissues

PLA-based scaffolds and other surgical devices, such as surgical sutures, plates, screws, stents, and components for vascular, tendon, and nerve regeneration, have been developed over many years. To date, a significant number of these products have been commercialized. Examples include surgical sutures like Vycril® (1974), Polysorb®, Radik®, and XLG® (based on PLGA copolymers), as well as plates and screws for internal bone fracture fixation like FIXSORB MX® and OSTEOTRANS MX® (based on HA/PLLA), or PLA-based stents such as REMEDY®, DESolve Cx®, MIRAGE®, ABSORB V G2®, and MAGNITUDE® (all derived from PLLA or PLLA/PDLLA).[172] There is a large literature on PLA-based materials, primarily on PLA copolymers with PGA, as well as PLA with other polyesters and natural polymers, and PLA composites, mostly with bioceramics, for medical applications.[170,172,182,183] Therefore, this topic will not be discussed in detail in this review, which specifically addresses PLA/PVM copolymers.

The drawback of PLA material for medical applications is its hydrophobicity which limits also degradability. Additionally, rigidity and brittleness are limitations for soft tissue. The main goal of introducing another monomer block to PLA-based materials is to improve the interface between tissue and scaffold material. The new block which was combined with PLA was prepared predominantly from another cyclic monomer which was mentioned earlier,[167,170] but there have also been attempts of the preparation of tissue scaffolds based on PLA/PVM copolymers.

One of the examples of such materials is the copolymer of PLA with HEA synthesized by Clement *et al.*[184] The authors prepared PLA-b-PHEA copolymer with a relatively short PHEA block to use it as a scaffold in nerve repair. They observed improved degradability and an increase in Schwann cell affinity due to the presence of a hydrophilic HEA block. Another example is the preparation of graft copolymer PLA-g-acylamide/N,N'-methylenebisacrylamide by grafting acrylamides from UV-activated PLA film.[185] The physicochemically modified films with hydrophilic and pH-responsive surfaces could potentially be used as cell culture substrates, scaffolds, or pH-sensitive absorbents.

Solid scaffolds are often produced as porous materials for tissue growth as well as devices for drug delivery. Various techniques such as phase separation, particulate leaching, electrospinning, and 3D printing are employed to create porous structures in scaffolds. The above methods were again used mainly for the preparation of scaffolds from the PLA copolymers with other biocompatible polyesters such as polyglycolide, poly(ε-caprolactone) or polyether – PEG.[171,186]

In the field of PLA/PVM copolymers, Spasova *et al.* combined the PLA block with a PDMAEMA block and used the resulting material to prepare fibrous mats *via* electrospinning.[187] The authors used two PLA stereoisomers *i.e.*, PLLA and PDLLA which resulted in the increase in melting temperature of the final copolymer. The presence of PDMAEMA blocks in mats material imparted hydrophilicity in contact with the body tissue. Moreover, the presence of tertiary amino groups imparted hemostatic and antibacterial properties which were shown by tests on blood cells on pathogenic microorganisms (see Fig. 10). Thus, the prepared PLA-based mats could have a possible application for wound healing as well as devices contacting with pathogenic microorganisms. Similarly, Toncheva *et al.* prepared antibacterial micro- and nanofibrous mats by electrospinning PLA grafted with PEG-acrylate.[188] These materials could find application as wound dressing materials or implants with antibacterial properties (reduced formation of bacterial biofilm).

An interesting PLA-based stimuli-responsive copolymer, promising for tissue engineering was prepared by Zhuang *et al.*[189] PLA-methacrylate was copolymerized radically with 2,2,6,6-tetrametylpiperidine-4-ylacrylamide (TAP). As a result of oxidation, the copolymer bearing PLA side chains and stable tetramethylpiperidine-N-oxyl radicals (PLA-g-PTAm) was obtained. The study of electrochemical properties indicated that prepared copolymer exhibited strongly reversible redox properties. Moreover, it exhibited good cell adhesion and improved cytocompatibility compared to the PTAm homopolymer attributed to the introduction of the biocompatible PLA moiety. These properties suggest that obtained electroactive material could have effects when in contact with fibroblasts, nerve cells, and osteoblasts which are sensitive to the electrical stimuli.[189]

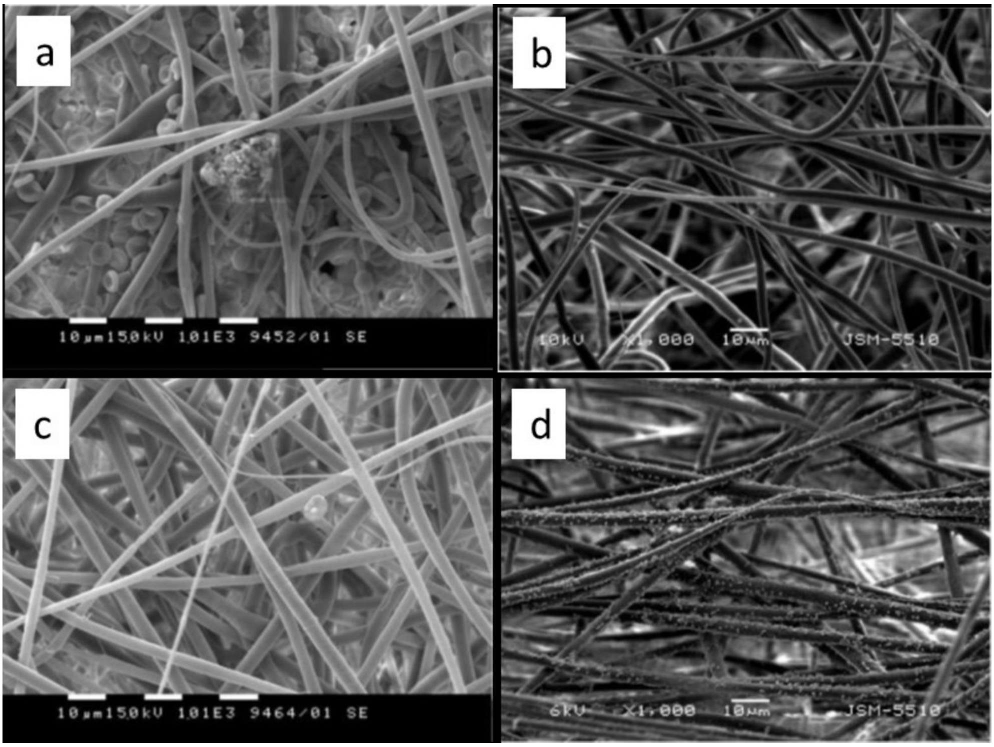

Figure 10. SEM micrographs of fibrous PLA-PDMAEMA mats after contact with human blood (a) and with *S.aureus* bacteria (b), and micrographs of high-molecular weight PLLA mats after contact with human blood (c) and with *S.aureus* bacteria (d) for comparison.[187] Adapted with permission from ACS, 2010.

4.3. Modification of the surface of inorganic medical devices

Copolymers of polylactide with certain vinyl monomers have shown utility in modifying the surfaces of metallic drug-eluting stents.[190] Typically, stents are coated with biodegradable polymers like PLLA, PLGA and PCL, however these coatings often experience defects such as cracking, peeling-off, and delamination. The reason for these problems is the difference in the physicochemical and mechanical properties between the metallic surface and the covering polymer. The physicochemical modification of the metallic stent surface is needed and the attachment of polymer brushes instead of biodegradable polymer alone seemed to fulfill this task. Thus, the authors covered Co-Cr alloy with PLA-based brushes composed of PHEMA-g-PLA copolymer growing from pretreated metal surface. The polymer layer loaded with the immunosuppressant - sirolimus exhibited improved durability, preventing peeling or delamination, and showed controlled drug release.

The functionalization of the inorganic surface with PHEMA-g-PLA brush copolymers was also performed for silica nanoparticles.[191] The authors activated the silica surface and initiated ATRP polymerization of HEMA, followed by ROP of lactide to form copolymer brushes on the surface of the silica particles. ATRP was performed again with an additional monomer, n-butyl acrylate (The procedure is shown in Fig. 11). The authors suggest that silica nanoparticles functionalized in this way could be useful in the field of biomaterials and chemical mechanical polishing.

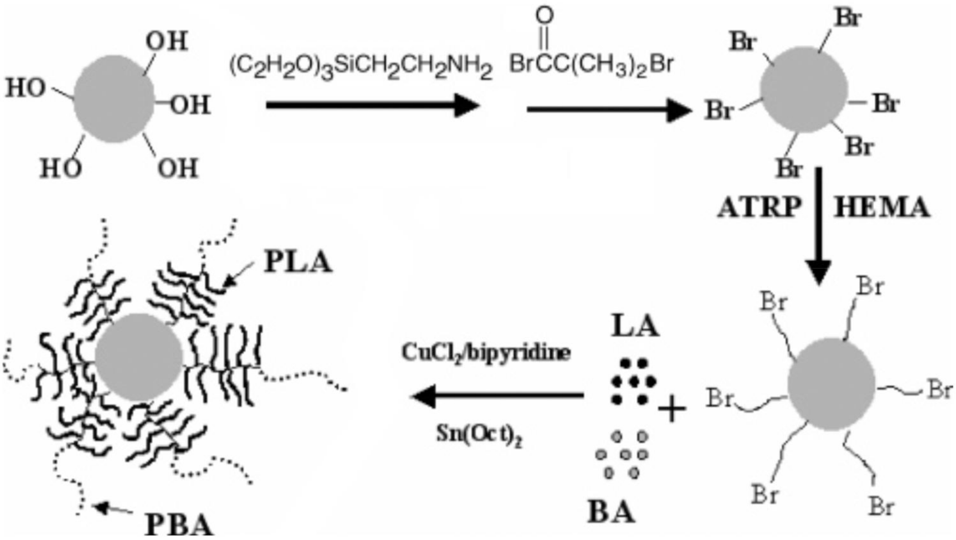

Figure 11. Reaction pathway of the preparation of comb-coil polymer brushes on the surface of silica nanoparticles.[191] Reproduced with permission from ACS, 2005.

5. Modification of PLA properties – synthesis of new materials for typical plastics applications

As mentioned in the introduction, polylactide (PLA) can be used as an alternative to traditional polymers in various industries such as textiles, electronics, and automotive. However, PLA's brittleness, with low elongation at break (up to 10%, typically ~5%) and impact strength (2–3 $\mathrm{kJ/m^2}$),[192] limits its widespread application. To address this, methods such as plasticization, copolymerization, and blending with flexible polymers or rubbers can be employed to reduce brittleness and enhance toughness, particularly impact toughness.

Plasticization generally results in a lower glass transition temperature of the matrix polymer and depends on the miscibility of the plasticizer with it. Therefore, plasticizers that are chemically similar to the polymer are typically employed. Small-molecular-weight plasticizers, which are the most efficient for PLA, include citric acid esters (such as triethyl citrate, tributyl citrate, acetyltriethyl citrate, and acetyltributyl citrate), but other ester-like plasticizers like glycerin triacetate, bis(2-ethylhexyl) adipate, sebacate, or laurate have also been tested.[193]

The use of small molecular weight plasticizers in melt blending often results in their evaporation and migration toward the surface of the final product. Therefore, oligomeric plasticizers (mainly PEG) and blends with more flexible polymers have been developed.[193] Blending PLA with other polymers, including poly(vinyl monomers) is a commonly used method to prepare materials based on PLA with modified physical properties.[194–198] However, it should be noted that the modification concerns comprehensive changes in properties, namely the improvement of the impact resistance and the elongation at break decreases brightness but usually results in lowering tensile strength and modulus. Instead of blends, copolymers are often synthesized which has this advantage over the blends that they avoid or at least limit incompatibility between different phases corresponding to different in-nature homopolymers. Both random and block copolymers of lactide/lactic acid were prepared by ring-opening polymerization and polycondensation. The first from the mentioned methods was effective in the synthesis of lactide copolymers with other cyclic monomers such as lactones, cyclic carbonates, and cyclic ethers.[193,199,200] However, PLA block was also combined with natural polymers or poly(vinyl monomers), particularly poly((meth)acrylates) as reported in the literature.

Block copolymers PLA/poly(meth)acrylate have modified thermal properties and usually increased toughness (increased impact strength) as in the case of block copolymers with PMMA and their blends with PLA[24] or block copolymers with poly(BD-co-MMA-co-BMA-co-HEMA) or poly(BD-co-MMA-co-BA-co-HEMA) (BD denotes butadiene).[201] The improvement of the same properties was also achieved in the case of PLA block copolymers with PMMA or PHEA or PtBA prepared by Wang *et al.*[23,202]

An interesting application was found for the copolymer (PLAMA-co-tBMA)-b-PEGMA which formed pH-sensitive micelles, *i.e.*, they were applied as additives to cement paste.[203] The presence of micelles altered the zeta potential of cement particles, leading to a better workability of cement paste through an accelerated rate of its hydration at later stages. As a final result, increased mechanical properties of the cement paste were observed.

Grafting PVM from polylactide by chemical reaction was performed to cover the PLA surface with another polymer. Thus, polylactide film was functionalized with a quaternary ammonium methacrylate by ATRP polymerization initiated from activated PLA surface.[204] The authors claim that these PLA films functionalized with charged methacrylate brushes with antimicrobial properties could be applied in packaging.

Graft copolymers - the special type of copolymers, consisting of blocks of different homopolymers, have been synthesized using polylactide chains incorporated both in main and side chains.[205] A variety of such copolymers was prepared *via* reactive blending/extrusion. Thus, although reactive blending/extrusion is considered as the method of compatible blends preparation, we decided to discuss in this review also such PLA-based materials containing blocks of poly(vinyl monomer) (or generally unsaturated monomer) because at reactive blending conditions, the initial homopolymers are effectively joined together forming graft copolymers. And the significance of this method in combining different homopolymers to obtain useful polymeric materials cannot be overlooked.

Grafting from polylactide or other polymer chains requires prior functionalization with reactive groups that react at processing conditions. One type of grafting is grafting through the radical process. At reactive blending conditions (high temperature and often the presence of radical initiators[205] radicals are generated along the polymer chain (along the PLA backbone). When another blended polymer is functionalized with unsaturated groups, the addition reaction results in grafting new polymer chains. Apart from the grafting process, crosslinking often occurs. For the purpose of polylactide plasticization during reactive blending/extrusion, PLA was often joined with PEG through grafting PEG-acrylate.[206–208]

Another type of grafting was achieved through the functionalization of one from the components with epoxy groups. Since PLA contains naturally –OH or –COOH groups,

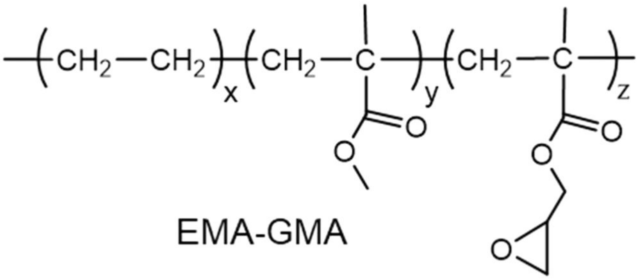

Figure 12. Structure of terpolymer EMA-GMA used as a compatibilizer in reactive blending of polyesters with different polymers.

they can react with epoxy groups linked to another blended polymer. Thus, some blended polymers were earlier functionalized with epoxy groups as *e.g.*, soybean oil[209] or natural rubber (NR).[210] PLA was also blended with commercial epoxy group containing compatibilizers as ethylene methyl acrylate-glycidyl methacrylate (EMA-GMA; trade name Lotader® AX8900) or ethylene butyl acrylate-glycidyl methacrylate (EBA-GMA; trade name Lotader® AX8750).[211,212] The compatibilizer structure is presented in Fig. 12. The above terpolymers were added to PLA alone or to its blends with other polymers or nanofillers.[213] The role of different compatibilizers (reacting with blended polymers due to the presence of reactive groups as well as many others not reacting) is to reduce the interfacial tension between separated phases and thereby decrease inclusions sizes.[198]

Other chain functionalization have also been used to link PLA with other polymers, with the functionalization with maleic anhydride (MAn) being particularly notable. PLA has been blended with many natural polymers by functionalizing PLA with MAn through radical attachment, followed by the reaction of the formed carboxyl groups with functional groups of cellulose or chitosan.[205] However, when joining natural rubber (NR) with PLA, it is primarily NR that is functionalized with maleic anhydride to enable the reaction with terminal PLA groups.[214,215]

Table 3 presents examples of compatible PLA/PVM blends prepared through reactive blending, effectively forming copolymers, along with the achieved modifications in properties. In some cases, potential applications for the resulting PLA-based materials have been suggested.

6. Conclusions and outlook

The significant area of application of block copolymers PLA/P(vinyl monomer) lies in biomedicine. In the field of biomedicine, PLA is combined with hydrophilic monomers to achieve self-organization into different micro/nanoparticles (with hydrophilic corona) for the delivery of biologically/pharmacologically active compounds or the preparation of thermo- and pH-responsive gels for tissue scaffolds. On the other hand, copolymers of PLA with hydrophilic blocks formed from vinyl monomers can serve as coatings for different medical devices that come into contact with body tissue. The inclusion of a hydrophilic component is crucial for ensuring good tolerance of the implanted device, such as a stent. With recent advancements in understanding the impact of traditionally

Table 3. (Co)polymers used for reactive blending with polylactide.

(Co)polymer to blend	Achieved toughening/plasticization	Possible application	Reference
PEG_A	T_g decrease by 15–24°, increase of elongation at break up to 380%	Flexible films	[206,207]
	38-fold increase in impact resistance, elongation at break 150%, efficient plasticization; partial crosslinking	—	[208]
biobased elastomer (PLBSI)	Significantly increased elongation at break, excellent processability	3D-printing material	[216]
Epoxidized soybean oil_ acrylate	Increase in impact strength (35 kJ/m^2) and elongation at break (11%)	Packaging, automotive, building and construction applications	[209]
NR_epoxy	Enormous increase in elongation at break, increase in shape recovery	Intelligent biomedical devices	[210]
MMA-co-GMA and PBAT	PLA/PBAT composites with equilibrated properties and melt stability	—	[217]
MMA-co-GMA and PVDF	Increased ductility	—	[218]
MMA-co-GMA and PASi-g-PMMA	Significant increase in impact strength (~100 kJ/m^2), improvement of heat resistance, preservation of transparency	—	[219]
MMA-co-BA-co-GMA (GACR)	Increase in tensile strength and elongation at break	—	[220]
MMA-BD-g-GMA; Core-shell particles added to PLA	Increase in impact strength and elongation at break	—	[221]
P(S-co-GMA) with PLA/ PMMA blend	Improved impact strength (by up to 60%), improved thermal properties and elongation at break with unaltered tensile strength and elastic modulus	—	[222]
EBA-GMA	Increase in impact strength; partial crosslinking	—	[212,223]
EBA-GMA	Increase in impact strength and elongation at brake to ~110 %dependent on blending temp.	—	[224]
EMA-GMA	Increase in impact strength	—	[211]
EMA-GMA and PP	Increase in elongation at break	—	[225]
EMA-GMA and LLDPE	Increase in impact strength (~50 kJ/m^2) and elongation at break up to 70%	—	[226]
EMA-GMA and PEBA	Great increase in the impact strength ~50 (70) kJ/m^2, and elongation at break up to 70%	Packaging and automotive parts	[227,228]
EMA-GMA and PEBA	Increase in fluidity, ductility and impact strength (elongation at break up to 70%)	—	[229]
EMA-GMA and PBAT	Increase in impact strength (62 kJ/m^2)	Packaging, agricultural film and 3D printing materials	[230]
EMA-GMA and PLA SC	Improvement of PLA melt stability, increased impact toughness (~65 kJ/m^2)	—	[231]
EMA-GMA and P(olefin)	Increase in impact strength (50 kJ/m^2)	—	[232]
EMA-GMA and PU	Improved impact strength (78 kJ/m^2)	—	[233]
EMA-GMA and EPDM	Increase in impact strength and elongation at break	—	[234]
EMA-GMA and nanofiller - zirconium phosphate	Increase in impact strength (71.5 kJ/ m^2) and elongation at break	—	[235]

(*continued*)

Table 3. Continued.

(Co)polymer to blend	Achieved toughening/plasticization	Possible application	Reference
EVMG and PLA SC	Impact toughness $>70\,kJ/m^2$ and heat resistance	—	[236]
NR_maleate	Increase in impact strength and elongation at break, improved thermal stability	—	[214,237]
NR_maleate	Improved thermal stability	—	[238]
NR_maleate	Increase in impact strength	—	[215]

PLBSI: poly (lactate/butanediol/sebacate/itaconate) bioelastomer containing 40% molar ratio of lactic acid to the total reactants; NR_epoxy: epoxidized natural rubber; PBAT: poly(butylene-adipate-co-terephtalate); PVDF: polyvinylidene fluoride; PASi-g-PMMA: a core-shell modifier with the crosslinked butyl acrylate and silicone copolymer as the core and PMMA as the shell; GACR: glycidyl methacrylate-functionalized methyl methacrylate–butyl acrylate core–shell copolymer; MMA-BD-g-GMA: glycidyl methacrylate-functionalized methyl methacrylate–butadiene core-shell particles; PP: polypropylene; LLDPE: linear low density polyethylene; PEBA: poly(ether-b-amide) elastomeric copolymer; PLA SC: polylactide stereocomplex (PDLLA + PLLA); P(olefin); PU: polyurethane; EFDM: ethylene-propylene-diene-rubber; EVMG: ethylene – vinyl acetate – glycidyl methacrylate elastomer; PEVA: poly(ethylene-*co*-vinyl acetate).
The meaning of other abbreviations is the same as for Table 1 and in the text of this section.

used polymers like PEG, there is great potential for replacing them in their “stealth” function with other polymers, including PVMs, to further develop drug delivery systems and materials for contact with living tissues.

It seems that currently developing non-medical applications of PLA/PVM copolymers are no less important. The application which uses polylactide/polystyrene block copolymer not directly but after removing etchable PLA block concerns porous membranes. These membranes can be employed in various areas such as water filtration, catalysis, and nanotemplating. Advances in the synthesis of complex copolymer architectures such as polymer brushes, have enabled the development of filtration membranes with efficient water uptake and desired permeability, expanding the range of materials currently in use. The application of well-defined porous polystyrene materials as templates for semiconductor production in various electronic applications, such as photovoltaic cells, also shows promising development prospect.

Block copolymers of PLA with PVM are also formed during reactive extrusion, a processing method rapidly developing and highly suitable for large-scale production of useful materials with properties modified for specific applications. In the case of PLA-based materials, reactive extrusion allows the inherently brittle PLA to be toughened, increasing flexibility and impact resistance by combining PLA chains with chains of different in-nature polymers. The grafted PVM units in reactive extrusion also act as compatibilizer between immiscible components in PLA blends. Reactive extrusion/blending, as forming PLA copolymers *in situ*, can lead to the largest (by mass) production and application of graft PLA copolymers including PLA/PVM. Although these materials combine bio-derived and petroleum-based polymers, they can help reduce the overall consumption of the latter while promoting partial degradability. This aligns with ongoing efforts to minimize the negative human impact on the environment.

We have no access to the current data regarding the market share of materials based on the PLA in combination with PVM. However, the global PLA production capacity in 2021 was about 670,000 tons.[239] The world’s leading manufacturer of polylactide is NatureWorks (USA) with the annual PLA production capacity of 150,000 ton (22% of the global production in 2021). They are currently realizing a new PLA manufacturing complex in Thailand (construction of the new production site began in June 2022 with an expected completion in the second half of 2024). Other leading suppliers also contribute to the ever-increasing production (TotalEnergies Corbion, France/Netherlands – 75,000 ton production capacity, 11%, Shandong Hongda Biotech, China – 24%, other Chinese suppliers −14% [239]) Nature Works produces and sells PLA under the tradename Ingeo™ for various purposes such as: (1) extrusion and thermoreforming, (2) injection molding, (3) films, (4) fibers and nonwovens, (5) 3D printing. All these techniques can be used also for PLA/PVM copolymers/blends to achieve specific modifications and, of course, taking into account the copolymer's ability to meet processing requirements.

Companies currently producing packaging materials (including films) or disposable tableware (that should be compostable) using commercial PLA can improve them by adding, for example, epoxidized soybean oil-acrylate to increase impact strength and elongation at break. The combination of PLA with other commercial polyesters such as PBAT (Ecoflex) with the addition of compatibilizer are promising as agricultural films and also packaging materials with increased impact strength. PLA is one of the most popular filaments for 3D printing techniques. Nanocomposites and blends with other polymers are prepared to increase the strength of printed items. Also additives of other polymers incorporated into the PLA matrix through reactive blending could strengthen PLA filaments for 3D printing on one hand and decrease the printing temperature on the other hand. PLA fibers and nonwoven produced for textile industry, as well as automotive and hygienic disposals could be also modified by the addition of other polymers. The same applies for the production of parts for electronics and daily use items (such as mobiles, computers, etc.). There is no point in listing all the possibilities here. It seems that the mass production of such materials may be developed soon, taking into account the dynamics of global polylactide production combined with the growing demand for environmentally friendly polymers.

Disclosure statement

No potential conflict of interest was reported by the authors.

Funding

This work was supported by the National Science Centre in Poland under Grant no 2018/31/B/ST8/01969. M. Grabowski acknowledges Bio-Med-Chem Doctoral School of the University of Lodz and Lodz Institutes of the Polish Academy of Sciences.

ORCID

Melania Bednarek http://orcid.org/0000-0003-1445-9878
Mateusz Grabowski http://orcid.org/0000-0003-1638-593X

References

1. Dorgan, J. R.; Lehermeier, H.; Mang, M. Thermal and Rheological Properties of Commercial-Grade Poly (Lactic Acid) S. *J. Polym. Environ.* **2000**, *8*, 1–9. . DOI: 10.1023/A:1010185910301.

2. Balla, E.; Daniilidis, V.; Karlioti, G.; Kalamas, T.; Stefanidou, M.; Bikiaris, N. D.; Vlachopoulos, A.; Koumentakou, I.; Bikiaris, D. N. Poly(Lactic Acid): A Versatile Biobased Polymer for the Future with Multifunctional Properties - From Monomer Synthesis, Polymerization Techniques and Molecular Weight Increase to PLA Applications. *Polymers*. **2021**, *13*, 1822. DOI: 10.3390/polym13111822.
3. Jimenez, A.; Peltzer, M.; Ruseckaite, R. *Poly(Lactic Acid) Science and Technology: Processing, Properties, Additives and Applications*; RSC: Cambridge, **2015**.
4. Nagarajan, V.; Mohanty, A. K.; Misra, M. Perspective on Polylactic Acid (PLA) Based Sustainable Materials for Durable Applications: Focus on Toughness and Heat Resistance. *ACS Sustainable Chem. Eng.* **2016**, *4*, 2899–2916. DOI: 10.1021/acssuschemeng.6b00321.
5. Auras, R.; Harte, B.; Selke, S. An Overview of Polylactides as Packaging Materials. *Macromol. Biosci.* **2004**, *4*, 835–864. DOI: 10.1002/mabi.200400043.
6. Södergård, A.; Stolt, M. Properties of Lactic Acid Based Polymers and Their Correlation with Composition. *Prog. Polym. Sci.* **2002**, *27*, 1123–1163. DOI: 10.1016/S0079-6700(02)00012-6.
7. Rasal, R. M.; Janorkar, A. V.; Hirt, D. E. Poly(Lactic Acid) Modifications. *Prog. Polym. Sci.* **2010**, *35*, 338–356. DOI: 10.1016/j.progpolymsci.2009.12.003.
8. Ulery, B. D.; Nair, L. S.; Laurencin, C. T. Biomedical Applications of Biodegradable Polymers. *J. Polym. Sci. B Polym. Phys.* **2011**, *49*, 832–864. DOI: 10.1002/polb.22259.
9. Armentano, I.; Bitinis, N.; Fortunati, E.; Mattioli, S.; Rescignano, N.; Verdejo, R.; Lopez-Manchado, M. A.; Kenny, J. M. Multifunctional Nanostructured PLA Materials for Packaging and Tissue Engineering. *Prog. Polym. Sci.* **2013**, *38*, 1720–1747. DOI: 10.1016/j.progpolymsci.2013.05.010.
10. Oh, J. K. Polylactide (PLA)-Based Amphiphilic Block Copolymers: Synthesis, Self-Assembly, and Biomedical Applications. *Soft Matter*. **2011**, *7*, 5096–5108. . DOI: 10.1039/c0sm01539c.
11. DeStefano, V.; Khan, S.; Tabada, A. Applications of PLA in Modern Medicine. *Eng. Regen.* **2020**, *1*, 76–87. DOI: 10.1016/j.engreg.2020.08.002.
12. Muller, A.; Borisov, O. *Self Organized Nanostructures of Amphiphilic Block Copolymers I*; Springer: Heidelberg, **2011**.
13. Hamley, I. *The Physics of Block Copolymers*; Oxford University Press: Oxford, **1998**.
14. Corrigan, N.; Jung, K.; Moad, G.; Hawker, C. J.; Matyjaszewski, K.; Boyer, C. Reversible-Deactivation Radical Polymerization (Controlled/Living Radical Polymerization): from Discovery to Materials Design and Applications. *Prog. Polym. Sci.* **2020**, *111*, 101311. DOI: 10.1016/j.progpolymsci.2020.101311.
15. Yildirim, I.; Weber, C.; Schubert, U. S. Old Meets New: Combination of PLA and RDRP to Obtain Sophisticated Macromolecular Architectures. *Prog. Polym. Sci.* **2018**, *76*, 111–150. DOI: 10.1016/j.progpolymsci.2017.07.010.
16. Gigmes, D.; Trimaille, T. Advances in Amphiphilic Polylactide/Vinyl Polymer Based Nano-Assemblies for Drug Delivery. *Adv. Colloid Interface Sci.* **2021**, *294*, 102483. DOI: 10.1016/j.cis.2021.102483.
17. Dove, A. P. Controlled Ring-Opening Polymerisation of Cyclic Esters: Polymer Blocks in Self-Assembled Nanostructures. *Chem. Commun.* **2008**, *48*, 6446–6470. DOI: 10.1039/b813059k.
18. Maharana, T.; Pattanaik, S.; Routaray, A.; Nath, N.; Sutar, A. K. Synthesis and Characterization of Poly(Lactic Acid) Based Graft Copolymers. *React. Funct. Polym.* **2015**, *93*, 47–67. DOI: 10.1016/j.reactfunctpolym.2015.05.006.
19. Stefaniak, K.; Masek, A. Green Copolymers Based on Poly(Lactic Acid)—Short Review. *Materials* **2021**, *14*, 5254. DOI: 10.3390/ma14185254.
20. Shin, J.; Kim, Y. W.; Kim, G. J. Sustainable Block Copolymer-Based Thermoplastic Elastomers. *Appl. Chem. Eng.* **2014**, *25*, 121–133. DOI: 10.14478/ace.2014-1025.
21. Song, J.; Xu, J.; Pispas, S.; Zhang, G. One-Pot Synthesis of Poly(L-Lactide)-b-Poly(Methyl Methacrylate) Block Copolymers. *RSC Adv.* **2015**, *5*, 38243–38247. DOI: 10.1039/C4RA17202G.

22. Tao, L.; Luan, B.; Pan, C. Y. Block and Star Block Copolymers by Mechanism Transformation. VIII Synthesis and Characterization of Triblock Poly(LLA-b-St-b-MMA) by Combination of ATRP and ROP. *Polymer* **2003**, *44*, 1013–1020. DOI: 10.1016/S0032-3861(02)00870-4.
23. Wang, W. W.; Ren, W. Y.; Jiang, L.; Dan, Y. Synthesis and Characterization of AB-Type Copolymers Poly(L-Lactide)-Block-Poly(Methyl Methacrylate) via a Convenient Route Combining ROP and ATRP from a Dual Initiator. *J. Appl. Polym. Sci.* **2010**, *118*, 2379–2388. DOI: 10.1002/app.32208.
24. Choochottiros, C.; Park, E.; Chin, I. J. Synthesis and Characterization of Polylactide-Poly(Methyl Methacrylate) Copolymer by Combining of ROP and AGET ATRP. *J. Ind. Eng. Chem.* **2012**, *18*, 993–1000. DOI: 10.1016/j.jiec.2011.11.153.
25. Zhao, Y.; Shuai, X.; Chen, C.; Xi, F. Synthesis of Novel Dendrimer-like Star Block Copolymers with Definite Numbers of Arms by Combination of ROP and ATRP. *Chem Commun.* **2004**, *4*, 1608–1609. DOI: 10.1039/b404143g.
26. Ye, C.; Zhao, G.; Zhang, M.; Du, J.; Zhao, Y. Precise Synthesis of ABCDE Star Quintopolymers by Combination of Controlled Polymerization and Azide-Alkyne Cycloaddition Reaction. *Macromolecules* **2012**, *45*, 7429–7439. DOI: 10.1021/ma3015118.
27. Kang, H. U.; Yu, Y. C.; Shin, S. J.; Youk, J. H. One-Step Synthesis of Block Copolymers Using a Hydroxyl-Functionalized Trithiocarbonate RAFT Agent as a Dual Initiator for RAFT Polymerization and ROP. *J. Polym. Sci. A Polym. Chem.* **2013**, *51*, 774–779. DOI: 10.1002/pola.26464.
28. Xia, Y.; Olsen, B. D.; Kornfield, J. A.; Grubbs, R. H. Efficient Synthesis of Narrowly Dispersed Brush Copolymers and Study of Their Assemblies: The Importance of Side Chain Arrangement. *J. Am. Chem. Soc.* **2009**, *131*, 18525–18532. DOI: 10.1021/ja908379q.
29. Wolf, F. F.; Friedemann, N.; Frey, H. Poly (Lactide) - Block -Poly (HEMA) Block Copolymers : An Orthogonal One-Pot Combination of ROP and ATRP, Using a Bifunctional Initiator. *Macromolecules* **2009**, *42*, 5622–5628. DOI: 10.1021/ma900894d.
30. Pratt, R. C.; Lohmeijer, B. G. G.; Long, D. A.; Lundberg, P. N. P.; Dove, A. P.; Li, H.; Wade, C. G.; Waymouth, R. M.; Hedrick, J. L. Exploration, Optimization, and Application of Supramolecular Thiourea-Amine Catalysts for the Synthesis of Lactide (Co)Polymers. *Macromolecules* **2006**, *39*, 7863–7871. DOI: 10.1021/ma061607o.
31. Seo, M.; Amendt, M. A.; Hillmyer, M. A. Cross-Linked Nanoporous Materials from Reactive and Multifunctional Block Polymers. *Macromolecules* **2011**, *44*, 9310–9318. DOI: 10.1021/ma2013942.
32. Zhao, C.; Wu, D.; Huang, N. A. N.; Zhao, H. Crystallization and Thermal Properties of PLLA Comb Polymer. *J. Polym. Sci. B Polym. Phys.* **2008**, *46*, 589–598. DOI: 10.1002/polb.21394.
33. Wu, D.; Yang, Y.; Cheng, X.; Liu, L.; Tian, J.; Zhao, H. Mixed Molecular Brushes with PLLA and PS Side Chains Prepared by AGET ATRP and Ring-Opening Polymerization. *Macromolecules* **2006**, *39*, 7513–7519. DOI: 10.1021/ma061141+.
34. Hu, F.; Neoh, K. G.; Kang, E. T. Synthesis of Folic Acid Functionalized PLLA-b-PPEGMA Nanoparticles for Cancer Cell Targeting. *Macromol. Rapid Commun.* **2009**, *30*, 609–614. DOI: 10.1002/marc.200800771.
35. Mao, J.; Ji, X.; Bo, S. Synthesis and PH/Temperature-Responsive Behavior of PLLA-b-PDMAEMA Block Polyelectrolytes Prepared via ROP and ATRP. *Macro. Chem. Phys.* **2011**, *212*, 744–752. DOI: 10.1002/macp.201000672.
36. Kryuchkov, M. A.; Detrembleur, C.; Bazuin, C. G. Linear Amphiphilic Diblock Copolymers of Lactide and 2-Dimethylaminoethyl Methacrylate Using Bifunctional-Initiator and One-Pot Approaches. *Polymer* **2014**, *55*, 2316–2324. DOI: 10.1016/j.polymer.2014.04.007.
37. Petzetakis, N.; Dove, A. P.; O'Reilly, R. K. Cylindrical Micelles from the Living Crystallization-Driven Self-Assembly of Poly(Lactide)-Containing Block Copolymers. *Chem. Sci.* **2011**, *2*, 955–960. DOI: 10.1039/C0SC00596G.

38. Themistou, E.; Battaglia, G.; Armes, S. P. Facile Synthesis of Thiol-Functionalized Amphiphilic Polylactide- Methacrylic Diblock Copolymers. *Polym. Chem.* **2014**, *5*, 1405–1417. DOI: 10.1039/C3PY01446K.
39. Yuan, W.; Zhang, J.; Wei, J.; Zhang, C.; Ren, J. Synthesis and Self-Assembly of PH-Responsive Amphiphilic Dendritic Star-Block Terpolymer by the Combination of ROP, ATRP and Click Chemistry. *Eur. Polym. J.* **2011**, *47*, 949–958. DOI: 10.1016/j.eurpolymj.2011.01.002.
40. Bagheri, M.; Motirasoul, F. Synthesis, Characterization, and Micellization of Cholesteryl-Modified Amphiphilic Poly(L-Lactide)-Block-Poly(Glycidyl Methacrylate) as a Nanocarrier for Hydrophobic Drugs. *J. Polym. Res.* **2013**, *20*, 59. DOI: 10.1007/s10965-012-0059-3.
41. Luo, H.; Santos, J. L.; Herrera-Alonso, M. Toroidal Structures from Brush Amphiphiles. *Chem. Commun.* **2014**, *50*, 536–538. DOI: 10.1039/c3cc46834h.
42. Huang, K.; Rzayev, J. Well-Defined Organic Nanotubes from Multicomponent Bottlebrush Copolymers. *J. Am. Chem. Soc.* **2009**, *131*, 6880–6885. DOI: 10.1021/ja901936g.
43. Yang, Y. Q.; Lin, W. J.; Zhao, B.; Wen, X. F.; Guo, X. D.; Zhang, L. J. Synthesis and Physicochemical Characterization of Amphiphilic Triblock Copolymer Brush Containing PH-Sensitive Linkage for Oral Drug Delivery. *Langmuir* **2012**, *28*, 8251–8259. DOI: 10.1021/la301099q.
44. Shi, P. J.; Li, Y. G.; Pan, C. Y. Block and Star Block Copolymers by Mechanism Transformation X. Synthesis of Poly(Ethylene Oxide) Methyl Ether/Polystyrene/Poly(L-Lactide) ABC Miktoarm Star Copolymers by Combination of RAFT and ROP. *Eur. Polym. J.* **2004**, *40*, 1283–1290. DOI: 10.1016/j.eurpolymj.2004.02.024.
45. Saeed, A. O.; Dey, S.; Howdle, S. M.; Thurecht, K. J.; Alexander, C. One-Pot Controlled Synthesis of Biodegradable and Biocompatible Co-Polymer Micelles. *J. Mater. Chem.* **2009**, *19*, 4529–4535. DOI: 10.1039/b821736j.
46. Nim, B.; Opaprakasit, P. Spectrochimica Acta Part A : Molecular and Biomolecular Spectroscopy Quantitative Analyses of Products from Chemical Recycling of Polylactide (PLA) by Alcoholysis with Various Alcohols and Their Applications as Healable Lactide-Based Polyurethanes. *Spectrochim. Acta. A Mol. Biomol. Spectrosc.* **2021**, *255*, 119684. DOI: 10.1016/j.saa.2021.119684.
47. Liu, G.; Hu, X.; Chen, C.; Ji, J. Construct Biomimetic Giant Vesicles via Self-Assembly of Poly(2-Methacryloyloxyethyl Phosphorylcholine)-Block-Poly(D,L-Lactide). *J. Appl. Polym. Sci.* **2010**, *118*, 3197–3202. DOI: 10.1002/app.32758.
48. Finnegan, M.; Mallon, G.; Leach, A.; Themistou, E. Electrosprayed Cysteine-Functionalized Degradable Amphiphilic Block Copolymer Microparticles for Low PH-Triggered Drug Delivery. *Polym. Chem.* **2019**, *10*, 5814–5820. DOI: 10.1039/C9PY01221D.
49. Vora, A.; Singh, K.; Webster, D. C. A New Approach to 3-Miktoarm Star Polymers Using a Combination of Reversible Addition-Fragmentation Chain Transfer (RAFT) and Ring Opening Polymerization (ROP) via “Click” Chemistry. *Polymer* **2009**, *50*, 2768–2774. DOI: 10.1016/j.polymer.2009.03.054.
50. Ko, N. R.; Yao, K.; Tang, C.; Oh, J. K. Synthesis and Thiol-Responsive Degradation of Polylactide-Based Block Copolymers Having Disulfide Junctions Using ATRP and ROP. *J. Polym. Sci. Part A: Polym. Chem.* **2013**, *51*, 3071–3080. DOI: 10.1002/pola.26335.
51. Messman, J. M.; Scheuer, A. D.; Storey, R. F. Synthesis and Characterization of A-B-a Triblock Copolymers Derived from Chloro-Telechelic Poly(l-Lactide): Combining Ring-Opening Polymerization (ROP) and Atom Transfer Radical Polymerization (ATRP). *Polymer* **2005**, *46*, 3628–3638. DOI: 10.1016/j.polymer.2005.03.023.
52. Blunden, B. M.; Lu, H.; Stenzel, M. H. Enhanced Delivery of the RAPTA-C Macromolecular Chemotherapeutic by Conjugation to Degradable Polymeric Micelles. *Biomacromolecules* **2013**, *14*, 4177–4188. DOI: 10.1021/bm4013919.
53. Handké, N.; Lahaye, V.; Bertin, D.; Delair, T.; Verrier, B.; Gigmes, D.; Trimaille, T. Elaboration of Glycopolymer-Functionalized Micelles from an N-Vinylpyrrolidone/Lactide-Based Reactive Copolymer Platform. *Macromol. Biosci.* **2013**, *13*, 1213–1220. DOI: 10.1002/mabi.201300102.

54. Sun, L.; Pitto-Barry, A.; Kirby, N.; Schiller, T. L.; Sanchez, A. M.; Dyson, M. A.; Sloan, J.; Wilson, N. R.; O'Reilly, R. K.; Dove, A. P. Structural Reorganization of Cylindrical Nanoparticles Triggered by Polylactide Stereocomplexation. *Nat. Commun.* **2014**, *5*, 5746. DOI: 10.1038/ncomms6746.
55. Pal, A.; Pal, S. Synthesis of Poly (Ethylene Glycol)-Block-Poly (Acrylamide)-Block-Poly (Lactide) Amphiphilic Copolymer through ATRP, ROP and Click Chemistry: Characterization, Micellization and PH-Triggered Sustained Release Behaviour. *Polymer* **2017**, *127*, 150–158. DOI: 10.1016/j.polymer.2017.08.048.
56. Akimoto, J.; Nakayama, M.; Sakai, K.; Okano, T. Molecular Design of Outermost Surface Functionalized Thermoresponsive Polymeric Micelles with Biodegradable Cores. *J. Polym. Sci. A Polym. Chem.* **2008**, *46*, 7127–7137. DOI: 10.1002/pola.23017.
57. Mespouille, L.; Nederberg, F.; Hedrick, J. L.; Dubois, P. Broadening the Scope of Functional Groups Accessible in Aliphatic Polycarbonates by the Introduction of RAFT Initiating Sites. *Macromolecules* **2009**, *42*, 6319–6321. DOI: 10.1021/ma900582z.
58. Hales, M.; Barner-Kowollik, C.; Davis, T. P.; Stenzel, M. H. Shell-Cross-Linked Vesicles Synthesized from Block Copolymers of Poly(D,L-Lactide) and Poly(N-Isopropyl Acrylamide) as Thermoresponsive Nanocontainers. *Langmuir* **2004**, *20*, 10809–10817. DOI: 10.1021/la0484016.
59. Kim, S. H.; Tan, J. P. K.; Nederberg, F.; Fukushima, K.; Yang, Y. Y.; Waymouth, R. M.; Hedrick, J. L. Mixed Micelle Formation through Stereocomplexation between Enantiomeric Poly(Lactide) Block Copolymers. *Macromolecules* **2009**, *42*, 25–29. DOI: 10.1021/ma801739x.
60. Hu, Y.; Darcos, V.; Monge, S.; Li, S. Synthesis and Self-Assembling of Poly(N-Isopropylacrylamide-Block-Poly(L -Lactide)-Block-Poly(N-Isopropylacrylamide) Triblock Copolymers Prepared by Combination of Ring-Opening Polymerization and Atom Transfer Radical Polymerization. *J. Polym. Sci.* **2013**, *51*, 3274–3283. DOI: 10.1002/pola.26721.
61. Zhang, W.; Wang, S.; Li, X.; Yuan, J.; Wang, S. Organic/Inorganic Hybrid Star-Shaped Block Copolymers of Poly(l-Lactide) and Poly(N-Isopropylacrylamide) with a Polyhedral Oligomeric Silsesquioxane Core: Synthesis and Self-Assembly. *Eur. Polym. J.* **2012**, *48*, 720–729. DOI: 10.1016/j.eurpolymj.2012.01.019.
62. Samarajeewa, S.; Ibricevic, A.; Gunsten, S. P.; Shrestha, R.; Elsabahy, M.; Brody, S. L.; Wooley, K. L. Degradable Cationic Shell Cross-Linked Knedel-like Nanoparticles: Synthesis, Degradation, Nucleic Acid Binding, and in Vitro Evaluation. *Biomacromolecules* **2013**, *14*, 1018–1027. DOI: 10.1021/bm3018774.
63. Du, N.; Guo, W.; Yu, Q.; Guan, S.; Guo, L.; Shen, T.; Tang, H.; Gan, Z. Poly(d,l-Lactic Acid)-: Block -Poly(N -(2-Hydroxypropyl)Methacrylamide) Nanoparticles for Overcoming Accelerated Blood Clearance and Achieving Efficient anti-Tumor Therapy. *Polym. Chem.* **2016**, *7*, 5719–5729. DOI: 10.1039/C6PY01113F.
64. Dirany, M.; Lacroix-Desmazes, P.; Vayer, M.; Erre, R.; Boutevin, B.; Sinturel, C. Polystyrene-Block-Polylactide Obtained by the Combination of Atom Transfer Radical Polymerization and Ring-Opening Polymerization with a Commercial Dual Initiator. *J. Appl. Polym. Sci.* **2011**, *122*, 2944–2951. DOI: 10.1002/app.34101.
65. Gorzolnik, B.; Davidson, P.; Beurroies, I.; Denoyel, R.; Daniel, G. Novel Functional Mesoporous Materials Obtained from Nanostructured Diblock Copolymers. *Macromol. Symp.* **2010**, *287*, 127–134. DOI: 10.1002/masy.201050118.
66. Zhang, L.; Nederberg, F.; Pratt, R. C.; Waymouth, R. M.; Hedrick, J. L.; Wade, C. G. Phosphazene Bases: A New Category of Organocatalysts for the Living Ring-Opening Polymerization of Cyclic Esters. *Macromolecules* **2007**, *40*, 4154–4158. DOI: 10.1021/ma070316s.
67. Vinas, J.; Chagneux, N.; Gigmes, D.; Trimaille, T.; Favier, A.; Bertin, D. SG1-Based Alkoxyamine Bearing a N-Succinimidyl Ester: A Versatile Tool for Advanced Polymer Synthesis. *Polymer* **2008**, *49*, 3639–3647. DOI: 10.1016/j.polymer.2008.06.017.

68. Ho, R. M.; Chiang, Y. W.; Tsai, C. C.; Lin, C. C.; Ko, B. T.; Huang, B. H. Three-Dimensionally Packed Nanohelical Phase in Chiral Block Copolymers. *J. Am. Chem. Soc.* **2004**, *126*, 2704–2705. DOI: 10.1021/ja039627i.
69. Jabbar, R.; Graffe, A.; Lessard, B.; Marić, M. Nitroxide-Mediated Synthesis of Styrenic-Based Segmented and Tapered Block Copolymers Using Poly(Lactide)-Functionalized TEMPO Macromediators. *J. Appl. Poly. Sci.* **2008**, *109*, 3185–3195. DOI: 10.1002/app.28377.
70. Rzayev, J.; Hillmyer, M. A. Nanoporous Polystyrene Containing Hydrophilic Pores from an ABC Triblock Copolymer Precursor. *Macromolecules* **2005**, *38*, 3–5. DOI: 10.1021/ma00020a042.
71. Stanford, M. J.; Dove, A. P. One-Pot Synthesis of a,ω -Chain End Functional, Stereoregular, Star-Shaped Poly(Lactide). *Macromolecules* **2009**, *42*, 141–147. DOI: 10.1021/ma801977e.
72. Crossland, E. J. W.; Ludwigs, S.; Hillmyer, M. A.; Steiner, U. Freestanding Nanowire Arrays from Soft-Etch Block Copolymer Templates. *Soft Matter.* **2007**, *3*, 94–98. DOI: 10.1039/b609780d.
73. Yu, T. L.; Huang, B. H.; Hung, W. C.; Lin, C. C.; Wang, T. C.; Ho, R. M. Preparation and Characterization of Poly(ε-Caprolactone)-b-Polyacrylonitrile (PCL-b-PAN) and Poly(l-Lactide)-b-Polyacrylonitrile (PLLA-b-PAN) Copolymers by Aluminum and Lithium Alkoxides Containing Double-Headed Initiators. *Polymer* **2007**, *48*, 4401–4411. DOI: 10.1016/j.polymer.2007.05.044.
74. Grabowski, M.; Kost, B.; Kubisa, P.; Bednarek, M. A New Approach to the Synthesis of Polylactide/Polyacrylonitrile Block Copolymers. *Polymers* **2022**, *14*, 1529. DOI: 10.3390/polym14081529.
75. Chung, T. M.; Wang, H. F.; Lin, T.; Chiang, Y. W.; Chen, Y. C.; Ko, B. T.; Ho, R. M. Helical Phase Driven by Solvent Evaporation in Self-Assembly of Poly(4-Vinylpyridine)-Block -Poly(l -Lactide) Chiral Block Copolymers. *Macromolecules* **2012**, *45*, 9727–9733. DOI: 10.1021/ma302159p.
76. Shin, S. J.; Yu, Y. C.; Seo, J. D.; Cho, S. J.; Youk, J. H. One-Step Synthesis of Poly(N-Vinylpyrrolidone)-b-Poly(l -Lactide) Block Copolymers Using a Dual Initiator for RAFT Polymerization and ROP. *J. Polym. Sci. Part A: Polym. Chem.* **2014**, *52*, 1607–1613. DOI: 10.1002/pola.27160.
77. Ramesh, K.; Mishra, A. K.; Patel, V. K.; Vishwakarma, N. K.; Biswas, C. S.; Paira, T. K.; Mandal, T. K.; Maiti, P.; Misra, N.; Ray, B. Synthesis of Well-Defined Amphiphilic Poly(d,l-Lactide)-b-Poly(N- Vinylpyrrolidone) Block Copolymers Using ROP and Xanthate-Mediated RAFT Polymerization. *Polymer* **2012**, *53*, 5743–5753. DOI: 10.1016/j.polymer.2012.10.009.
78. Hira, S. K.; Ramesh, K.; Gupta, U.; Mitra, K.; Misra, N.; Ray, B.; Manna, P. P. Methotrexate-Loaded Four-Arm Star Amphiphilic Block Copolymer Elicits CD8+ T Cell Response against a Highly Aggressive and Metastatic Experimental Lymphoma. *ACS Appl. Mater. Interfaces.* **2015**, *7*, 20021–20033. DOI: 10.1021/acsami.5b04905.
79. Mishra, A. K.; Park, J.; Joseph, K. L. V.; Maiti, S.; Kwak, J.; Choi, C.; Hyun, S.; Kim, J. K. Synthesis and Self-Assembly of Amphiphilic and Biocompatible Poly(Vinyl Alcohol)-Block-Poly(L-Lactide) Copolymer. *Polymer* **2016**, *100*, 28–36. DOI: 10.1016/j.polymer.2016.08.005.
80. Ojha, U.; Kulkarni, P.; Singh, J.; Faust, R. Syntheses, Characterization, and Properties of Multiblock Copolymers Consisting of Polyisobutylene and Poly(L-Lactide) Segments. *J. Polym. Sci. A Polym. Chem.* **2009**, *47*, 3490–3505. DOI: 10.1002/pola.23428.
81. Frick, E. M.; Hillmyer, M. A. Synthesis and Characterization of Polylactide-Block-Polyisoprene-Block-Polylactide Triblock Copolymers: New Thermoplastic Elastomers Containing Biodegradable Segments. *Macromol. Rapid Commun.* **2000**, *21*, 1317–1322. DOI: 10.1002/1521-3927(20001201)21:18<1317::AID-MARC1317>3.0.CO;2-B.

82. Gramlich, W. M.; Theryo, G.; Hillmyer, M. A. Copolymerization of Isoprene and Hydroxyl Containing Monomers by Controlled Radical and Emulsion Methods. *Polym. Chem.* **2012**, *3*, 1510–1516. DOI: 10.1039/c2py20072d.
83. Bates, F. Polymer-Polymer Phase Behavior. *Science* **1991**, *251*, 898–905. DOI: 10.1126/science.251.4996.898.
84. Feng, H.; Lu, X.; Wang, W.; Kang, N. G.; Mays, J. W. Block Copolymers: Synthesis, Self-Assembly, and Applications. *Polymers* **2017**, *9*, 494. DOI: 10.3390/polym9100494.
85. Hamley, J. *Block Copolymers in Solution: Fundamentals and Applications*; Wiley & Sons, Ltd: Chichester, UK, **2005**.
86. Zhang, L.; Lin, J.; Lin, S. Self-Assembly Behavior of Amphiphilic Block Copolymer/Nanoparticle Mixture in Dilute Solution Studied by Self-Consistent-Field Theory/Density Functional Theory. *Macromolecules* **2007**, *40*, 5582–5592. DOI: 10.1021/ma070986y.
87. Blanazs, A.; Armes, S. P.; Ryan, A. J. Self-Assembled Block Copolymer Aggregates: From Micelles to Vesicles and Their Biological Applications. *Macromol. Rapid Commun.* **2009**, *30*, 267–277. DOI: 10.1002/marc.200800713.
88. Rodriguezhernandez, J.; Checot, F.; Gnanou, Y.; Lecommandoux, S. Toward "Smart" Nano-Objects by Self-Assembly of Block Copolymers in Solution. *Prog. Polym. Sci.* **2005**, *30*, 691–724. DOI: 10.1016/j.progpolymsci.2005.04.002.
89. Otsuka, H.; Nagasaki, Y.; Kataoka, K. Self-Assembly of Block Copolymers. *Mater. Today* **2001**, *4*, 30–36. DOI: 10.1016/S1369-7021(01)80036-5.
90. Webber, S. E. Polymer Micelles: An Example of Self-Assembling Polymers. *J. Phys. Chem. B* **1998**, *102*, 2618–2626. DOI: 10.1021/jp980386o.
91. Nishiyama, N.; Kataoka, K. Nanostructured Devices Based on Block Copolymer Assemblies for Drug Delivery: Designing Structures for Enhanced Drug Function. *Adv. Polym. Sci.* **2006**, *193*, 67–101. DOI: 10.1007/12_025.
92. Kulthe, S. S.; Choudhari, Y. M.; Inamdar, N. N.; Mourya, V. Polymeric Micelles: Authoritative Aspects for Drug Delivery. *Des. Monomers Polym.* **2012**, *15*, 465–521. DOI: 10.1080/1385772X.2012.688328.
93. Kowalczuk, A.; Trzcinska, R.; Trzebicka, B.; Müller, A. H. E.; Dworak, A.; Tsvetanov, C. B. Loading of Polymer Nanocarriers: Factors, Mechanisms and Applications. *Prog. Polym. Sci.* **2014**, *39*, 43–86. DOI: 10.1016/j.progpolymsci.2013.10.004.
94. Englert, C.; Brendel, J. C.; Majdanski, T. C.; Yildirim, T.; Schubert, S.; Gottschaldt, M.; Windhab, N.; Schubert, U. S. Pharmapolymers in the 21st Century: Synthetic Polymers in Drug Delivery Applications. *Prog. Polym. Sci.* **2018**, *87*, 107–164. DOI: 10.1016/j.progpolymsci.2018.07.005.
95. Zhu, M.; Whittaker, A. K.; Han, F. Y.; Smith, M. T. Journey to the Market: The Evolution of Biodegradable Drug Delivery Systems. *Appl. Sci.* **2022**, *12*, 935. DOI: 10.3390/app12020935.
96. Perumal, S.; Atchudan, R.; Lee, W. A Review of Polymeric Micelles and Their Applications. *Polymers* **2022**, *14*, 2510. DOI: 10.3390/polym14122510.
97. Niculescu, A. G.; Grumezescu, A. M. Polymer-Based Nanosystems-A Versatile Delivery Approach. *Materials* **2021**, *14*, 6812. DOI: 10.3390/ma14226812.
98. Lassalle, V.; Ferreira, M. L. PLA Nano- and Microparticles for Drug Delivery: An Overview of the Methods of Preparation. *Macromol. Biosci.* **2007**, *7*, 767–783. DOI: 10.1002/mabi.200700022.
99. Sedush, N. G.; Kadina, Y. A.; Razuvaeva, E. V.; Puchkov, A. A.; Shirokova, E. M.; Gomzyak, V. I.; Kalinin, K. T.; Kulebyakina, A. I.; Chvalun, S. N. Nanoformulations of Drugs Based on Biodegradable Lactide Copolymers with Various Molecular Structures and Architectures. *Nanotechnol. Russia.* **2021**, *16*, 421–438. DOI: 10.1134/S2635167621040121.
100. Vlachopoulos, A.; Karlioti, G.; Balla, E.; Daniilidis, V.; Kalamas, T.; Stefanidou, M.; Bikiaris, N. D.; Christodoulou, E.; Koumentakou, I.; Karavas, E.; Bikiaris, D. N. Poly(Lactic Acid)-Based Microparticles for Drug Delivery Applications: An Overview of Recent Advances. *Pharmaceutics* **2022**, *14*, 359. DOI: 10.3390/pharmaceutics14020359.

101. Wang, J.; Li, S.; Han, Y.; Guan, J.; Chung, S.; Wang, C.; Li, D. Poly(Ethylene Glycol)-Polylactide Micelles for Cancer Therapy. *Front. Pharmacol.* **2018**, *9*, 202. DOI: 10.3389/fphar.2018.00202.
102. Leibler, L. Theory of Microphase Separation in Block Copolymers. *Macromolecules* **1980**, *13*, 1602–1617. DOI: 10.1021/ma60078a047.
103. Lynd, N. A.; Meuler, A. J.; Hillmyer, M. A. Polydispersity and Block Copolymer Self-Assembly. *Prog. Polym. Sci.* **2008**, *33*, 875–893. DOI: 10.1016/j.progpolymsci.2008.07.003.
104. Matsushita, Y. Microphase Separation (of Block Copolymers). In *Encyclopedia of Polymeric Nanomaterials*; Springer-Verlag: Berlin Heidelberg, **2014**. DOI: 10.1007/978-3-642-36199-9.
105. Pulingam, T.; Foroozandeh, P.; Chuah, J. A.; Sudesh, K. Exploring Various Techniques for the Chemical and Biological Synthesis of Polymeric Nanoparticles. *Nanomaterials* **2022**, *12*, 576. DOI: 10.3390/nano12030576.
106. Wei, H.; Zhuo, R. X.; Zhang, X. Z. Design and Development of Polymeric Micelles with Cleavable Links for Intracellular Drug Delivery. *Prog. Polym. Sci.* **2013**, *38*, 503–535. DOI: 10.1016/j.progpolymsci.2012.07.002.
107. Bawa, K. K.; Oh, J. K. Stimulus-Responsive Degradable Polylactide-Based Block Copolymer Nanoassemblies for Controlled/Enhanced Drug Delivery. *Mol. Pharm.* **2017**, *14*, 2460–2474. DOI: 10.1021/acs.molpharmaceut.7b00284.
108. Sah, H.; Thoma, L. A.; Desu, H. R.; Sah, E.; Wood, G. C. Concepts and Practices Used to Develop Functional PLGA-Based Nanoparticulate Systems. *Int. J. Nanomed.* **2013**, *8*, 747–765. DOI: 10.2147/IJN.S40579.
109. Khan, I.; Gothwal, A.; Sharma, A. K.; Kesharwani, P.; Gupta, L.; Iyer, A. K.; Gupta, U. PLGA Nanoparticles and Their Versatile Role in Anticancer Drug Delivery. *Crit. Rev. Ther. Drug Carrier Syst.* **2016**, *33*, 159–193. DOI: 10.1615/CritRevTherDrugCarrierSyst.2016015273.
110. Cabral, H.; Miyata, K.; Osada, K.; Kataoka, K. Block Copolymer Micelles in Nanomedicine Applications. *Chem. Rev.* **2018**, *118*, 6844–6892. DOI: 10.1021/acs.chemrev.8b00199.
111. Coumes, F.; Beauté, L.; Domurado, D.; Li, S.; Lecommandoux, S.; Coudane, J.; Darcos, V. Self-Assembly of Well-Defined Triblock Copolymers Based on Poly(Lactic Acid) and Poly(Oligo(Ethylene Glycol) Methyl Ether Methacrylate) Prepared by ATRP. *RSC Adv.* **2016**, *6*, 53370–53377. DOI: 10.1039/C6RA07535E.
112. Kalelkar, P. P.; Collard, D. M. Tricomponent Amphiphilic Poly(Oligo(Ethylene Glycol) Methacrylate) Brush-Grafted Poly(Lactic Acid): Synthesis, Nanoparticle Formation, and in Vitro Uptake and Release of Hydrophobic Dyes. *Macromolecules* **2020**, *53*, 4274–4283. DOI: 10.1021/acs.macromol.9b02467.
113. Plichta, A.; Kowalczyk, S.; Kamiński, K.; Wasyłeczko, M.; Więckowski, S.; Olędzka, E.; Nałęcz-Jawecki, G.; Zgadzaj, A.; Sobczak, M. ATRP of Methacrylic Derivative of Camptothecin Initiated with PLA Tpward Three-Arm Star Block Copolymer Conjugates with Favorable Drug Release. *Macromolecules* **2017**, *50*, 6439–6450. DOI: 10.1021/acs.macromol.7b01350.
114. Nehate, C.; Moothedathu Raynold, A. A.; Haridas, V.; Koul, V. Comparative Assessment of Active Targeted Redox Sensitive Polymersomes Based on PPEGMA-S-S-PLA Diblock Copolymer with Marketed Nanoformulation. *Biomacromolecules* **2018**, *19*, 2549–2566. DOI: 10.1021/acs.biomac.8b00178.
115. Cunningham, A.; Oh, J. K. New Design of Thiol-Responsive Degradable Polylactide-Based Block Copolymer Micelles. *Macromol. Rapid Commun.* **2013**, *34*, 163–168. DOI: 10.1002/marc.201200532.
116. Sun, L.; Wei, H.; Zhang, X.; Meng, C.; Kang, G.; Ma, W.; Ma, L.; Wang, B.; Yu, C. Synthesis of Polymeric Micelles with Dual-Functional Sheddable PEG Stealth for Enhanced Tumor-Targeted Drug Delivery. *Polym. Chem.* **2020**, *11*, 4469–4476. DOI: 10.1039/D0PY00653J.
117. Samarajeewa, S.; Shrestha, R.; Elsabahy, M.; Karwa, A.; Li, A.; Zentay, R. P.; Kostelc, J. G.; Dorshow, R. B.; Wooley, K. L. In Vitro Efficacy of Paclitaxel-Loaded Dual-Responsive

Shell Cross-Linked Polymer Nanoparticles Having Orthogonally Degradable Disulfide Cross-Linked Corona and Polyester Core Domains. *Mol. Pharm.* **2013**, *10*, 1092–1099. DOI: 10.1021/mp3005897.

118. Kozma, G. T.; Shimizu, T.; Ishida, T.; Szebeni, J. Anti-PEG Antibodies: Properties, Formation, Testing and Role in Adverse Immune Reactions to PEGylated Nano-Biopharmaceuticals. *Adv. Drug Deliv. Rev.* **2020**, *154-155*, 163–175. DOI: 10.1016/j.addr.2020.07.024.
119. Long, L. X.; Zhao, J.; Li, K.; He, L. G.; Qian, X. M.; Liu, C. Y.; Wang, L. M.; Yang, X. Q.; Sun, J.; Ren, Y.; et al. Synthesis of Star-Branched PLA-b-PMPC Copolymer Micelles as Long Blood Circulation Vectors to Enhance Tumor-Targeted Delivery of Hydrophobic Drugs in Vivo. *Mater. Chem. Phys.* **2016**, *180*, 184–194. DOI: 10.1016/j.matchemphys.2016.05.062.
120. Wang, T.; Tang, X.; Han, J.; Ding, Y.; Guo, W.; Pei, M. Biodegradable Self-Assembled Nanoparticles of Galactose-Containing Amphiphilic Triblock Copolymers for Targeted Delivery of Paclitaxel to HepG2 Cells. *Macromol. Biosci.* **2016**, *16*, 774–783. DOI: 10.1002/mabi.201500413.
121. Ravenelle, F.; Vachon, P.; Rigby-Jones, A. E.; Sneyd, J. R.; Le Garrec, D.; Gori, S.; Lessard, D.; Smith, D. C. Anaesthetic Effects of Propofol Polymeric Micelle: A Novel Water Soluble Propofol Formulation. *Br. J. Anaesth.* **2008**, *101*, 186–193. DOI: 10.1093/bja/aen147.
122. Ramesh, K.; Gundampati, R. K.; Singh, S.; Mitra, K.; Shukla, A.; Jagannadham, M. V.; Chattopadhyay, D.; Misra, N.; Ray, B. Self-Assembly, Doxorubicin-Loading and Antibacterial Activity of Well-Defined ABA-Type Amphiphilic Poly(N-Vinylpyrrolidone)-b-Poly(d,l-Lactide)-b-Poly(N-Vinyl Pyrrolidone) Triblock Copolymers. *RSC Adv.* **2016**, *6*, 25864–25876. DOI: 10.1039/C5RA23239B.
123. Jiménez-Sánchez, G.; Pavot, V.; Chane-Haong, C.; Handké, N.; Terrat, C.; Gigmes, D.; Trimaille, T.; Verrier, B. Preparation and in Vitro Evaluation of Imiquimod Loaded Polylactide-Based Micelles as Potential Vaccine Adjuvants. *Pharm. Res.* **2015**, *32*, 311–320. DOI: 10.1007/s11095-014-1465-5.
124. Lacroix, C.; Humanes, A.; Coiffier, C.; Gigmes, D.; Verrier, B.; Trimaille, T. Polylactide-Based Reactive Micelles as a Robust Platform for MRNA Delivery. *Pharm. Res.* **2020**, *37*, 30. DOI: 10.1007/s11095-019-2749-6.
125. Barz, M.; Armiñán, A.; Canal, F.; Wolf, F.; Koynov, K.; Frey, H.; Zentel, R.; Vicent, M. J. P(HPMA)-Block-P(LA) Copolymers in Paclitaxel Formulations: Polylactide Stereochemistry Controls Micellization, Cellular Uptake Kinetics, Intracellular Localization and Drug Efficiency. *J. Control. Release* **2012**, *163*, 63–74. DOI: 10.1016/j.jconrel.2012.05.024.
126. Qian, W.; Song, T.; Ye, M.; Xu, P.; Lu, G.; Huang, X. PAA-: G -PLA Amphiphilic Graft Copolymer: Synthesis, Self-Assembly, and Drug Loading Ability. *Polym. Chem.* **2017**, *8*, 4098–4107. DOI: 10.1039/C7PY00762K.
127. Ahmadi, E.; Zarghami, N.; Jafarabadi, M. A.; Alizadeh, L.; Khojastehfard, M.; Yamchi, M. R.; Salehi, R. Enhanced Anticancer Potency by Combination Chemotherapy of HT-29 Cells with Biodegradable, PH-Sensitive Nanoparticles for Co-Delivery of Hydroxytyrosol and Doxorubicin. *J. Drug Deliv. Sci. Technol.* **2019**, *51*, 721–735. DOI: 10.1016/j.jddst.2019.03.003.
128. Karanikolopoulos, N.; Zamurovic, M.; Pitsikalis, M.; Hadjichristidis, N. Poly(DL-Lactide)-b-Poly(N,N-Dimethylamino-2-Ethyl Methacrylate): Synthesis, Characterization, Micellization Behavior in Aqueous Solutions, and Encapsulation of the Hydrophobic Drug Dipyridamole. *Biomacromolecules* **2010**, *11*, 430–438. DOI: 10.1021/bm901151g.
129. Lin, W.; Yao, N.; Qian, L.; Zhang, X.; Chen, Q.; Wang, J.; Zhang, L. PH-Responsive Unimolecular Micelle-Gold Nanoparticles-Drug Nanohybrid System for Cancer Theranostics. *Acta Biomater.* **2017**, *58*, 455–465. DOI: 10.1016/j.actbio.2017.06.003.
130. Qian, X.; Long, L.; Shi, Z.; Liu, C.; Qiu, M.; Sheng, J.; Pu, P.; Yuan, X.; Ren, Y.; Kang, C. Star-Branched Amphiphilic PLA-b-PDMAEMA Copolymers for Co-Delivery of MiR-21 Inhibitor and Doxorubicin to Treat Glioma. *Biomaterials* **2014**, *35*, 2322–2335. DOI: 10.1016/j.biomaterials.2013.11.039.

131. Black, K. C. L.; Ibricevic, A.; Gunsten, S. P.; Flores, J. A.; Gustafson, T. P.; Raymond, J. E.; Samarajeewa, S.; Shrestha, R.; Felder, S. E.; Cai, T.; et al. In Vivo Fate Tracking of Degradable Nanoparticles for Lung Gene Transfer Using PET and C^{a}erenkov Imaging. *Biomaterials* **2016**, *98*, 53–63. DOI: 10.1016/j.biomaterials.2016.04.040.
132. Hu, Y.; Darcos, V.; Monge, S.; Li, S.; Zhou, Y.; Su, F. Tunable Thermo-Responsive P(NIPAAm-Co-DMAAm)-b-PLLA-b-P(NIPAAm-Co-DMAAm) Triblock Copolymer Micelles as Drug Carriers. *J. Mater. Chem. B* **2014**, *2*, 2738–2748. DOI: 10.1039/c3tb21793k.
133. Hu, Y.; Darcos, V.; Monge, S.; Li, S.; Zhou, Y.; Su, F. Thermo-Responsive Release of Curcumin from Micelles Prepared by Self-Assembly of Amphiphilic P(NIPAAm-Co-DMAAm)-b-PLLA-b-P(NIPAAm-Co-DMAAm) Triblock Copolymers. *Int. J. Pharm.* **2014**, *476*, 31–40. DOI: 10.1016/j.ijpharm.2014.09.029.
134. Wu, C.; Ying, A.; Ren, S. Fabrication of Polymeric Micelles with Core-Shell-Corona Structure for Applications in Controlled Drug Release. *Colloid Polym. Sci.* **2013**, *291*, 827–834. DOI: 10.1007/s00396-012-2794-8.
135. Li, P.; Zhang, Z.; Su, Z.; Wei, G. Thermosensitive Polymeric Micelles Based on the Triblock Copolymer Poly(d,l-Lactide)-b-Poly(N-Isopropyl Acrylamide)-b-Poly(d,l-Lactide) for Controllable Drug Delivery. *J. Appl Polymer Sci.* **2017**, *134*, 1–6. DOI: 10.1002/app.45304.
136. Dai, X. H.; Jin, H.; Cai, M. H.; Wang, H.; Zhou, Z. P.; Pan, J. M.; Wang, X. H.; Yan, Y. S.; Liu, D. M.; Sun, L. Fabrication of Thermosensitive, Star-Shaped Poly(L-Lactide)-Block-Poly(N-Isopropylacrylamide) Copolymers with Porphyrin Core for Photodynamic Therapy. *React. Funct. Polym.* **2015**, *89*, 9–17. DOI: 10.1016/j.reactfunctpolym.2015.02.002.
137. Tsai, H. C.; Tsai, C. H.; Lin, S. Y.; Jhang, C. R.; Chiang, Y. S.; Hsiue, G. H. Stimulated Release of Photosensitizers from Graft and Diblock Micelles for Photodynamic Therapy. *Biomaterials* **2012**, *33*, 1827–1837. DOI: 10.1016/j.biomaterials.2011.11.014.
138. Lu, M.; Chen, F.; Noy, J. M.; Lu, H.; Stenzel, M. H. Enhanced Antimetastatic Activity of the Ruthenium Anticancer Drug RAPTA-C Delivered in Fructose-Coated Micelles. *Macromol. Biosci.* **2017**, *17*, 1–11. DOI: 10.1002/mabi.201600513.
139. Dai, X.-H.; Wang, Z.-M.; Pan, J.-M.; Yuan, S.-S.; Yan, Y.-S.; Liu, D.-M.; Sun, L. Star-Shaped Poly(l-Lactide)-b-Poly(Lactobionamidoethyl Methacrylate) with Porphyrin Core: Synthesis, Self-Assemby. *J. Biomater. Sci. Polym. Ed.* **2014**, *25*, 1755–1770. DOI: 10.1080/09205063.2014.946878.
140. Hillmyer, M. A. Nanoporous Materials from Block Copolymer Precursors. *Adv. Polym. Sci.* **2005**, *190*, 137–181. DOI: 10.1007/12_002.
141. Grande, D.; Penelle, J.; Davidson, P.; Beurroies, I.; Denoyel, R. Functionalized Ordered Nanoporous Polymeric Materials: From the Synthesis of Diblock Copolymers to Their Nanostructuration and Their Selective Degradation. *Micropor. Mesopor. Mat.* **2011**, *140*, 34–39. DOI: 10.1016/j.micromeso.2010.10.007.
142. Xiang, L.; Li, Q.; Li, C.; Yang, Q.; Xu, F.; Mai, Y. Block Copolymer Self-Assembly Directed Synthesis of Porous Materials with Ordered Bicontinuous Structures and Their Potential Applications. *Adv. Mater.* **2023**, *35*, e2207684. DOI: 10.1002/adma.202207684.
143. Olson, D. A.; Chen, L.; Hillmyer, M. A. Templating Nanoporous Polymers with Ordered Block Copolymers. *Chem. Mater.* **2008**, *20*, 869–890. DOI: 10.1021/cm702239k.
144. Hampu, N.; Werber, J. R.; Chan, W. Y.; Feinberg, E. C.; Hillmyer, M. A. Next-Generation Ultrafiltration Membranes Enabled by Block Polymers. *ACS Nano.* **2020**, *14*, 16446–16471. DOI: 10.1021/acsnano.0c07883.
145. Zalusky, A. S.; Olayo-Valles, R.; Taylor, C. J.; Hillmyer, M. A. Mesoporous Polystyrene Monoliths. *J. Am. Chem. Soc.* **2001**, *123*, 1519–1520. DOI: 10.1021/ja003936g.
146. Zalusky, A. S.; Olayo-Valles, R.; Wolf, J. H.; Hillmyer, M. A. Ordered Nanoporous Polymers from Polystyrene-Polylactide Block Copolymers. *J. Am. Chem. Soc.* **2002**, *124*, 12761–12773. DOI: 10.1021/ja0278584.
147. Wolf, J. H.; Hillmyer, M. A. Ordered Nanoporous Poly(Cyclohexylethylene). *Langmuir* **2003**, *19*, 6553–6560. DOI: 10.1021/la0341862.

148. Rzayev, J.; Hillmyer, M. Nanoporous Polystyrene Containing Hydrophilic Pores from an ABC Triblock Copolymer Precursor. *J. Am. Chem. Soc.* **2005**, *38*, 3–5. DOI: 10.1021/ja01344a068.
149. Rzayev, J.; Hillmyer, M. A. Nanochannel Array Plastics with Tailored Surface Chemistry. *J. Am. Chem. Soc.* **2005**, *127*, 13373–13379. DOI: 10.1021/ja053731d.
150. Phillip, W. A.; Rzayev, J.; Hillmyer, M. A.; Cussler, E. L. Gas and Water Liquid Transport through Nanoporous Block Copolymer Membranes. *J. Memb. Sci* **2006**, *286*, 144–152. DOI: 10.1016/j.memsci.2006.09.028.
151. Jackson, E. A.; Lee, Y.; Radlauer, M. R.; Hillmyer, M. A. Well-Ordered Nanoporous ABA Copolymer Thin Films via Solvent Vapor Annealing, Homopolymer Blending, and Selective Etching of ABAC Tetrablock Terpolymers. *ACS Appl. Mater. Interfaces.* **2015**, *7*, 27331–27339. DOI: 10.1021/acsami.5b08856.
152. Seo, M.; Hillmyer, M. Reticulated Nanoporous Polymers by Controlled Polymerization-Induced Microphase Separation. *Labour's Lost Lead* **2012**, *336*, 1422–1426. DOI: 10.5040/9780755621101.0007.
153. Seo, M.; Kim, S.; Oh, J.; Kim, S. J.; Hillmyer, M. A. Hierarchically Porous Polymers from Hyper-Cross-Linked Block Polymer Precursors. *J. Am. Chem. Soc.* **2015**, *137*, 600–603. DOI: 10.1021/ja511581w.
154. Larsen, M. B.; Van Horn, J. D.; Wu, F.; Hillmyer, M. A. Intrinsically Hierarchical Nanoporous Polymers via Polymerization-Induced Microphase Separation. *Macromolecules* **2017**, *50*, 4363–4371. DOI: 10.1021/acs.macromol.7b00808.
155. Hampu, N.; Bates, M. W.; Vidil, T.; Hillmyer, M. A. Bicontinuous Porous Nanomaterials from Block Polymers Radically Cured in the Disordered State for Size-Selective Membrane Applications. *ACS Appl. Nano Mater.* **2019**, *2*, 4567–4577. DOI: 10.1021/acsanm.9b00922.
156. Vidil, T.; Hampu, N.; Hillmyer, M. A. Nanoporous Thermosets with Percolating Pores from Block Polymers Chemically Fixed above the Order-Disorder Transition. *ACS Cent. Sci.* **2017**, *3*, 1114–1120. DOI: 10.1021/acscentsci.7b00358.
157. Chan, W. Y.; Hillmyer, M. A. Disordered Triblock Polymers for Nanoporous Materials with Tunable Surface Properties for Ultrafiltration Applications. *ACS Appl. Polym. Mater.* **2022**, *4*, 8009–8020. DOI: 10.1021/acsapm.2c00065.
158. Anderson, E. L.; Saba, S. A.; Loomis, D. J.; Bühlmann, P.; Hillmyer, M. A. Functionalized Mesoporous Polymers with Enhanced Performance as Reference Electrode Frits. *ACS Appl. Nano Mater.* **2018**, *1*, 139–144. DOI: 10.1021/acsanm.7b00058.
159. Phillip, W. A.; O'Neill, B.; Rodwogin, M.; Hillmyer, M. A.; Cussler, E. L. Self-Assembled Block Copolymer Thin Films as Water Filtration Membranes. *ACS Appl. Mater. Interfaces.* **2010**, *2*, 847–853. DOI: 10.1021/am900882t.
160. Bolton, J.; Bailey, T. S.; Rzayev, J. Large Pore Size Nanoporous Materials from the Self-Assembly of Asymmetric Bottlebrush Block Copolymers. *Nano Lett.* **2011**, *11*, 998–1001. DOI: 10.1021/nl103747m.
161. Ho, R. M.; Chen, C. K.; Chiang, Y. W.; Ko, B. T.; Lin, C. C. Tubular Nanostructures from Degradable Core-Shell Cylinder Microstructures in Chiral Diblock Copolymers. *Adv. Mater.* **2006**, *18*, 2355–2358. DOI: 10.1002/adma.200601135.
162. Hampu, N.; Werber, J. R.; Hillmyer, M. A. Co-Casting Highly Selective Dual-Layer Membranes with Disordered Block Polymer Selective Layers. *ACS Appl. Mater. Interfaces.* **2020**, *12*, 45351–45362. DOI: 10.1021/acsami.0c13726.
163. Crossland, E. J. W.; Cunha, P.; Scroggins, S.; Moratti, S.; Yurchenko, O.; Steiner, U.; Hillmyer, M. A.; Ludwigs, S. Soft-Etch Mesoporous Hole-Conducting Block Copolymer Templates. *ACS Nano.* **2010**, *4*, 962–966. DOI: 10.1021/nn901447a.
164. Lo, K.-H.; Tseng, W.-H.; Ho, R.-M. In-Situ Formation of CdS Nanoarrays by Pore-Filling Nanoporous Templates from Degradable Block Copolymers. *Macromolecules* **2007**, *40*, 2621–2624. DOI: 10.1021/ma0628580.
165. Runge, M. B.; Dutta, S.; Bowden, N. B. Synthesis of Comb Block Copolymers by ROMP, ATRP, and ROP and Their Assembly in the Solid State. *Macromolecules* **2006**, *39*, 498–508. DOI: 10.1021/ma052012g.

166. Sveinbjörnsson, B. R.; Weitekamp, R. A.; Miyake, G. M.; Xia, Y.; Atwater, H. A.; Grubbs, R. H. Rapid Self-Assembly of Brush Block Copolymers to Photonic Crystals. *Proc. Natl. Acad. Sci. U S A* **2012**, *109*, 14332–14336. DOI: 10.1073/pnas.1213055109.
167. Tekale, S. U.; Rottenberg, Y.; Ingle, R. D.; Domb, A. J.; Pawar, R. P. Recent Developments in Biodegradable Block Copolymers. *Polym. Adv. Techs.* **2021**, *32*, 3877–3899. DOI: 10.1002/pat.5460.
168. Li, G.; Zhao, M.; Xu, F.; Yang, B.; Li, X.; Meng, X.; Teng, L.; Sun, F.; Li, Y. Synthesis and Biological Application of Polylactic Acid. *Molecules* **2020**, *25*, 5023. DOI: 10.3390/molecules25215023.
169. Ebrahimi, F.; Ramezani Dana, H. Poly Lactic Acid (PLA) Polymers: From Properties to Biomedical Applications. *Int. J. Polym. Mater. Polym. Biomater.* **2022**, *71*, 1117–1130. DOI: 10.1080/00914037.2021.1944140.
170. Ghalia, M. A.; Dahman, Y. Biodegradable Poly(Lactic Acid)-Based Scaffolds: Synthesis and Biomedical Applications. *J. Polym. Res.* **2017**, *24*, 74. DOI: 10.1007/s10965-017-1227-2.
171. Gritsch, L.; Conoscenti, G.; La Carrubba, V.; Nooeaid, P.; Boccaccini, A. R. Polylactide-Based Materials Science Strategies to Improve Tissue-Material Interface without the Use of Growth Factors or Other Biological Molecules. *Mater. Sci. Eng. C Mater. Biol. Appl.* **2019**, *94*, 1083–1101. DOI: 10.1016/j.msec.2018.09.038.
172. Moya-Lopez, C.; González-Fuentes, J.; Bravo, I.; Chapron, D.; Bourson, P.; Alonso-Moreno, C.; Hermida-Merino, D. Polylactide Perspectives in Biomedicine: From Novel Synthesis to the Application Performance. *Pharmaceutics* **2022**, *14*, 1673. DOI: 10.3390/pharmaceutics14081673.
173. Ranakoti, L.; Gangil, B.; Bhandari, P.; Singh, T.; Sharma, S.; Singh, J.; Singh, S. Promising Role of Polylactic Acid as an Ingenious Biomaterial in Scaffolds, Drug Delivery, Tissue Engineering, and Medical Implants: Research Developments, and Prospective Applications. *Molecules* **2023**, *28*, 485. DOI: 10.3390/molecules28020485.
174. Castañeda-Rodríguez, S.; González-Torres, M.; Ribas-Aparicio, R. M.; Del Prado, M. L.; Leyva, G.; Gürer, E. S.; Sharifi, J. Recent Advances in Modified Poly (Lactic Acid) as Tissue Engineering Materials. *J. Biol. Eng.* **2023**, *17*, 21. DOI: 10.1186/s13036-023-00338-8.
175. Pawar, R. P.; Tekale, S. U.; Shisodia, S.; Totre, J.; Domb, A. J. Biomedical Applications of Poly (Lactic Acid). *Rec. Pat. Regen. Med.* **2014**, *4*, 40–51. DOI: 10.2174/2210296504666140402235024.
176. Gaytán, I.; Burelo, M.; Loza-Tavera, H. Current Status on the Biodegradability of Acrylic Polymers: Microorganisms, Enzymes and Metabolic Pathways Involved. *Appl. Microbiol. Biotechnol.* **2021**, *105*, 991–1006. DOI: 10.1007/s00253-020-11073-1.
177. Nelson, D. M.; Ma, Z.; Leeson, C. E.; Wagner, W. R. Extended and Sequential Delivery of Protein from Injectable Thermoresponsive Hydrogels. *J. Biomed. Mater. Res. A* **2012**, *100*, 776–785. DOI: 10.1002/jbm.a.34015.
178. Ma, Z.; Nelson, D. M.; Hong, Y.; Wagner, W. R. Thermally Responsive Injectable Hydrogel Incorporating Methacrylate- Polylactide for Hydrolytic Lability. *Biomacromolecules* **2010**, *11*, 1873–1881. DOI: 10.1021/bm1004299.
179. Guan, J.; Hong, Y.; Ma, Z.; Wagner, W. R. Protein-Reactive, Thermoresponsive Copolymers with High Flexibility and Biodegradability. *Biomacromolecules* **2008**, *9*, 1283–1292. DOI: 10.1021/bm701265j.
180. Zhu, Y.; Jiang, H.; Ye, S. H.; Yoshizumi, T.; Wagner, W. R. Tailoring the Degradation Rates of Thermally Responsive Hydrogels Designed for Soft Tissue Injection by Varying the Autocatalytic Potential. *Biomaterials* **2015**, *53*, 484–493. DOI: 10.1016/j.biomaterials.2015.02.100.
181. Fathi, A.; Mithieux, S. M.; Wei, H.; Chrzanowski, W.; Valtchev, P.; Weiss, A. S.; Dehghani, F. Elastin Based Cell-Laden Injectable Hydrogels with Tunable Gelation, Mechanical and Biodegradation Properties. *Biomaterials* **2014**, *35*, 5425–5435. DOI: 10.1016/j.biomaterials.2014.03.026.
182. Donate, R.; Monzón, M.; Alemán-Domínguez, M. E. Additive Manufacturing of PLA-Based Scaffolds Intended for Bone Regeneration and Strategies to Improve Their Biological Properties. *E-Polymers* **2020**, *20*, 571–599. DOI: 10.1515/epoly-2020-0046.

183. Vacaras, S.; Baciut, M.; Lucaciu, O.; Dinu, C.; Baciut, G.; Crisan, L.; Hedesiu, M.; Crisan, B.; Onisor, F.; Armencea, G.; et al. Understanding the Basis of Medical Use of Poly-Lactide-Based Resorbable Polymers and Composites–A Review of the Clinical and Metabolic Impact. *Drug Metab. Rev.* **2019**, *51*, 570–588. DOI: 10.1080/03602532.2019.1642911.
184. Clément, B.; Decherchi, P.; Féron, F.; Bertin, D.; Gigmes, D.; Trimaille, T.; Marqueste, T. Poly(D,L-Lactide)-Block-Poly(2-Hydroxyethyl Acrylate) Block Copolymers as Potential Biomaterials for Peripheral Nerve Repair: In Vitro and in Vivo Degradation Studies. *Macromol. Biosci.* **2011**, *11*, 1175–1184. DOI: 10.1002/mabi.201100067.
185. Rahman, M.; Sreearunothai, P.; Opaprakasit, P. Development and Characterization of Photoinduced Acrylamide-Grafted Polylactide Films for Biomedical Applications. *Int. J. Polym. Sci.* **2017**, *2017*, 1–11. DOI: 10.1155/2017/5651398.
186. Contreras-Cáceres, R.; Cabeza, L.; Perazzoli, G.; Díaz, A.; López-Romero, J. M.; Melguizo, C.; Prados, J. Electrospun Nanofibers: Recent Applications in Drug Delivery and Cancer Therapy. *Nanomaterials* **2019**, *9*, 656. DOI: 10.3390/nano9040656.
187. Spasova, M.; Manolova, N.; Paneva, D.; Mincheva, R.; Dubois, P.; Rashkov, I.; Maximova, V.; Danchev, D. Polylactide Stereocomplex-Based Electrospun Materials Possessing Surface with Antibacterial and Hemostatic Properties. *Biomacromolecules* **2010**, *11*, 151–159. DOI: 10.1021/bm901016y.
188. Toncheva, A.; Mincheva, R.; Kancheva, M.; Manolova, N.; Rashkov, I.; Dubois, P.; Markova, N. Antibacterial PLA/PEG Electrospun Fibers: Comparative Study between Grafting and Blending PEG. *Eur. Polym. J.* **2016**, *75*, 223–233. DOI: 10.1016/j.eurpolymj.2015.12.019.
189. Zhuang, X.; Zhang, H.; Chikushi, N.; Zhao, C.; Oyaizu, K.; Chen, X.; Nishide, H. Biodegradable and Electroactive TEMPO-Substituted Acrylamide/Lactide Copolymers. *Macromol. Biosci.* **2010**, *10*, 1203–1209. DOI: 10.1002/mabi.201000031.
190. Bedair, T. M.; Cho, Y.; Joung, Y. K.; Han, D. K. Biodegradable Polymer Brush as Nanocoupled Interface for Improving the Durability of Polymer Coating on Metal Surface. *Colloids Surf. B Biointerfaces* **2014**, *122*, 808–817. DOI: 10.1016/j.colsurfb.2014.08.025.
191. Zhao, H.; Kang, X.; Liu, L. Comb-Coil Polymer Brushes on the Surface of Silica Nanoparticles. *Macromolecules* **2005**, *38*, 10619–10622. DOI: 10.1021/ma051822p.
192. Auras, R. *Poly (Lactic Acid): Encyclopedia of Polymer Science and Technology*; Wiley & Sons, Inc., New Jersey, **2010**; pp 967–983
193. Liu, H.; Zhang, J. Research Progress in Toughening Modification of Poly(Lactic Acid). *J. Polym. Sci. B Polym. Phys.* **2011**, *49*, 1051–1083. DOI: 10.1002/polb.22283.
194. Zhao, X.; Hu, H.; Wang, X.; Yu, X.; Zhou, W.; Peng, S. Super Tough Poly(Lactic Acid) Blends: A Comprehensive Review. *RSC Adv.* **2020**, *10*, 13316–13368. DOI: 10.1039/D0RA01801E.
195. Nofar, M.; Sacligil, D.; Carreau, P. J.; Kamal, M. R.; Heuzey, M. C. Poly (Lactic Acid) Blends: Processing, Properties and Applications. *Int. J. Biol. Macromol.* **2019**, *125*, 307–360. DOI: 10.1016/j.ijbiomac.2018.12.002.
196. Hamad, K.; Kaseem, M.; Ayyoob, M.; Joo, J.; Deri, F. Polylactic Acid Blends: The Future of Green, Light and Tough. *Prog. Polym. Sci.* **2018**, *85*, 83–127. DOI: 10.1016/j.progpolymsci.2018.07.001.
197. Sangeetha, V. H.; Deka, H.; Varghese, T. O.; Nayak, S. K. State of the Art and Future Prospectives of Poly(Lactic Acid) Based Blends and Composites. *Polym. Compos.* **2018**, *39*, 81–101. DOI: 10.1002/pc.23906.
198. Kfoury, G.; Raquez, J. M.; Hassouna, F.; Odent, J.; Toniazzo, V.; Ruch, D.; Dubois, P. Recent Advances in High Performance Poly(Lactide): from "Green" Plasticization to Super-Tough Materials via (Reactive) Compounding. *Front. Chem.* **2013**, *1*, 32. DOI: 10.3389/fchem.2013.00032.
199. Pang, X.; Zhuang, X.; Tang, Z.; Chen, X. Polylactic Acid (PLA): Research, Development and Industrialization. *Biotechnol. J.* **2010**, *5*, 1125–1136. DOI: 10.1002/biot.201000135.

200. Puthumana, M.; Santhana Gopala Krishnan, P.; Nayak, S. K. Chemical Modifications of PLA through Copolymerization. *Int. J. Polym. Anal. Charact* **2020**, *25*, 634–648. DOI: 10.1080/1023666X.2020.1830650.
201. Choochottiros, C.; Chin, I. J. Potential Transparent PLA Impact Modifiers Based on PMMA Copolymers. *Eur. Polym. J.* **2013**, *49*, 957–966. DOI: 10.1016/j.eurpolymj.2012.12.008.
202. Wang, W. W.; Jiang, L.; Ren, W. Y.; Zhang, C. M.; Man, C. Z.; Nguyen, T. P.; Dan, Y. The Crystallinity, Thermal Properties and Microscopic Morphology of Di-Block Copolymers of l-Lactide and Several Acrylates. *RSC Adv.* **2016**, *6*, 31934–31946. DOI: 10.1039/C5RA24327K.
203. Zhu, Y. Y.; Hu, J.; Ma, Y. W.; Xie, H. B.; Guo, W. H.; Wei, J. X.; Yu, Q. J. The Effect of Micelles with Random PH-Sensitive/Hydrophobic Structure on the Workability, Hydration Process and Microstructure of Cement Paste. *RSC Adv.* **2017**, *7*, 17085–17094. DOI: 10.1039/C6RA26643F.
204. Kalelkar, P. P.; Geng, Z.; Cox, B.; Finn, M. G.; Collard, D. M. Surface-Initiated Atom-Transfer Radical Polymerization (SI-ATRP) of Bactericidal Polymer Brushes on Poly(Lactic Acid) Surfaces. *Colloids Surf. B Biointerfaces* **2022**, *211*, 112242. DOI: 10.1016/j.colsurfb.2021.112242.
205. Coudane, J.; Van Den Berghe, H.; Mouton, J.; Garric, X.; Nottelet, B. Poly(Lactic Acid)-Based Graft Copolymers: Syntheses Strategies and Improvement of Properties for Biomedical and Environmentally Friendly Applications: A Review. *Molecules* **2022**, *27*, 4135. DOI: 10.3390/molecules27134135.
206. Choi, K. M.; Choi, M. C.; Han, D. H.; Park, T. S.; Ha, C. S. Plasticization of Poly(Lactic Acid) (PLA) through Chemical Grafting of Poly(Ethylene Glycol) (PEG) via in Situ Reactive Blending. *Eur. Polym. J.* **2013**, *49*, 2356–2364. DOI: 10.1016/j.eurpolymj.2013.05.027.
207. Choi, K. M.; Lim, S. W.; Choi, M. C.; Kim, Y. M.; Han, D. H.; Ha, C. S. Thermal and Mechanical Properties of Poly(Lactic Acid) Modified by Poly(Ethylene Glycol) Acrylate through Reactive Blending. *Polym. Bull.* **2014**, *71*, 3305–3321. DOI: 10.1007/s00289-014-1251-x.
208. Georgia, K.; Raquez, J. M.; Hassouna, F.; Leclere, P.; Toniazzo, V.; Ruch, D.; Dubois, P. Toughening of Poly(Lactide) Using Polyethylene Glycol Methyl Ether Acrylate: Reactive versus Physical Blending. *Polym. Eng. Sci.* **2015**, *55*, 1408–1419. DOI: 10.1002/pen.
209. Quiles-Carrillo, L.; Duart, S.; Montanes, N.; Torres-Giner, S.; Balart, R. Enhancement of the Mechanical and Thermal Properties of Injection-Molded Polylactide Parts by the Addition of Acrylated Epoxidized Soybean Oil. *Mater. Des.* **2018**, *140*, 54–63. DOI: 10.1016/j.matdes.2017.11.031.
210. Chen, Y.; Chen, K.; Wang, Y.; Xu, C. Biobased Heat-Triggered Shape-Memory Polymers Based on Polylactide/Epoxidized Natural Rubber Blend System Fabricated via Peroxide-Induced Dynamic Vulcanization: Co-Continuous Phase Structure, Shape Memory Behavior, and Interfacial Compatibilization. *Ind. Eng. Chem. Res.* **2015**, *54*, 8723–8731. DOI: 10.1021/acs.iecr.5b02195.
211. Feng, Y.; Zhao, G.; Yin, J.; Jiang, W. Reactive Compatibilization of High-Impact Poly(Lactic Acid)/Ethylene Copolymer Blends Catalyzed by N,N-Dimethylstearylamine. *Polym. Int.* **2014**, *63*, 1263–1269. DOI: 10.1002/pi.4632.
212. Liu, H.; Guo, L.; Guo, X.; Zhang, J. Effects of Reactive Blending Temperature on Impact Toughness of Poly(Lactic Acid) Ternary Blends. *Polymer* **2012**, *53*, 272–276. DOI: 10.1016/j.polymer.2011.12.036.
213. Li, W.; Zhang, Y.; Wu, D.; Li, Z.; Zhang, H.; Dong, L.; Sun, S.; Deng, Y.; Zhang, H. The Effect of Core–Shell Ratio of Acrylic Impact Modifier on Toughening PLA. *Adv. Polym. Technol.* **2017**, *36*, 491–501. DOI: 10.1002/adv.21632.
214. Mohammad, N.; Arsad, A.; Rahmat, A.; Abdullah Sani, N.; Ali Mohsin, M. Influence of Compatibilizer on the Structure Properties of Polylactic Acid/Natural Rubber Blends. *Polym. Sci. Ser. A* **2016**, *58*, 177–185. DOI: 10.1134/S0965545X16020164.

215. Pongsathit, S.; Pattamaprom, C. Irradiation Grafting of Natural Rubber Latex with Maleic Anhydride and Its Compatibilization of Poly(Lactic Acid)/Natural Rubber Blends. *Radiat. Phys. Chem* **2018**, *144*, 13–20. DOI: 10.1016/j.radphyschem.2017.11.006.
216. Hu, X.; Kang, H.; Li, Y.; Geng, Y.; Wang, R.; Zhang, L. Preparation, Morphology and Superior Performances of Biobased Thermoplastic Elastomer by in Situ Dynamical Vulcanization for 3D-Printed Materials. *Polymer* **2017**, *108*, 11–20. DOI: 10.1016/j.polymer.2016.11.045.
217. Sui, X.; Zhao, X.; Wang, Z.; Sun, S. Super-Ductile and Stiff PBAT/PLA Biodegradable Composites Balanced with Random PMMA-Co-GMA Copolymer as Compatibilizer. *Polym. Int.* **2022**, *72*, 333–341. DOI: 10.1002/pi.6471.
218. Zhang, Y.; Gu, X.; Ni, C.; Li, F.; Li, Y.; You, J. Improvement of PLLA Ductility by Blending with PVDF: Localization of Compatibilizers at Interface and Its Glycidyl Methacrylate Content Dependency. *Polymers* **2020**, *12*, 1846. DOI: 10.3390/POLYM12081846.
219. Jiang, Y.; Li, Z.; Song, S.; Sun, S.; Li, Q. Highly-Modified Polylactide Transparent Blends with Better Heat-Resistance, Melt Strength, Toughness and Stiffness Balance Due to the Compatibilization and Chain Extender Effects of Methacrylate-Co-Glycidyl Methacrylate Copolymer. *J. Appl. Polym. Sci.* **2021**, *138*, 1–12. DOI: 10.1002/app.50124.
220. Li, W.; Wu, D.; Sun, S.; Wu, G.; Zhang, H.; Deng, Y.; Zhang, H.; Dong, L. Toughening of Polylactide with Epoxy-Functionalized Methyl Methacrylate–Butyl Acrylate Copolymer. *Polym. Bull.* **2014**, *71*, 2881–2902. DOI: 10.1007/s00289-014-1228-9.
221. Hao, Y.; Liang, H.; Bian, J.; Sun, S.; Zhang, H.; Dong, L. Toughening of Polylactide with Epoxy-Functionalized Methyl Methacrylate-Butadiene Copolymer. *Polym. Int.* **2014**, *63*, 660–666. DOI: 10.1002/pi.4561.
222. Anakabe, J.; Zaldua Huici, A. M.; Eceiza, A.; Arbelaiz, A. The Effect of the Addition of Poly(Styrene-Co-Glycidyl Methacrylate) Copolymer on the Properties of Polylactide/Poly(Methyl Methacrylate) Blend. *J. Appl. Polym. Sci.* **2016**, *133*, 1–10. DOI: 10.1002/app.43935.
223. Liu, H.; Chen, F.; Liu, B.; Estep, G.; Zhang, J. Super Toughened Poly(Lactic Acid) Ternary Blends by Simultaneous Dynamic Vulcanization and Interfacial Compatibilization. *Macromolecules* **2010**, *43*, 6058–6066. DOI: 10.1021/ma101108g.
224. Yuryev, Y.; Mohanty, A. K.; Misra, M. A New Approach to Supertough Poly(Lactic Acid): A High Temperature Reactive Blending. *Macro. Mater. Eng.* **2016**, *301*, 1443–1453. DOI: 10.1002/mame.201600242.
225. Xu, Y.; Loi, J.; Delgado, P.; Topolkaraev, V.; McEneany, R. J.; Macosko, C. W.; Hillmyer, M. A. Reactive Compatibilization of Polylactide/Polypropylene Blends. *Ind. Eng. Chem. Res.* **2015**, *54*, 6108–6114. DOI: 10.1021/acs.iecr.5b00882.
226. Zolali, A. M.; Favis, B. D. Toughening of Cocontinuous Polylactide/Polyethylene Blends via an Interfacially Percolated Intermediate Phase. *Macromolecules* **2018**, *51*, 3572–3581. DOI: 10.1021/acs.macromol.8b00464.
227. Zhang, K.; Nagarajan, V.; Misra, M.; Mohanty, A. K. Supertoughened Renewable PLA Reactive Multiphase Blends System: Phase Morphology and Performance. *ACS Appl. Mater. Interfaces.* **2014**, *6*, 12436–12448. DOI: 10.1021/am502337u.
228. Jauzein, T.; Huneault, M. A.; Heuzey, M. C. Crystallinity and Mechanical Properties of Polylactide/Ether-Amide Copolymer Blends. *J. Appl. Polym. Sci.* **2017**, *134*, 1–10. DOI: 10.1002/app.44677.
229. Vachon, A.; Pépin, K.; Balampanis, E.; Veilleux, J.; Vuillaume, P. Y. Compatibilization of PLA/PEBA Blends via Reactive Extrusion: A Comparison of Different Coupling Agents. *J. Polym. Environ.* **2017**, *25*, 812–827. DOI: 10.1007/s10924-016-0860-x.
230. Wu, N.; Zhang, H. Mechanical Properties and Phase Morphology of Super-Tough PLA/PBAT/EMA-GMA Multicomponent Blends. *Mater. Lett* **2017**, *192*, 17–20. DOI: 10.1016/j.matlet.2017.01.063.
231. Deng, S.; Bai, H.; Liu, Z.; Zhang, Q.; Fu, Q. Toward Supertough and Heat-Resistant Stereocomplex-Type Polylactide/Elastomer Blends with Impressive Melt Stability via in

Situ Formation of Graft Copolymer during One-Pot Reactive Melt Blending. *Macromolecules* **2019**, *52*, 1718–1730. DOI: 10.1021/acs.macromol.8b02626.

232. Sui, G.; Wang, K.; Xu, S.; Liu, Z.; Zhang, Q.; Du, R.; Fu, Q. The Combined Effect of Reactive and High-Shear Extrusion on the Phase Morphologies and Properties of PLA/OBC/EGMA Ternary Blends. *Polymer* **2019**, *169*, 66–73. DOI: 10.1016/j.polymer.2019.02.044.
233. Lin, W.; He, Y.; Qu, J. P. Super-Tough and Highly-Ductile Poly(l-Lactic Acid)/Thermoplastic Polyurethane/Epoxide-Containing Ethylene Copolymer Blends Prepared by Reactive Blending. *Macromol. Mater. Eng.* **2019**, *304*, 1–6. 304 DOI: 10.1002/mame.201900020.
234. Piontek, A.; Vernaez, O.; Kabasci, S. Compatibilization of Poly(Lactic Acid) (PLA) and Bio-Based Ethylene-Propylene-Diene-Rubber (EPDM) via Reactive Extrusion with Different Coagents. *Polymers* **2020**, *12*, 605. DOI: 10.3390/polym12030605.
235. Zhu, C.; Lu, X.; Li, Y.; Deng, Y.; Lu, J.; Liu, Z.; Wu, H.; Tong, Y.; Qu, J. Enhancing Toughness of PLA/ZrP Nanocomposite through Reactive Melt-Mixing by Ethylene-Methyl Acrylate-Glycidyl Methacrylate Copolymer. *Polymers* **2022**, *14*, 3748. DOI: 10.3390/polym14183748.
236. Wu, B.; Zeng, Q.; Niu, D.; Yang, W.; Dong, W.; Chen, M.; Ma, P. Design of Supertoughened and Heat-Resistant PLLA/Elastomer Blends by Controlling the Distribution of Stereocomplex Crystallites and the Morphology. *Macromolecules* **2019**, *52*, 1092–1103. DOI: 10.1021/acs.macromol.8b02262.
237. Mohammad, N. N. B.; Arsad, A.; Choi, H. J.; Ngadi, N.; Desa, M. S. Z. M. Influences of Pristine Carbon Nanotube on the Rheological Properties of Compatibilized Polylactic Acid/Natural Rubber Nanocomposite. *Mater. Today Proc.* **2021**, *39*, 951–955. DOI: 10.1016/j.matpr.2020.04.211.
238. Sookprasert, P.; Hinchiranan, N. Morphology, Mechanical and Thermal Properies of Poly(Lactic Acid) (PLA)/Natural Rubber (NR) Blends Compatibilized by NR-Graft-PLA. *Mater. Res. Soc.* **2017**, *32*, 788–800. DOI: 10.1557/jmr.2017.9.
239. Prismane Consulting. Polylactic Acid Market Overview-2021 https://prismaneconsulting.com/blog-details/polylactic-acid-market-overview-2021.